ABSTRACT

Title of Dissertation: SEISMIC ASSESSMENT OF CURVED BRIDGES USING MODAL PUSHOVER ANALYSIS

Mohamed Salah Eldin Ibrahim Ahmed,
Doctor of Philosophy, 2010

Dissertation Directed By: Professor Chung C. Fu
Department of Civil and Environmental Engineering

The assessment of existing bridge structures against earthquake threat has become a major issue lately, motivated by the maturity of seismic design of new structures, on one side, and by the recognition of the inadequate level of seismic protection, the aging and the constant need of maintenance of the existing ones, on the other. While nonlinear time history analysis (NL-THA) is the most rigorous procedure to compute seismic demands, many seismic-prone countries, such as United States, New Zealand, Japan and Italy, have recently released standards for the assessment of buildings, all of which include the use of the non-linear static analysis procedure (NSP), the so-called pushover. The nonlinear static analysis procedure has a relatively long history. It was first specified by (FEMA-273, 1997) and later updated by (FEMA-356, 2000) as an analytical procedure that can be used in systematic rehabilitation of structures. Also, (ATC-40, 1996), developed by the Applied Technology Council, applied the NSP as a seismic assessment tool. These methods were applied only for buildings. Recently Chopra and

Goel (2002) proposed the modal pushover analysis (MPA) procedure that considers the effect of higher modes on the behavior of buildings.

This research investigation is intended to evaluate the accuracy of the modal pushover analysis (MPA) procedure in estimating seismic demands for curved bridges after proposing some modifications that would render the MPA procedure applicable for bridges. For verification purpose, the nonlinear time history analysis (NL-THA) is also performed in order to quantify the accuracy of MPA. Three bridges were analyzed using both the MPA and NL-THA in addition to the standard pushover analysis (SPA). Maximum Demand displacements, total base shear and plastic rotations obtained from SPA and MPA are compared with the corresponding values resulting from the NL-THA. Comparison shows a good agreement between MPA and NL-THA results and MPA is deemed to be accurate enough for practical use. Furthermore, to evaluate the applicability of the MPA method for a wide range of bridges, a parametric study using both the MPA and NL-THA is performed. Results from the MPA for demand displacement and base shear are compared with results from the NL-THA. Also, the influence of different parameters on the behavior of curved bridges is studied. Parameters included the girder cross section (steel I vs. steel BOX), span length, number of spans, radius of curvature, and pier height. Pier height is found to have the most significant effect on bridge behavior as well as span length, while radius of curvature is found to have less influence on the behavior of curved bridges.

SEISMIC ASSESSMENT OF CURVED BRIDGES USING MODAL PUSHOVER ANALYSIS

By

Mohamed Salah Eldin Ibrahim Ahmed

Dissertation submitted to the Faculty of the Graduate School of the
University of Maryland, College Park, in partial fulfillment
of the requirements for the degree of
Doctor of Philosophy
2010

Advisory Committee:
Professor Chung C. Fu, Chair/Advisor
Professor M. Sherif Aggour
Professor Amde M. Amde
Professor Charles W. Schwartz
Professor Amr Baz

ACKNOWLEDGEMENTS

I would like to take this opportunity to thank my advisor, Dr. Chung C. Fu, for his knowledge and guidance during my studies. His advice was very crucial for the success of this work. I have truly enjoyed my time working for him, and I appreciate his enthusiasm for learning.

I also thank my committee members: Dr. Aggour, Dr. Amde, Dr. Schwartz and Dr. Baz for their valuable time reading my work and providing their insight and comments.

Financial support provided by Dr. Fu and the Bridge Engineering Software and Technology (BEST) Center is gratefully acknowledged.

Special thanks are to my wife and my daughters for encouraging and supporting me during pursuit of my degree.

Finally, I would like to thank all my family members for their patience and support throughout the course of this research. My sincere appreciation goes to my brother, mother and sister.

Table of Contents

LIST OF TABLES

LIST OF FIGURES

1. INTRODUCTION

1.1 INTRODUCTION

The use of horizontally curved girders in the design of highway bridges and interchanges in large urban areas has increased dramatically in recent years. In fact, nationwide, over one-third of all steel superstructure bridges constructed today are curved. The primary reason for the increase is that curved bridges offer an economical means of satisfying the demand placed on highway structures by predetermined roadway alignment and tight geometric restrictions to maintain required traffic design speeds. In addition, curved bridges result in an aesthetically superior solution that has motivated increased use of designs which utilize curved configurations. There will be a likewise increased need for curved superstructure bridges that will facilitate smooth traffic flow off of interstate highways and other major roadways.

Today, curved girders are widely used in bridge superstructures. The designer has many choices including material (concrete vs. steel), cross section shape (tub girder vs. I-beam), etc. Furthermore, the past three decades have resulted in advances in optimizing curved bridge design, resulting in innovative, aesthetically pleasing structures. However, due to the addition of curvature, the design and construction of bridges becomes immensely more complicated than that of straight bridges. While the girders, stringers, and floor beams of straight bridges can be designed by systematically isolating each member and applying standard loads, curved bridges must be designed with careful consideration to system-wide behavior. In essence, the addition of curvature adds torsion to the system that results in significant warping and distortional stresses within the member cross sections. Furthermore, "secondary members" such as cross frames and diaphragms that provide stability in straight bridges become primary load carrying members in curved bridges.

1.2 BACKGROUND AND MOTIVATIONS

The assessment of existing bridge structures against earthquake threat has become a major issue lately, motivated by the maturity of seismic design of new structures, on one side, and by the recognition of the inadequate level of seismic protection, the aging and the constant need of maintenance of the existing ones, on the other. While nonlinear time history analysis (NL-THA) is the most rigorous procedure to compute seismic demands, many seismic-prone countries, such as United States, New Zealand, Japan and Italy, have recently released standards for the assessment of buildings, all of which include the use of the non-linear static analysis method, the so-called pushover.

Pushover is a widely used analytical tool for the evaluation of the structural behavior in the inelastic range and the identification of the locations of structural weaknesses as well as of failure mechanisms. Nevertheless, the method is limited by the assumption that the response of the structure is controlled by its fundamental mode.

The seismic demands are computed by nonlinear static analysis of the structure subjected to monotonically increasing lateral forces with an invariant spatial distribution until a predetermined target displacement is reached at a monitoring point. The target displacement is determined from the deformation of an equivalent single-degree-of-freedom (SDOF) system.

The nonlinear static analysis method has a relatively long history; its fundamentals were laid out in the work of (Freeman, Nicoletti, & Tyrell, 1975) and (Fajfar & Fischinger, 1989). Since then, extension of the standard pushover analysis (SPA) to consider higher modes effects has attracted attention, the effort being to match as closely as possible the results of the nonlinear time history analysis. In an early effort (Sasaki, Freeman, & Paret, 1998) used the multi-mode pushover procedure to identify the effects of higher modes in pushover analysis of buildings by appropriately extending the capacity spectrum method (CSM), which directly compares building capacity to earthquake demand; separate pushover curves were derived for each mode, without an attempt to combine modal responses. (Bracci, Kunnath, & Reinhorn, 1997), (Gupta & Kunnath, 2000), and (Antoniou, Rovithakis, & Pinho, 2002) developed a series of 'adaptive' multi-mode pushover analysis methods, involving redefinition of the loading pattern, which is determined by modal combination rules (e.g. SRSS of modal loads) at each stage of the response during which the dynamic characteristics of the structure change (usually at each step when a new plastic hinge forms). While in the aforementioned adaptive methods modal superposition is carried out at the level of loading, in the modal pushover analysis (MPA) proposed by (Chopra & Goel, 2002), subsequently improved by the same authors (Chopra & Goel, 2004), pushover analyses are carried out separately for each significant mode, and the contributions from individual modes to calculated response quantities (displacements, drifts, etc.) are combined using an appropriate combination rule (SRSS or CQC). Although the rule of superposition of modal responses does not apply in the inelastic range of the response (modes are not uncoupled anymore), (Chopra & Goel, 2004) have shown that the error, taking the results of nonlinear THA as the benchmark, is typically smaller than in the case that superposition is carried out at the level of loading (with fixed loading pattern), as recommended in the (FEMA-356, 2000) Guidelines; these guidelines adopt the nonlinear static procedure (NSP), i.e. pushover analysis, carried out with two different loading patterns, one based on first mode loading ('triangular' distribution) and one with 'modal' distribution (SRSS combination of elastic modal loads).

In another recent development, (Aydinoglu, 2004) has proposed the so-called 'incremental response spectrum analysis (IRSA)', wherein each time a new hinge forms in a structure, elastic modal spectrum analysis is performed, taking into account the changes in the dynamic properties of the structure.

From the previously-mentioned studies attempting to account for higher modes in pushover analysis, only that of (Aydinoglu, 2004), which focuses mainly on buildings, includes an application to a bridge structure; the IRSA procedure is used, taking one or eight modes into account, without detailed discussion of the resulting differences. At the same time as (Aydinoglu, 2004), another study by (Kappos, Paraskeva, & Sextos, 2004) involving higher mode effects in pushover analysis of bridges appeared. It applies a multi-modal pushover procedure generally similar to that of (Chopra & Goel, 2002) to an actual curved bridge considering its first three transverse modes, and compares the resulting displacements with those of single mode pushover and of time history analysis for spectrum-compatible records. Also, in the studies by (Fischinger, Beg, Isakovic, Tomazevic, & Zarnic, 2004) and (Isakovic & Fischinger, 2006) slightly different versions of these three methods, as well as IRSA, are used for the analysis of hypothetical irregular, torsionally sensitive bridges, and results are compared.

Recently (Pinho, Antoniou, Casarotti, & Lopez, 2005) applied a number of existing pushover procedures ('standard' and adaptive), as well as a new version of adaptive pushover (called 'displacement-based adaptive pushover') to a number of idealized bridges (regular and irregular), and compared with results from incremental inelastic dynamic analysis. (Paraskeva, Kappos, & Sextos, 2006) extended the MPA procedure previously proposed by (Chopra & Goel, 2002), which was found to provide good results for buildings and can be implemented using standard software tools, to the case of bridges. They also quantified the relative accuracy of three inelastic analysis methods, i.e. SPA, MPA, and NL-THA, by focusing on the realistic case of a long and curved-in-plan, actual bridge, analyzed with the aid of a three-dimensional model. The study was subsequently improved by (Kappos & Paraskeva, 2008), and improved modal pushover analysis method was proposed which gave better results comparing to the THA results.

This approach has been extensively developed and a large number of variants, of increasing accuracy but also of greater complexity, are available. While many studies are available dealing with the application of pushover to building structures, the situation is quite different when bridges are considered. The number of studies are very limited, among those are Aydinoglu (2004), Kappos et al. (2004), Pinho et al. (2005), Paraskeva et al. (2006), Kappos and Paraskeva (2008) and, in addition, several issues have been raised that are still awaiting a satisfactory solution.

Actually, the dynamic response of bridge structures is often contributed by several modes, which hinders conceptually the reduction of a multi-degrees-of-freedom (MDOF) structure into an equivalent single-degree-of-freedom (SDOF) oscillator. Furthermore, while buildings behave essentially as vertical cantilevers, bridges may vibrate according to complex patterns, which make more problematic the selection of the "reference DOF" representing the displacement of the equivalent SDOF oscillator.

This study represents a further attempt to investigate the subject. Considering that computational burden and records availability, the main obstacles to dynamic analysis, have been largely overcome nowadays, a precondition for this study has been the choice of retaining what is considered the only other reason for favoring an approximate static approach, i.e. simplicity. Along this line, attention is focused on the modal pushover approach which was first introduced by Chopra and Goel (2002), which might be viewed as an upper-bound level of sophistication for a non-linear static analysis. The investigation is made on three reinforced concrete bridges of considerable length and importance which was built in the '90. Due to one of the bridges' highly irregular configuration, it may well represent an extreme case to test the applicability of the procedure. After verifying the MPA method results, a parametric study was carried out in order to study the effect of different parameters on the behavior of steel curved bridges.

1.3 OBJECTIVES

The main objective of this study is to evaluate the applicability of the modal pushover analysis (MPA) procedure to curved bridges and quantify its accuracy. Due to the nature of bridges, which extend horizontally rather than buildings that extend vertically, some considerations and modifications are proposed to make this method applicable for bridges. This main objective includes the following steps:

1) Considering a realistic case of a long and curved-in-plan bridge, in order to quantify the relative accuracy of the MPA method with other inelastic analysis methods, i.e. SPA, and NL-THA.

2) Definition of the control node: control node is the node used to monitor displacement of the structure. Its displacement versus the base-shear forms the capacity (pushover) curve of the structure. Different control nodes are investigated in order to define the most appropriate point that gives the most accurate results with regard to realistic pushover curves and maximum demand displacement.

3) Evaluation of the modal force distributions applied to the structure while performing the pushover analysis for each mode either using the elastic mode

shape load or the resulting deformed shape after pushing over the structure with the corresponding modal load pattern.

4) Estimation of the displacement demand and response quantities.

5) Extend the case study to consider another realistic bridge in addition to a modified model based on the second bridge in order to evaluate the accuracy of the MPA method and also investigate the influence of skewness on the behavior of bridges.

6) Carry out a parametric study for different configurations of horizontally curved steel bridges in order to evaluate the applicability of MPA to a wide range of bridges and study the effect of various parameters such as steel girder cross section, span length, radius of curvature and pier column's height on the behavior of curved bridges during a large seismic event.

1.4 ORGANIZATION OF THE WORK

The present chapter presents an overview of the study along with its objectives. Methods to estimate seismic demands on elastic and inelastic structures are reviewed in Chapter 2, where the derivation and underlying assumptions of MPA procedure for bridges are also presented. Chapter 3 describes the three structural systems to be analyzed to verify the MPA procedure, and also the ensemble of ground motions considered. Studying the applicability of the MPA to bridges, along with proposed modifications, is presented in Chapter 4 which is titled "Evaluation of MPA procedure for bridges."

Chapter 5 describes the parametric study to be performed for different bridge configurations. Results and findings of the parametric study are reviewed in chapter 6. Summary and conclusions are presented in chapter 7. Appendix A includes the calculations of different parameters needed to define plastic hinges as well as nonlinear link elements needed to perform modal pushover and nonlinear time history analyses using the SAP2000. Appendix B includes an investigation of the influence of the number of transverse mode shapes to be included in the analysis. A sample of input files for analyzing and designing different bridge configurations with steel I & BOX cross sections using DESCUS I&II are presented in Appendix C. Lastly, Appendix D includes a sample input data files needed to create one bridge model for analysis in SAP2000 using both the MPA and NL-THA.

2. METHODS TO ESTIMATE SEISMIC DEMANDS

2.1 INTRODUCTION

Conventional dynamic analysis and modal pushover analysis procedures to determine seismic demands for elastic and inelastic structures are presented in this chapter. These procedures have been presented by Chopra and Goel (2002) which have emphasis on buildings and will be reviewed in the following sections. First, two versions of modal analysis, response history analysis (RHA) and response spectrum analysis (RSA), for linearly elastic systems are reviewed. Then, standard equations of motion for inelastic MDOF systems are expressed in terms of elastic modal coordinates. Although, these modal equations are not uncoupled in contrast to elastic systems, their coupling is shown to be weak and thus neglected to develop the uncoupled modal response history analysis (UMRHA) procedure as was explained in Chopra and Goel (2002). The peak "modal" responses, which can be determined by a pushover analysis for each "mode", are then combined according to an appropriate modal combination rule. In order to apply the modal pushover (MPA) procedure to the case of bridges; a set of additional assumptions and decisions regarding alternative procedures that can be used are needed. It will be reviewed as the extended MPA procedure for bridges.

2.2 ELASTIC MULTISTORY BUILDINGS

2.2.1 Modal Response History Analysis (RHA)

The differential equations governing the response of a multistory building to horizontal earthquake ground motion $\ddot{u}_g(t)$ are as follows:

$$m\ddot{u} + c\dot{u} + ku = -m\iota\,\ddot{u}_g(t) \tag{2.1}$$

Where **u** is the vector of N lateral floor displacements relative to the ground, **m**, **c**, and **k** are the mass, classical damping, and lateral stiff matrices of the system; each element of the influence vector $\boldsymbol{\iota}$ is equal to unity.

The right side of Eq. (2.1) can be interpreted as effective earthquake forces:

$$p_{eff}(t) = -m\iota\,\ddot{u}_g(t) \tag{2.2}$$

The spatial distribution of these forces over the height of the building is defined by the vector s = mι and their time variation by $\ddot{u}_g(t)$. This force distribution can be expanded as a summation of modal inertia force distribution s_n (Chopra, 2001)

$$m\,\iota = \sum_{n=1}^{N} s_n = \sum_{n=1}^{N} \Gamma_n m\,\phi_n \tag{2.3}$$

Where ϕ_n is the *n*th natural vibration mode of the structure, and

$$\Gamma_n = \frac{L_n}{M_n} \qquad L_n = \phi_n^T m\,\iota \qquad M_n = \phi_n^T m \phi_n \tag{2.4}$$

The effective earthquake forces can then be expressed as

$$p_{eff}(t) = \sum_{n=1}^{N} p_{eff,n}(t) = \sum_{n=1}^{N} -s_n \ddot{u}_g(t) \tag{2.5}$$

The contribution of the *n*th mode to **s** and to $\mathbf{p_{eff}}$ ***(t)*** is:

$$s_n = \Gamma_n m \phi_n \qquad p_{eff,n}(t) = -s_n \ddot{u}_g(t) \tag{2.6}$$

The response of the MDOF system to $\mathbf{p_{eff,\mathit{n}}}$ ***(t)*** is entirely in the *nth*-mode, with no contributions from other modes. The equations governing the response of the system are

$$m\ddot{u} + c\dot{u} + ku = -s_n \ddot{u}_g(t) \tag{2.7}$$

By utilizing the orthogonality property of modes, it can be demonstrated that none of the modes other than the *n*th mode contribute to the response. Then the floor displacements are:

$$u_n(t) = \phi_n q_n(t) \tag{2.8}$$

Where the modal coordinate $q_n(t)$ is governed by

$$\ddot{q}_n + 2\zeta_n \omega_n \dot{q}_n + \omega_n^2 q_n = -\Gamma_n \ddot{u}_g(t) \tag{2.9}$$

In which ω_n is the natural vibration frequency and ζ_n is the damping ratio for the *n*th mode. The solution $q_n(t)$ can readily be obtained by comparing Eq. (2.9) to the equation of motion for the *n*th-mode elastic SDOF system, an SDOF system with vibration properties-natural frequency ω_n and damping ration ζ_n –of the *nth*-mode of the MDOF system, subjected to $\ddot{u}_g(t)$:

$$\ddot{D}_n + 2\zeta_n \omega_n \dot{D}_n + \omega_n^2 D_n = -\ddot{u}_g(t) \tag{2.10}$$

Comparing Equations (2.9) and (2.10) gives

$$q_n(t) = \Gamma_n D_n(t) \tag{2.11}$$

And substituting in Eq. (2.8) gives the floor displacements

$$u_n(t) = \Gamma_n \phi_n D_n(t) \tag{2.12}$$

Any response quantity *r (t)* –displacements, internal element forces, etc.- can be expressed by:

$$r_n(t) = r_n^{st} A_n(t) \tag{2.13}$$

Where r_n^{st} denotes the modal static response, the static value of *r* due to external forces s_n, and

$$A_n(t) = \omega_n^2 D_n(t) \tag{2.14}$$

is the pseudo-acceleration response of the *n*th-mode SDOF system (Chopra, 2001; Section 12.1). The two analyses that lead to r_n^{st} and $A_n(t)$ are shown schematically in Figure 2-1.

Equations (2.12) and (2.13) represent the response of the MDOF system to $\mathbf{p}_{\mathbf{eff,n}}$ ***(t)***. Therefore, the response of the system to the total excitation $\mathbf{p}_{\mathbf{eff}}$ ***(t)*** is:

$$u(t) = \sum_{n=1}^{N} u_n(t) = \sum_{n=1}^{N} \Gamma_n \phi_n D_n(t) \tag{2.15}$$

$$r(t) = \sum_{n=1}^{N} r_n(t) = \sum_{n=1}^{N} r_n^{st} A_n(t) \tag{2.16}$$

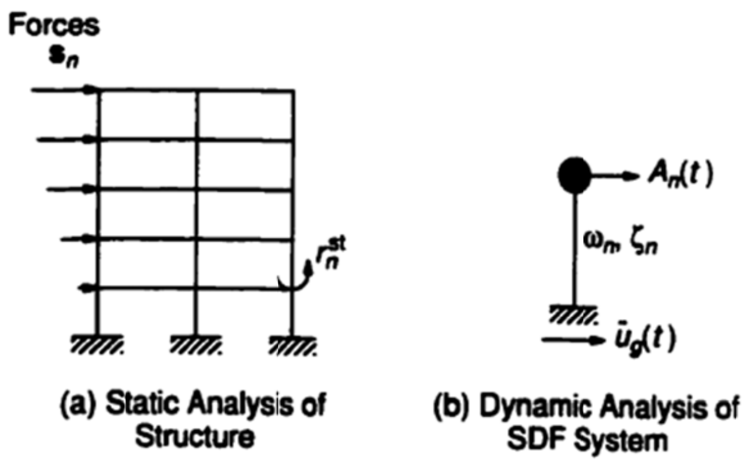

Figure 2-1 Conceptual explanation of modal response history analysis of elastic MDOF systems.

(Source: (Chopra & Goel, 2001))

This is the classical modal RHA procedure wherein Eq. (2.9) is the standard modal equation governing $q_n(t)$, Eqs. (2.12) and (2.13) define the contribution of the *n*th-mode to the response, and Eqs. (2.15) and (2.16) reflect combining the response contributions of all modes. However, these standard equations have been derived in an unconventional way. In contrast to the classical derivation found in textbooks

(Chopra, 2001; Sections 12.4 and 13.1.3), the modal expansion of the spatial distribution of the effective earthquake forces was used.

2.2.2 Modal Response Spectrum Analysis (RSA)

The peak value r_o of the total response $r(t)$ can be estimated directly from the response spectrum for the ground motion without carrying out the response history analysis (RHA) implied in Eqs. (2.9)-(2.16). In such a response spectrum analysis (RSA), the peak value r_{no} of the nth-mode contribution $r_n(t)$ to response $r(t)$ is determined from

$$r_{no} = r_n^{st} A_n \tag{2.17}$$

Where A_n is the ordinate $A(T_n,\zeta_n)$ of the pseudo-acceleration response (or design) spectrum for the nth-mode SDOF system, and $T_n=2\pi/\omega_n$ is the natural vibration period of the nth-mode of the MDOF system.

The peak modal responses are combined according to the Square-Root-of-Sum-of-Squares (SRSS) or the Complete Quadratic Combination (CQC) rules. The SRSS rule, which is valid for structures with well-separated natural frequencies such as multistory buildings with symmetric plan, provides an estimate of the peak value of the total response:

$$r_o \approx \left(\sum_{n=1}^{N} r_{no}^2 \right)^{1/2} \tag{2.18}$$

2.2.3 Modal Pushover Analysis (MPA)

To develop a pushover analysis procedure consistent with RSA, it is noted that static analysis of the structure subjected to lateral forces

$$f_{no} = \Gamma_n m \phi_n A_n \tag{2.19}$$

will provide the same value of r_{no}, the peak nth-mode response as in Eq. (2.17) (Chopra, 2001; Section 13.8.1). Alternatively, this response value can be obtained by static analysis of the structure subjected to lateral forces distributed over the building height according to

$$s_n^* = m \phi_n \tag{2.20}$$

and the structure is pushed to the roof displacement, u_{rno}, the peak value of the roof displacement due to the nth-mode, which from Eq. (2.12) is

$$u_{rno} = \Gamma_n \phi_{rn} D_n \tag{2.21}$$

where $D_n = A_n/\omega_n^2$. Obviously D_n and A_n are available from the response (or design) spectrum.

The peak modal responses, r_{no} , each determined by one pushover analysis, can be combined according to Eq. (2.18) to obtain an estimate of the peak value r_o of the total response. This modal pushover analysis (MPA) for linearly elastic systems is equivalent to the well-known RSA procedure (Section 2.2.2).

2.3 INELASTIC MULTISTORY BUILDINGS

2.3.1 Nonlinear Response History Analysis (NL-RHA)

For each structural element of a building, the initial loading curve is idealized as bilinear, and the unloading and reloading curves differ from the initial loading branch. Thus, the relations between lateral forces f_s at the N floor levels and the lateral displacements u are not single valued, but depend on the history of the displacements:

$$\mathrm{f}_s = \mathrm{f}_s(\mathrm{u}, \mathrm{sign}\,\dot{\mathrm{u}}) \tag{2.22}$$

With this generalization for inelastic systems, Eq. (2.1) becomes

$$m\ddot{u} + c\dot{u} + \mathrm{f}_s(\mathrm{u}, \mathrm{sign}\ \dot{\mathrm{u}}) = -m\iota\,\ddot{u}_g(t) \tag{2.23}$$

The standard approach is to solve directly these coupled equations, leading to the "exact" nonlinear response history analysis (RHA).

Although classical modal analysis (Section 2.2.1) is not valid for inelastic systems, it is useful for later reference to transform Eq. (2.23) to the modal coordinates of the corresponding linear system. Each structural element of this elastic system is defined to have the same stiffness as the initial stiffness of the structural element of the inelastic system. Both systems have the same mass and damping. Therefore, the natural vibration periods and modes of the corresponding linear system are the same as the vibration properties of the inelastic system undergoing small oscillations (within the linear range).

Expanding the displacements of the inelastic system in terms of the natural vibration modes of the corresponding linear system gives

$$\mathrm{u}(t) = \sum_{n=1}^{N} \phi_n q_n(t) \tag{2.24}$$

Substituting Eq. (2.24) in Eq. (2.23), premultiplying by ϕ_n^T, and using the mass and classical damping orthogonality property of modes gives

$$\ddot{q}_n + 2\zeta_n \omega_n \dot{q}_n + \frac{F_{sn}}{M_n} = -\Gamma_n \ddot{u}_g(t) \qquad n = 1,2,\dots. N \tag{2.25}$$

Where the only term that differs from Eq. (2.9) involves

$$F_{sn} = F_{sn}(q, sign\,\dot{q}) = \phi_n^T\, \mathrm{f_s}(\mathrm{u}, \mathrm{sign}\,\dot{\mathrm{u}}) \tag{2.26}$$

This resisting force depends on all modal coordinates q_n (t), contained in **q**, implying coupling of modal coordinates because of yielding of the structure.

Equation (2.25) represents N equations in the modal coordinates q_n. unlike Eq. (2.9) for linearly elastic systems; these equations are coupled for inelastic systems. Simultaneously solving these coupled equations and using Eq. (2.24) will, in principle, give the same results for **u** (t) as obtained directly from Eq. (2.23). However, Eq. (2.25) is rarely solved because it offers no particular advantage over Eq. (2.23).

2.3.2 Uncoupled Modal Response History Analysis (UMRHA)

Neglecting the coupling of the N equations in modal coordinates [Eq. (2.25)] leads to the uncoupled modal response history analysis (UMRHA) procedure. This approximate RHA procedure is the preliminary step in developing a modal pushover analysis procedure for inelastic systems.

The spatial distribution $\mathbf{s}$ of the effective earthquake forces is expanded into the modal contributions $\mathbf{s_n}$ according to Eq. (2.3), where $\boldsymbol{\phi}_n$ are now the modes of the corresponding linear system. The equations governing the response of the inelastic system to $\mathbf{p}_{\mathbf{eff},n}\,\boldsymbol{(t)}$ given by Eq.(2.6b) are

$$m\ddot{u} + c\dot{u} + \mathrm{f}_s(\mathrm{u}, \mathrm{sign}\,\dot{\mathrm{u}}) = -s_n\,\ddot{u}_g(t) \tag{2.27}$$

The solution of Eq. (2.27) for inelastic systems will no longer be described by Eq. (2.8) because $q_r(t)$ will generally be nonzero for “modes” other than the nth ”mode”, implying that other “modes” will also contribute to the solution. For linear elastic systems, however, $q_r\,(t)$=0 for all modes other than the nth-mode; therefore, it is reasonable to expect that the nth “mode” should be dominant even for inelastic systems. Approximating the response of the structure to excitation $\mathbf{p}_{\mathbf{eff,n}}\;\boldsymbol{(t)}$ by Eq. (2.8), substituting Eq. (2.8) in Eq. (2.27) and premultiplying by $\boldsymbol{\phi}_n^{\,T}$ gives Eq. (2.25), except for the important approximation that F_{sn} now depends only on one modal coordinate, q_n :

$$F_{sn} = F_{sn}(q_n, sign\dot{q}_n) = \phi_n^T\ \mathrm{f}_s(q_n, \mathrm{sign}\ \dot{q}_n) \tag{2.28}$$

with this approximation, solution of Eq. (2.25) can be expressed by Eq. (2.11) where $D_n(t)$ is governed by

$$\ddot{D}_n + 2\zeta_n \omega_n \dot{D}_n + \frac{F_{sn}}{L_n} = -\ddot{u}_g(t) \tag{2.29}$$

and

$$F_{sn} = F_{sn}(D_n, sign\dot{D}_n) = \phi_n^T \, \mathrm{f_s}(D_n, \mathrm{sign}\, \dot{D}_n) \tag{2.30}$$

is related to $F_{sn}(q_n, sign\dot{q}_n)$ because of Eq. (2.11).

Equation (2.29) may be interpreted as the governing equation for the *n*th-mode inelastic SDOF system, an SDOF system with (1) small amplitude vibration properties-natural frequency ω_n and damping ratio ζ_n – of the *n*th mode of the corresponding linear MDOF system; (2) unit mass; and (3) F_{sn}/L_n-D_n relation between resisting force F_{sn}/L_n and modal coordinate D_n defined by Eq. (2.30). Although Eq. (2.25) cab be solved in its original form, Eq. (2.29) can be solved conveniently by standard software because it is of the same form as the SDOF system excited by ground acceleration $\ddot{u}_g(t)$, and the peak value of $D_n(t)$ can be estimated from the inelastic response (or design) spectrum (Chopra, 2001; Sections 7.6 and 7.12.1). Introducing the *n*th-mode inelastic SDOF system also permitted extension of the well-established concepts for elastic systems to inelastic systems. Compare Eqs. (2.25) and (2.29) to Eqs. (2.9) and (2.10); note that Eq. (2.11) applies to both systems.

Solution of the nonlinear Eq. (2.29) formulated in this manner provides $D_n(t)$, which substituted into Eq. (2.12) gives the floor displacements of the structure associated with the *n*th-mode inelastic SDOF system. Any floor displacement, story drift, or another deformation response quantity $r(t)$ is given by Eqs. (2.13) and (2.14), where $A_n(t)$ is now the pseudo-acceleration response of the *n*th-mode inelastic SDOF system. The two analyses that lead to r_n^{st} and $A_n(t)$ are shown in Figure 2-2. Equations (2.13) and (2.14) represent the response of the inelastic MDOF system to $\mathbf{p}_{\mathbf{eff},\mathbf{n}}(\mathbf{t})$, the *n*th-mode contribution to $\mathbf{p}_{\mathbf{eff}}(\mathbf{t})$. Therefore the response of the system to the total excitation $\mathbf{p}_{\mathbf{eff}}(\mathbf{t})$ is given by Eqs. (2.15) and (2.16). This is the UMRHA procedure.

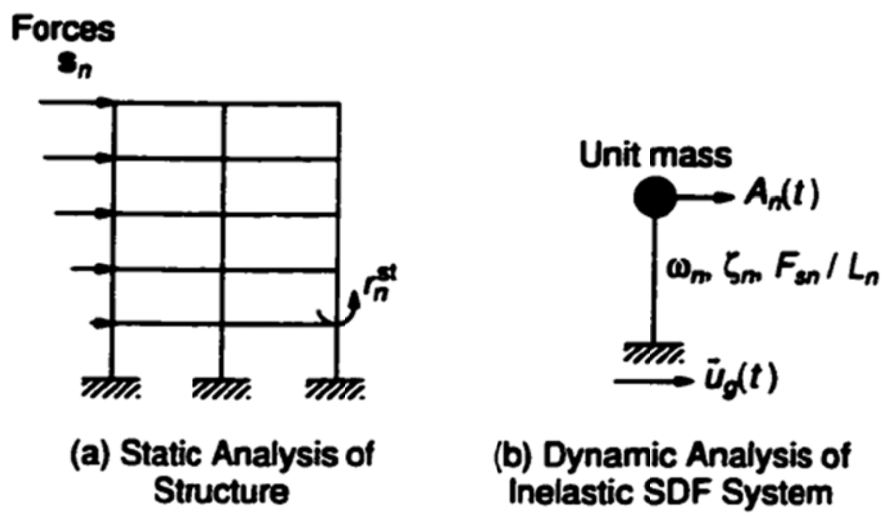

Figure 2-2 Conceptual explanation of uncoupled modal response history analysis of inelastic MDOF systems.

(Source: (Chopra & Goel, 2001))

2.3.2.1 Properties of the *n*th-mode Inelastic SDOF System

To determine the F_{sn}/L_n - D_n relation in Eq. (2.29), the relationship between lateral forces $\mathbf{f}_s$ and $\boldsymbol{D_n}$ in Eq. (2.30) should be determined by nonlinear static analysis of the structure as the structure undergoes displacements $\boldsymbol{u}=\boldsymbol{D_n \phi_n}$ with increasing $\boldsymbol{D_n}$. However, most commercially available software cannot implement such displacement controlled analysis. An alternative approach, which is an approximation, is to conduct a force controlled nonlinear static analysis of the structure subjected to lateral forces distribution over the building height according to Eq. (2.20). When implemented by commercially available software, such nonlinear static analysis provides the so-called pushover curve, which is a plot of base shear V_{bn} against roof displacement u_{rn}. A bilinear idealization of this pushover curve for the *n*th-mode is shown in Figure 2-3a. At the yield point, the base shear is V_{bny} and roof displacement is u_{rny}.

To convert this $V_{bn} - u_{rn}$ pushover curve to the $F_{sn}/L_n - D_n$ relation, the two sets of forces and displacements are related as follows:

$$F_{sn} = \frac{V_{bn}}{\Gamma_n} \qquad\qquad D_n = \frac{u_{rn}}{\Gamma_n \phi_{rn}} \tag{2.31}$$

Equation (2.31) enables conversion of the pushover curve to the desired $F_{sn}/L_n - D_n$ relation shown in Figure 2-3b, where the yield values of F_{sn}/L_n *and* D_n *are*

$$\frac{F_{sny}}{L_n} = \frac{V_{bny}}{M_n^*} \qquad\qquad D_{ny} = \frac{u_{rny}}{\Gamma_n \phi_{rn}} \tag{2.32}$$

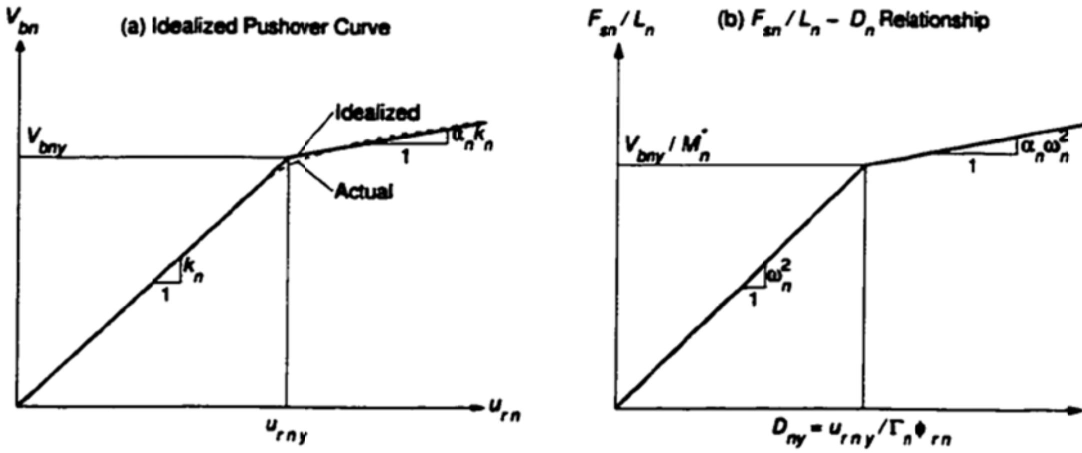

Figure 2-3 Properties of the *n*th-mode inelastic SDOF system from the pushover curve.
(Source: (Chopra & Goel, 2001))

in which $M_n^* = L_n \Gamma_n$ is the effective modal mass (Chopra, 2001; Section 13.2.5). The two are related through

$$\frac{F_{sny}}{L_n} = \omega_n^2 D_{ny} \tag{2.33}$$

implying that the initial slope of the curve in Figure 2-3b is ω_n^2. Knowing F_{sny}/L_n and D_{ny} from Eq. (2.32), the elastic vibration period T_n of the *n*th-mode SDOF system is computed from

$$T_n = 2\pi \left(\frac{L_n D_{ny}}{F_{sny}} \right)^{1/2} \tag{2.34}$$

This value of T_n , which may differ from the period of the corresponding linear system, should be used in Eq. (2.29). In contrast, the initial slope of the pushover curve in Figure 2-3a is $k_n=\omega_n^2 L_n$, which is not meaningful quantity.

2.3.2.2 Step-by-step UMRHA Procedure

The inelastic response of an N-story building with plan symmetric about two orthogonal axes to earthquake ground motion along an axis of symmetry can be estimated as a function of time by the UMRHA procedure developed, which is summarized next as a sequence of steps; (Chopra & Goel, 2001):

1. Compute the natural frequencies, ω_n , and modes, ϕ_n , for linearly elastic vibration of the building.

2. For the *n*th-mode, develop the base shear – roof-displacement ($V_{bn} – u_{rn}$) pushover curve for the force distribution s_n^* [Eq. (2.20)].

3. Idealize the pushover curve as a bilinear curve with post-yield stiffness ration α_n (Figure 2-3a).

4. Convert the idealized pushover curve to the $F_{sn}/L_n – D_n$ relation (Figure 2-3b) by utilizing Eq. (2.32).

5. Compute the deformation history, $D_n(t)$, and pseudo-acceleration history, $A_n(t)$, of the *n*th mode inelastic SDOF system (Figure 2-2b) with force-deformation relation of Figure 2-3b.

6. Calculate histories of various responses by Eqs. (2.12) and (2.13).

7. Repeat steps 2-6 for as many modes as required for sufficient accuracy. Typically, the first two or three modes will suffice.

8. Combine the modal responses using Eqs. (2.15) and (2.16) to determine the total response.

9. Calculate the peak value, r_o , of the total response $r(t)$ obtained in step 8.

2.3.3 Modal Pushover Analysis (MPA)

2.3.3.1 MPA Procedure A

A pushover analysis procedure is presented next to estimate the peak response r_{no} of the inelastic MDOF system to effective earthquake forces $\mathbf{p}_{\mathbf{eff,n}}(\boldsymbol{t})$. Consider a nonlinear static analysis of the structure subjected to lateral forces distributed over the building height according to $\mathbf{s}_\mathbf{n}^*$ [Eq. (2.20)], with the structure is pushed to the roof displacement $\boldsymbol{u_{rno}}$. This value of the roof displacement is given by Eq. (2.21) where $\boldsymbol{D_n}$, the peak value of $\boldsymbol{D_n (t)}$, is now determined by solving Eq. (2.29), as described in Section 2.3.2; alternatively, it can be determined from the inelastic response (or design) spectrum. At this roof displacement, the pushover analysis provides an estimate of the peak value $\boldsymbol{r_{no}}$ of any response $\boldsymbol{r_n(t)}$: floor displacements, story drifts, joint rotations, plastic hinge rotations, etc.

This pushover analysis, although somewhat intuitive for inelastic buildings, seems reasonable. It provides results for elastic buildings that are identical to the well-known

RSA procedure (section 2.2.2) because, as mentioned earlier, the lateral force distribution used possesses two properties: (1) it appears to be the most rational choice among all invariant distribution of forces; and (2) it provides the exact modal response for elastic systems.

The response value $\boldsymbol{r_{no}}$ is an estimate of the peak value of the response of the inelastic system to $\mathbf{p_{eff,n}(t)}$, governed by Eq. (2.27). As shown in sections 2.2.2 and 2.2.3, for elastic systems, $\boldsymbol{r_{no}}$ also represents the exact peak value of the *n*th-mode contribution $\boldsymbol{r_n(t)}$ to response $\boldsymbol{r(t)}$. Thus, we will refer to $\boldsymbol{r_{no}}$ as the peak modal response even in the case of inelastic systems.

The peak modal responses $\boldsymbol{r_{no}}$, each determined by one pushover analysis, are combined using an appropriate modal combination rule, e.g. Eq. (2.18), to obtain an estimate of the peak value $\boldsymbol{r_o}$ of the total response. “This application of modal combination rules to inelastic systems obviously lacks a theoretical basis. However, it seems reasonable because it provides results for elastic buildings that are identical to the well-known RSA procedure”, (Chopra & Goel, 2002).

Step-by-step MPA Procedure A

The peak inelastic response of a building to earthquake excitation can be estimated by the MPA procedure just developed, which is summarized next as a sequence of steps:

1. Compute the natural frequencies, ω_n , and modes, ϕ_n , for linearly elastic vibration of the building.

2. For the *n*th-mode, develop the base shear – roof-displacement ($V_{bn} - u_{rn}$) pushover curve for the force distribution s_n^* [Eq. (2.20)].

3. Idealize the pushover curve as a bilinear curve with post-yield stiffness ration α_n (Figure 2-3a).

4. Convert the idealized pushover curve to the $F_{sn}/L_n - D_n$ relation (Figure 2-3b) by utilizing Eq. (2.32).

5. Compute the peak deformation, D_n, of the *n*th-mode inelastic SDOF system (Figure 2-2b) with force-deformation relation of Figure 2-3b by solving Eq. (2.29), or from the inelastic response (or design) spectrum.

6. Calculate the peak roof displacement u_{rno} associated with the *n*th-mode inelastic SDOF system from Eq. (2.21).

7. At u_{rno}, extract from the pushover database values of other desired responses, r_{no} .

8. Repeat steps 3 to 7 for as many modes as required for sufficient accuracy. Typically, the first two or three modes will suffice.

9. Determine the total response by combining the peak modal responses using the SRSS combination rule of Eq. (2.18). From the total rotation of a plastic hinge, subtract the yield value of hinge rotation to determine the hinge plastic rotation.

Procedure A mainly determines the peak deformations when the earthquake hazard is given in terms of ground motion records. In order to simplify the MPA procedure to facilitate its implementation in engineering practice – where the earthquake hazard is defined in term of a smooth design spectrum corresponding to a selected exceedence probability – procedures B and C will be summarized in the following sections.

2.3.3.2 MPA Procedure B

In the MPA Procedure A, the seismic demand due to each (say, *i*th) ground motion is determined by calculating $(D_n)_i$,$(u_{rno})_i$, $(r_{no})_i$, and $(r_{MPA})_i$, and then the median of $(r_{MPA})_i$ (i=1, 2, 3…) gives $\hat{r}_{MPA}$. The first simplification estimates the median value of "modal" seismic demands $\hat{r}_{no}$ directly from the deformation $\hat{D}_n$ of the *n*th mode inelastic SDOF system, which was determined from the median spectrum for the ensemble of ground motions.

Step-by-step MPA Procedure B

1. Compute the natural frequencies, ω_n , and modes, ϕ_n , for linearly elastic vibration of the building.

2. For the nth-mode, develop the base shear – roof-displacement ($V_{bn} - u_{rn}$) pushover curve for the force distribution s_n^* [Eq. (2.20)].

3. Idealize the pushover curve as a bilinear curve with post-yield stiffness ration α_n (Figure 2-3a).

4. Convert the idealized pushover curve to the $F_{sn}/L_n - D_n$ relation (Figure 2-3b) by utilizing Eq. (2.32).

5. Compute the peak deformation, D_n, of the nth-mode inelastic SDOF system (Figure 2-2b) with force-deformation relation of Figure 2-3b by solving Eq. (2.29), or from the inelastic response (or design) spectrum.

6. Repeat step 5 for all excitations and obtain $(D_n)_i$ for each excitation.

7. Calculate $\hat{D}_n$, the median value of $(D_n)_i$, by

$$\hat{x} = \exp\left[\frac{\sum_{i=1}^{n} \ln x_i}{n}\right] \tag{2.35}$$

8. Calculate the median peak roof displacement $\hat{u}_{rno}$ associated with the nth mode inelastic SDOF system from

$$\hat{u}_{rno} = \Gamma_n \phi_{rn} \hat{D}_n \tag{2.36}$$

9. Extract other desired responses, $\hat{r}_{no}$, from the pushover database values at roof displacement $\hat{u}_{rno}$.

10. Repeat steps 3 to 9 for as many modes as required for sufficient accuracy; usually the first two or three modes will suffice.

11. Determine the total response $\hat{r}_{MPA}$ by combining the peak modal responses $\hat{r}_{no}$ using appropriate modal combination rule, e.g., the SRSS combination rule:

$$\hat{r}_{MPA} = \left(\sum_{n=1}^{J} \hat{r}_{no}^{2} \right)^{1/2} \tag{2.37}$$

2.3.3.3 MPA Procedure C

Procedure B requires nonlinear RHA of the *n*th-mode inelastic SDOF system (step 5) for each ground motion. Procedure C avoids this computation by determining $\hat{D}_n$ from the median deformation spectrum for inelastic SDOF systems for constant yield-strength-reduction-factor R_y, (Chopra, 2001). Steps 5-7 in procedure B to determine $\hat{D}_n$ are replaced by the following steps:

5. Compute the yield strength reduction factor R_{yn} for the *n*th-mode inelastic SDOF system from

$$R_{yn} = \frac{\hat{D}_{n,elastic}}{D_{ny}} \tag{2.38}$$

Where $\hat{D}_{n,elastic}$ is the spectral ordinate of the median elastic deformation spectrum at period T_n; D_{ny} is the yield deformation of the nth-mode inelastic SDOF system obtained in step 4.

6. Compute the peak deformation of the nth-mode inelastic SDOF system with $R_y = R_{yn}$ for every ground motion and determine the median deformation, $\hat{D}_n$. A plot of $\hat{D}_n$ against T_n is the median deformation spectrum for $R_y = R_{yn}$ and damping ratio ζ_n.

7. Obtain $\hat{D}_n$ from this median deformation spectrum at period T_n.

2.4 PROPOSED EXTENSION TO APPLY MPA FOR BRIDGES

2.4.1 Introduction

According to the MPA procedure developed by Chopra and Goel (2002, 2004), standard pushover analysis is performed for each mode independently, wherein the elastic modal forces are applied as invariant seismic load patterns. Modal pushover curves are then plotted and can be converted to capacity diagrams using modal conversion parameters from ATC-40 (1996) and Chopra and Goel (2002). Response quantities are separately estimated for each individual mode, and then superimposed using an appropriate modal combination rule.

2.4.2 MPA procedure for Bridges

Using the extended MPA procedure for the case of bridges includes additional considerations due to the fact that bridges are extending horizontally, contrary to the case of a building which extends vertically. Paraskeva et al. (2006) followed by same authors; (Kappos & Paraskeva, 2008) suggested a set of additional assumptions and decisions regarding alternative procedures that can be used which are needed in order to apply the method in the case of bridges. A key issue is the selection of an appropriate point for monitoring the displacement demand (and also for drawing the pushover curve for each mode). Other issues include the way a pushover curve is bilinearized before being transformed into a capacity curve, the use of the ‘capacity spectrum’ for defining the earthquake demand for each mode and then combining modal responses, and the number of modes that should be considered in the case of bridges.

2.4.2.1 Control Node

Control node is the node used to monitor displacement of the structure. Its displacement versus the base-shear forms the capacity (pushover) curve of the structure. The control node should satisfy two conditions:

- Its location is expected to have maximum displacement.
- Its displacement should reflect the behavior of the structure.

This means that the control node displacement should be affected by the yielding or inelastic behavior of any member that contributes to the stiffness of the structure in the direction under consideration. The latter condition is an essential one that may cause significant error if it is not satisfied while the former condition seems to be more flexible. The selection of an appropriate monitoring point for bridges (in buildings it is typically the roof) is a critical issue for modal pushover analysis (MPA) of bridges. Natural choices for the monitoring point in a bridge are the deck mass center as proposed in (Eurocode 8, 2004), or the top of the nearest to it pier, if the displacement of the two is practically the same, i.e. for monolithic or hinged pier-to-deck connections, but not for sliding or flexible connections (e.g. through pot bearings or elastomeric bearings). By analogy to building structures in (Chopra, 2001), it can also be selected as the point of the deck that corresponds to the location (x_n^*) along the longitudinal axis of the bridge of an equivalent SDOF system, defined by the location of the resultant of the modal load pattern applied to the bridge; which can be calculated from the properties of the MDOF system using the following relationship:

$$x_n^* = \frac{\sum_{j=1}^{N} x_j m_j \phi_{jn}}{\sum_{j=1}^{N} m_j \phi_{jn}} \tag{2.39}$$

in which, x_j is the distance of the *j*th mass from a (selected) point of the MDOF system (in a bridge, the left abutment is a natural choice), and ϕ_{jn} is the value of ϕ_n at the *j*th mass; x_n^* is essentially independent of the way the mode is normalized. It is noted that whereas in buildings locating the SDOF system to a height above the ground defined by equation (2.39) ensures that the overturning moment at its base is the same as that resulting in the MDOF structure from the application of the modal load pattern (see step 2, section 2.4.3), in bridges it simply ensures that the moment at the abutments resulting from applying the base shear at a distance x_n^* is the same as that resulting from the modal loads applied on the actual (MDOF) bridge.

Another proposal by Paraskeva et al. (2006) for the monitoring point of the bridge was also used in the present study is the top of the pier that exhibits the most critical plastic rotation (again, for identical pier and deck displacements), which does not have to be the same for all individual analyses (i.e. for all modes). An initial analysis of the structure for each mode is required in the last case, to define the most critical location that will be used for constructing the relevant pushover curve (Figure 2-4); even this extra effort is not always enough when multiple earthquake intensities are considered, since the location of the critical point might change as the bridge enters the inelastic range and the relative contribution of each mode possibly changes. In this study, effect of the selection of the monitoring point on the shape of the pushover curve will be studied considering the three different proposals of control node mentioned before.

2.4.2.2 Pushover Curve

The pushover analysis method is the process where the structure is subjected to monotonically increasing lateral forces with an invariant distribution until the structure reaches a predetermined target displacement or collapses. The distribution of lateral inertia forces varies continuously during earthquake response. Loading pattern is the most important factor affecting the relative magnitudes of shears, moments, and deformations. If an invariant load pattern is used, the basic assumptions are that the distribution of inertia forces will be reasonably constant throughout the earthquake and that the maximum deformations obtained from this invariant load pattern will be comparable to those expected in the design earthquake. Different load patterns were implemented before to represent the distribution of lateral inertia forces on bridges. Patterns like the uniform load pattern, a modal load pattern corresponding to the fundamental mode or load pattern based on the modal forces combined were previously used.

In this study, separate pushover analyses were carried out for force distributions; $s_n^* = m\phi_n$, where **m** is the mass matrix of the structure, for each significant mode, $\boldsymbol{\phi_n}$, of the bridge as was explained in section 2.3.3.

Also, a critical issue in MPA is the way that response quantities individually calculated for each mode are superimposed, in the sense that modal contributions should correspond to the same earthquake intensity. Most of the currently available procedures; (FEMA-356, 2000), (ATC-40, 1996), or (Eurocode 8, 2004), developed for SPA require that the pushover curve be idealized as a bilinear curve (Figure 2-4—left), so that a yield point and ductility factor can be defined and then be used to appropriately reduce the elastic response spectra representing the seismic action considered for assessment. Paraskeva et al. (2006) suggested doing this once using the full pushover curve.

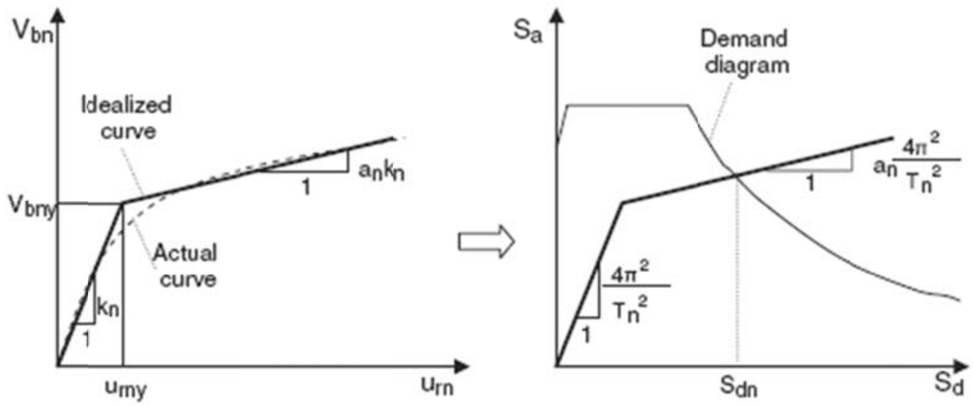

Figure 2-4 Idealized pushover curve of the *n*th mode of the MDOF system, and corresponding capacity curve for the *n*th mode of the equivalent inelastic SDOF system.

2.4.2.3 Demand Displacement

Several procedures are available [(Chopra & Goel, 2002), (FEMA-356, 2000), (ATC-40, 1996), (Eurocode, 2004)] for defining the earthquake displacement demand associated with each of the pushover curves derived from the modal pushover analysis. In this study the concept of capacity and demand spectra [(Sasaki et al., 1998), (ATC-40, 1996)] is used for defining the displacement demand for a given earthquake intensity. The difference is instead of reducing the elastic spectra with ductility-dependent damping factors, as applied in the standard capacity spectrum method adopted by (ATC-40, 1996), inelastic spectra is used for estimating the displacement demand at the monitoring point. This is equally simple, more consistent, and more accurate as shown in a number of studies; (Kappos & Petrains, 2001) and (Fajfar, 1999).

In this study, the formula proposed by Fajfar (1999), was used

$$S_a = \frac{S_{ae}}{R_\mu} \tag{2.40}$$

$$S_d = \frac{\mu}{R_\mu} S_{de} = \frac{\mu}{R_\mu} \frac{T^2}{4\pi^2} S_{ae} = \mu \frac{T^2}{4\pi^2} S_a \tag{2.41}$$

Where μ is the ductility factor defined as the ratio between the maximum displacement and the yield displacement, and R_μ is the reduction factor due to ductility, i.e. due to the hysteretic energy dissipation of ductile structures. Several proposals have been made for the reduction factor R_μ. In this study, the formula proposed by (Vidic, Fajfar, & Fischinger, 1994) was used. They provide reasonably accurate results, very simple and suited for the use in the capacity spectrum method format.

$$R_\mu = (\mu - 1)\frac{T}{T_o} + 1, \quad T \leq T_o \tag{2.42}$$

$$R_\mu = \mu\,, \quad T \geq T_o \tag{2.43}$$

$$T_o = 0.65\,\mu^{0.3} T_c \quad \leq T_c \tag{2.44}$$

T_c is the characteristic period of the ground motion. It is typically defined as the transition period where the constant acceleration segment of the response spectrum passes to the constant velocity segment of the spectrum.

Starting from the typical elastic design spectrum (as will be discussed in section 3.5.1), and using equations (2.40) – (2.44), the demand spectra for the constant ductility factors μ in the Acceleration-Displacement Response Spectrum (ADRS) format can be obtained.

This calculated displacement demand refers to SDOF system and should be correlated to those of the actual bridge. In order to convert the displacement demand of the *n*th mode inelastic SDOF system to the peak displacement of the monitoring point, equation 2.32b will be used. Then response quantities of interest corresponding to that displacement demand of the *n*th mode can be evaluated.

2.4.2.4 Number of modes considered

It is noted that in the case of bridges, the number of modes that have to be considered is significantly higher than in the case of buildings; where considered modes should contribute to 90% of the total mass (a criterion commonly used in seismic codes). In fact, in order to capture all modes whose masses contribute to at least 90% of the total mass of a complex bridge structure, it might need up to a few hundred modes. On the other hand, work carried out by Paraskeva et al. (2006) and results from current study for bridge no. 1 have shown that there is little merit in adding modes whose participation factor is very low (say less than 1%), and less rigid rules than the 90% one (calibrated only for buildings) could be adopted.

2.4.3 Step-by-step Extended MPA procedure for Bridges

1. Compute the natural periods, T_n and modes ϕ_n, for linearly elastic vibration of the structure.

2. Carry out separate pushover analyses for force distribution, $s_n^* = m\phi_n$, where m is the mass matrix of the structure, for each significant mode of the bridge, and construct the base shear vs displacement of the monitoring point (V_{bn}–u_{rn}) pushover curve for each mode. Gravity loads are applied before each MPA, and P-Δ effects are included, if significant (e.g. bridges with tall piers). It is noted that the value of the lateral deck displacement due to gravity loads, u_{rg}, is negligible for a bridge with nearly symmetrically distributed gravity loading.

3. The pushover curve must be idealized as a bilinear curve so that a yield point and ductility factor can be defined and then used to appropriately reduce the elastic response spectra representing the seismic action considered for assessment. This idealization can be done in a number of ways, some more involved than others; it is suggested to do this once as recommended by Paraskeva et al. (2006) (as opposed, for instance, to the (ATC-40, 1996) procedure) using the full pushover curve (i.e. analysis up to 'failure' of the structure, defined by a drop in peak strength of about 20%) and the equal energy absorption rule (equal areas under the actual and the bilinear curve). Remaining steps of the MPA procedure can be applied even if a different method for producing a bilinear curve is used.

4. Converting the idealized pushover curve ($V_{bn} - u_{cn}$) of the multi-degree-of-freedom (MDOF) system (calculated in Step 3) to a capacity diagram, as shown in Figure 2-4—right. The base shear forces and the corresponding displacements in each pushover curve are converted to spectral accelerations (S_a) and spectral displacements (S_d), respectively, of an equivalent single-degree-of-freedom (SDOF) system, using the relationships [Chopra and Goel (2002), ATC-40(1996)]:

$$S_a = \frac{V_{bn}}{M_n^*} \tag{2.45}$$

$$S_d = \frac{u_{cn}}{\Gamma_n \phi_{cn}} \tag{2.46}$$

Wherein ϕ_{cn} is the value of the mode shape ϕ_n at the reference (or monitoring) point, $M_n^* = L_n \cdot \Gamma_n$ is the effective modal mass, $L_n = \phi_n^T m \cdot 1$, $\Gamma_n = L_n / M_n$, and $M_n = \phi_n^T m \phi_n$ is the generalized mass, for the nth natural mode. For inelastic behavior, the procedure used here for estimating the displacement demand at the monitoring point is based on the use of inelastic spectra previously explained in section 2.4.2.3

5. Conversion of the displacement demand of the nth mode inelastic SDOF system to the peak displacement of the monitoring point, u_{cn} of the bridge, using Equation (2.46).

6. If the structure remains elastic or close to the yield point, the procedure suggested in section 2.4.2.3 is used to estimate seismic demands for the bridge. For cases that significant inelasticity develops in the structure, a correction is made to the displacement of the monitoring point of the bridge, which was calculated at the previous step, to estimate the modified control point displacement u'_{cn} . The response displacements of the structure are evaluated by extracting from the database of the individual pushover analyses the values of the desired responses at which the displacement at the control point is equal to u_{cn} (see equation 2.46). These displacements are then applied to derive a new vector ϕ_n', which is the deformed shape (affected by inelastic effects) of the bridge subjected to the given modal load pattern. The target displacement at the monitoring point for each pushover analysis is calculated again with the use of ϕ_n', according to:

$$u'_{cn} = \Gamma'_n \cdot \phi'_{cn} \cdot S_{dn} \tag{2.47}$$

Wherein S_{dn} is the displacement of the SDOF system and Γ'_n is Γ_n recalculated using ϕ'_n.

7. The response quantities of interest (displacements, plastic hinge rotations, forces in the piers) are evaluated by extracting from the database of the individual pushover analyses the values of the desired responses r_n, due to the combined

effects of gravity and lateral loads for the analysis step at which the displacement at the control point is equal to u'_{cn} (see equation 2.47).

8. Steps 3 to 7 are repeated for as many modes as required for sufficient accuracy.

9. The total value for any desired response quantity (and each level of earthquake intensity considered) can be determined by combining the peak 'modal' responses, r_{no} using an appropriate modal combination rule, e.g. the SRSS combination rule, or the CQC rule. This simple procedure was used for displacements, total base shear and plastic hinge rotations in the present study, which were the main quantities used for assessing the bridges analyzed (whose response to service gravity loading was, of course, elastic).

3. STRUCTURAL SYSTEMS AND GROUND MOTIONS

3.1 INTRODUCTION

This chapter is intended to provide a description of the bridges used as examples in the assessment of the proposed MPA method when applied to bridges. General descriptions for these bridges, including geometry and material in addition to the considered earthquake ground motion records will be presented. Considerations and assumptions needed to perform the analysis, if any, will be mentioned. Results of analysis will be presented in the next chapter.

A series of seven design examples was presented by the Federal HighWay Administration (FHWA) to illustrate the AASHTO requirements for seismic design of bridges. The study was performed by BERGER/ABAM Engineers, Inc. of Seattle, Washington and presented in FHWA manuals FHWA-SA-97-006 through 012. Two bridges of those examples were chosen to be analyzed in this study along with a third bridge model (based on the second example) in order to verify the proposed MPA procedure's accuracy.

The first bridge studied in this thesis is bridge number 5 of the FHWA examples mentioned above (FHWA, 1996-b). The second bridge is bridge number 4 of the FHWA examples (FHWA, 1996-a). The third one is the same as the second bridge with some geometry modifications. All three bridges models were analyzed using both the MPA and the nonlinear time history analysis, NL-THA, methods. Detailed description of these bridges will be presented in the following sections.

The finite element program SAP2000 advanced version 14 (CSI, 2009) was implemented to perform analyses. SAP2000 has the capability of performing nonlinear time history analysis as well as nonlinear static analysis. The capability of the program was used to plot the capacity (pushover curve) in the case of the MPA procedure while target displacement were calculated manually using the procedure steps presented in the previous chapter.

3.2 BRIDGE NO. 1 (9-SPAN BRIDGE)

This bridge is example No. 5 of the FHWA series (FHWA, 1996-b). The bridge has nine continuous spans totaling 1488 feet and consisting of two units:

- Unit 1: a four-span tangent unit
- Unit 2: a five-span curved unit with a radius of curvature equals 1300 feet.

The superstructure is composed of four steel plate girders with a composite cast-in-place concrete deck. The structural elements, seat type elements, and single column intermediate piers are all cast-in-place concrete supported on steel H-piles. All structure elements are oriented normal to the centerline of the bridge. Figure 3-1 through Figure 3-4 provide details about bridge configuration.

In the longitudinal direction, the pinned intermediate pier columns (Pier numbers 1, 2, and 3 in Unit 1, and pier numbers 6 and 7 in Unit 2) are assumed to resist the entire longitudinal seismic force. The seat type abutments and the expansion joint at pier No. 4 will accommodate significant motion in the longitudinal direction and provide restraint in the transverse direction. The two units of the bridge are assumed to act independently for longitudinal motion. This behavior is illustrated in Figure 3-5.

In the transverse direction, the structure is assumed to act as a two-rigid link system pivoting at the abutments with maximum transverse displacement at pier No. 4. All of the intermediate piers and abutments are assumed to participate in resisting the transverse seismic force. This behavior is illustrated in Figure 3-6. The intermediate pier foundations were modeled with equivalent linear spring stiffnesses for the pile group.

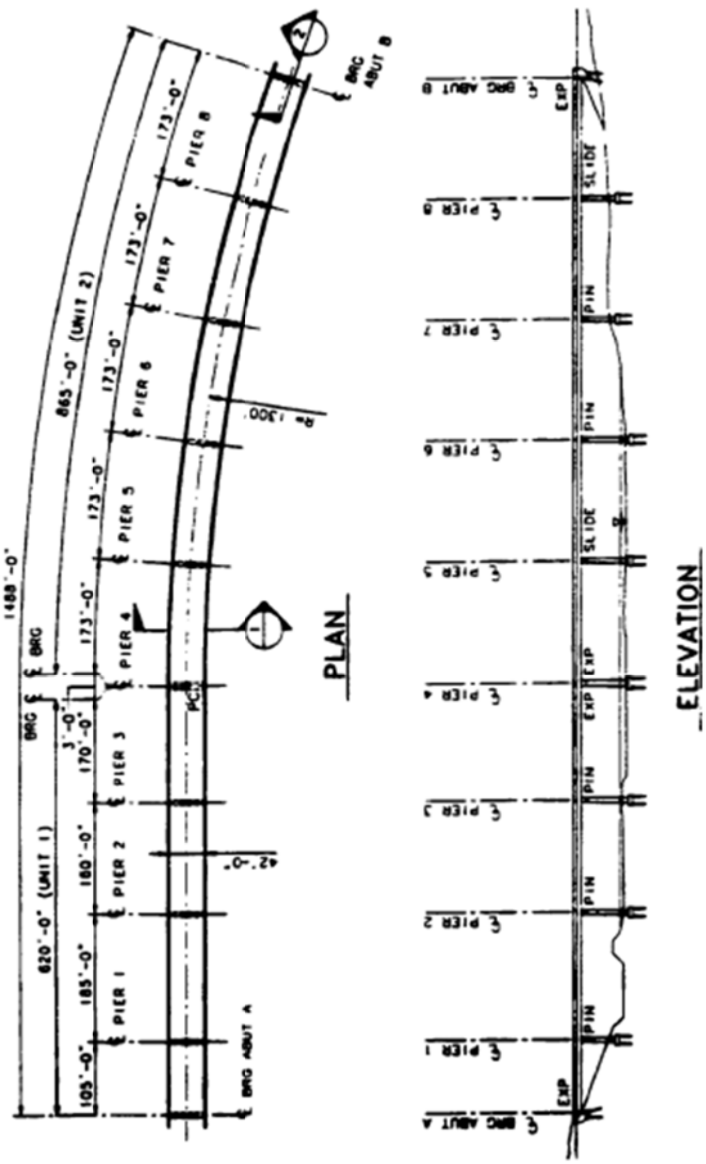

Figure 3-1 Bridge No. 1 – Plan and Elevation

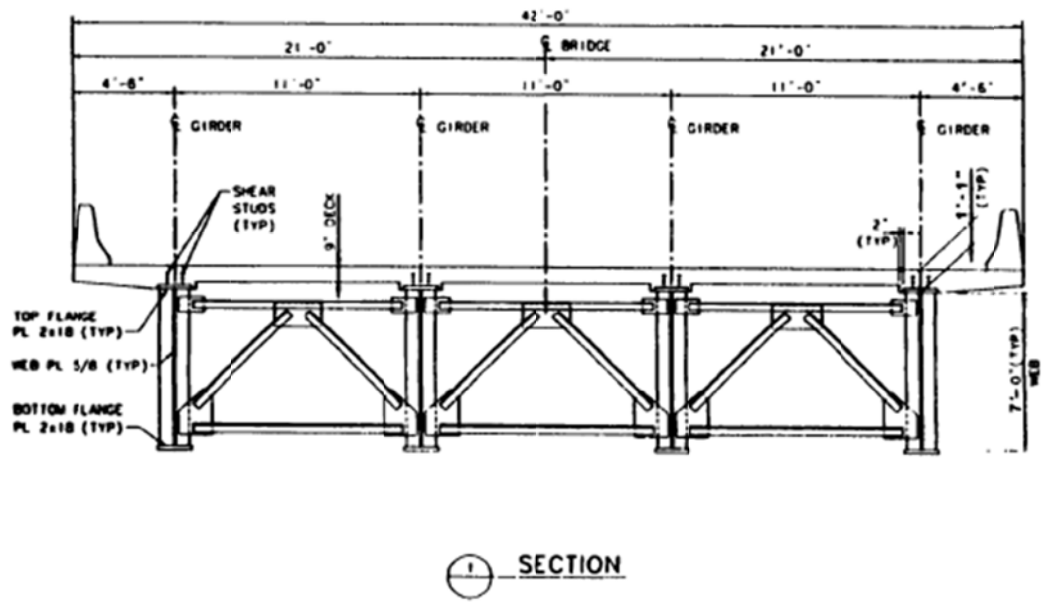

Figure 3-2 Bridge No. 1 – Typical Cross Section

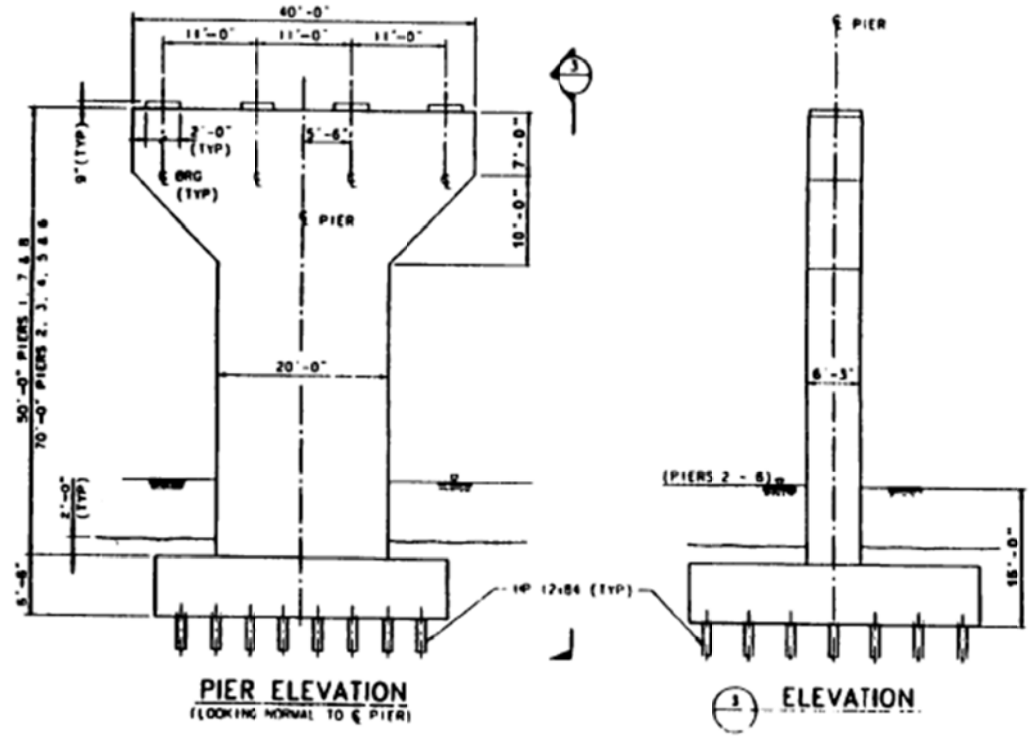

Figure 3-3 Bridge No. 1 – Intermediate Pier Elevations

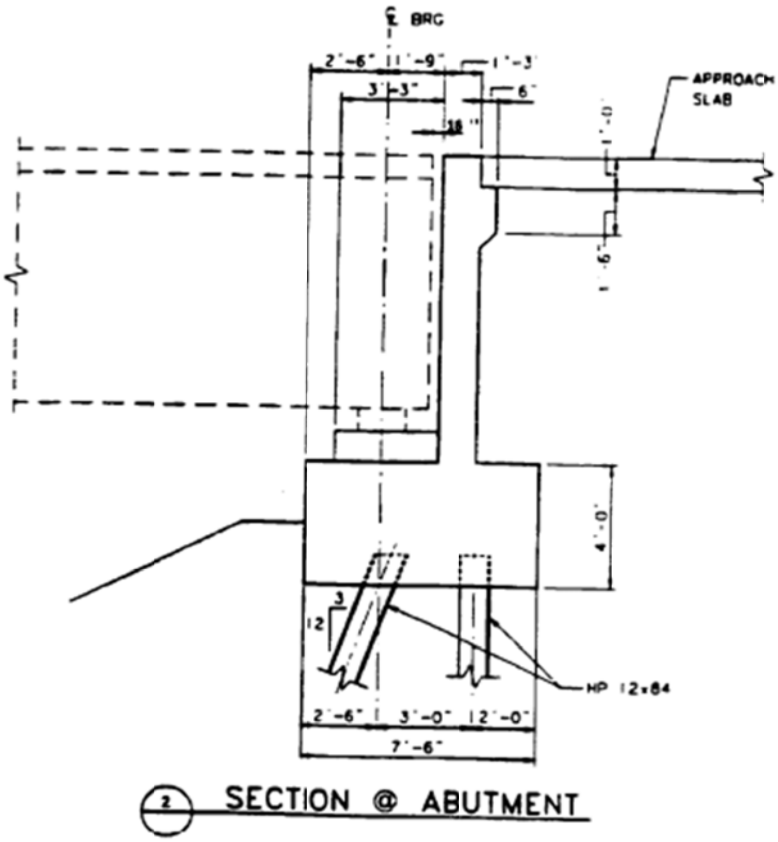

Figure 3-4 Bridge No. 1 – Seat-Type Abutment

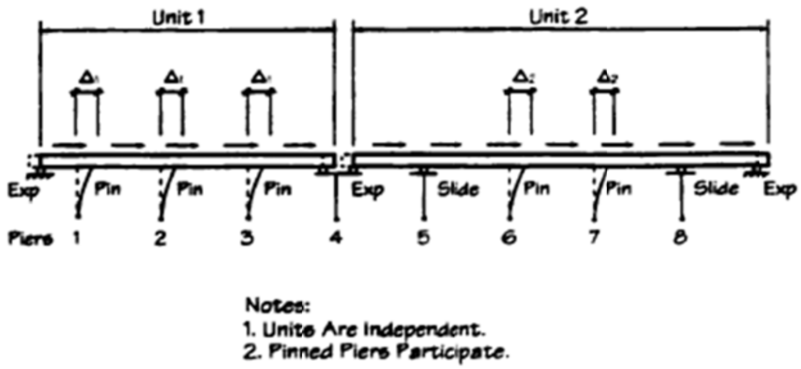

Figure 3-5 Bridge No. 1 – Longitudinal Seismic Behavior

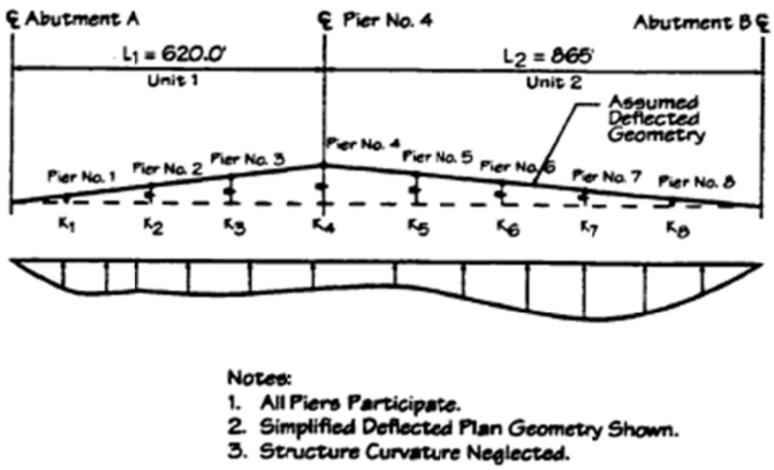

Figure 3-6 Bridge No. 1 – Transverse Seismic Behavior

3.2.1 Finite element model

The structural analysis program SAP2000 advanced version 14.0 (CSI, 2009) was used to perform analyses. As shown in Figure 3-7, the model includes a single line of three-dimensional frame elements for the superstructure and each of the intermediate piers.

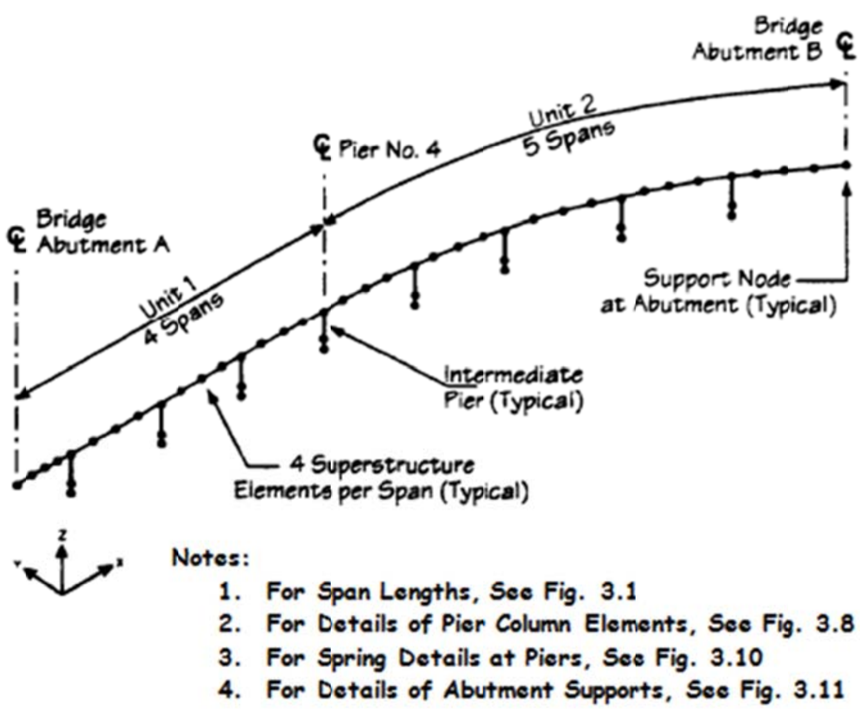

Figure 3-7 Bridge No. 1 – Finite Element Model of Bridge

3.2.1.1 Superstructure

The superstructure has been modeled with four elements per span. The nodes and work lines of the elements are located along the center of gravity of the superstructure. The density has been adjusted to include additional dead loads from traffic barriers, wearing surface overlay, and stay-in-place metal forms. The total weight of these additional dead loads is 2.4 kips per linear foot of superstructure.

The centroid of the superstructure has been located eight feet above the top of the pier to account for the height of the bearings and leveling pedestal. The connection of the superstructure to the pier is made in a SAP2000 model with the rigid link elements shown in Figure 3-8 as the top elements of the piers. Properties of the superstructure and its elements are shown below.

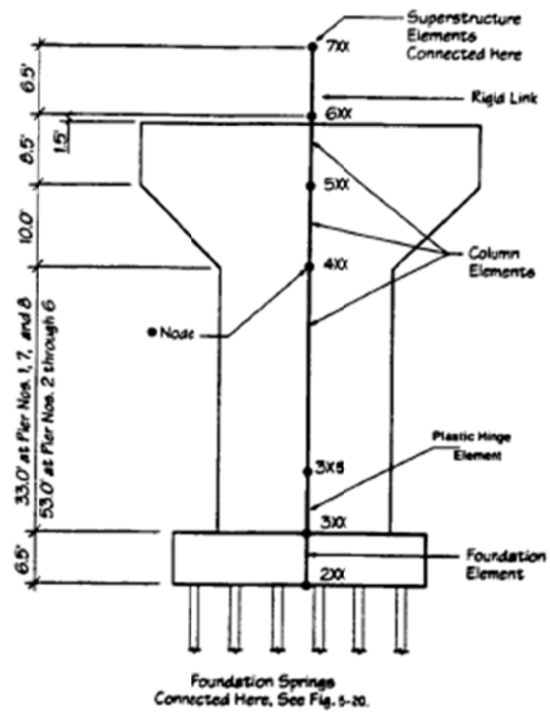

Figure 3-8 Bridge No. 1 – Details of Pier Column Elements

The superstructure area and moments of inertia include the concrete deck, the girder webs, and both flanges with steel transformed to concrete using a modular ratio, n=8.

$L = 1488$ ft	Overall length of bridge.
$L_1 = 620$ ft	Length of Unit 1.
$L_2 = 865$ ft	Length of Unit 2.
$A_d = 60\ ft^2$	Cross section area of superstructure and deck. (Steel transformed to concrete with n=8)
$I_{zd} = 518\ ft^4$	Moment of inertia of superstructure about a horizontal axis. (Steel transformed to concrete with n=8)
$I_{yd} = 9003\ ft^4$	Moment of inertia of superstructure about a vertical axis. (Steel transformed to concrete with n=8)
$f_c^{'} = 4000$ psi	Compressive strength of concrete.
$E_c = 3600$ ksi	Young's modulus of concrete.
$J = 5.906\ ft^4$	Torsional constant of superstructure.

The torsional constant of the superstructure is calculated using only the deck. The contribution to torsional resistance offered by warping of the steel sections has been ignored since it is too small.

3.2.1.2 Substructure

The intermediate piers are modeled with three-dimensional frame elements that represent the individual columns. Figure 3-8 shows the relationship between the actual pier and the stick model of the three-dimensional frame elements. Four elements were used for the column between the top of the footing (node 3xx) and the bearing (node 6xx). The first element from the bottom is the plastic hinge element which represents the inelastic behavior of the column. . Length of the plastic hinge was calculated using the following formula, (Priestly, Seible, & Calvi, 1996):

$$L_p = 0.08L + 0.15 f_{ye} d_{bl} \geq 0.3 f_{ye} d_{bl} \tag{3.1}$$

Where:

d_{bl} is the diameter of the longitudinal reinforcement (ft).

f_{ye} is the effective yield strength of steel reinforcement (ksi).

L is the distance from the critical section of the plastic hinge to the point of contra-flexure (ft).

In this example, L = the clear height of the column since the column base is pinned. The second element is the actual column element. The third element represents the varying section between the column section and the column head, which is modeled by the fourth element. The moments of the inertia for the column and the plastic hinge elements are based on a cracked section calculated using the moment-curvature and moment-rotation curves as will be discussed in Appendix A. Foundation springs are connected to the node (2xx) at the base of the pile cap. There are no elements to model the abutments, only support nodes as shown in Figure 3-7.

In the actual structure, internal forces are transferred between the superstructure and the pier through the bearings. In the seismic model, the superstructure forces are transferred at the single point where the superstructure and pier intersect. At pinned piers, node (6xx) in Figure 3-8 transfers shears from the superstructure in all directions, and is released for moment in the longitudinal direction. At Piers Nos. 4, 5, and 8 which are free to move longitudinally, only transverse shears are transferred.

Figure 3-9 shows modeling details for the connection at the top of Pier No. 4, which is the location of the expansion joint between Unit 1 and Unit 2.

If the ends of the adjacent superstructure elements are connected directly to node (741) and these element ends are released for longitudinal translation and rotation, the node (741) is still attached to the top of the rigid link and will receive the tributary mass from each end of the attached superstructure. This will result in longitudinal shears being transmitted to Pier No. 4 though the super structure is free to move longitudinally there and should transfer no shear.

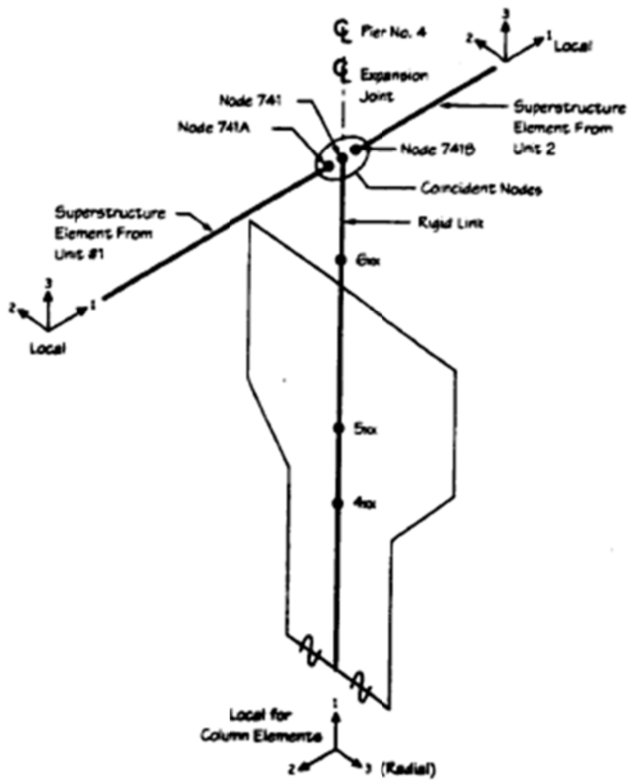

Figure 3-9 Bridge No. 1 – Details at Pier No. 4 Expansion Joint

To model the behavior of the expansion joint correctly, three coincident nodes are defined at the top of the rigid link. The two additional nodes (741A and 741B) are used to define connectivity, which will result in correct forces for Pier No. 4. The end of the superstructure element from Unit 1 is connected to one of the nodes (741A), the end of the superstructure element from Unit 2 is connected to another node (741B), and the third node (741) is connected to the top of the rigid link of the pier column elements. Local coordinate systems and release constraints of each of the three nodes are defined. This prevents the column top node (741) from picking up lumped mass from the adjacent superstructure elements in the longitudinal direction, for which the superstructure is free to move. The three coincident elements are given the same displacements in the transverse direction.

Piers Nos. 5 and 8 have sliding bearings to allow unrestrained longitudinal motion. Translational and rotational releases are provided at the top end of the rigid link element. The direction for the releases is in the local column coordinate system, and so is oriented tangential to the point of curvature at the center of the pier.

At the sliding piers and the expansion locations, several types of bearings could be used to accommodate the expected displacements. Elastomeric bearings with provision for sliding between the bearing and the girder under large displacements would work. The transverse restraint would be provided by girder stops to transfer transverse seismic forces to Piers Nos. 4, 5, and 8 and the abutments.

Foundation Stiffness

The intermediate pier foundations were modeled with equivalent spring stiffnesses for the pile group. Details of the spring supports are shown in Figure 3-10. For this bridge, all the intermediate piers use the same foundation springs. The spring stiffnesses are developed for the local pier support coordinate geometry and are input into SAP2000 model with the same orientation as the local pier columns. The local axes for the spring support nodes are identified differently in Figure 3-10 from the local axis of the column elements. The pier foundation stiffnesses used in the model for producing final design forces are the stiffnesses of the pile group only without any stiffness contribution from the soil below the pile cap or contribution of flexibility of the cap itself. The cap was assumed to be rigid. Values of the stiffnesses for foundation springs provided by (FHWA, 1996-b) are used in this study.

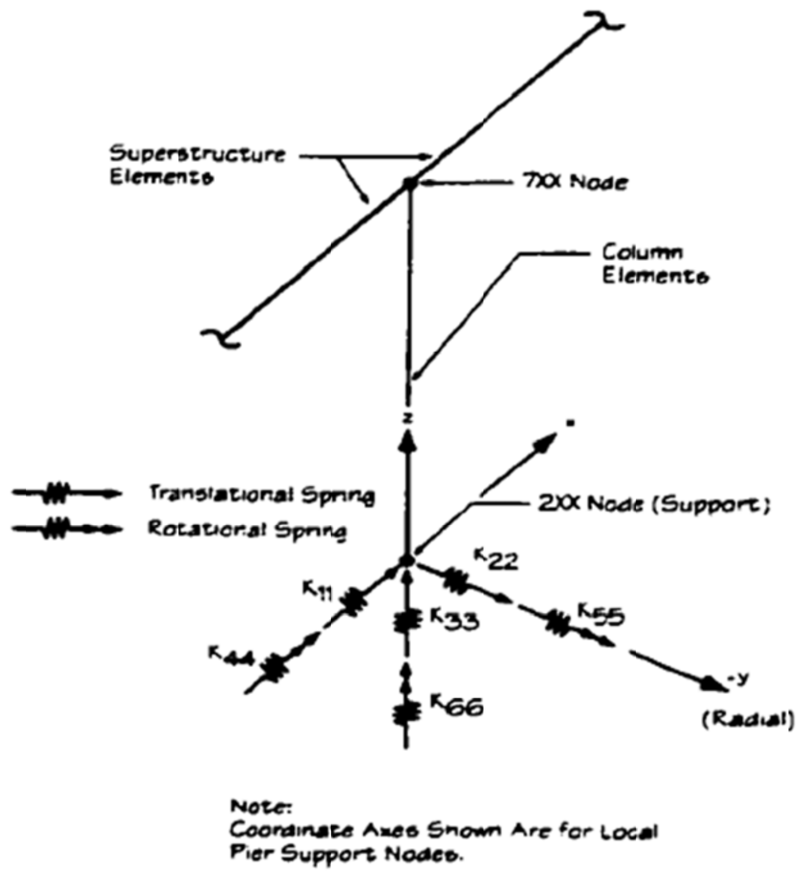

Figure 3-10 Bridge No. 1 – Details of Supports for Spring Foundation Model

The abutments have been modeled with a combination of full restraints (vertical translation and superstructure torsional rotation) and an equivalent spring stiffness (transverse translation), as shown in Figure 3-11. Other degrees of freedom are released.

SAP2000 allows for springs and releases relative to the local coordinate geometry; the longitudinal direction at the abutment nodes is oriented along the axis of the superstructure element connected at that node. The transverse direction is perpendicular to the longitudinal direction in the global x-y plane. The abutment restraints and transverse spring act at these nodes, which are oriented in the local node's coordinate geometry. The gap between the superstructure and the abutment was set at 18″ as shown in Figure 3-4 so the superstructure will not get in contact with the abutment during the longitudinal movement.

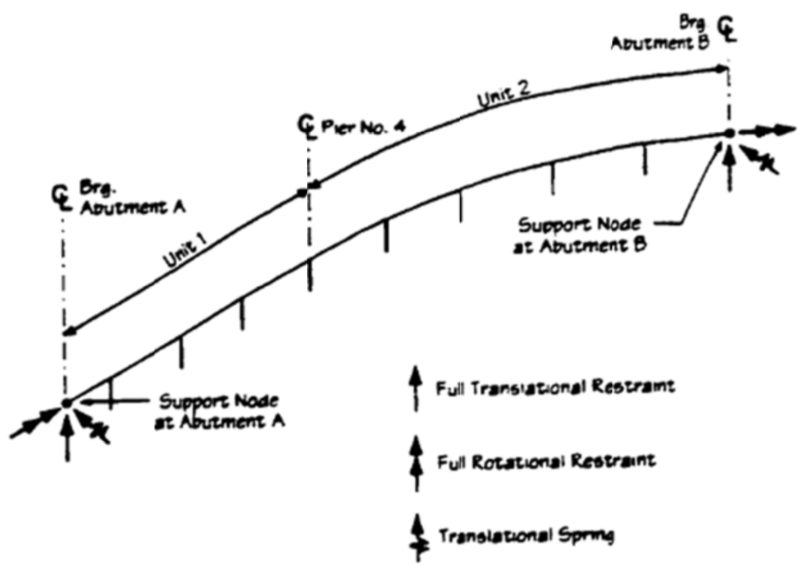

Figure 3-11 Bridge No. 1 – Details of Abutment Supports

Moment-Curvature of Columns

In this study, moment-curvature was used to estimate moment of inertia for columns in order to have accurate results, especially for stiffness of the springs that represent the plastic hinges. The moment of inertia was calculated using a cracked section. Figure 3-12 shows a cross section in the Pier Column.

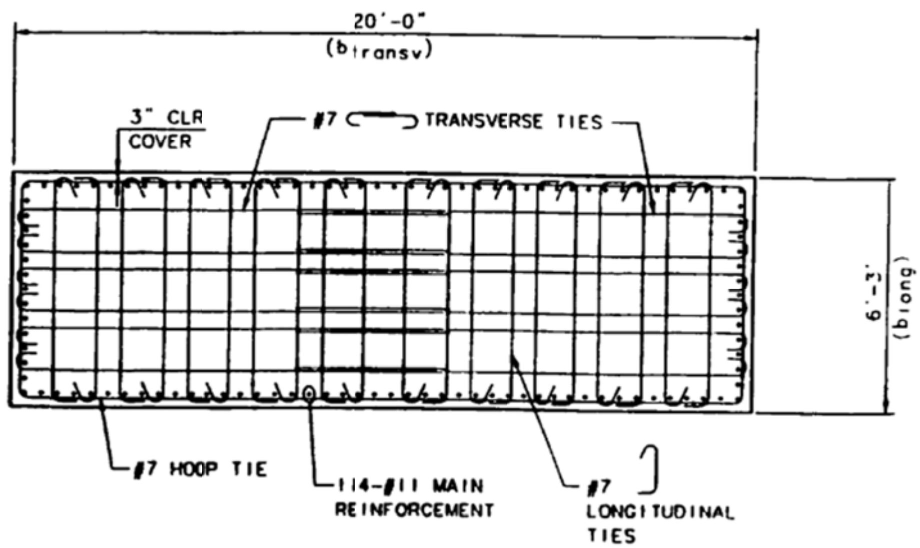

Figure 3-12 Bridge No. 1 – Cross Section in the Column

The yield curvature can be approximated as (Priestly et. al. (1996))

$$\phi_y = \frac{M_n}{E_c I_e} \tag{3.2}$$

Where:

ϕ_y is the curvature at yield estimated by using a bilinear curve to represent the M-ϕ curve

M_n is the nominal moment corresponding to ϕ_y

E_c is the concrete modulus of elasticity I_e is the effective moment of inertia

Using this equation, I_e can be calculated directly from the M-ϕ curve. Also, from the M-ϕ curve, the moment rotation (M-θ) curve can be developed. The moment-rotation curve is generated in order to estimate the flexural stiffness of the nonlinear springs used to represent the plastic hinges.

Calculations for different values needed to define the plastic hinge properties for the pushover analysis as well as springs stiffnesses for the time history analysis will be presented in Appendix A.

3.3 BRIDGE NO. 2 (3-SPAN BRIDGE)

As previously mentioned, this bridge is one of the FHWA examples series (FHWA, 1996-a). It consists of three spans. The total length is 320 feet with span lengths of 100, 120, and 100 feet, respectively. All substructure elements are oriented at a 30-degree skew from a line perpendicular to a straight bridge centerline alignment. Figure 3-13 shows a plan and elevation of the bridge. The superstructure is a cast-in-place concrete box girder with two interior webs. The intermediate bents have a crossbeam integral with the box girder and two round columns that are pinned at the top of spread footing foundations. Figure 3-14 shows a cross section through the bridge with an elevation of an intermediate bent. The seat type abutments are on spread footings, as shown in Figure 3-15, and the intermediate bents are all cast-in-place concrete. Framing of the box girder superstructure is shown in Figure 3-16.

In the longitudinal direction, the intermediate bent columns are assumed to resist the entire longitudinal seismic force. The seat type abutments (Figure 3-15) will allow free longitudinal movement of the superstructure and will not provide longitudinal restraint.

In the transverse direction, the superstructure is assumed to act as a simply supported beam spanning laterally between abutments with the maximum transverse displacement at the center of the middle span. The intermediate bents are assumed to participate in resisting the transverse seismic force along with the superstructure. A shear key provides transverse restraint to enable transfer of transverse seismic forces to the abutment.

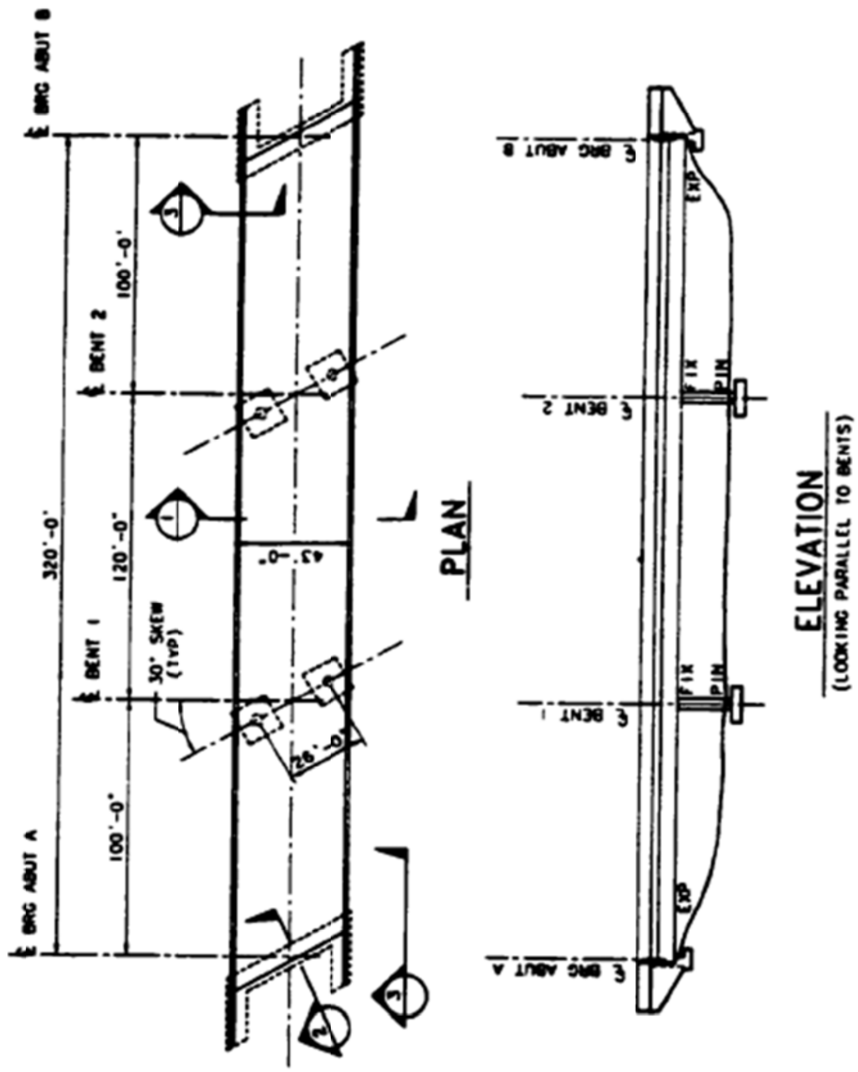

Figure 3-13 Bridge No. 2 – Plan and Elevation

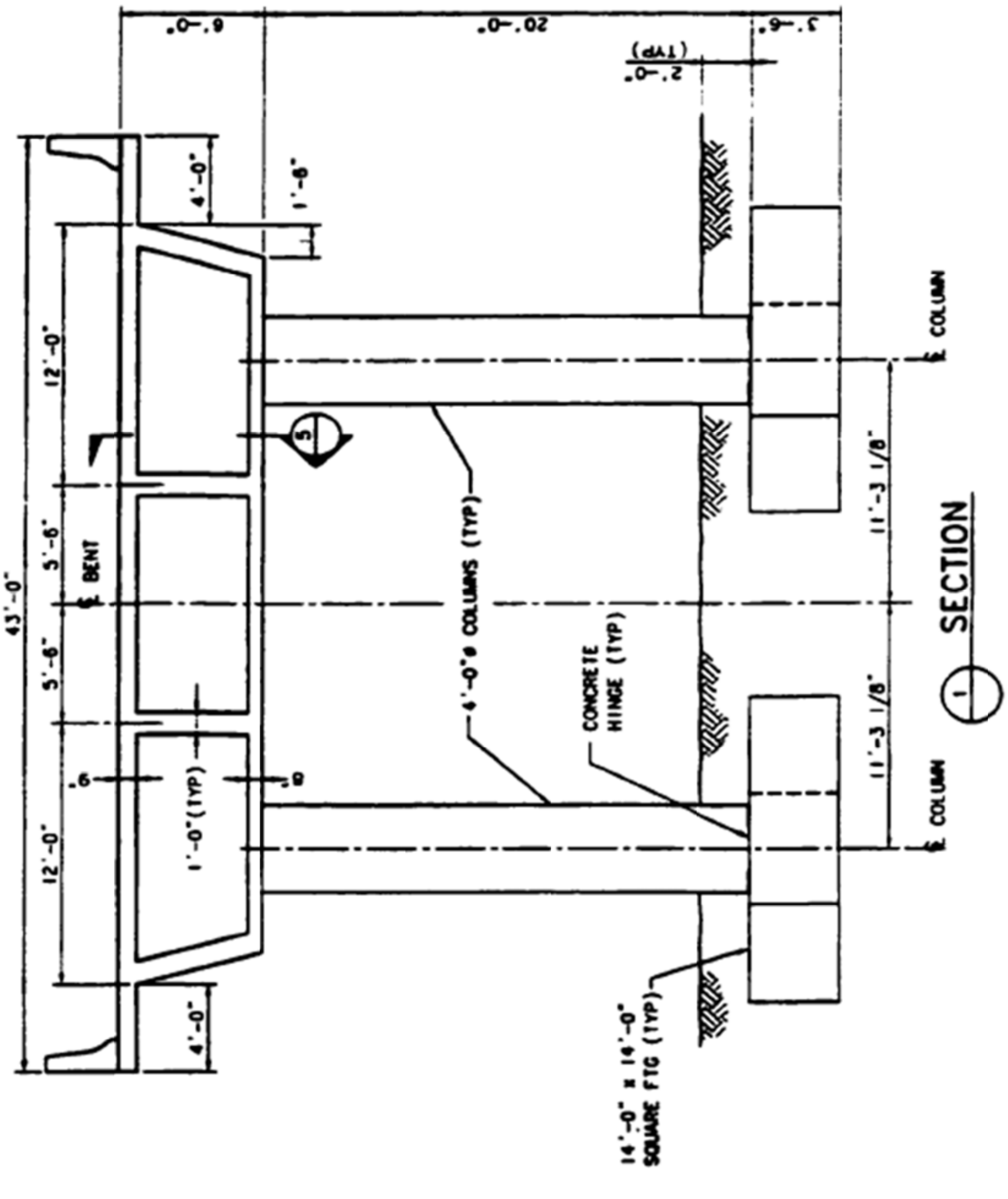

Figure 3-14 Bridge No. 2 – Typical Cross Section

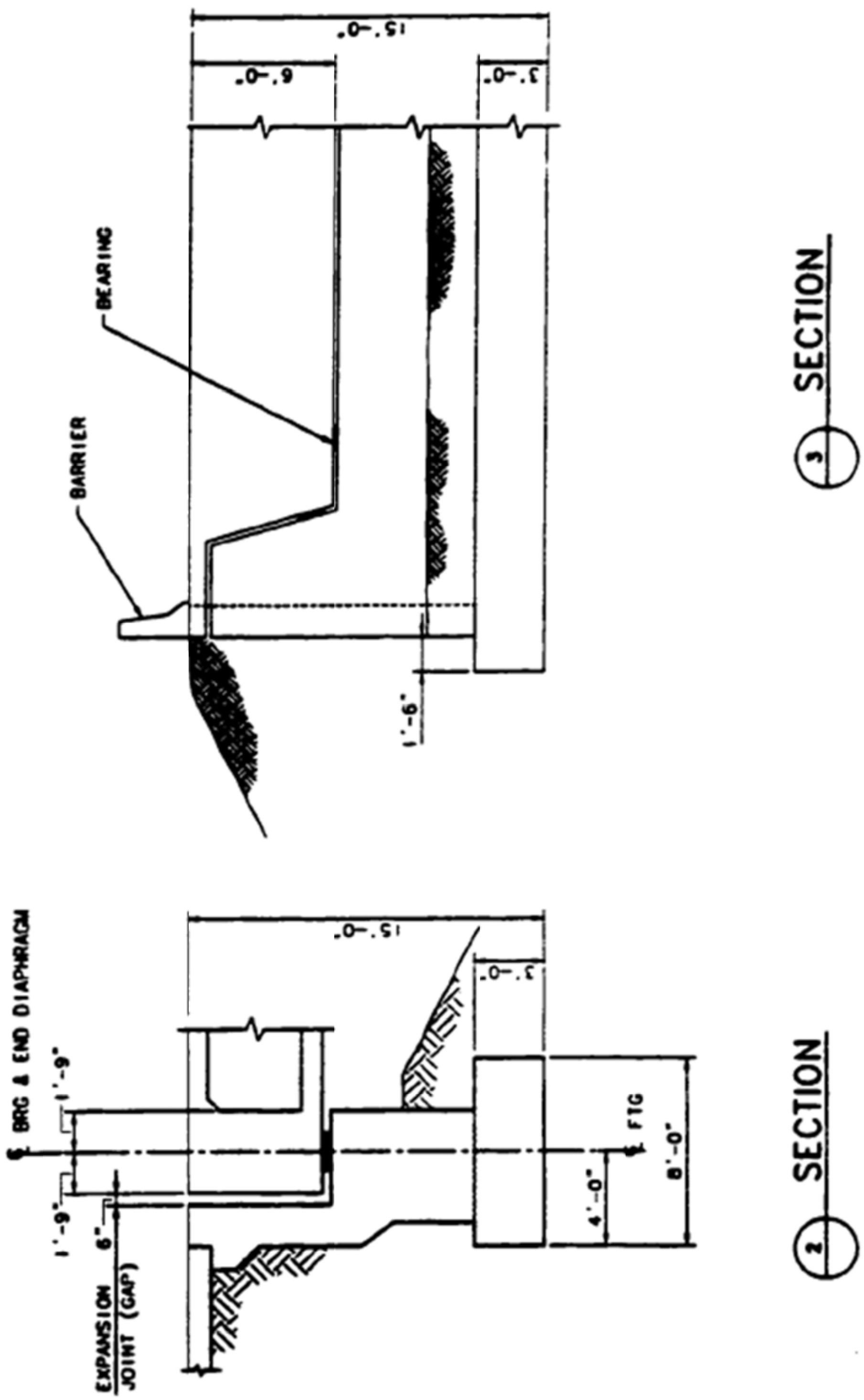

Figure 3-15 Bridge No. 2 – Seat Type Abutment

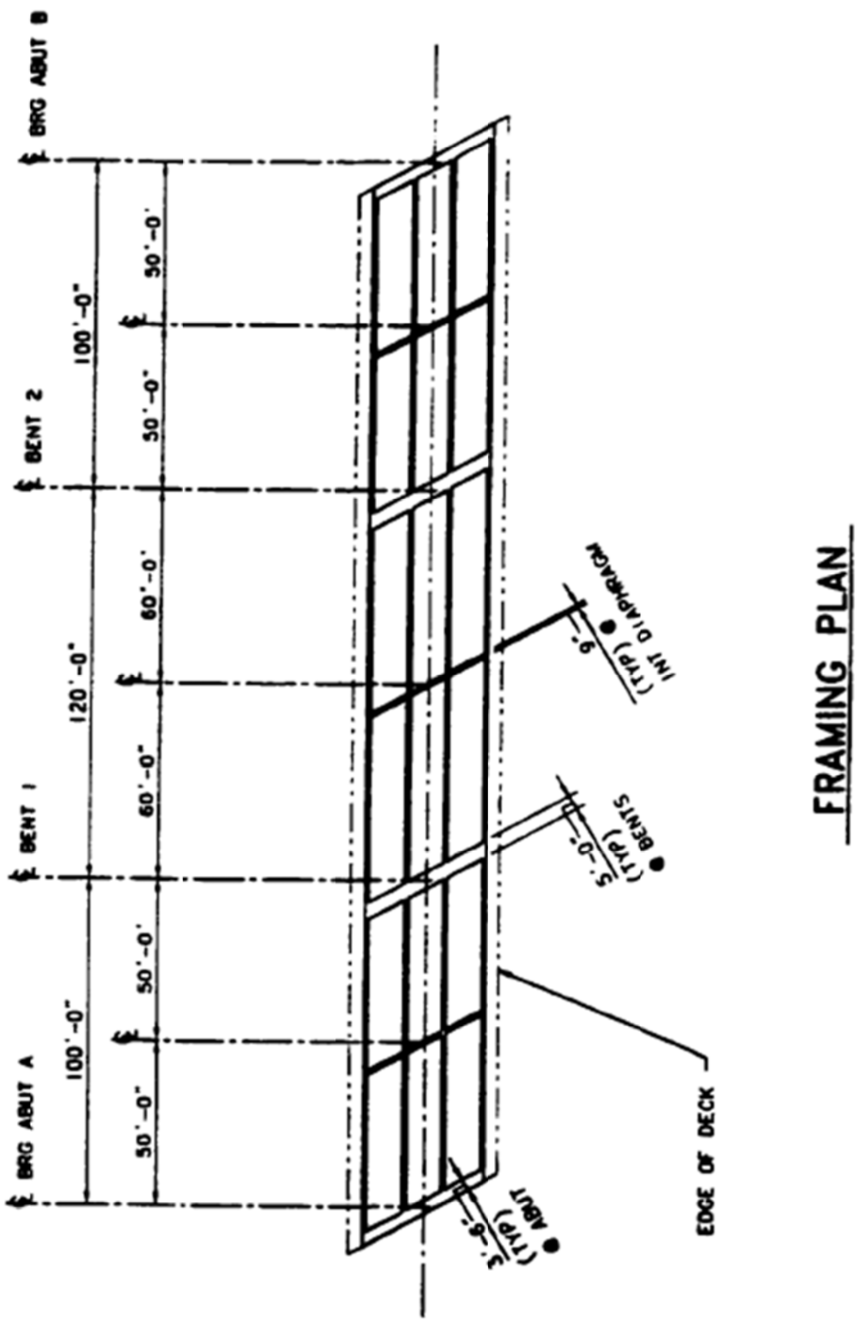

Figure 3-16 Bridge No. 2 – Box Girder Framing Plan

3.3.1 Finite Element Model

The structural analysis program SAP2000 version 14 was used to perform the analyses. As shown in Figure 3-17, the model includes a single line of three dimensional frame elements for the superstructure and individual element for the cap beam and columns of the intermediate bents.

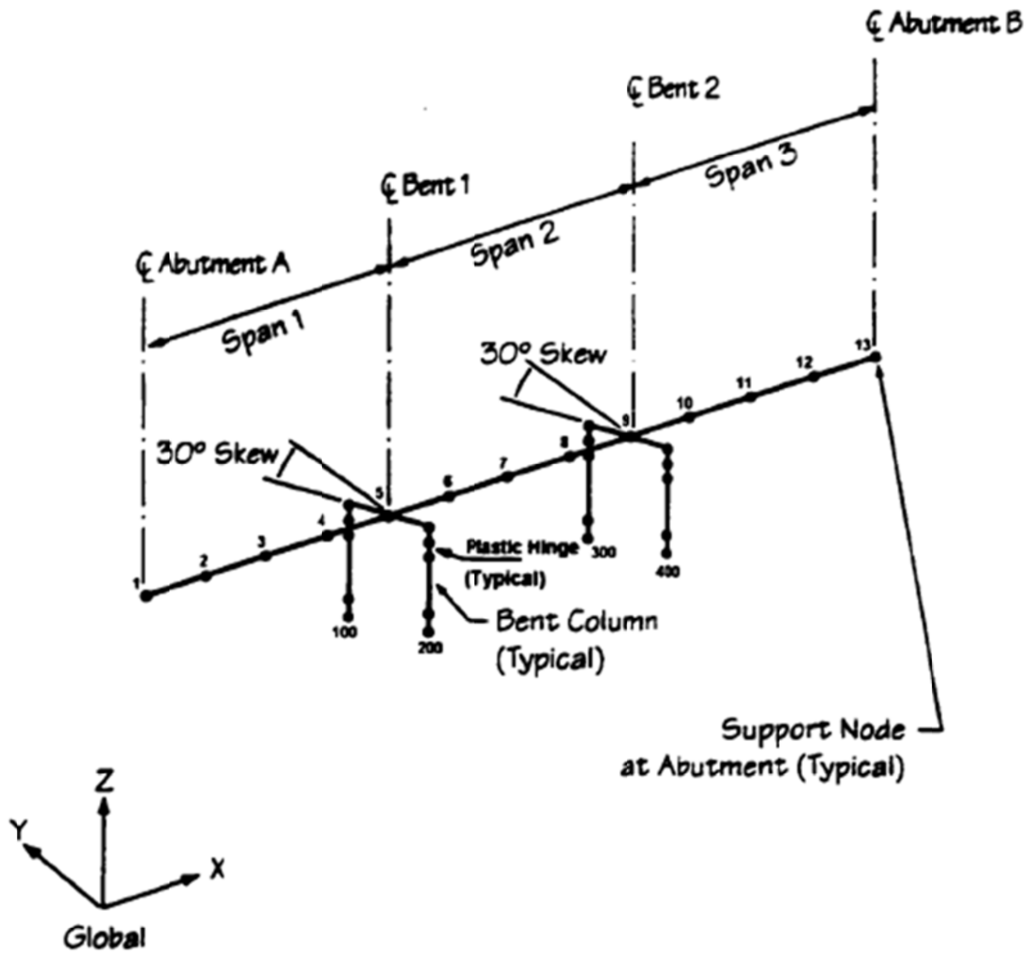

Figure 3-17 Bridge No. 2 – Finite Element Model

3.3.1.1 Superstructure

The superstructure has been modeled with four elements per span and the work lines of the elements are located along the centroid of the superstructure. The total mass of the structure was lumped to the nodes of the superstructure (nodes 1-13 in Figure 3-17). An additional load of 2.35 kips per linear foot of superstructure was considered to represent loads from traffic barriers and wearing surface overlay. The weight of the mid-span diaphragms was lumped to the nodes of the mid-spans. Weight of the cap beams and half weight of the bents were lumped to nodes of the superstructure corresponding to bents (nodes 5 and 9 in Figure 3-17) since weight of the bent columns is not significant. The properties of the structure used in the seismic model (both superstructure and substructure) are shown in table 3-1. Determination of the moment of inertia and torsional stiffness of the superstructure are based on uncracked cross sectional properties because the superstructure is expected to respond linearly to seismic loadings. The presence of skew is accounted for only in the orientation of the substructure elements, and is not considered in determination of the superstructure properties.

Table 3-1 Bridge No. 2 – Section Properties for the Bridge Model

Element Properties	CIP Box Superstructure	Bent Cap Beam	Bent Column
Area (ft^2)	72.74	27.00	12.57
I_x – Torsion (ft^4)	1177	100000 (1)	25.13
I_y – (ft^4)	401	100000 (2)	9.00
I_{z-} (ft^4)	9697	100000 (3)	9.00

Notes:

1. This value has been increased for force distribution to bent columns. Actual value is $I_x = 139\ ft^4$
2. This value has been increased for force distribution to bent columns. Actual value is $I_y = 90\ ft^4$
3. This value has been increased for force distribution to bent columns. Actual value is $I_z = 63\ ft^4$

3.3.1.2 Substructure

The bents and abutments are skewed 30 degrees from the center line of the superstructure. Since the bent columns are circular, which gives the same properties at any angle; properties of the bent columns were input in the global coordinates in order to have compatible results for the MPA and the nonlinear time history analysis without recourse to transform from local coordinates to global coordinate.

There are no elements to model the abutments; only support nodes are shown in Figure 3-17. The bents are modeled with three-dimensional frame elements that represent the cap beams and individual columns. Figure 3-18 shows the relationship between the actual bent and the stick model. Since columns are pinned to the column bases, two elements were used to model each column between the top of footing and the soffit of the box girder superstructure; the upper element represents the plastic hinge while the lower one represents the rest of column. A rigid link was used to model the connection between

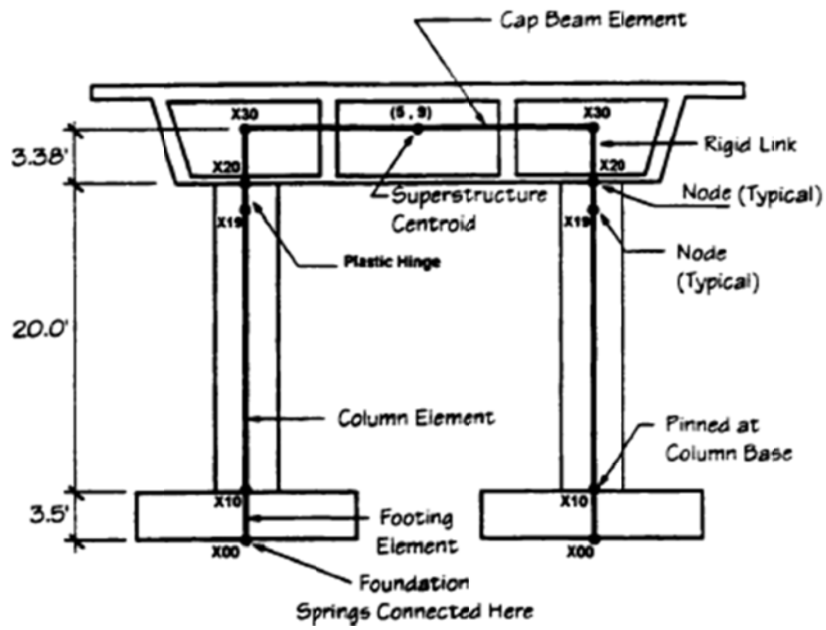

Figure 3-18 Bridge No. 2 – Details of Bent Elements

The column top and the center of gravity for the cap beam. Foundations are represented by a three-dimensional element with the same properties of the footing which approximates a rigid link due to its high stiffness. The node at the top of the footing (X10) is released for rotation in both plan direction to model the pinned column base. Stiff elements (with increased stiffness properties as shown in Table 3-1) were used to model the cap beams for distribution of loads between the columns without having deformation to cap beams in order to match the behavior of the superstructure.

Foundation springs are connected to the node (X00) at the base of the footing, Figure 3-19. The moments of inertia for columns were calculated based on the cracked section using M-ϕ curve. (Refer to Appendix A)

Foundation Stiffness

The intermediate bent foundations were modeled with equivalent spring stiffnesses for the spread footing. Details of the spring supports are shown in Figure 3-19. For this bridge, all of the intermediate bent footings use the same foundation springs.

The stiffnesses are developed for the local bent supports and transformed to global support when input to SAP2000 program so as to have compatible results for the MPA analysis and the nonlinear time history analysis. Values of stiffnesses for foundation springs provided by (FHWA, 1996-a) are used in this study.

The abutments have been modeled with a combination of full restraints (vertical translation and superstructure torsional rotation) and an equivalent spring stiffness (transverse translation), as shown in Figure 3-19. Other degrees of freedom are all released.

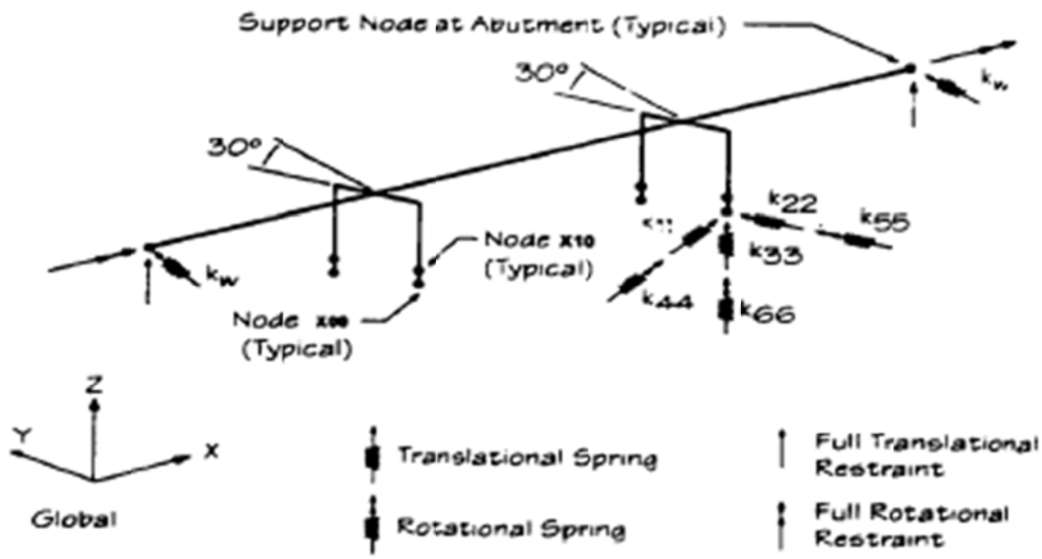

Figure 3-19 Bridge No. 2 – Details of Spring Supports

Moment-Curvature for Bent Columns

The moment of inertia for bent columns was calculated using cracked section. Moment-curvature curve was used to estimate moment of inertia for bent columns. Calculations for different values needed to define the plastic hinge properties for the pushover analysis as well as springs stiffnesses for the time history analysis will be presented in Appendix A.

3.4 BRIDGE NO. 3 (3-SPAN BRIDGE – NO SKEW)

Bridge no. 3, as shown in Figure 3-20, is the same as bridge no. 2 with only one modification. This modification was related to the skew angle. In bridge no. 3, the skew angle was set to zero in order to assess the effect of skew on the dynamic behavior of this bridge. This modification does not affect modeling of the superstructure since the superstructure is represented by a single line of three dimensional frame elements. The substructure is represented by individual elements for the cap beam and columns of the intermediate bents. Properties of bridge no. 2 (listed in Table 3-1) are still valid for bridge no. 3.

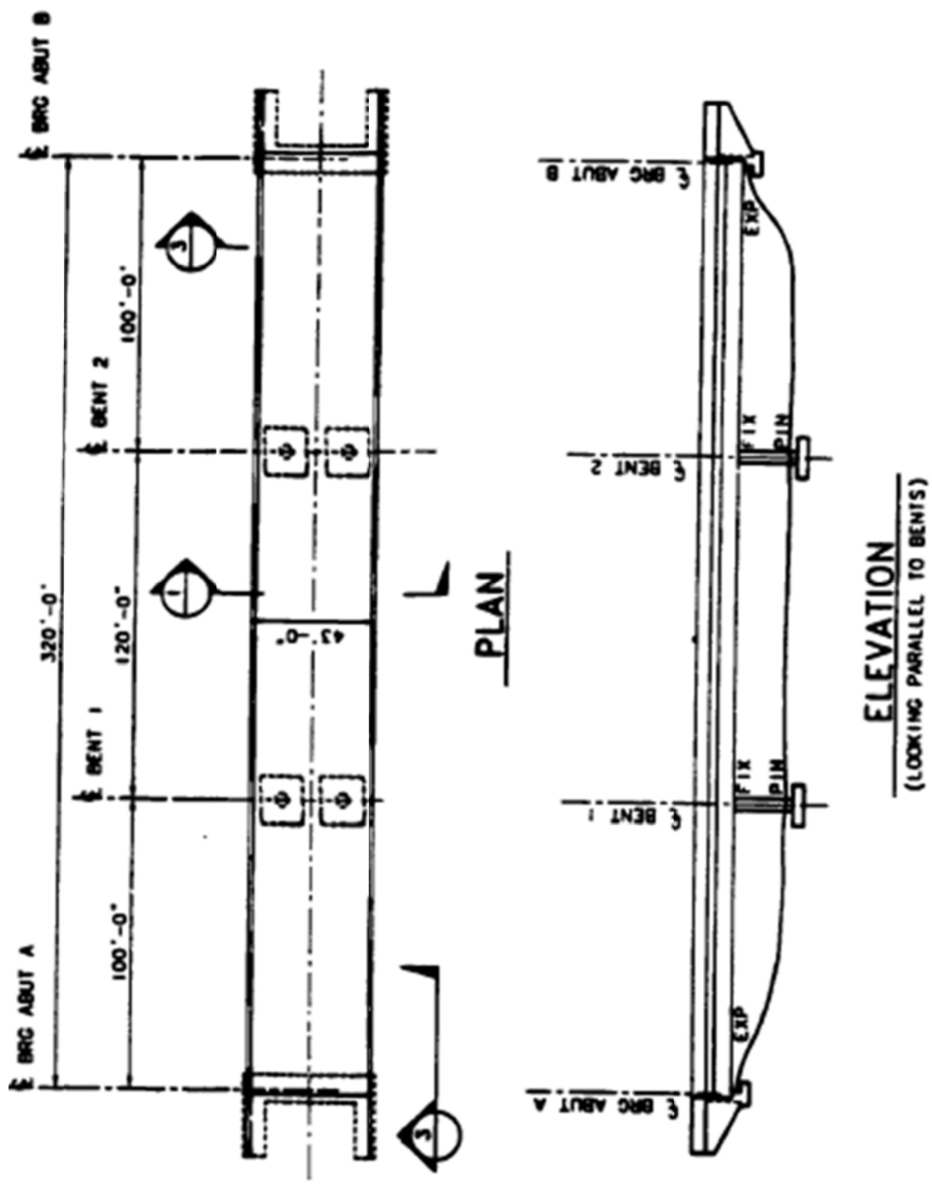

Figure 3-20 Bridge No. 3 – Plan and Elevation

3.5 SEISMIC LOADING

In the previous sections, the modeling of the bridges used as examples in this study was discussed. After modeling the bridges, we need to apply load. In this section, the seismic loading applied to each bridge will be discussed.

In order to perform the MPA, design response spectrum as shown in Figure 3-21 will be needed. The new AASHTO guide specifications for LRFD seismic bridge design (AASHTO, 2009) implements hazard maps to estimate parameters used to develop design response spectrum. National ground-motion maps are based on probabilistic national ground motion mapping conducted by the U.S. Geological Survey (USGS) having a seven percent chance of exceedence in 75yr. Values for Peak Ground Acceleration (*PGA*), response spectrum ordinate for short period (S_s), and response spectrum ordinate for long period (S_1) can be obtained from either the hazard maps in these guide specifications or the USGS seismic parameters program accompanying these guide specification. In this study, the USGS seismic parameters program was used in order to generate the design response spectrum for different bridge models.

Figure 3-22 shows the program input screen used to specify seismic parameters. For any site location, we start by specifying the location by either using the longitude and latitude of site location or the zip code of the site. The program will then calculate the map parameters (PGA, S_s, and S_1) which will be used to calculate the design parameters

(A_s, SD_s, and SD_1). Once all these parameters are calculated, then the program can generate the design response spectrum for that site location as shown in Figure 3-23 .

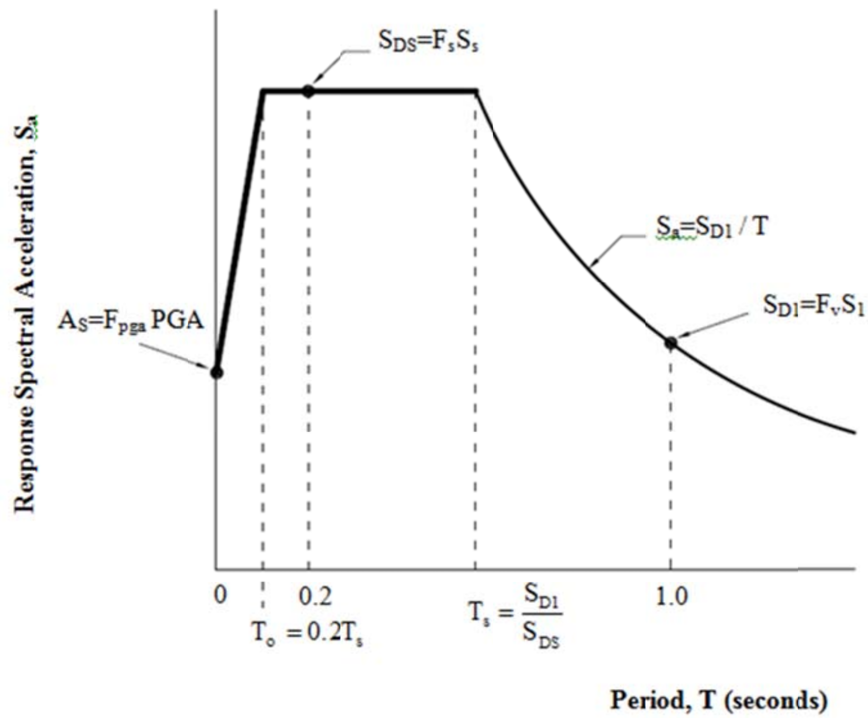

Figure 3-21 Design Response Spectrum, Construction Using Three-Point Method

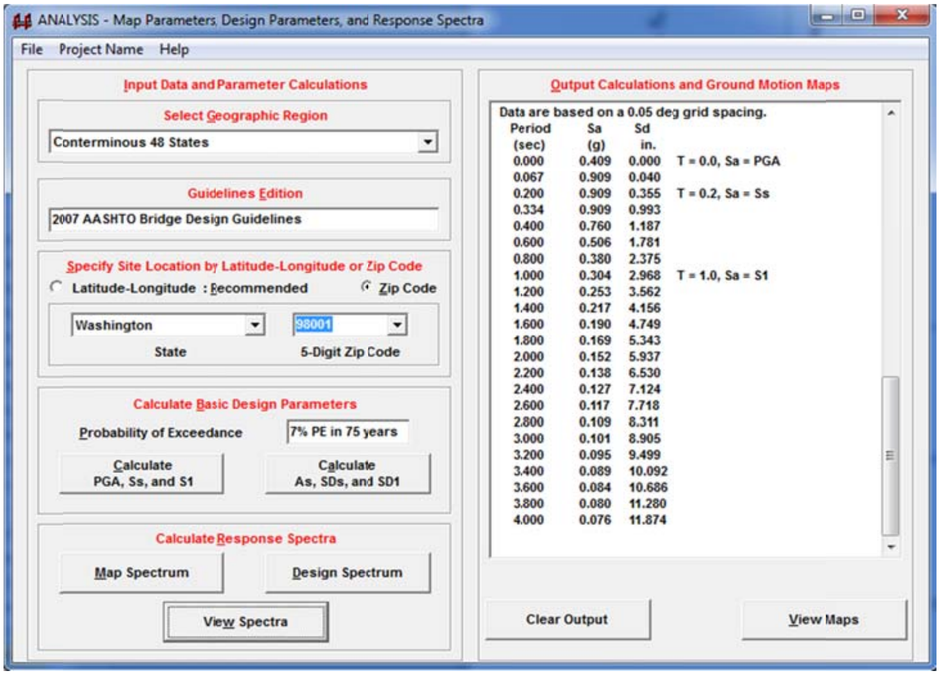

Figure 3-22 USGS Program input screen

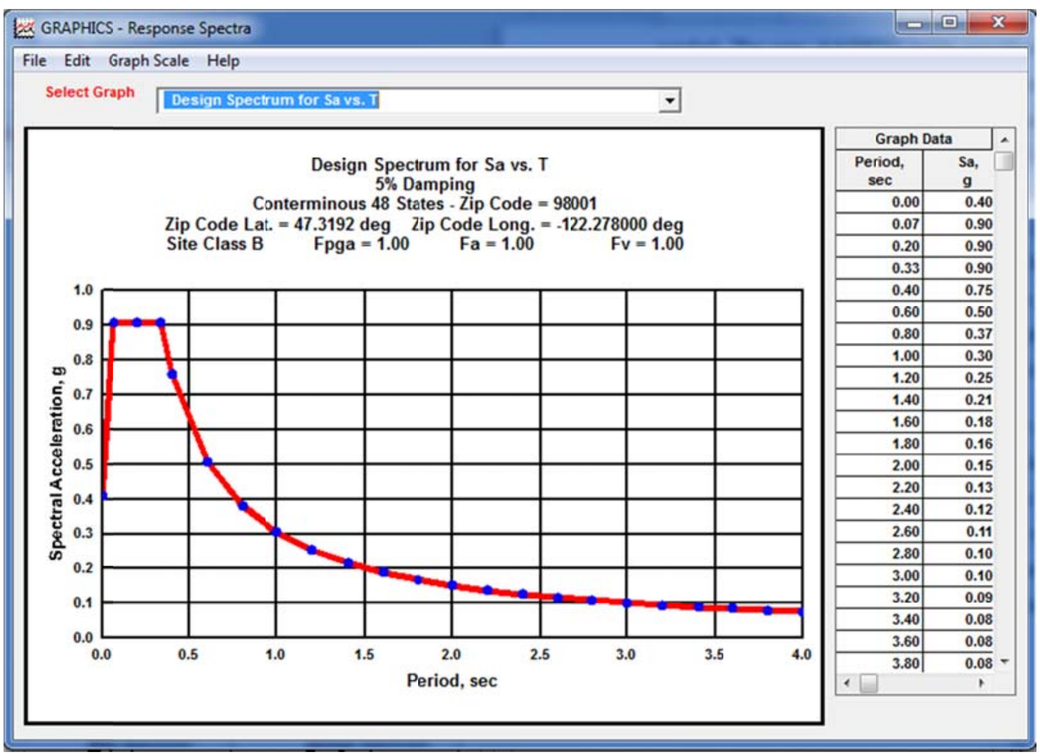

Figure 3-23 Generated Design Response Spectrum using USGS Program

3.5.1 Design Response Spectrum

In this section, design response spectrums generated, for each bridge model, using the USGS seismic parameters program will be discussed.

3.5.1.1 Bridge No 1

This bridge is to be built across a large river and flood plain in the inland pacific Northwest zone in a seismic zone with an acceleration coefficient of PGA = 0.15g according to (FHWA, 1996-b). It is assumed that the column size of the intermediate piers in not controlled by seismic loading because the bridge crosses the flood plain and main channel of a sizable river. Flow issues and ice loading have dictated the size requirements for the pier columns. Due to the issue previously discussed, the bridge is expected to respond linearly to seismic loading of PGA = 0.15g. In order to ensure that the bridge response is in the inelastic range, the bridge will be assessed for higher values of PGA. An acceleration coefficient (PGA) of 0.45g and 0.60g were used in this study. Figure 3-24 shows the design response spectra (5% damped) used for this bridge.

3.5.1.2 Bridge No. 2

The bridge is to be built in the western united states in a seismic zone with an acceleration coefficient of PGA = 0.3g according to (FHWA, 1996-a). The bridge will be assessed for two different spectra, the design response spectrum as well as 1.5 times the design response spectrum. Design response spectra (5% damped) for this bridge are shown in Figure 3-25.

3.5.1.3 Bridge No. 3

As mentioned before, bridge no. 3 is the same as bridge no. 2 with some modifications. The same seismic response spectra of bridge no. 2 are used for both bridges.

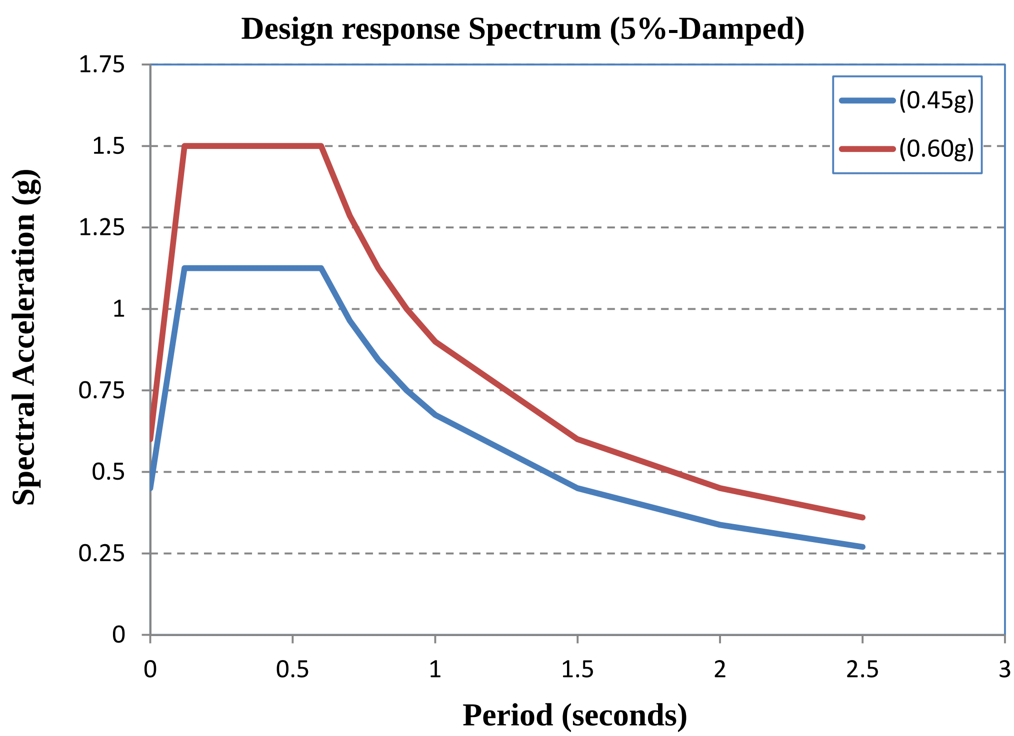

Figure 3-24 Bridge No. 1 – Damped Response Spectrum (5%-Damped)

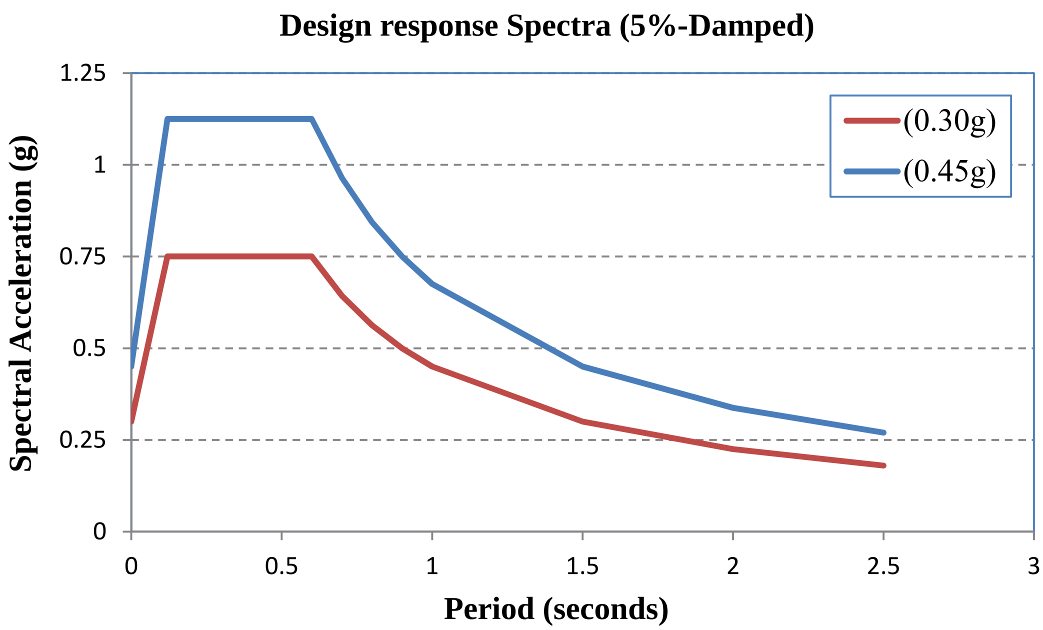

Figure 3-25 Bridge No.2 – Damped Response Spectra (5% Damped)

3.5.2 Acceleration Time Histories

In this study, nonlinear time history analysis (NL-THA) was performed to the three bridges in order to compare its results with the MPA analysis results. Three actual acceleration histories were implemented in this study; which were adjusted to match the design response spectrum for each analysis case. A uniform damping value of 3% was assumed for all analyses. Those actual acceleration time histories are:

- El Centro 1940
- Northridge 1994, Century City Lacc North.
- Santa Monica 1994, City Hall Grounds.

Acceleration time-histories used in this study were obtained from PEER NGA Database (PEER, 2005) and are shown below:

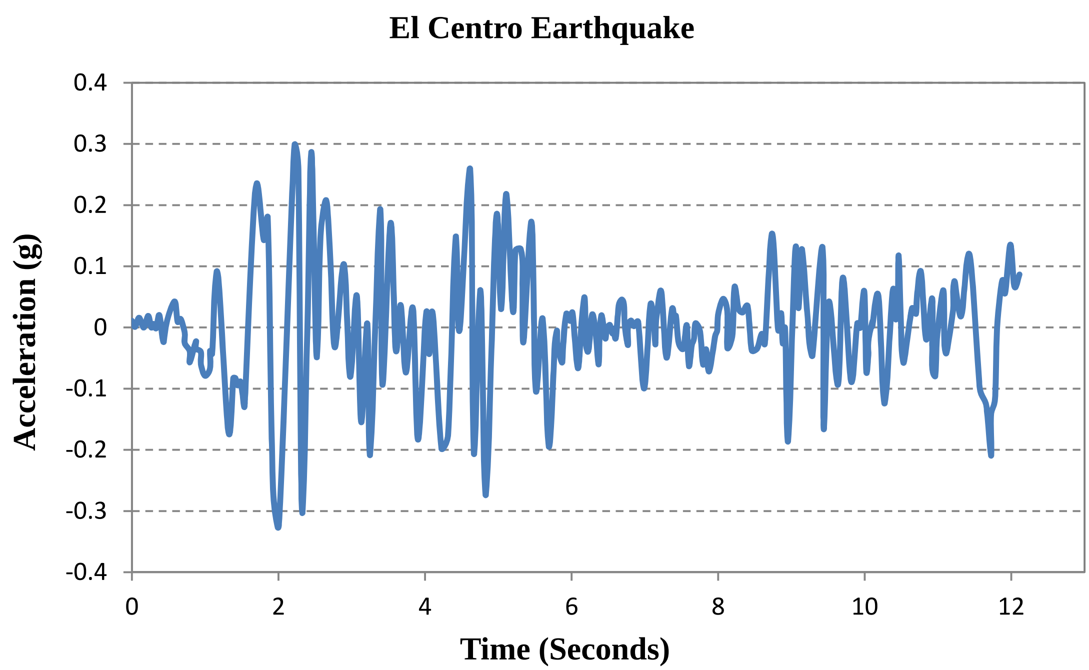

Figure 3-26 Acceleration Time-History of the El Centro Earthquake

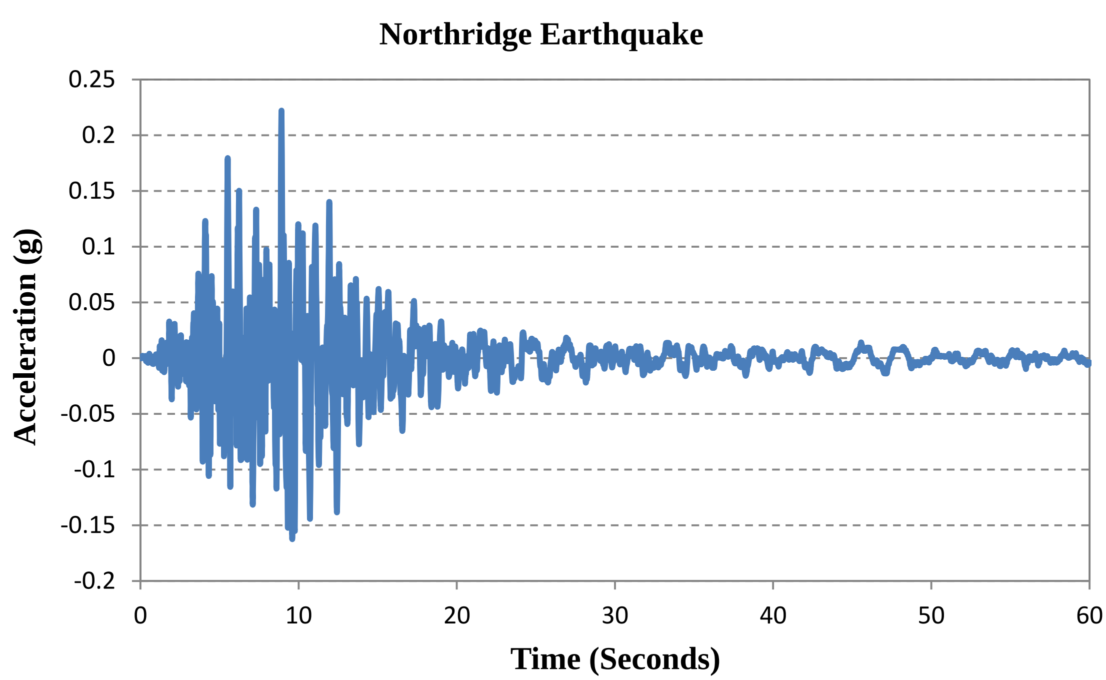

Figure 3-27 Acceleration Time-History of the Northridge-Century City Earthquake

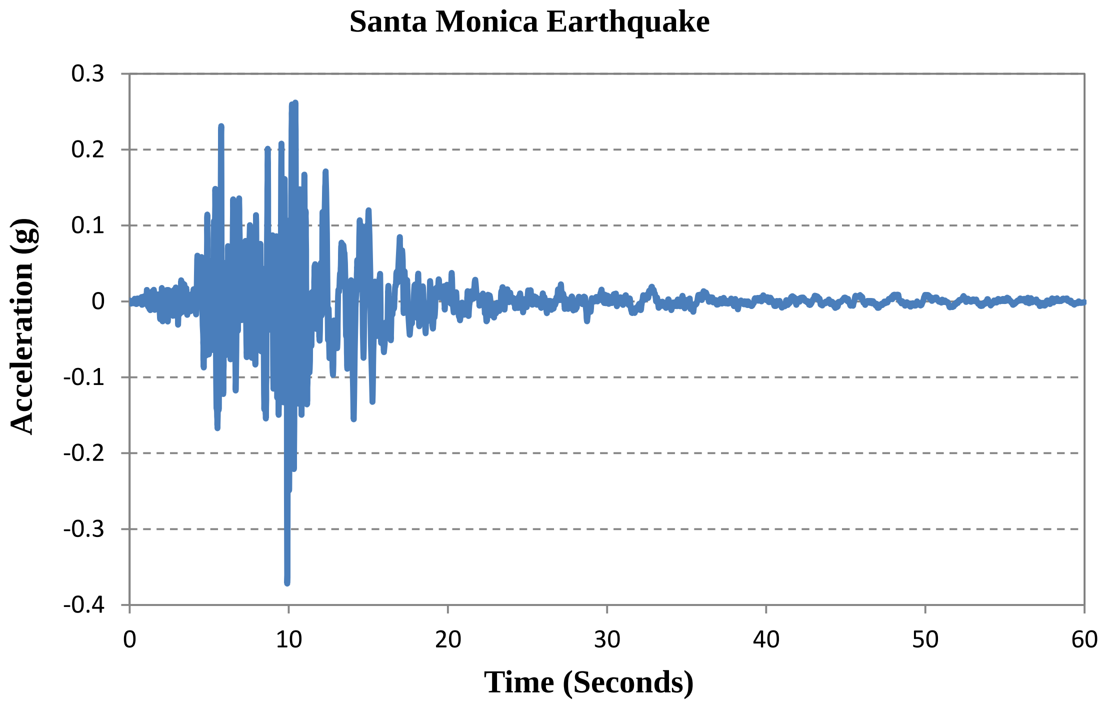

Figure 3-28 Acceleration Time-History of the Santa Monica Earthquake

4. EVALUATION OF MPA PROCEDURE FOR BRIDGES

4.1 INTRODUCTION

The recently developed MPA procedure has been tested by only few researchers for the case of bridges. Being an approximate method, however, it should obviously be evaluated comprehensively before practical application to bridge evaluation and design. The bridges analyzed in this chapter were previously present in chapter 3. Each bridge is analyzed for three different ground motions. The objective of this chapter is to evaluate the accuracy of the MPA procedure in estimating demands for different real bridges.

Definition of the control node was discussed in section 2.4.2.1 as (1) the node of maximum displacement and (2) the node which displacement reflects the behavior of the structure. According to this, three locations were proposed for the monitoring point in the case of bridges. These locations will be evaluated and results will be illustrated and discussed in this chapter as first task when analyzing bridge no. 1 model.

Developing pushover curve and estimation of the demand displacement were discussed in sections 2.4.2.2, 2.4.2.3 and 2.4.3 for either elastic or inelastic behavior of the structure. The objective of this chapter is to evaluate the accuracy of the MPA procedure for three different real bridges and different ground motion ensembles. In this chapter, maximum seismic demand displacement of monitoring point is predicted using the standard pushover analysis (SPA), MPA (without inelastic behavior correction for demand displacement), and the modified MPA (using modified control point displacement u'_{cn}) and then compared with the average demand displacement of the same node obtained from the nonlinear time history (NL-THA) analysis using three different ground acceleration histories closely matching the design response spectrum. The accuracy in estimating demands from the MPA procedure is presented and analyzed.

4.2 RESULTS FOR BRIDGE NO. 1

4.2.1 Effect of Control Node

In order to evaluate the selection of an appropriate point for monitoring the demand displacement and also for drawing the pushover curve, bridge no. 1 was selected to be analyzed. As mentioned in section 3.2, it has nine spans with total length of 1488 feet and consists of two separate units (4 spans tangent, unit 1, and 5 spans curved, unit 2, respectively). It crosses the flood plain and main channel of a sizable river. Unit 2 of the bridge is characterized by a large curvature in plan (radius equal to 1300 ft). The superstructure is composed of four steel plate girders with a composite cast-in-place concrete deck of a 42 ft wide. Piers are single-column cast-in-place concrete rectangular sections widened at the pier top. Piers are supported on steel H-piles. All substructure elements are oriented normal to the centerline of the bridge. Figure 4-1shows the finite element modeling of the bridge. The bridge is assessed using SPA and MPA as well as NL-THA for three acceleration time histories matching the design response spectrum. In the analyses presented in the following, the focus is on the transverse response of the bridge, as it is well known that this is the response most affected by higher modes.

Seismic load is applied perpendicular to a straight line between the two end nodes at the abutments. The transverse seismic load is applied in a direction making an angle of 11° (clockwise) with the global y-axis. Analyses are carried out using the SAP2000 program. The reference finite element model utilizes appropriate plastic hinges (software built-in plastic hinges) and nonlinear links for static and time history inelastic analyses, respectively.

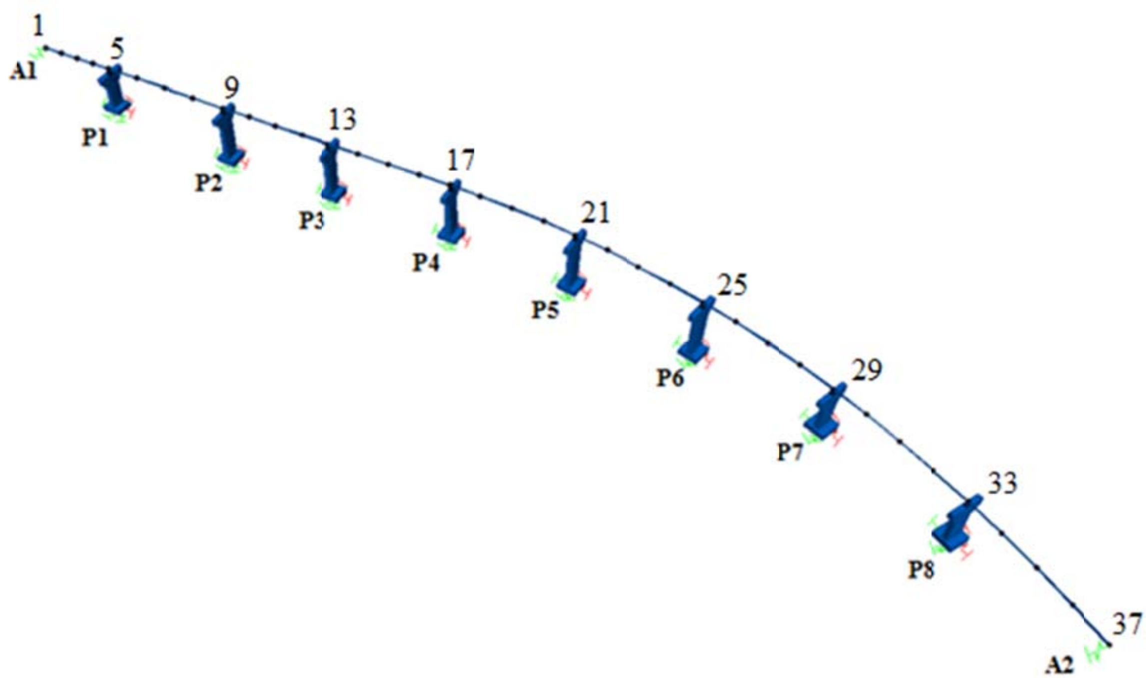

Figure 4-1 Finite Element Model of Bridge No. 1

4.2.1.1 Dynamic characteristics

The dynamic characteristics required within the context of the MPA approach, were determined using standard eigenvalue analysis. Figure 4-2 through Figure 4-4 illustrate the first four fundamental transverse mode shapes of the bridge (modes 5, 7, 9, and 12) with the corresponding natural periods. Table 4-1 lists the locations of different control nodes (mass center, equivalent SDOF system location calculated from equation (2.39) and most critical pier for each of the four modes) for the main transverse modes of the bridge. Tables 4.2-4.4 list the modal periods and frequencies, modal participation factors, and modal participating mass ratios, respectively.

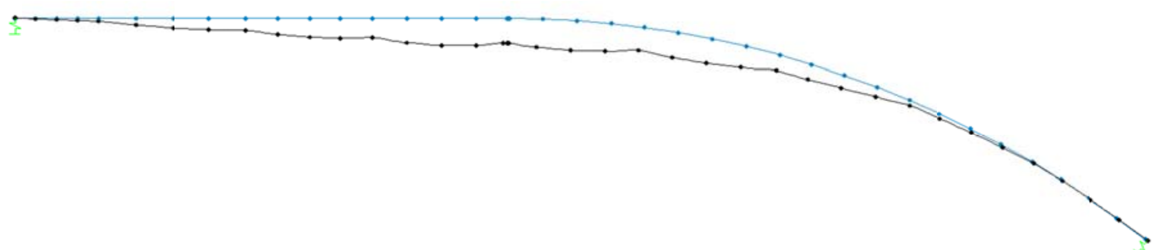

Mode 5: T_5=1.028s

Figure 4-2 Deformed Shape of Mode 5 (Bridge No. 1)

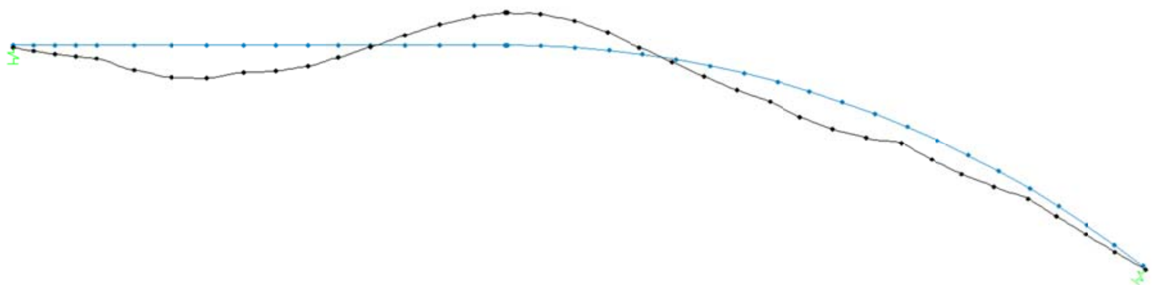

Mode 7: T_7=0.86376s

Figure 4-3 Deformed Shape of Mode 7 (Bridge No. 1)

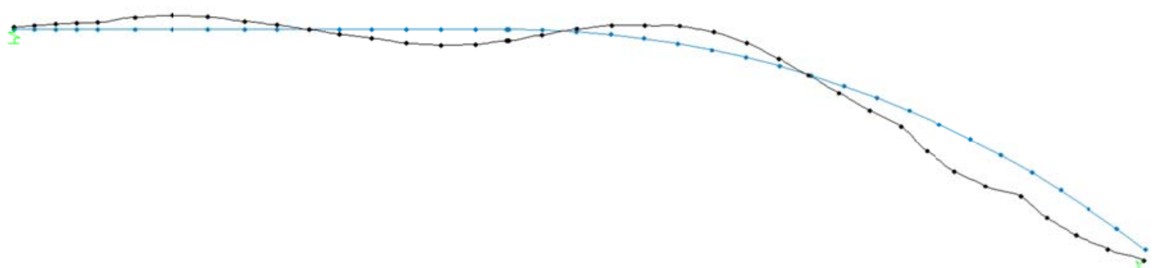

Mode 9: T_9=0.75944s

Figure 4-4 Deformed Shape of Mode 9 (Bridge No. 1)

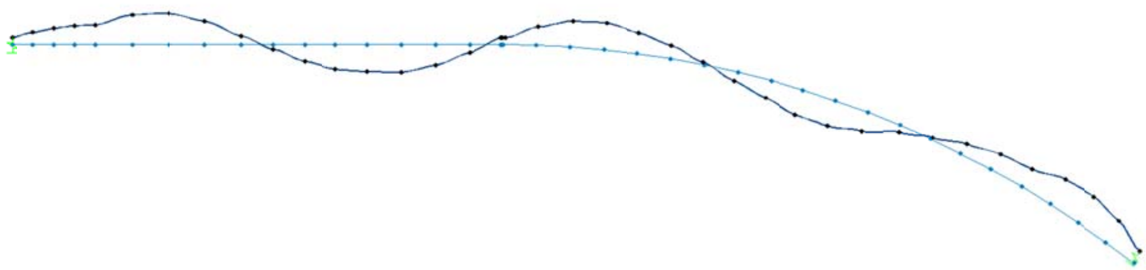

Mode 12: T_{12}=0.6756s

Figure 4-5 Deformed Shape of Mode 12 (Bridge No. 1)

Table 4-1 Locations of different Control Nodes for the Main Transverse Modes of the Bridge

		Mode 5	Mode 7	Mode 9	Mode12
$X_{mass\ center}/L$	(a)	0.5	0.5	0.5	0.5
X_{SDOF}/L	(b)	0.413	0.4866	0.5038	0.5205
$X_{critical\ pier}/L$	(c)	0.44	0.44	0.9	0.9

Where: L = Total Length

Table 4-2 Modal Periods and Frequencies (Bridge No. 1)

OutputCase	StepType	StepNum	Period	Frequency	CircFreq	Eigenvalue
			Sec	Cyc/sec	rad/sec	rad2/sec2
MODAL	Mode	1.000000	2.218319	4.5079E-01	2.8324E+00	8.0225E+00
MODAL	Mode	2.000000	1.767226	5.6586E-01	3.5554E+00	1.2641E+01
MODAL	Mode	3.000000	1.075853	9.2950E-01	5.8402E+00	3.4108E+01
MODAL	Mode	4.000000	1.075853	9.2950E-01	5.8402E+00	3.4108E+01
MODAL	Mode	5.000000	1.028028	9.7274E-01	6.1119E+00	3.7355E+01
MODAL	Mode	6.000000	0.954703	1.0474E+00	6.5813E+00	4.3313E+01
MODAL	Mode	7.000000	0.863764	1.1577E+00	7.2742E+00	5.2914E+01
MODAL	Mode	8.000000	0.820088	1.2194E+00	7.6616E+00	5.8700E+01
MODAL	Mode	9.000000	0.759435	1.3168E+00	8.2735E+00	6.8451E+01
MODAL	Mode	10.000000	0.757447	1.3202E+00	8.2952E+00	6.8811E+01
MODAL	Mode	11.000000	0.704497	1.4195E+00	8.9187E+00	7.9543E+01
MODAL	Mode	12.000000	0.675598	1.4802E+00	9.3002E+00	8.6493E+01
MODAL	Mode	13.000000	0.659078	1.5173E+00	9.5333E+00	9.0884E+01
MODAL	Mode	14.000000	0.642600	1.5562E+00	9.7778E+00	9.5604E+01
MODAL	Mode	15.000000	0.609872	1.6397E+00	1.0302E+01	1.0614E+02
MODAL	Mode	16.000000	0.595508	1.6792E+00	1.0551E+01	1.1132E+02
MODAL	Mode	17.000000	0.571567	1.7496E+00	1.0993E+01	1.2084E+02
MODAL	Mode	18.000000	0.540418	1.8504E+00	1.1627E+01	1.3518E+02
MODAL	Mode	19.000000	0.517591	1.9320E+00	1.2139E+01	1.4736E+02
MODAL	Mode	20.000000	0.504123	1.9836E+00	1.2464E+01	1.5534E+02
MODAL	Mode	21.000000	0.496003	2.0161E+00	1.2668E+01	1.6047E+02
MODAL	Mode	22.000000	0.440906	2.2681E+00	1.4251E+01	2.0308E+02
MODAL	Mode	23.000000	0.402141	2.4867E+00	1.5624E+01	2.4412E+02
MODAL	Mode	24.000000	0.380742	2.6264E+00	1.6502E+01	2.7233E+02
MODAL	Mode	25.000000	0.358059	2.7928E+00	1.7548E+01	3.0793E+02
MODAL	Mode	26.000000	0.343527	2.9110E+00	1.8290E+01	3.3453E+02
MODAL	Mode	27.000000	0.327286	3.0554E+00	1.9198E+01	3.6856E+02
MODAL	Mode	28.000000	0.318963	3.1352E+00	1.9699E+01	3.8804E+02
MODAL	Mode	29.000000	0.318927	3.1355E+00	1.9701E+01	3.8813E+02
MODAL	Mode	30.000000	0.310327	3.2224E+00	2.0247E+01	4.0994E+02
MODAL	Mode	31.000000	0.296041	3.3779E+00	2.1224E+01	4.5046E+02
MODAL	Mode	32.000000	0.281906	3.5473E+00	2.2288E+01	4.9677E+02
MODAL	Mode	33.000000	0.274613	3.6415E+00	2.2880E+01	5.2350E+02
MODAL	Mode	34.000000	0.270628	3.6951E+00	2.3217E+01	5.3903E+02
MODAL	Mode	35.000000	0.265566	3.7655E+00	2.3660E+01	5.5978E+02

Table 4-3 Modal Participation Factors (Bridge No. 1)

OutputCase	StepType	StepNum	Period Sec	UX Kip-s2	UY Kip-s2	UZ Kip-s2
MODAL	Mode	1.000000	2.218319	16.286228	-5.372288	0.004721
MODAL	Mode	2.000000	1.767226	-16.445294	5.089E-07	0.040074
MODAL	Mode	3.000000	1.075853	-4.330441	0.765917	-1.699E-06
MODAL	Mode	4.000000	1.075853	7.151030	-0.184556	-6.905E-07
MODAL	Mode	5.000000	1.028028	1.955644	22.351909	-0.019497
MODAL	Mode	6.000000	0.954703	2.901254	-0.994532	0.034382
MODAL	Mode	7.000000	0.863764	3.238172	9.892469	0.129679
MODAL	Mode	8.000000	0.820088	0.205518	0.060828	-2.349733
MODAL	Mode	9.000000	0.759435	4.756829	6.231181	0.136658
MODAL	Mode	10.000000	0.757447	1.399897	1.544784	-0.361869
MODAL	Mode	11.000000	0.704497	0.165094	0.000361	4.706851
MODAL	Mode	12.000000	0.675598	-1.797084	-5.369813	-0.124753
MODAL	Mode	13.000000	0.659078	-0.039422	0.188224	-4.603131
MODAL	Mode	14.000000	0.642600	0.011032	-0.001256	-0.338536
MODAL	Mode	15.000000	0.609872	0.972471	-2.216504	-0.088038
MODAL	Mode	16.000000	0.595508	-5.002939	2.946858	-0.000015
MODAL	Mode	17.000000	0.571567	-0.145966	0.191084	0.242052
MODAL	Mode	18.000000	0.540418	-0.618305	-2.664868	0.064822
MODAL	Mode	19.000000	0.517591	-0.043632	-0.049828	12.455965
MODAL	Mode	20.000000	0.504123	0.198835	-3.004847	0.095216
MODAL	Mode	21.000000	0.496003	-0.068450	-0.000071	-8.943761
MODAL	Mode	22.000000	0.440906	0.337685	1.147661	0.001842
MODAL	Mode	23.000000	0.402141	0.040200	-3.124260	0.000302
MODAL	Mode	24.000000	0.380742	0.120389	-2.083737	-0.007920
MODAL	Mode	25.000000	0.358059	-0.217638	-1.410582	0.005131
MODAL	Mode	26.000000	0.343527	-0.008290	-0.204530	0.003092
MODAL	Mode	27.000000	0.327286	-0.305469	-2.866016	-0.003343
MODAL	Mode	28.000000	0.318963	0.039457	7.468300	-0.000825
MODAL	Mode	29.000000	0.318927	0.261722	-0.000097	-5.420651
MODAL	Mode	30.000000	0.310327	-2.397523	-6.721389	-0.002090
MODAL	Mode	31.000000	0.296041	-0.000101	3.484902	-6.676E-07
MODAL	Mode	32.000000	0.281906	-0.402962	0.000060	-0.990414
MODAL	Mode	33.000000	0.274613	0.749481	-0.226454	0.088614
MODAL	Mode	34.000000	0.270628	0.217984	-0.014398	-0.791710
MODAL	Mode	35.000000	0.265566	0.551684	-0.187383	0.044023

Table 4-4 Modal Participating Mass Ratios (Bridge No. 1)

StepType	StepNum	Period Sec	UX	UY	UZ	SumUX	SumUY	SumUZ
Mode	1.000000	2.218319	0.28367	0.03087	2.410E-08	0.28367	0.03087	2.410E-08
Mode	2.000000	1.767226	0.28924	2.770E-16	1.736E-06	0.57291	0.03087	1.760E-06
Mode	3.000000	1.075853	0.02006	0.00063	3.120E-15	0.59296	0.03149	1.760E-06
Mode	4.000000	1.075853	0.05469	3.643E-05	5.155E-16	0.64765	0.03153	1.760E-06
Mode	5.000000	1.028028	0.00409	0.53432	4.110E-07	0.65174	0.56585	2.171E-06
Mode	6.000000	0.954703	0.00900	0.00106	1.278E-06	0.66075	0.56691	3.449E-06
Mode	7.000000	0.863764	0.01121	0.10466	1.818E-05	0.67196	0.67157	2.163E-05
Mode	8.000000	0.820088	4.517E-05	3.957E-06	0.00597	0.67200	0.67157	0.00599
Mode	9.000000	0.759435	0.02420	0.04153	2.019E-05	0.69620	0.71310	0.00601
Mode	10.000000	0.757447	0.00210	0.00255	0.00014	0.69830	0.71565	0.00615
Mode	11.000000	0.704497	2.915E-05	1.394E-10	0.02395	0.69833	0.71565	0.03010
Mode	12.000000	0.675598	0.00345	0.03084	1.683E-05	0.70178	0.74649	0.03012
Mode	13.000000	0.659078	1.662E-06	3.789E-05	0.02291	0.70179	0.74653	0.05303
Mode	14.000000	0.642600	1.302E-07	1.688E-09	0.00012	0.70179	0.74653	0.05315
Mode	15.000000	0.609872	0.00101	0.00525	8.379E-06	0.70280	0.75178	0.05316
Mode	16.000000	0.595508	0.02677	0.00929	2.328E-13	0.72956	0.76107	0.05316
Mode	17.000000	0.571567	2.279E-05	3.905E-05	6.334E-05	0.72959	0.76111	0.05322
Mode	18.000000	0.540418	0.00041	0.00759	4.543E-06	0.73000	0.76870	0.05323
Mode	19.000000	0.517591	2.036E-06	2.655E-06	0.16773	0.73000	0.76870	0.22096
Mode	20.000000	0.504123	4.228E-05	0.00966	9.801E-06	0.73004	0.77836	0.22097
Mode	21.000000	0.496003	5.011E-06	5.453E-12	0.08648	0.73005	0.77836	0.30745
Mode	22.000000	0.440906	0.00012	0.00141	3.667E-09	0.73017	0.77977	0.30745
Mode	23.000000	0.402141	1.728E-06	0.01044	9.858E-11	0.73017	0.79021	0.30745
Mode	24.000000	0.380742	1.550E-05	0.00464	6.782E-08	0.73019	0.79485	0.30745
Mode	25.000000	0.358059	5.066E-05	0.00213	2.846E-08	0.73024	0.79698	0.30745
Mode	26.000000	0.343527	7.350E-08	4.474E-05	1.034E-08	0.73024	0.79702	0.30745
Mode	27.000000	0.327286	9.979E-05	0.00878	1.208E-08	0.73034	0.80581	0.30745
Mode	28.000000	0.318963	1.665E-06	0.05965	7.361E-10	0.73034	0.86546	0.30745
Mode	29.000000	0.318927	7.326E-05	1.003E-11	0.03177	0.73041	0.86546	0.33921
Mode	30.000000	0.310327	0.00615	0.04832	4.723E-09	0.73656	0.91378	0.33921
Mode	31.000000	0.296041	1.099E-11	0.01299	4.818E-16	0.73656	0.92676	0.33921
Mode	32.000000	0.281906	0.00017	3.864E-12	0.00106	0.73673	0.92676	0.34027
Mode	33.000000	0.274613	0.00060	5.484E-05	8.489E-06	0.73733	0.92682	0.34028
Mode	34.000000	0.270628	5.082E-05	2.217E-07	0.00068	0.73738	0.92682	0.34096
Mode	35.000000	0.265566	0.00033	3.755E-05	2.095E-06	0.73771	0.92686	0.34096

4.2.1.2 Pushover Curves

Applying the modal load pattern of the 5th, 7th, 9th and 12th modes in the transverse direction of the bridge, the corresponding pushover curves were derived with respect to the deck displacement at the location of: (1) pier location nearest to deck mass center point; (2) the position of the corresponding equivalent SDOF system; (3) the most critical pier (in terms of maximum plastic rotation) for each individual modal load pattern. To identify the most critical pier in order to construct the pushover curve with respect to that location, a preliminary pushover analysis for each mode is needed. After carrying out these analyses, it was decided to draw the pushover curve of both the 5th and 7th modes (first & second fundamental transverse modes) in terms of the deck displacement at pier no. 4 (P4), see Figure 4-1 and that of the 9th and 12th modes (third & fourth fundamental transverse modes) in terms of the deck displacement at pier no. 8 (P8). The pushover curves were then idealized as bilinear curves. Bilinearization is carried out using equal energy absorption concept. The bilinearized pushover curves for the four transverse modes were converted to the capacity curves. Curves were drawn with respect to the mass center of the deck, position of equivalent SDOF system and critical pier locations as shown in Figure 4-6.

It is noted that these curves are not necessarily representative of the actual response of all structural members of the bridge. For example, the capacity curves corresponding to modes 9 and 12 are rather linear (with respect to deck mass center and equivalent SDOF system), hence conveying the impression that the bridge does not enter the inelastic range when subjected to the 9th or 12th modal load pattern. In reality, it is only the central pier region (pier no. 4) that responds elastically in that case, whereas the edge piers do enter the inelastic range; this is due to the form of those higher modal load patterns which are not critical for the central region of the bridge (see Figure 4-4 and Figure 4-5).

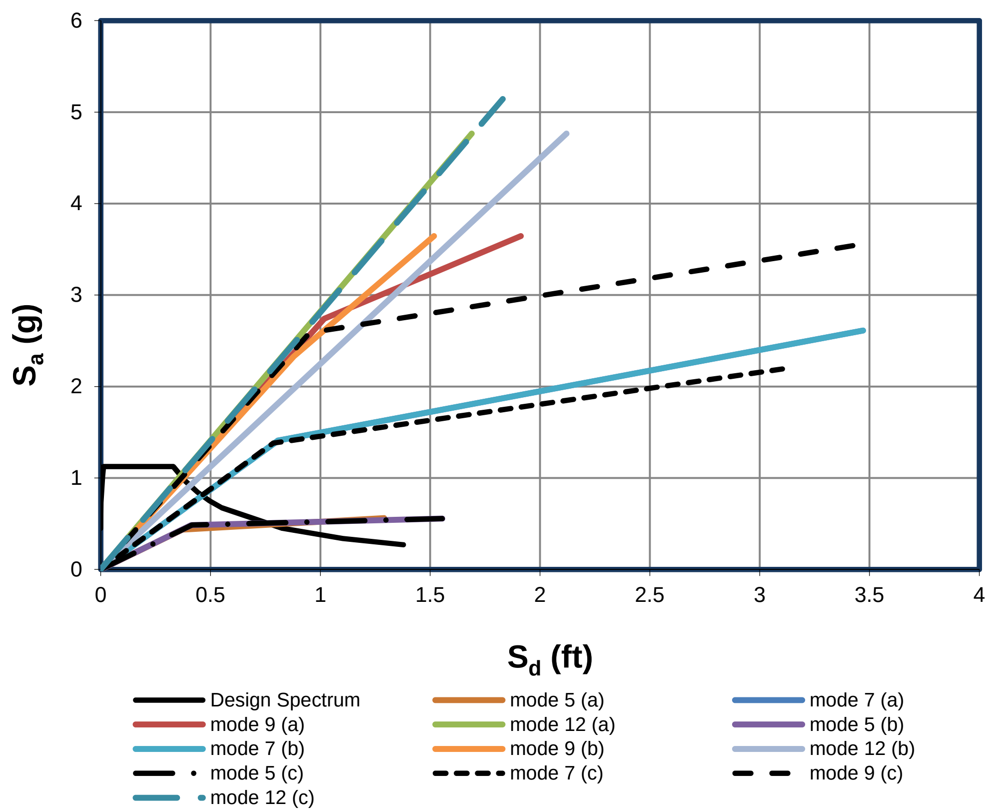

Figure 4-6 Capacity curves derived with respect to the deck displacement: (a) at the location of the deck mass center; (b) at the location of the equivalent SDOF system; and (c) at the location of the most critical pier for each mode. (The elastic spectrum of the design earthquake is also shown)

By comparing the capacity curves constructed with respect to the three different control node locations, it is clear that the capacity curves produced using the most critical pier location are more representative of the actual behavior of the bridge, since they indicate that at some stage of the response one or more piers of the structure yield. In the studied bridge, the capacity curves of Figure 4-6 using the most critical pier indicate that yielding of the structure will initiate from its response to the fundamental transverse mode (5^{th} mode) followed by yielding due to the 7^{th} mode then the 9^{th} mode.

4.2.2 Demand Displacement

The inelastic spectra based version of CSM is used to define the displacement demand for a given earthquake intensity. To investigate the effect of the level of inelasticity on the calculated response, different levels of excitation were considered, i.e. peak ground acceleration PGA=0.45g and 0.60g.

Figure 4-7 illustrate the deck displacements of bridge no. 1 derived from modal pushover analysis using modal load pattern of mode no. 5 (bridge responded inelastically to this load pattern), while Figure 4-8 illustrate the total deck displacements of bridge no. 1 derived using modal pushover analysis (after combining modal displacements from all four modal load patterns), with respect to different control point locations for excitation of PGA=0.45g. Considering the first four transverse modes assures that these modes contribute to 75% of the total mass of the bridge structure. Adding more modes in order to capture all modes whose masses contribute to at least 90% of the total mass of the bridges (a criterion commonly used in seismic codes) was also studied (as shown in Appendix B) and based on the results, it was found that there was little merit in adding modes whose participation factor is very low, say less than 1%, and less rigid rules than the 90% one (calibrated only for buildings) could be adopted.

Inelasticity developed in the bridge behavior was not considered and the peak displacement of the monitoring point of the bridge, u_{cn}, was calculated using equation (2.46) (no correction was made to control point displacement). It was found that deck displacements derived with respect to different control points are not identical, but rather the estimated deformed shape of the bridge depends on the monitoring point selected for drawing the pushover curve. This would also be explained due to the fact that u_{cn} will differ because of the deviation of the elastic mode shape ϕ_n from the actual deformed shape of the structure, and also the spectral displacement S_d is dependent on the selection of monitoring point if the structure exhibits inelastic behavior.

Same trends were also noticed for ground excitation of PGA = 0.60g as shown in Figure 4-9 and Figure 4-10. Deck displacements derived with respect to the control point of deck mass center are different from those displacements derived with respect to either control point of equivalent SDOF system or most critical pier which were found to be rather identical.

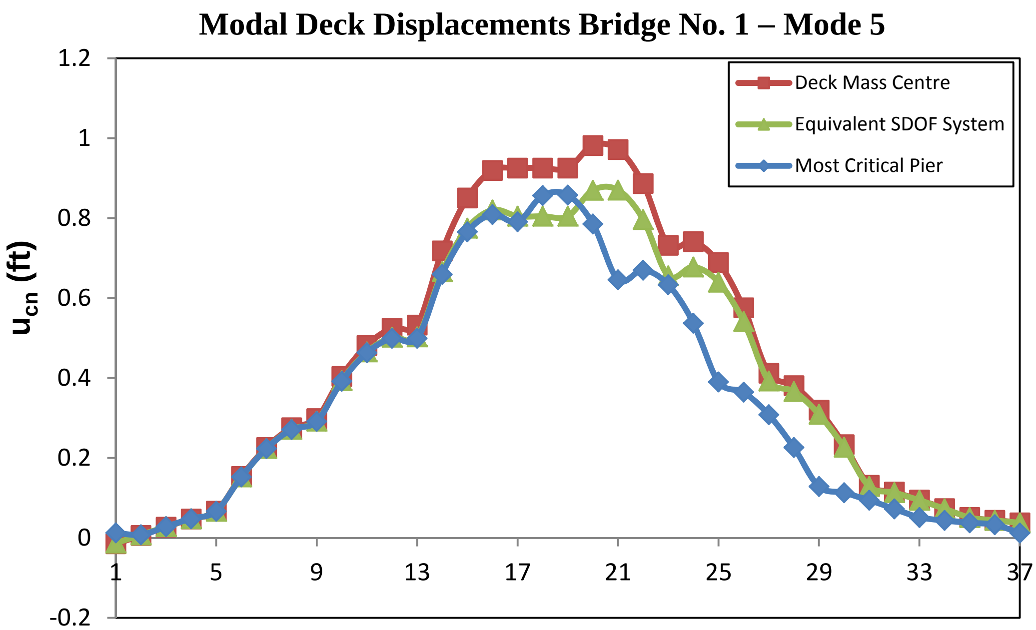

Figure 4-7 Modal deck displacements derived with respect to different control points – Mode 5 load (Ag=0.45)

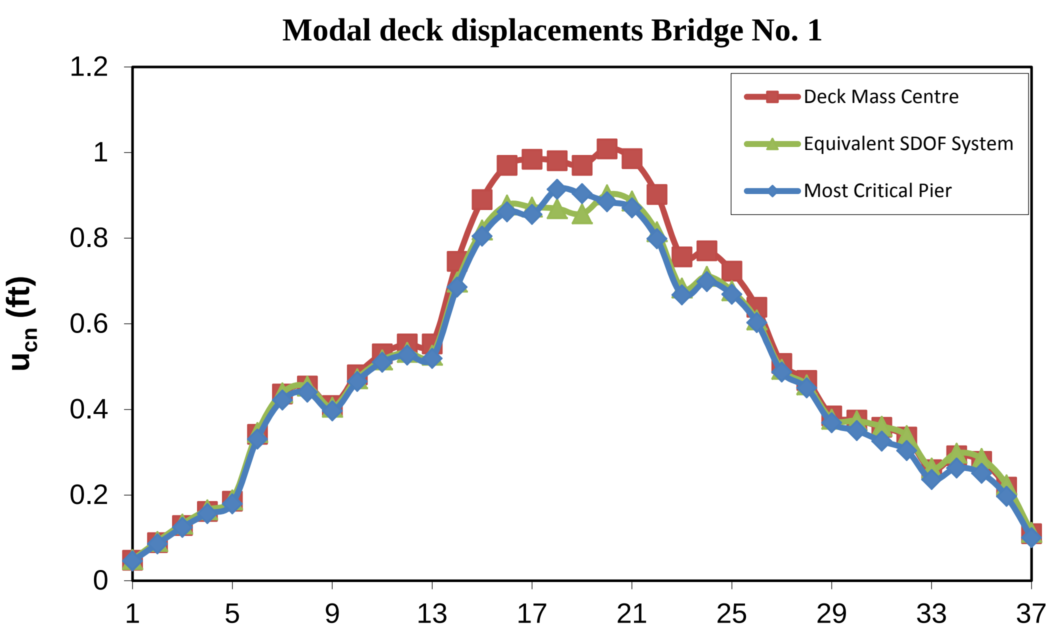

Figure 4-8 Modal deck displacements derived with respect to different control points – u_{cn} (A_g=0.45)

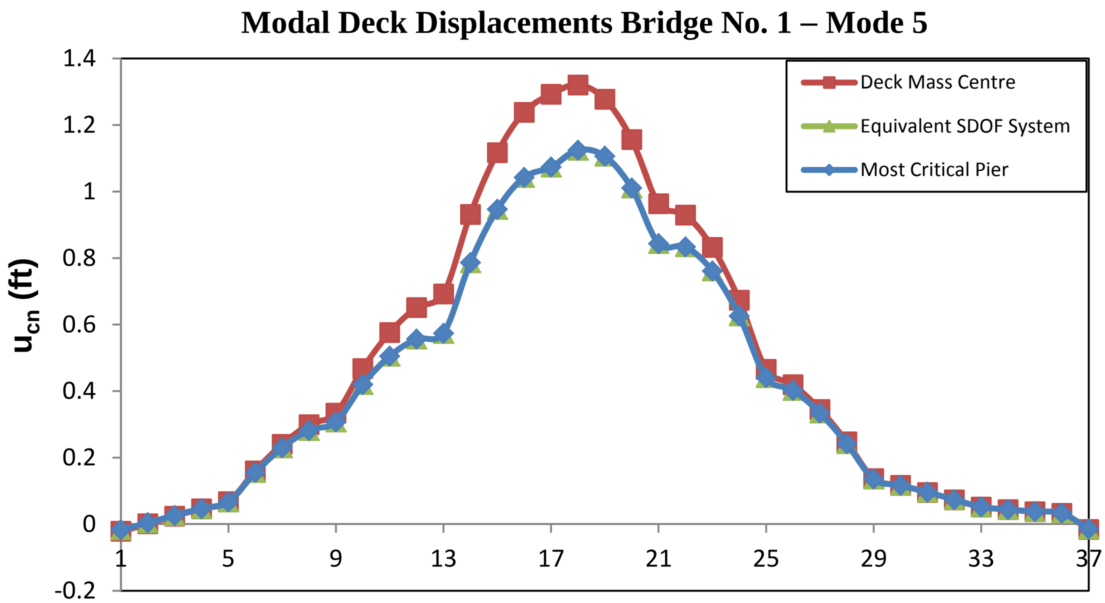

Figure 4-9 Modal deck displacements derived with respect to different control points – Mode 5 load (A_g=0.60)

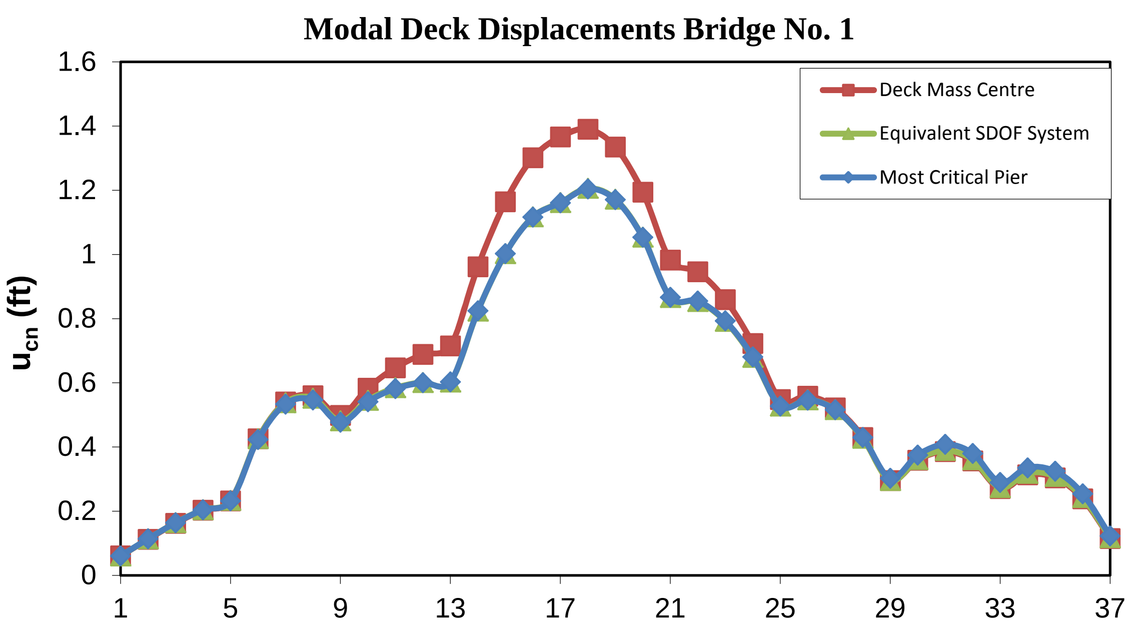

Figure 4-10 Modal deck displacements derived with respect to different control points – u_{cn} (Ag=0.60)

In order to take the inelastic behavior of the bridge into account and to apply the proposed modified MPA method where an improved target displacement of the monitoring point (u'_{cn}) is calculated (from equation (2.40), the actual deformed shape of the structure (ϕ'_n) will be used. For example, the actual deformed shapes of the modal load pattern of mode 5 (as shown in Figure 4-7 and Figure 4-9 for ground excitation of PGA = 0.45g and 0.60g respectively) will be used as the new modal load ϕ'_n, and then the modified target displacement u'_{cn} will be calculated.

Figure 4-11 to Figure 4-14 illustrate the deck displacements of the studied bridge calculated from the modified MPA procedure using u'_{cn} as a target displacement for different ground acceleration intensities. It is noted that deck displacements derived with respect to different control points are rather identical and differences are significantly reduced and results are deemed acceptable for all practical purposes.

Based on the previous findings, the most critical pier location can be considered as the most practical choice for the monitoring point for either drawing the pushover curve or calculating the maximum demand displacement whether inelasticity was already developed in the bridge or it is still responding elastically to the seismic load.

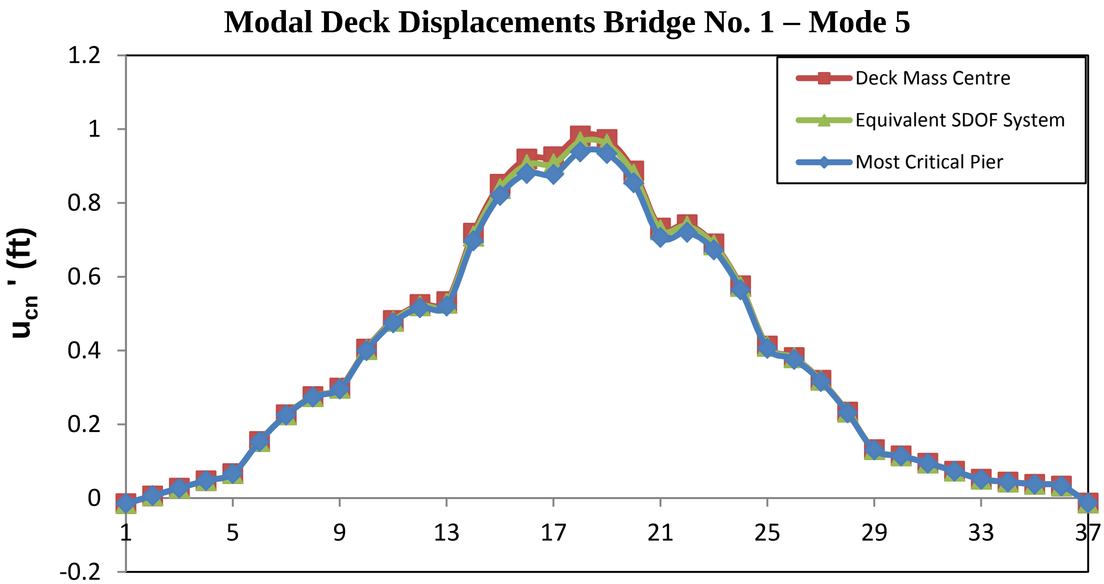

Figure 4-11 Modal deck displacements derived with respect to different control points –mode 5 load only using u'_{cn} as target displacement according to the improved MPA procedure (A_g=0.45)

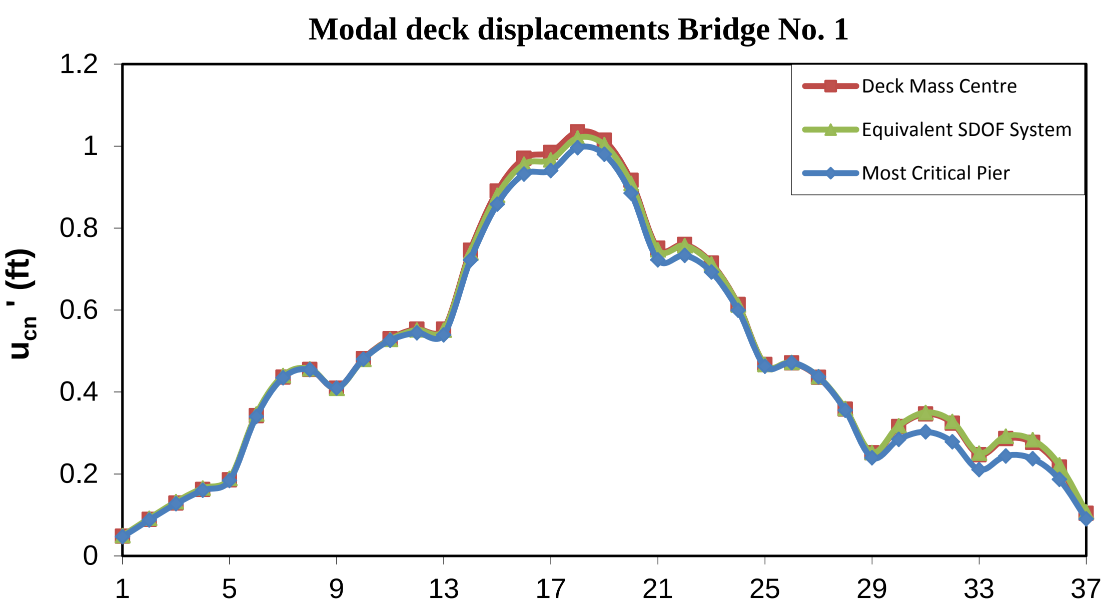

Figure 4-12 Modal deck displacements derived with respect to different control points – using u'_{cn} as target displacement according to the improved MPA procedure (A_g=0.45)

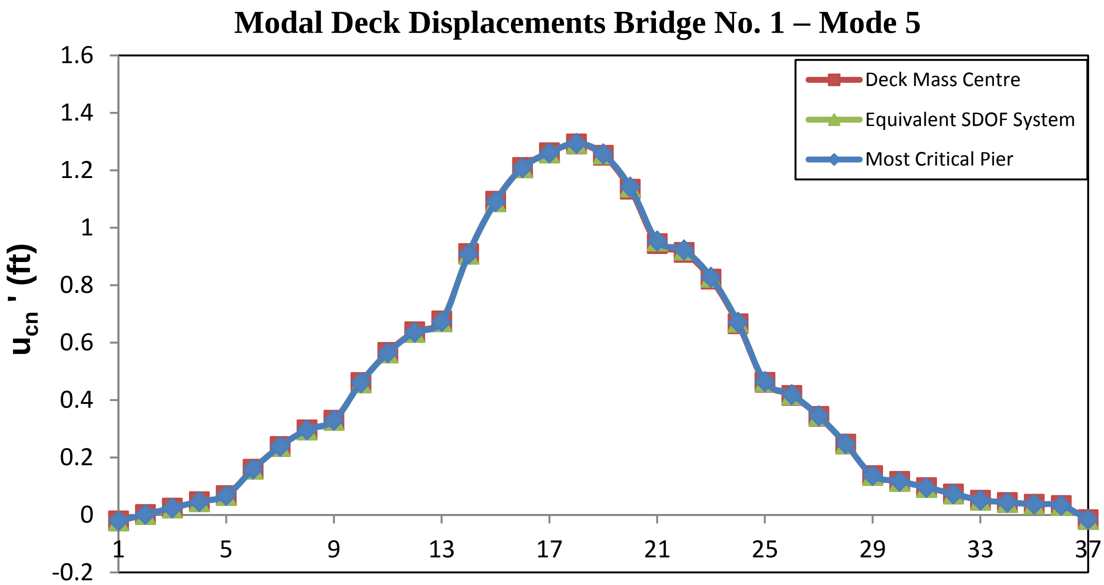

Figure 4-13 Modal deck displacements derived with respect to different control points –mode 5 load only using u'_{cn} as target displacement according to the improved MPA procedure (A_g=0.60)

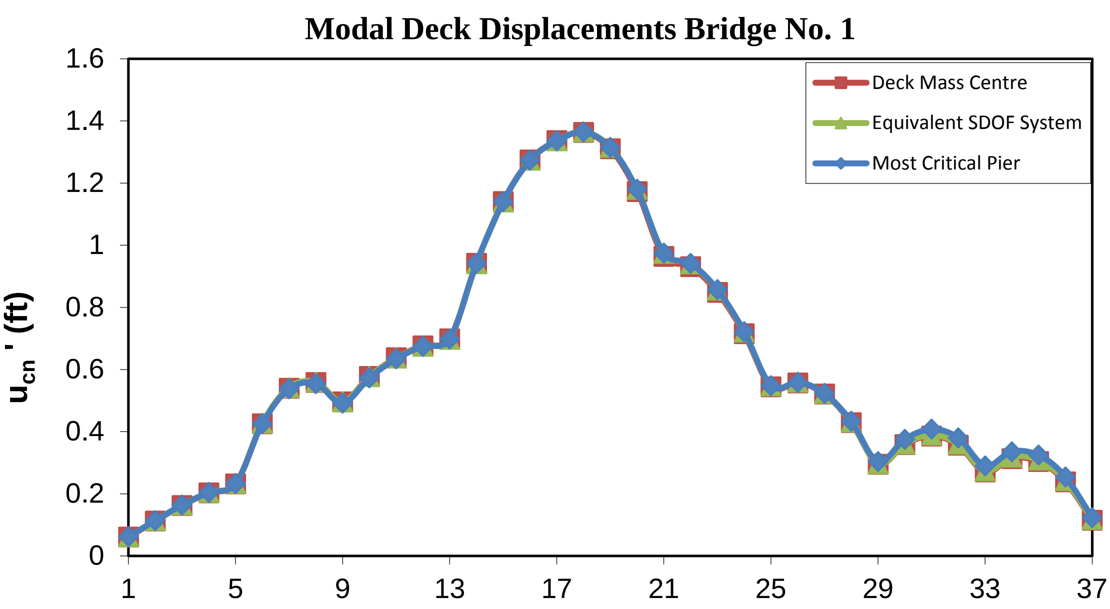

Figure 4-14 Modal deck displacements derived with respect to different control points – using u'_{cn} as target displacement according to the improved MPA procedure (A_g=0.60)

Evaluation of different procedures

Results of the standard and modal pushover approaches were evaluated by comparing them with those from the NL-THA, the latter is considered to be the most rigorous procedure to compute seismic demands. To this effect, a set of three real time acceleration records compatible with the design spectrum was used in the NL-THA analyses. The deck displacements determined from each of the SPA and MPA analyses with respect to the control point of the most critical pier were compared with those from NL-THA for increasing levels of earthquake excitation, as shown in Figure 4-15 and Figure 4-16 for PGA = 0.45g and 0.60g respectively.

It is noted that the deck displacements shown in the figures as the THA case are the average of the peak displacements recorded in the structure during the three time-history analyses.

As shown in Figure 4-15, it is observed that the SPA procedure poorly predicts the transverse displacements at the end areas of the bridge and gave better estimates only in the area of the central piers; such area is dominated by the first fundamental transverse mode. MPA procedure which accounts for four transverse modes predicts well the deck displacements of the bridge. On the other hand, the modified MPA procedure that also accounts for four transverse modes with a correction made to the demand displacement is much closer to NL-THA and gave better predictions at the end areas of the bridge from that of the SPA. As the level of excitation increases and higher mode contributions become more significant (see Figure 4-16).

Modal deck displacements Bridge No. 1

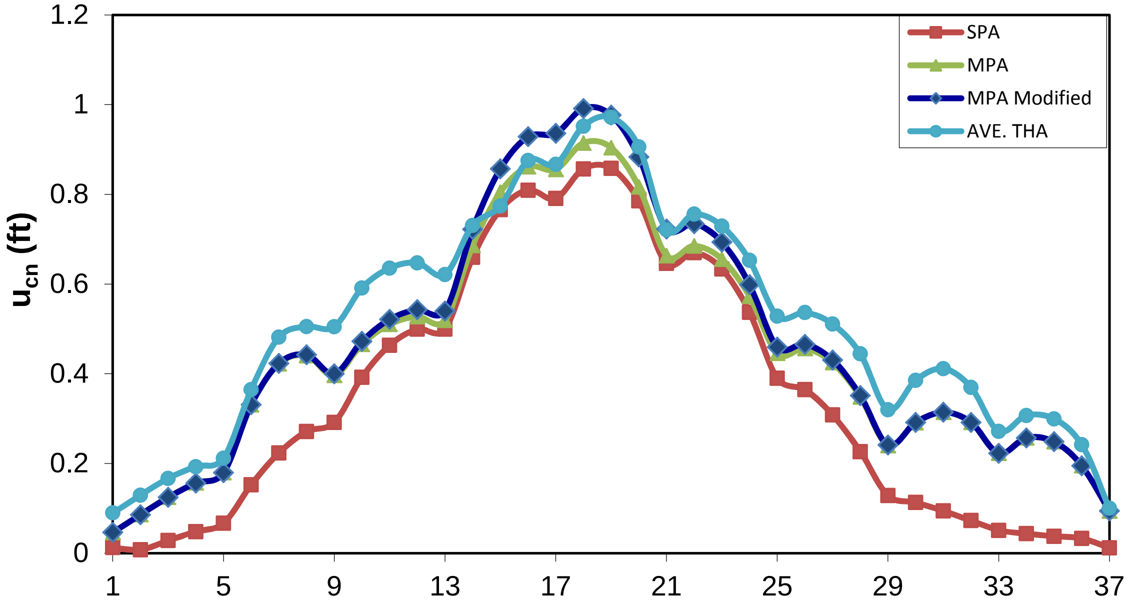

Figure 4-15 Deck displacements at pier locations for bridge no. 1 calculated from SPA, MPA, modified MPA and THA, for PGA = 0.45g

Modal Deck Displacements Bridge No. 1

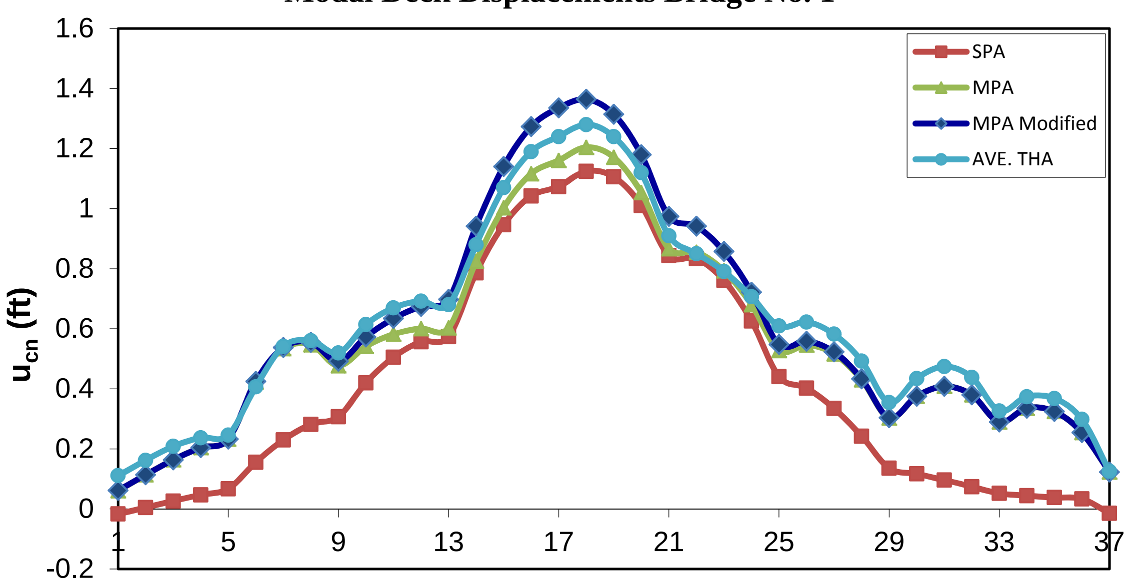

Figure 4-16 Deck displacements at pier locations for bridge no. 1 calculated from SPA, MPA, modified MPA and THA, for PGA = 0.60g

The displacement profile derived by the modified MPA method tends to match that obtained by the NL-THA, whereas predictions from SPA become less accurate as the level of inelasticity increases. The consideration of higher modes and the correction made to the target displacement significantly improve the accuracy of the predicted deck displacements.

Table 4-5 lists the deck displacement of bridge no. 1 for the case of earthquake intensity of PGA = 0.45g calculated using different pushover analyses as well as the NL-THA as the benchmark to compare with others cases. As shown in the table, modified MPA procedure provided the best estimate of deck displacement. The difference between the maximum displacement calculated using the modified MPA (at pier no. 4) and that of the NL-THA is 8% and the modified MPA displacement profile is closely matching that profile derived from NL-THA with differences ranging from 13% at pier no. 6 to 21% at pier no. 2. Same observations were noted in the case of applying ground acceleration with increased intensity, PGA = 0.60g as shown in Table 4-6 where the structure enters deeper into the inelastic range. The difference between maximum demand displacements calculated using the modified MPA (at pier no. 4) and that of the NL-THA is 8% and the displacement profile derived using modified MPA is closely matching that profile derived from NL-THA with differences ranging from 3% at pier no. 3 to 14% at pier no. 7.

Table 4-5 Modal Deck Displacement for Bridge No. 1 for PGA = 0.45g

Deck Location		A1	P1	P2	P3	P4	P5	P6	P7	P8	A2
AVE. THA	Disp. (ft)	0.090	0.212	0.505	0.621	0.867	0.721	0.529	0.320	0.272	0.101
SPA	Disp. (ft)	0.013	0.067	0.291	0.499	0.791	0.646	0.390	0.129	0.051	0.012
	Diff. (%)	-86%	-68%	-42%	-20%	-9%	-10%	-26%	-60%	-81%	-88%
MPA	Disp. (ft)	0.046	0.179	0.397	0.519	0.856	0.663	0.446	0.240	0.223	0.094
	Diff. (%)	-49%	-15%	-21%	-16%	-1%	-8%	-16%	-25%	-18%	-6%
Modified MPA	Disp. (ft)	0.046	0.179	0.400	0.540	0.936	0.723	0.460	0.241	0.223	0.094
	Diff. (%)	-48%	-15%	-21%	-13%	8%	0%	-13%	-25%	-18%	-6%

Disp. = Deck Displacement in the transverse direction in feet.

$$Diff.\ (\%) = \frac{\delta_{\mathrm{PO}} - \delta_{\mathrm{THA}}}{\delta_{\mathrm{THA}}}$$

Where δ_{PO} is the deck displacement from pushover analysis, and δ_{THA} is the deck displacement from time history analysis.

Table 4-6 Modal Deck Displacement for Bridge No. 1 for PGA = 0.60g

Deck Location		A1	P1	P2	P3	P4	P5	P6	P7	P8	A2
AVE. THA	Disp. (ft)	0.111	0.246	0.520	0.680	1.240	0.910	0.609	0.354	0.326	0.126
SPA	Disp. (ft)	-0.017	0.067	0.307	0.574	1.073	0.844	0.441	0.136	0.052	-0.014
	Diff. (%)	-115%	-73%	-41%	-16%	-13%	-7%	-28%	-62%	-84%	-111%
MPA	Disp. (ft)	0.061	0.232	0.477	0.603	1.161	0.867	0.528	0.303	0.290	0.123
	Diff. (%)	-45%	-5%	-8%	-11%	-6%	-5%	-13%	-15%	-11%	-2%
Modified MPA	Disp. (ft)	0.065	0.237	0.492	0.698	1.336	0.974	0.548	0.304	0.290	0.124
	Diff. (%)	-41%	-4%	-5%	3%	7.7%	7%	-10%	-14%	-11%	-1.6%

Disp. = Deck Displacement in the transverse direction in feet.

$$Diff.\ (\%) = \frac{\delta_{\mathrm{PO}} - \delta_{\mathrm{THA}}}{\delta_{\mathrm{THA}}}$$

Where δ_{PO} is the deck displacement from pushover analysis, and δ_{THA} is the deck displacement from time history analysis.

4.2.3 Total Base Shear and Plastic Rotations

In order to further evaluate the results obtained from the MPA analysis, comparison is also performed for total base shear and plastic hinges' rotations at the bottom of piers between results from the SPA and MPA with corresponding values from the NL-THA procedure for increasing levels of earthquake excitation.

As for the base shear, both SPA and MPA underestimated the total base shear with regard to results from the NL-THA method for different earthquake intensities as listed in tables 4-7 and 4-8.

For PGA=0.45g, SPA underestimates the base shear by about 33% while MPA gives a better results and underestimates the base shear by only 28%. On the other hand, for PGA=0.60g base shear is underestimated by 33% and 26% for SPA and MPA, respectively.

Tables 4-7 and 4-8 list the plastic rotations at the bottom of the piers derived using the SPA and MPA for different excitation levels; 0.45g and 0.60g, respectively along with rotations derived from the NL-THA. It is observed that SPA poorly predicts plastic rotations for both cases considered while MPA provided better predictions with differences range between 8.8% to 25.7% and 3.5% to 31.9% for PGA=0.45g and 0.60g, respectively. Another significant advantage of the MPA method is that it is able to capture the plastic hinge development at P2 and P7 for PGA=0.60g, something the SPA failed to do, hence, the overall degree of agreement between MPA and NL-THA is deemed quite satisfactory.

Table 4-7 Total Base shear and Plastic rotations at bottom of piers for Bridge no. 1 (PGA=0.45g)

	Base Shear	Plastic Rotation							
		P1	P2	P3	P4	P5	P6	P7	P8
THA	**12069**	**0.000461**	**0.001694**	**0.002614**	**0.00469**	**0.00337**	**0.002511**	**0.000639**	**0.000593**
SPA	8107.41	0	0	0.000716	0.0042	0.00203	0	0	0
Diff. (%)	-32.8%	-	-	-72%	-10.5%	-29.8%	-	-	-
MPA	8640	0	0.0013	0.002	0.00428	0.00255	0.001864	0	0
Diff. (%)	-28%	-	-23.3%	-23.5%	-8.8%	-24%	-25.7%	-	-

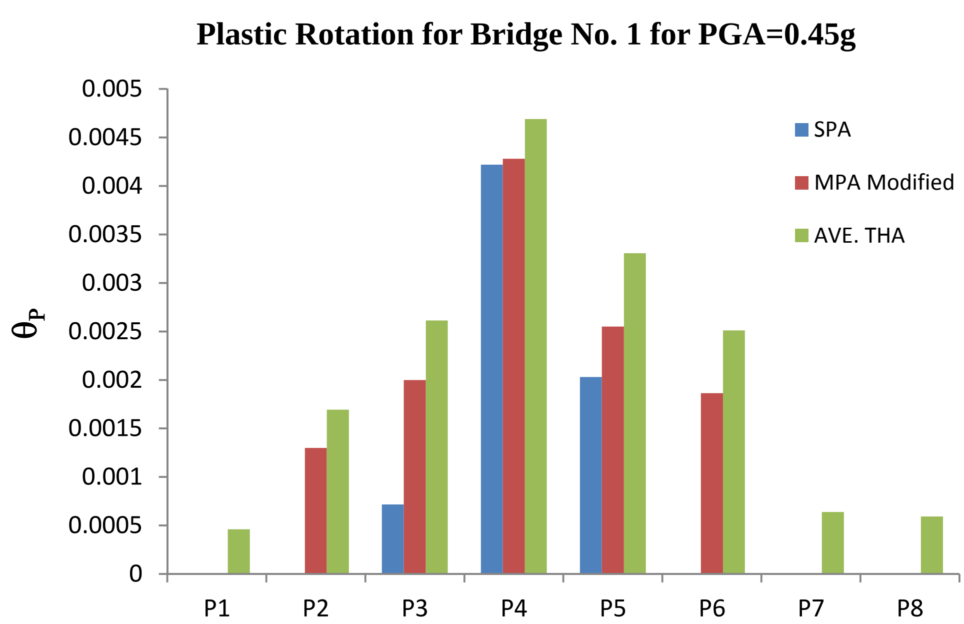

Figure 4-17 Rotations of plastic hinges at bottom of piers of Bridge no. 1, PGA=0.45g

Table 4-8 Total Base shear and Plastic rotations at bottom of piers for Bridge no. 1 (PGA=0.60g)

	Base Shear	Plastic Rotation							
		P1	P2	P3	P4	P5	P6	P7	P8
THA	**12764**	**0.00067**	**0.00243**	**0.004882**	**0.00692**	**0.006054**	**0.00405**	**0.0011**	**0.0009**
SPA	8529.5	0	0	0.0012	0.005	0.00345	0.00082	0	0
Diff. (%)	-33.2%	-	-	-72%	-10.5%	-43%	-80%	-	-
MPA	9355.32	0	0.0018	0.00375	0.0066	0.00585	0.0033	0.00075	0
Diff. (%)	-26%	-	-25%	-23.2%	-4.6%	-3.5%	-19.5%	-31.9%	-

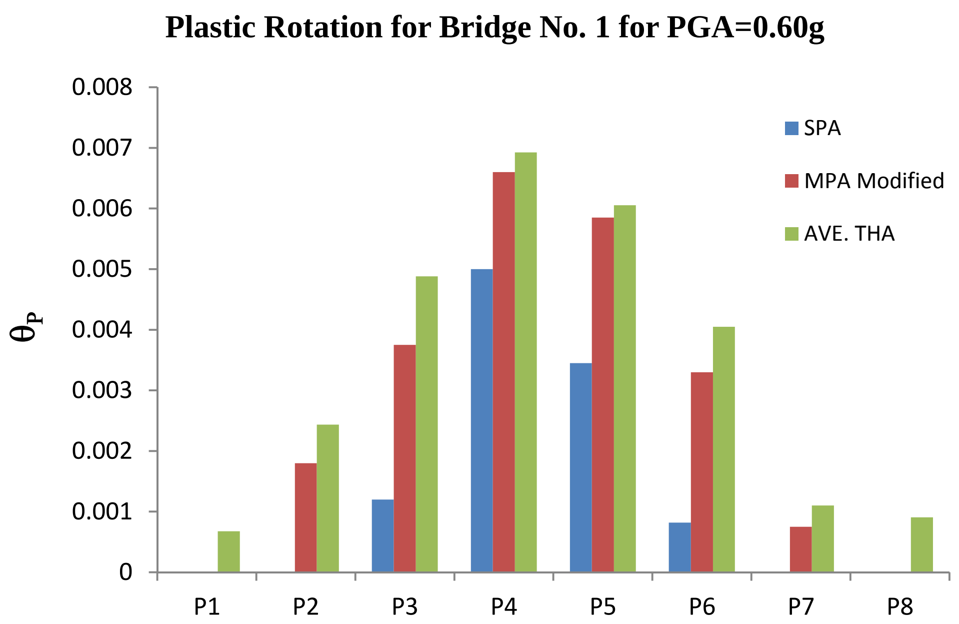

Figure 4-18 Rotations of plastic hinges at bottom of piers of Bridge no. 1, PGA=0.60g

4.3 RESULTS FOR BRIDGE NO. 2

A general description of the bridge was previously presented in section 3.3. The bridge is assessed using the modified MPA procedure with respect to control point at the most critical pier location as it showed to give the most accurate results. NL-THAs are also performed using three different acceleration time histories matching the demand spectrum in the transverse direction in order to compare results. Analyses are carried out using the SAP2000 program (CSI, 2009). Figure 4-19 shows the finite element modeling of the bridge.

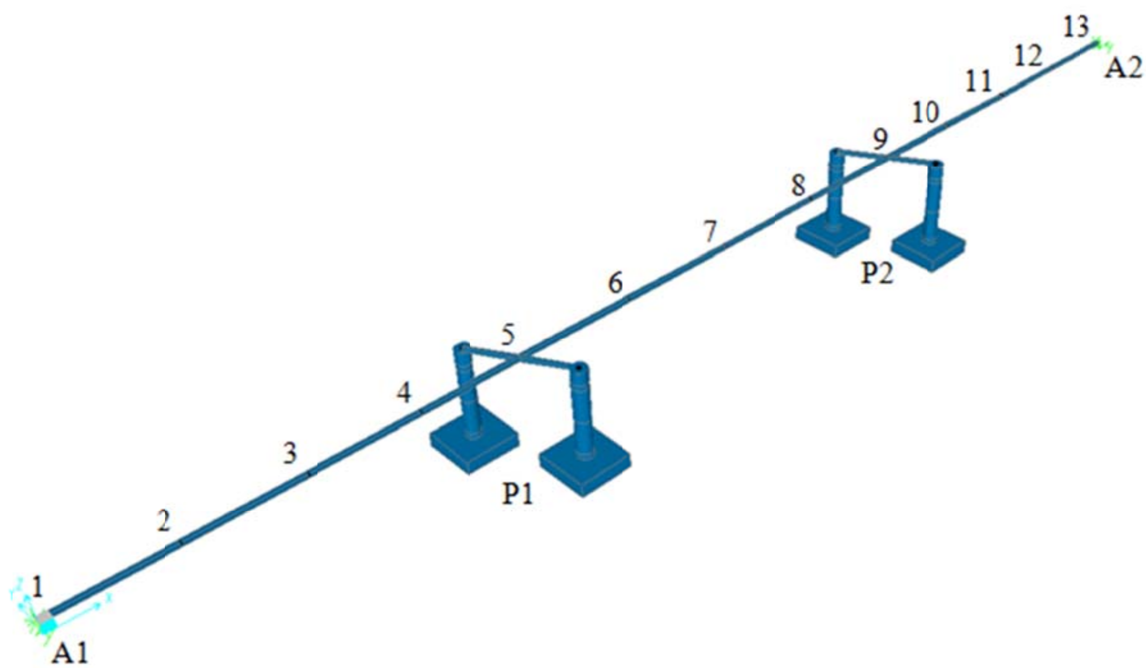

Figure 4-19 Finite Element Model of Bridge No. 2

4.3.1 Dynamic Characteristics

The dynamic characteristics required within the context of the MPA approach, were determined using standard eigenvalue analysis. Figure 4-20 and Figure 4-21 illustrate the first two fundamental transverse mode shapes of the bridge (modes 2 and 4) with the corresponding natural periods. Modal periods and frequencies are listed in Table 4-9, modal participation factors are listed in Table 4-10, and modal participating mass ratios are listed in Table 4-11.

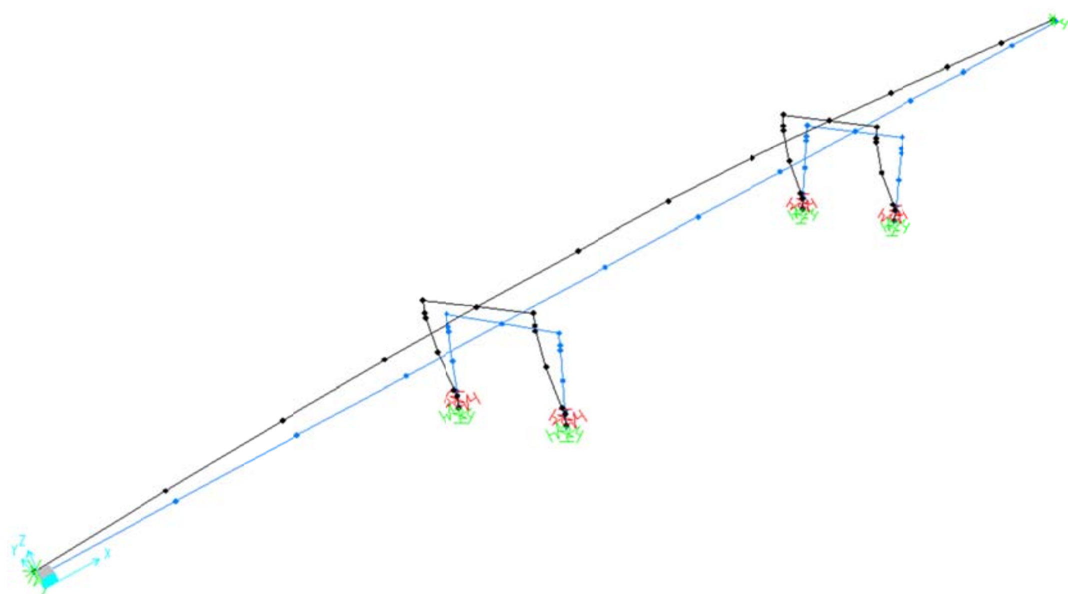

Mode 2: T_2=0.5621s

Figure 4-20 Deformed Shape of Mode 2 (Bridge No. 2)

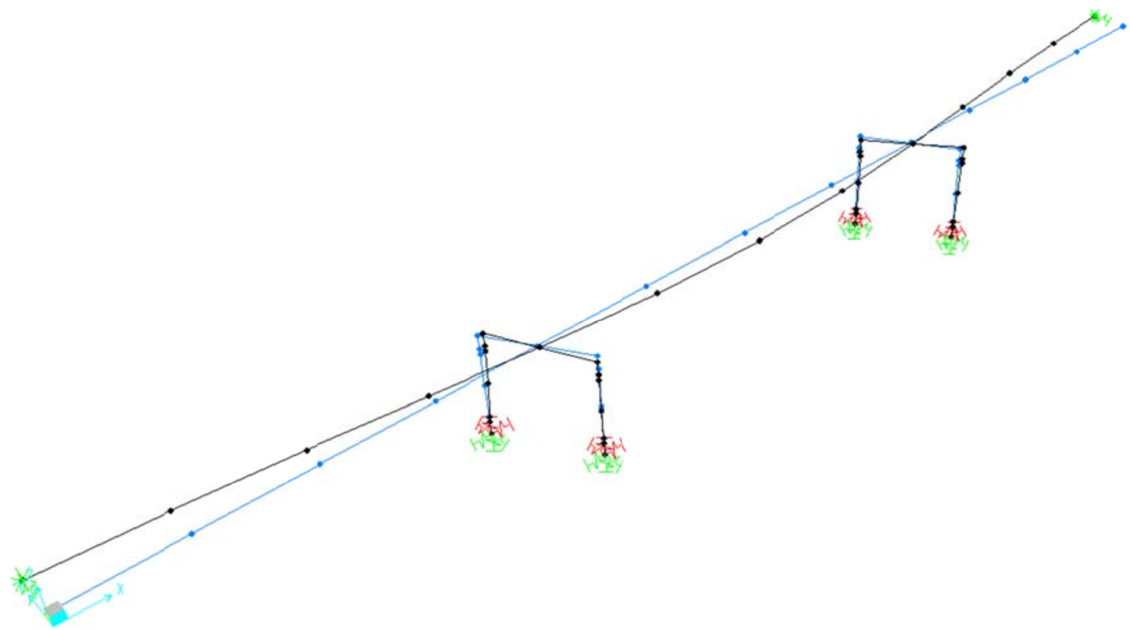

Mode 4: T_4=0.12516s

Figure 4-21 Deformed Shape of Mode 4 (Bridge No. 2)

Table 4-9 Modal Periods and Frequencies (Bridge No. 2)

OutputCase	StepType	StepNum	Period Sec	Frequency Cyc/sec	CircFreq rad/sec	Eigenvalue rad2/sec2
Modal	Mode	1.000000	0.966007	1.0352E+00	6.5043E+00	4.2306E+01
Modal	Mode	2.000000	0.526100	1.9008E+00	1.1943E+01	1.4263E+02
Modal	Mode	3.000000	0.210878	4.7421E+00	2.9795E+01	8.8777E+02
Modal	Mode	4.000000	0.125163	7.9896E+00	5.0200E+01	2.5200E+03
Modal	Mode	5.000000	0.081535	1.2265E+01	7.7061E+01	5.9385E+03
Modal	Mode	6.000000	0.068764	1.4543E+01	9.1373E+01	8.3491E+03
Modal	Mode	7.000000	0.048488	2.0624E+01	1.2958E+02	1.6792E+04
Modal	Mode	8.000000	0.034272	2.9178E+01	1.8333E+02	3.3610E+04
Modal	Mode	9.000000	0.030670	3.2605E+01	2.0486E+02	4.1969E+04
Modal	Mode	10.000000	0.024273	4.1198E+01	2.5885E+02	6.7004E+04
Modal	Mode	11.000000	0.022045	4.5361E+01	2.8501E+02	8.1233E+04
Modal	Mode	12.000000	0.018333	5.4547E+01	3.4273E+02	1.1747E+05

Table 4-10 Modal Participation Factors (Bridge No. 2)

OutputCase	StepType	StepNum	Period Sec	UX Kip-s2	UY Kip-s2	UZ Kip-s2
Modal	Mode	1.000000	0.966007	11.908197	0.254998	0.000000
Modal	Mode	2.000000	0.526100	0.273393	-11.131288	0.000000
Modal	Mode	3.000000	0.210878	-1.907E-12	-9.051E-14	0.000000
Modal	Mode	4.000000	0.125163	-0.001474	-4.179216	0.000000
Modal	Mode	5.000000	0.081535	1.396E-11	2.655E-13	0.000000
Modal	Mode	6.000000	0.068764	-3.028E-11	-8.692E-13	0.000000
Modal	Mode	7.000000	0.048488	0.000825	0.654170	0.000000
Modal	Mode	8.000000	0.034272	0.008127	-0.000365	0.000000
Modal	Mode	9.000000	0.030670	7.547E-11	1.627E-12	0.000000
Modal	Mode	10.000000	0.024273	5.445E-10	1.165E-11	0.000000
Modal	Mode	11.000000	0.022045	-0.000359	0.122636	0.000000
Modal	Mode	12.000000	0.018333	0.004605	-0.000223	0.000000

Table 4-11 Modal Participating Mass Ratios (Bridge No. 2)

OutputCase	StepType	StepNum	Period Sec	UX	UY	UZ	SumUX	SumUY
Modal	Mode	1.000000	0.966007	0.99947	0.00046	0.00000	0.99947	0.00046
Modal	Mode	2.000000	0.526100	0.00053	0.87331	0.00000	1.00000	0.87377
Modal	Mode	3.000000	0.210878	0.00000	0.00000	0.00000	1.00000	0.87377
Modal	Mode	4.000000	0.125163	1.531E-08	0.12310	0.00000	1.00000	0.99687
Modal	Mode	5.000000	0.081535	0.00000	0.00000	0.00000	1.00000	0.99687
Modal	Mode	6.000000	0.068764	0.00000	0.00000	0.00000	1.00000	0.99687
Modal	Mode	7.000000	0.048488	4.794E-09	0.00302	0.00000	1.00000	0.99989
Modal	Mode	8.000000	0.034272	4.655E-07	9.366E-10	0.00000	1.00000	0.99989
Modal	Mode	9.000000	0.030670	0.00000	0.00000	0.00000	1.00000	0.99989
Modal	Mode	10.000000	0.024273	0.00000	0.00000	0.00000	1.00000	0.99989
Modal	Mode	11.000000	0.022045	9.086E-10	0.00011	0.00000	1.00000	1.00000
Modal	Mode	12.000000	0.018333	1.494E-07	3.512E-10	0.00000	1.00000	1.00000

4.3.2 Evaluation of Different Response Quantities

Displacement demands were derived for bridge no. 2 using the inelastic spectra. The demand spectrum was the design one or multiple of it. The bridge was subsequently assessed using NL-THA, for ground acceleration records matching the demand spectra. Peak ground accelerations of (PGA) 0.30g and 0.45g were considered. Comparison is performed for the maximum demand displacement in the transverse direction, total base shear and rotations of plastic hinges.

Evaluation of different procedures

Results of the standard and modal pushover approaches were evaluated by comparing them with those from the NL-THA, the latter is considered to be the most rigorous procedure to compute seismic demands. To this effect, a set of three real time acceleration records compatible with the design spectrum was used in the NL-THA analyses. The deck displacements determined from each of the SPA and MPA analyses with respect to the control point of the most critical pier were compared with those from NL-THA for increasing levels of earthquake excitation, as shown in Figure 4-22 and Figure 4-23 for PGA = 0.30g and 0.45g respectively.

It is noted that the deck displacements shown in the figures as the THA case are the average of the peak displacements recorded in the structure during the three time-history analyses. As shown in Figure 4-22, it is observed that the SPA procedure predicts well the transverse displacements of the bridge and slightly underestimated the maximum displacement demand at the mid-span point of the middle span by 5% (2.57 inches compared to the 2.70 inches predicted by NL-THA); such area is dominated by the first fundamental transverse mode. Similarly, MPA procedure which accounts for two transverse modes predicts well the deck displacements (2.62 inches compared to the 2.70 inches predicted by NL-THA) of the bridge with only 3% difference and slightly improved the displacement profile from that obtained from SPA with regards to results derived from the NL-THA. The reason for such close results obtained from the SPA and MPA analyses would be to the fact that the first fundamental transverse mode (mode 2) contributes to approximately 88% of the mass of the bridge (as shown in Table 4-11).

As the level of excitation increases, the displacement profiles derived by the MPA as well as SPA methods tend to match that obtained by the NL-THA as shown in Figure 4-23 for the case of earthquake intensity equals 1.5 times the design earthquake intensity. MPA slightly overestimated the maximum demand displacement by only 2% (4.1 inches, compared to the 3.936 inches predicted by NL-THA).

Also shown in Figure 4-24 and Figure 4-25 are the plastic rotations at the top of the piers derived using the MPA for different excitation levels; 0.30g and 0.45g, respectively, along with those rotations predicted from the NL-THA. For the case of seismic intensity of PGA = 0.30g, MPA underestimates the plastic rotation by about 13% at pier 1 and by 28% at pier 2. On the other hand, as the level of seismic loading increases; PGA = 0.45g, MPA overestimates the plastic rotation by only 3% at pier 1 and by 4% at pier 2.

For the base shear, MPA predicts very well the total base shear of the bridge. For the first level of earthquake excitation (PGA=0.30g), a total base shear of 3059.06 kips was predicted compared to 2983.02 kips from the NL-THA case with a difference of only 2.5%. On the other hand, for PGA=0.45g, a base shear value of 4124.8 kips was predicted compared to a value of 3877.23 kips from NL-THA with a difference of 6.4%.

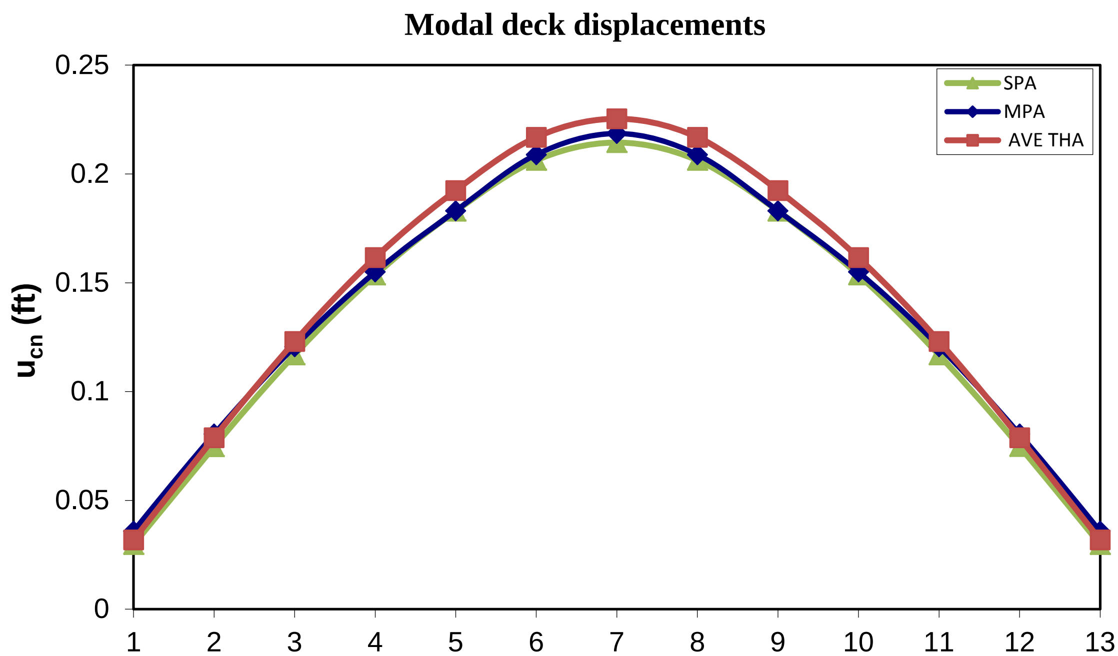

Figure 4-22 Deck displacements for bridge no. 2 calculated from SPA, MPA and THA, for PGA = 0.30g

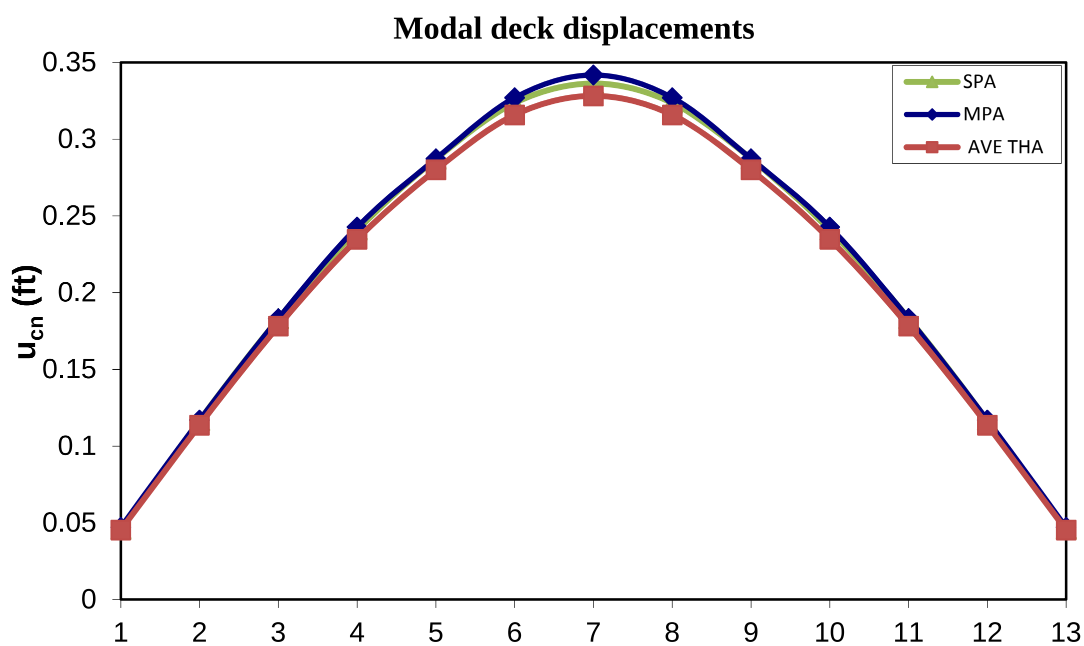

Figure 4-23 Deck displacements for bridge no. 2 calculated from SPA, MPA and THA, for PGA = 0.45g

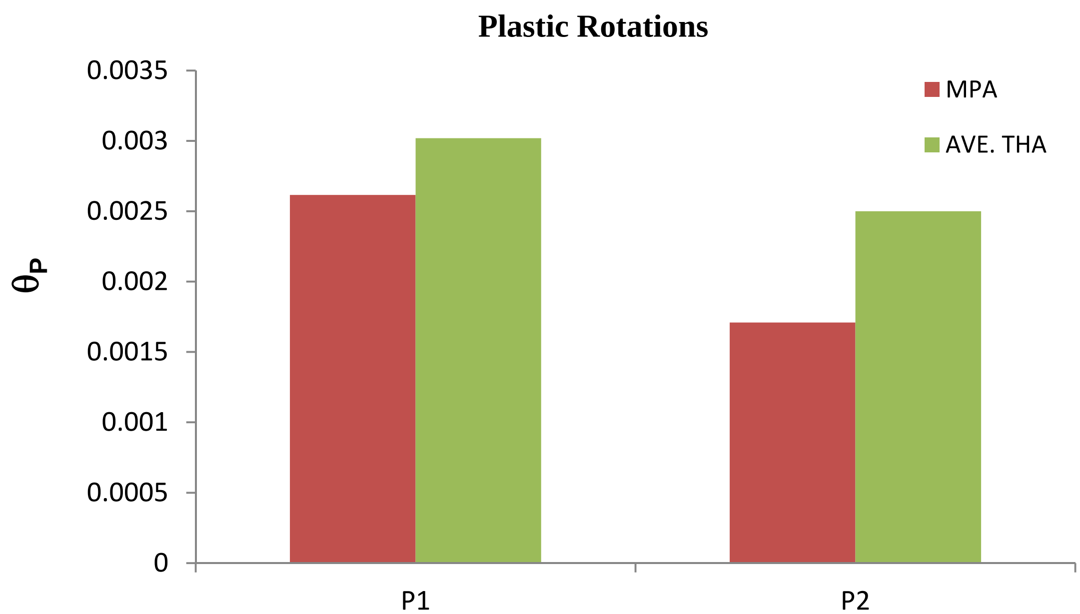

Figure 4-24 Plastic rotations at the top of the piers for bridge no. 2, for PGA = 0.30g

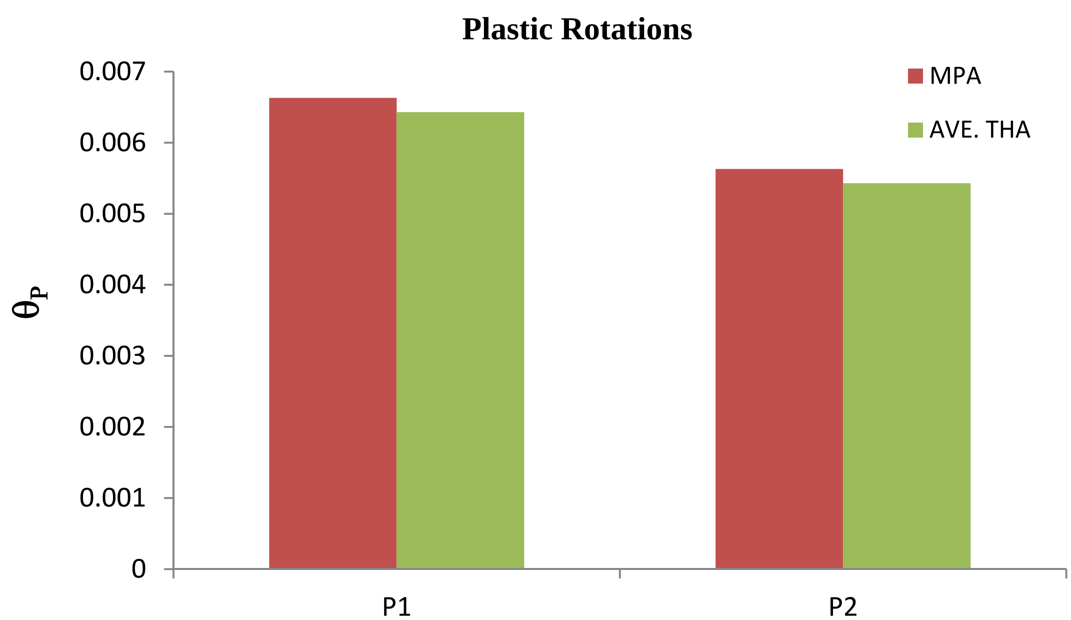

Figure 4-25 Plastic rotations at the top of the piers for bridge no. 2, for PGA = 0.45g

4.4 RESULTS OF BRIDGE NO 3

As mentioned before, this bridge is the same as bridge no. 2 with only one modification; no skew angle was considered for this bridge instead of 30 degrees for bridge no. 2. A general description of this bridge was previously presented in section 3.4. The same considerations, which were considered for bridge no. 2, are applied here. The bridge is assessed using the modified MPA procedure with respect to control point at the most critical pier location as it showed to give the most accurate results. NL-THAs are also performed in the transverse direction using three different acceleration time histories matching the demand spectrum in order to compare results. Figure 4-26 shows the finite element modeling of the bridge. Behavior of this bridge will be assessed and compared with behavior of bridge no. 2 in order to study the effect of skewness on the overall behavior of the bridge.

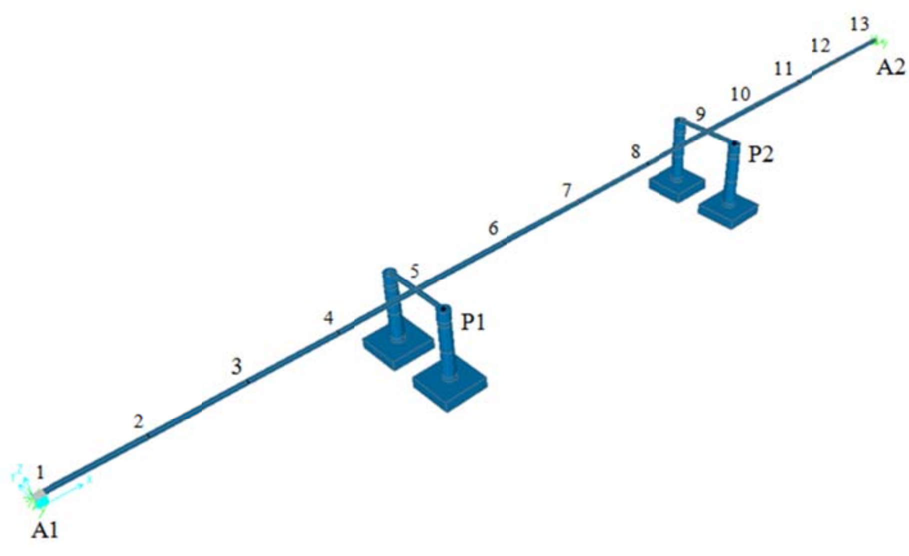

Figure 4-26 Finite Element Model of Bridge No. 3

4.4.1 Dynamic Characteristics

The dynamic characteristics required within the context of the MPA approach, were determined using standard eigenvalue analysis. Figure 4-27 and Figure 4-28 illustrate the first two fundamental transverse mode shapes of the bridge (modes 2 and 4) with the corresponding natural periods. Modal periods and frequencies are listed in Table 4-12, modal participation factors are listed in Table 4-13, and modal participating mass ratios are listed in Table 4-14.

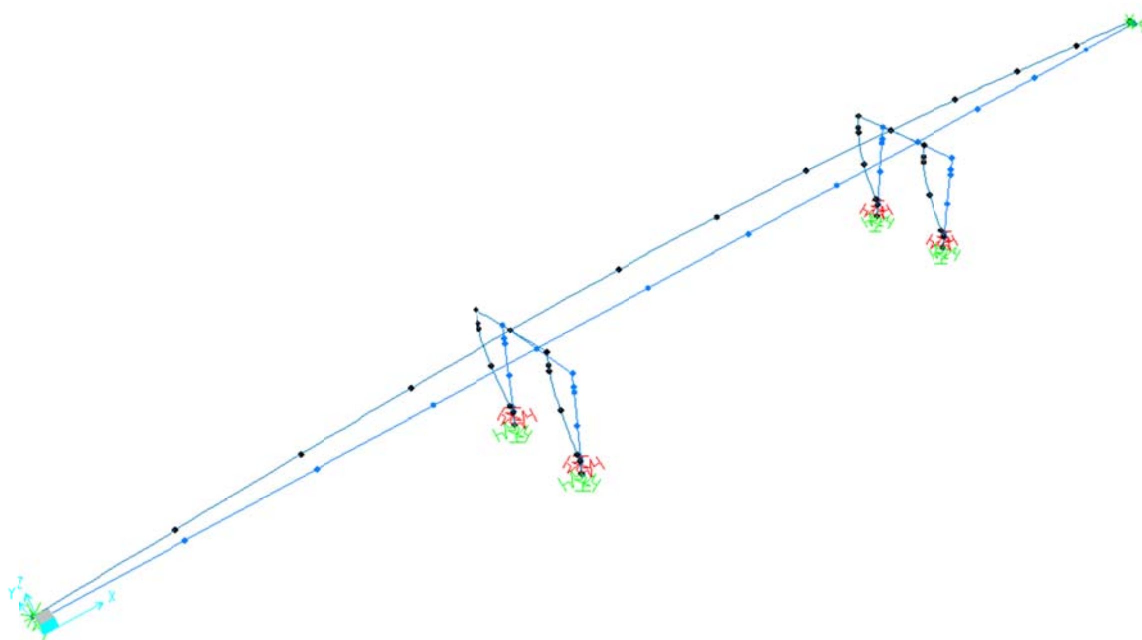

Mode 2: T_2=0.52406s

Figure 4-27 Deformed Shape of Mode 2 (Bridge No. 3)

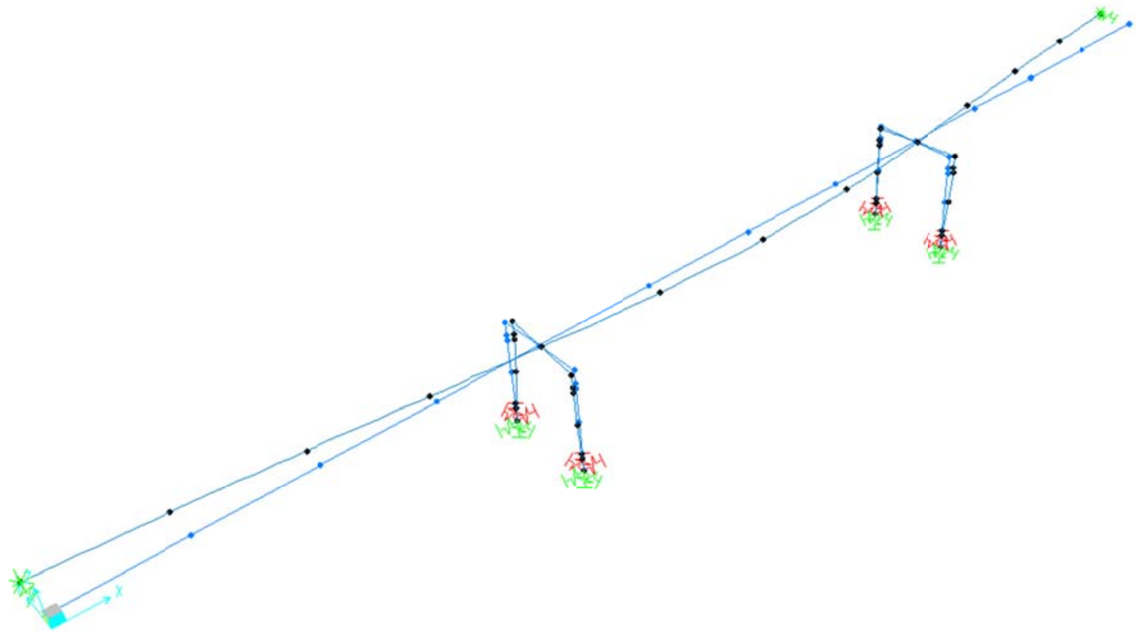

Mode 4: T_4=0.12519s

Figure 4-28 Deformed Shape of Mode 4 (Bridge No. 3)

Table 4-12 Modal Periods and Frequencies (Bridge No. 3)

OutputCase	StepType	StepNum	Period Sec	Frequency Cyc/sec	CircFreq rad/sec	Eigenvalue rad2/sec2
Modal	Mode	1.000000	0.968387	1.0326E+00	6.4883E+00	4.2098E+01
Modal	Mode	2.000000	0.524058	1.9082E+00	1.1989E+01	1.4375E+02
Modal	Mode	3.000000	0.210797	4.7439E+00	2.9807E+01	8.8845E+02
Modal	Mode	4.000000	0.125188	7.9880E+00	5.0190E+01	2.5191E+03
Modal	Mode	5.000000	0.081528	1.2266E+01	7.7068E+01	5.9395E+03
Modal	Mode	6.000000	0.068767	1.4542E+01	9.1370E+01	8.3484E+03
Modal	Mode	7.000000	0.048492	2.0622E+01	1.2957E+02	1.6789E+04
Modal	Mode	8.000000	0.034272	2.9178E+01	1.8333E+02	3.3610E+04
Modal	Mode	9.000000	0.030672	3.2603E+01	2.0485E+02	4.1964E+04
Modal	Mode	10.000000	0.024274	4.1197E+01	2.5885E+02	6.7002E+04
Modal	Mode	11.000000	0.022045	4.5362E+01	2.8502E+02	8.1235E+04
Modal	Mode	12.000000	0.018333	5.4547E+01	3.4273E+02	1.1746E+05

Table 4-13 Modal Participation factors (Bridge No. 3)

OutputCase	StepType	StepNum	Period Sec	UX Kip-s2	UY Kip-s2	UZ Kip-s2
Modal	Mode	1.000000	0.968387	11.911335	-1.556E-11	0.000000
Modal	Mode	2.000000	0.524058	-3.548E-12	-11.134043	0.000000
Modal	Mode	3.000000	0.210797	3.015E-12	1.392E-13	0.000000
Modal	Mode	4.000000	0.125188	3.765E-12	-4.179684	0.000000
Modal	Mode	5.000000	0.081528	1.358E-11	-3.930E-14	0.000000
Modal	Mode	6.000000	0.068767	-3.140E-11	-5.819E-14	0.000000
Modal	Mode	7.000000	0.048492	6.695E-11	0.653963	0.000000
Modal	Mode	8.000000	0.034272	0.008077	-3.169E-16	0.000000
Modal	Mode	9.000000	0.030672	-7.757E-11	-1.548E-15	0.000000
Modal	Mode	10.000000	0.024274	5.559E-10	-5.962E-14	0.000000
Modal	Mode	11.000000	0.022045	8.288E-10	0.122801	0.000000
Modal	Mode	12.000000	0.018333	0.004576	1.046E-13	0.000000

Table 4-14 Modal Participating Mass Ratios (Bridge No. 3)

OutputCase	StepType	StepNum	Period Sec	UX	UY	UZ
Modal	Mode	1.000000	0.968387	1.00000	0.00000	0.00000
Modal	Mode	2.000000	0.524058	0.00000	0.87374	0.00000
Modal	Mode	3.000000	0.210797	0.00000	0.00000	0.00000
Modal	Mode	4.000000	0.125188	0.00000	0.12313	0.00000
Modal	Mode	5.000000	0.081528	0.00000	0.00000	0.00000
Modal	Mode	6.000000	0.068767	0.00000	0.00000	0.00000
Modal	Mode	7.000000	0.048492	0.00000	0.00301	0.00000
Modal	Mode	8.000000	0.034272	4.598E-07	0.00000	0.00000
Modal	Mode	9.000000	0.030672	0.00000	0.00000	0.00000
Modal	Mode	10.000000	0.024274	0.00000	0.00000	0.00000
Modal	Mode	11.000000	0.022045	0.00000	0.00011	0.00000
Modal	Mode	12.000000	0.018333	1.476E-07	0.00000	0.00000

4.4.2 Evaluation of Different Response Quantities

Displacement demands were derived for bridge no. 3 using the inelastic spectra. The demand spectra were the same as that used for bridge no. 2. The bridge was subsequently assessed using NL-THA, for ground acceleration records matching the demand spectra. Analyses were performed for two levels of seismic load intensity. Peak ground accelerations (PGA) of 0.30g and 0.45g were considered. Comparison is performed for the maximum demand displacement in the transverse direction, total base shear and rotations of plastic hinges.

Evaluation of different procedures

Results of the standard and modal pushover approaches were evaluated by comparing them with those from the NL-THA, the latter is considered to be the most rigorous procedure to compute seismic demands. A set of three real time acceleration records compatible with the design spectra was used in the NL-THA analyses. The deck displacements determined from each of the SPA and MPA analyses with respect to the control point of the most critical pier were compared with those from NL-THA for increasing levels of earthquake excitation, as shown in Figure 4-29 and Figure 4-30 for PGA = 0.30g and 0.45g respectively.

It is noted that the deck displacements shown in the figures as the THA case are the average of the peak displacements recorded in the structure during the three time-history analyses.

As shown in Figure 4-29, it is observed that the SPA procedure predicts well the transverse displacements of the bridge and slightly underestimated the maximum demand displacement by 6% as compared to the NL-THA results at the mid-span point of the middle span (2.33 inches compared to the 2.47 inches predicted by NL-THA); such area is dominated by the first fundamental transverse mode. Similarly, MPA procedure which accounts for two transverse modes predicts well the deck displacements, it underestimated the maximum demand displacement by only 3% difference as compared to the NL-THA results (2.39 inches compared to the 2.47 inches predicted by NL-THA).

As noticed before, SPA results matched closely the results from MPA analyses and that would be referred to the fact that the first fundamental transverse mode (mode 2) contributed to approximately 87% of the total mass of the bridge (as shown in Table 4-14).

As the level of excitation increases, the displacement profiles derived by the MPA as well as SPA method tend to match that obtained from the NL-THA as shown in Figure 4-30 for the case of earthquake intensity equals 1.5 times the design earthquake (PGA = 0.45g). MPA slightly overestimated the maximum demand displacement by 4% as compared to the NL-THA results (4.05 inches, compared to the 3.888 inches predicted by NL-THA).

Also shown in Figure 4-31 and Figure 4-32 are the plastic rotations at the top of the piers derived using the MPA for different excitation levels; 0.30g and 0.45g, respectively, along with those rotations predicted from the NL-THA. For the case of seismic intensity of PGA = 0.30g, MPA underestimates the plastic rotation by about 24% at pier 1 and 21% at pier 2. On the other hand, as the level of seismic loading increases; PGA = 0.45g, MPA overestimates the plastic rotation by only 8% at pier 1 and underestimated it by 1% at pier 2.

For the base shear, MPA also predicts very well the total base shear of the bridge as was noted in bridge no. 2. For the first level of earthquake excitation (PGA=0.30g), a total base shear of 2895.3 kips was predicted comparing to 2762.77 kips from the NL-THA case with a difference of only 4.8%. On the other hand, for PGA=0.45g, a base shear value of 4011.89 kips was predicted compared to a value of 3864.66 kips from NL-THA with a difference of 4.0%.

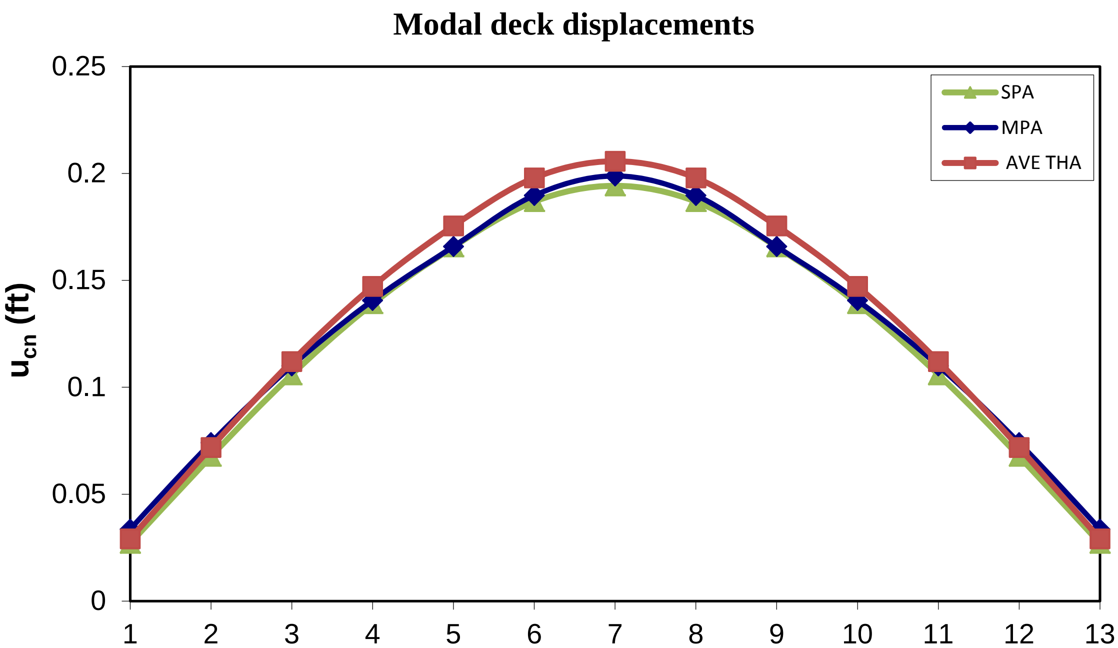

Figure 4-29 Deck displacements for bridge no. 3 calculated from SPA, MPA and THA, for PGA = 0.30g

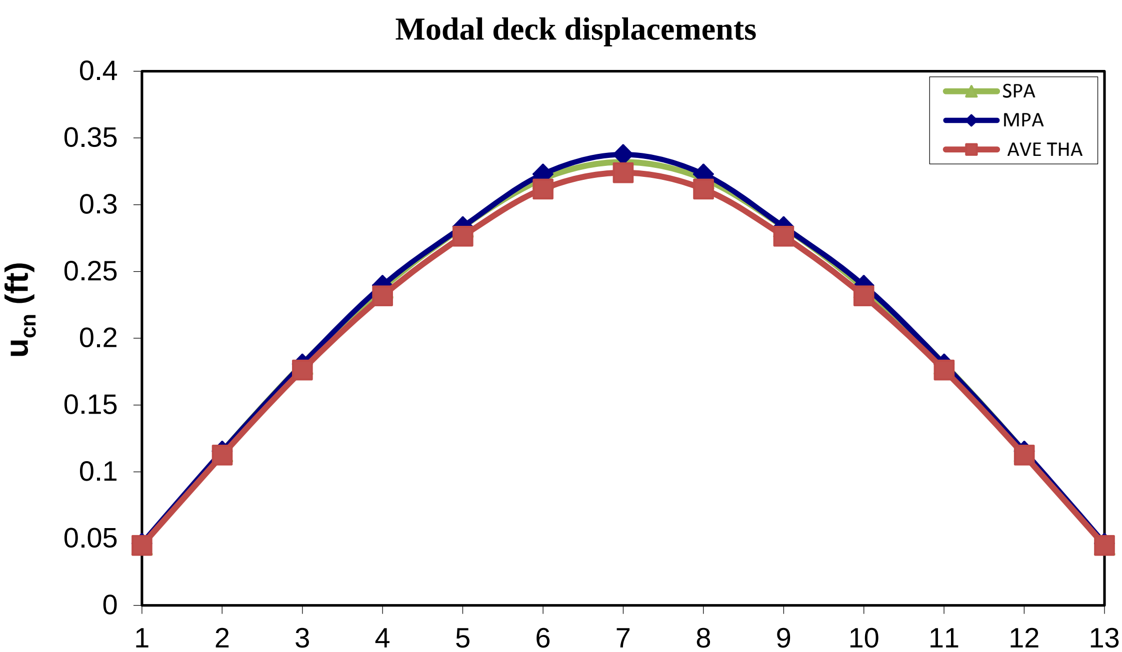

Figure 4-30 Deck displacements for bridge no. 3 calculated from SPA, MPA and THA, for PGA = 0.45g

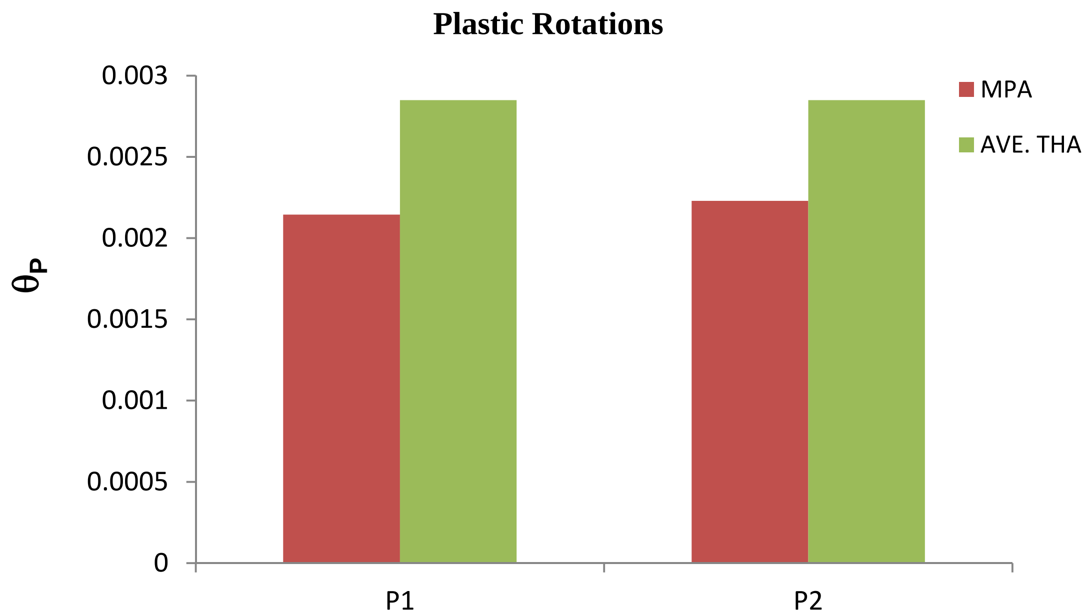

Figure 4-31 Plastic rotations at the top of the piers for bridge no. 3, for PGA = 0.30g

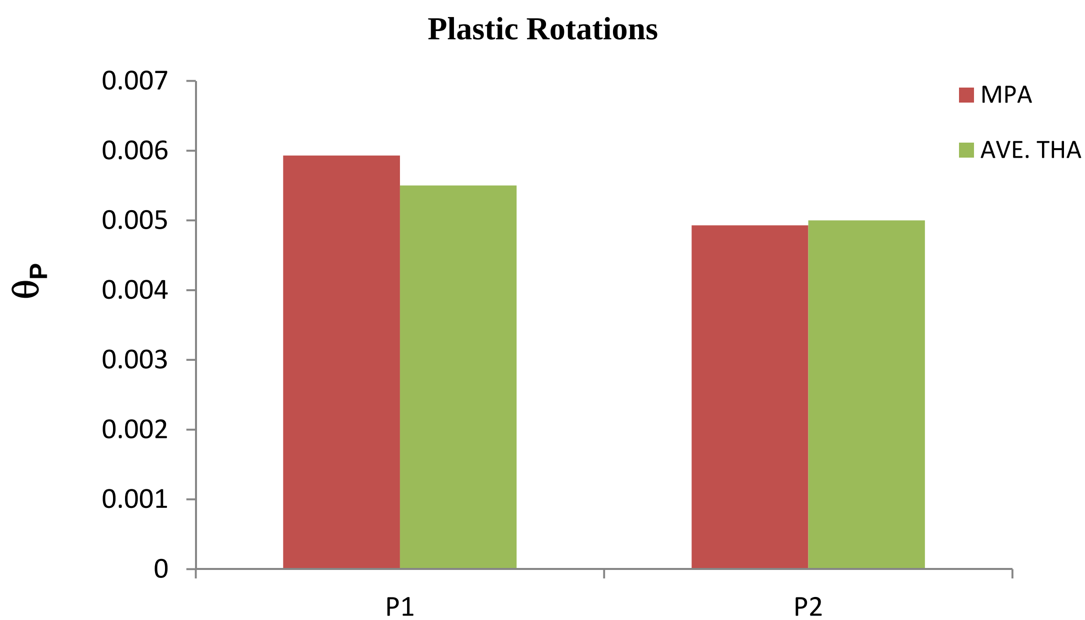

Figure 4-32 Plastic rotations at the top of the piers for bridge no. 3, for PGA = 0.45g

4.5 COMPARISON BETWEEN RESULTS OF BRIDGES NO. 2 AND NO. 3

In order to study the effect of skewness on estimating the demand displacement of bridges using MPA, bridges no. 2 and 3 were studied. These two bridges are the same with only one difference: bridge no. 2 has a skew angle of 30 degrees from a line perpendicular to a straight bridge centerline alignment while bridge no. 3 is not skewed.

Comparison is made for many parameters in the transverse direction as listed in Table 4-15. By examining the data shown, skewness found to have a little contribution to bridge behavior. That effect took place on the bridge behavior through changing the natural period of the 1st fundamental mode from 0.5621 to 0.52406 seconds (7.25% difference). Both participation factor and mass participation factor were almost the same and had less than 1% difference. Demand displacement of the control node for the first level of earthquake excitation (PGA = 0.30g) increased due to skew angle by 9.5%, 10.39%, and 9.9% for the NL-THA, SPA, and MPA, respectively. On the other hand, for the second level of earthquake (PGA = 0.45g), demand displacement of the control node was very close and slightly changed by only 1.2% for all cases.

Same observations were noted for the comparison of total base shear. For PGA=0.30g, total base shear increased due to skew angle by 9% while for PGA=0.45g, base shear increase slightly by only 2%.

Table 4-15 Comparison of properties and transverse demands for bridge no. 2 and bridge no. 3

		Bridge No. 2	Bridge No. 3	Ratio
1st Fundamental Transverse Mode	Natural Period	0.5621	0.52406	1.07258
	Participation Factor	11.1312	11.134	0.9997
	Mass Participation Factor	87.331%	87.374%	0.9995
2nd Fundamental Transverse Mode	Natural Period	0.12516	0.1252	0.9996
	Participation Factor	4.1792	4.1796	0.9999
	Mass Participation Factor	12.31%	12.313%	0.9997
NL-THA (0.30g)	Demand Displacement (ft)	0.22536	0.20571	1.0955
SPA		0.2144219	0.194233	1.1039
MPA		0.218591	0.198826	1.099
NL-THA (0.45g)		0.32822	0.32401	1.012
SPA		0.33625	0.331968	1.012
MPA		0.34181	0.33759	1.012
NL-THA (0.30g)	Base Shear (kips)	2983.02	2762.776	1.080
MPA		3159.06	2895.3	1.091
NL-THA (0.45g)		3877.23	3864.66	1.005
MPA		4124.8	4011.89	1.028

$$\text{Ratio} = \frac{\text{Parameter Value}_{\text{Bridge no. 2}}}{\text{Parameter Value}_{\text{Bridge no. 3}}}$$

4.6 COMPARISON WITH PREVIOUS RESEARCH

Different Nonlinear Static Procedures (NSP) were developed that can be used for seismic analysis and rehabilitation of structures. (FEMA-273, 1997) and (FEMA-356, 2000) applied the Displacement Coefficient Method (DCM) while the Applied Technology Council developed (ATC-40, 1996) that utilized the Capacity Spectrum Method (CSM) for the assessment of Buildings. For the case of bridges, (AlAyed, 2002) evaluated the applicability of NSP by implementing the DCM and CSM to bridges.

For comparison purposes and to further evaluate the MPA results with regard to other performance-based seismic analyses, results from the current study will be compared with the results from (AlAyed, 2002) study for the first two bridges studied in the previous sections, bridge no. 1 and bridge no. 2. Comparison will be performed for maximum transverse demand displacement, total base shear, and rotations of plastic hinges.

Table 4-16 lists comparison of results obtained using NL-THA, MPA, and DCM methods. Both MPA and DCM are predicting the responses very well and in good agreement with the most rigorous method, NL-THA procedure.

For long curved-in-plan bridge, bridge no. 1, MPA tends to overestimate the maximum demand displacement for the level of earthquake studied while DCM underestimates it. For other response quantities, both methods tend to underestimate the responses.

For regular bridge like bridge no. 2 studied, both methods underestimate the demand displacement for lower level of earthquake excitation while for higher levels of earthquake excitation, they overestimate demand displacements. On the other hand, total base shear is always overestimated by both methods for different levels of earthquake load.

Table 4-16 Comparison of results obtained using NL-THA, MPA, and DCM methods

		Displacement (Inch.)	**Rotation (rad)**	**Base shear (Kips)**
Bridge No. 1	**THA (0.45g)**	**0.87**	**0.00469**	**12069**
	MPA	0.9358	0.00428	8640
	Diff. (%)	+6.3%	-8.8%	-28%
	DCM	0.83	0.00456	8467
	Diff. (%)	-5.7%	-3%	-30%
Bridge No. 2	**THA (0.30g)**	**0.225**	**0.00302**	**2983.02**
	MPA	0.218	0.00262	3059.06
	Diff. (%)	-3.2%	-13%	+2.5%
	DCM	0.215	0.00325	3076.33
	Diff. (%)	-4.5%	+8%	+3.12%
	THA (0.45g)	**0.3282**	**0.00643**	**3877.23**
	MPA	0.3418	0.00663	4124.8
	Diff. (%)	+4.1%	+3%	+6.4%
	DCM	0.335	0.00727	4134.33
	Diff. (%)	+2.0%	+14%	+7%

5. PARAMETRIC STUDY

5.1 INTRODUCTION

The developed MPA procedure has been tested for three bridges in order to evaluate the applicability of the procedure in estimating the demand displacements. Being an approximate method, however, it should be evaluated comprehensively before practical application to curved bridge evaluation and design. The objective of this chapter is to expand the previously obtained results and evaluate the accuracy of the MPA procedure in estimating the demand displacement and bas shear for a wide range of curved bridges.

Different parameters may affect the behavior of curved bridges under seismic loading and consequently the estimated demand displacement derived from the MPA. Among these parameters are curvature, span configuration, cross sectional geometry and pier height. A parametric study is performed in order to quantify the effect of such parameters on estimating the demand displacement and base shear using the MPA procedure and compare the results with those obtained from the NL-THA.

5.2 ANALYSIS CASES

To study the effect of various bridge parameters on the response of curved bridges and the accuracy of the estimated demand displacements derived using the MPA procedure, a parametric study was performed which focused on the variation of span configuration and length, bridge cross-section geometry, radius of curvature and pier height.

Two bridge cross-section shapes were considered.

- Steel-I girder cross section.
- Steel Box girder cross section.

For each cross-section type, six typical bridge models were considered:

- Two span – 240, and 240 feet long;
- Two span – 180, and 180 feet long;
- Two span – 120, and 120 feet long;
- Three span – 180, 240, and 180 feet long;
- Three span – 140, 180, and 140 feet long;
- Three span – 100, 120, and 100 feet long.

Each of the typical bridge models was analyzed twice using different pier height. First, pier height was taken as 50 feet, and then changed to 20 feet in the second analysis. It was assumed that the pier and abutment foundations are stiff and fixed restraints were assumed in all bridge models.

Each of the above 24 bridges was configured as curved bridges with radii of 500, 1000, and 1600 feet, resulting in 72 bridge configurations. These configurations need to be designed first according to the code and design standards and then evaluated using both the MPA and the NL-THA procedures.

The bridge models' cross sections were analyzed and designed using the software DESCUS I (Fu, DESCUS I, 2009) for curved I Girder and DESCUS II (Fu, DESCUS II, 2009) for Box Girder Bridges, respectively. Descus input files for analyzing and designing bridge models are provided in Appendix C.

The computer programs DESCUS I & II will perform the complete analysis of a horizontally curved bridge composed of flanged steel sections or steel box sections, respectively, which act either compositely or noncompositely with a concrete deck. The program can be run using either Working Stress Design (WSD) method, the Load Factor Design (LFD) method or the Load and Resistance Factor Design (LRFD) method. The bridge may be of arbitrary plan configuration and can be continuous and skewed over supports. The girders may have a high degree of curvature and may be nonconcentric.

The program models the bridge structure as a two-dimensional grid in a stiffness format with three degrees-of-freedom at each nodal point (corresponding to torsion, shear, and bending moment). All nodal locations, member connectivity, and properties are generated internally from basic input. All dead load (DL) computations are performed automatically within the program to satisfy the construction conditions specified by AASHTO. Additional dead load (DL) and superimposed dead load (SDL) are allowed to input to combine with the program-generated dead load. All live load (LL) computations also are performed automatically where the AASHTO truck and lane loadings are applied to an influence surface previously generated for the entire bridge.

In this study, bridge models were analyzed and designed according to the Load and Resistance Factor Design (LRFD) method.

For each bridge, two different cross sections were designed. The first one is typical cross section (1), depending on the span length, which is utilized along the span length of the bridge except at the pier locations where a second cross section (Typical cross section (2)) is used that extended to one fourth of the span length on each side of the pier.

Figure 5-1 through Figure 5-12 show typical cross sections with dimensions designed for use in the current study. Figure 5-13 shows a typical finite element model.

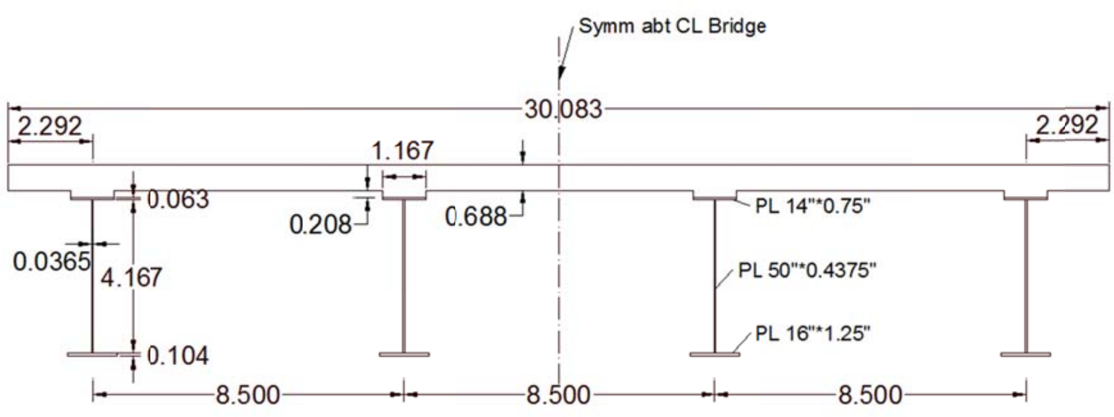

Figure 5-1 Typical steel I cross section (1) for L = 120ft

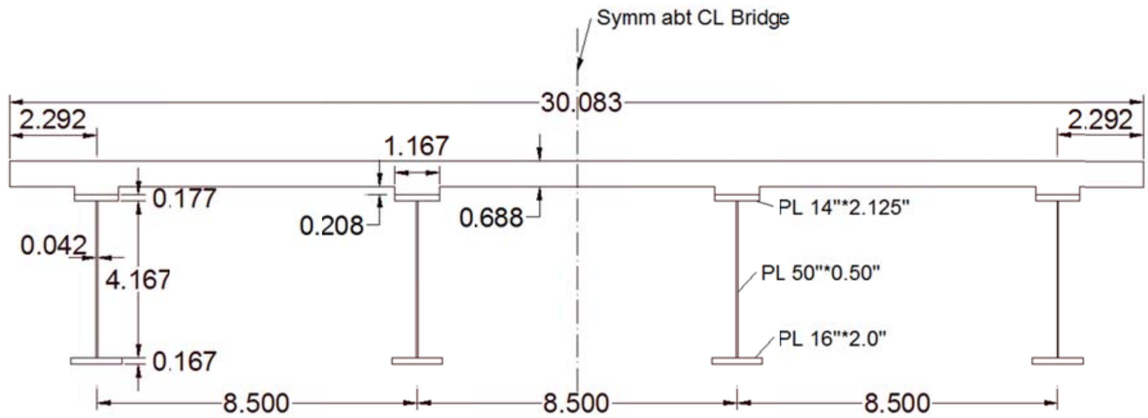

Figure 5-2 Typical steel I cross section (2) for L = 120ft at pier location

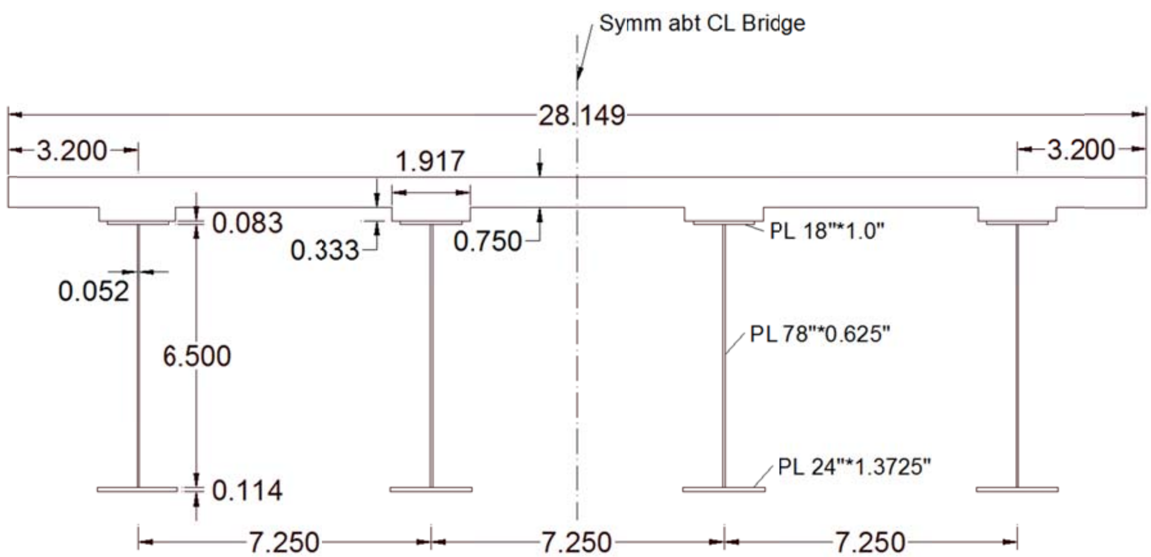

Figure 5-3 Typical steel I cross section (1) for L = 180ft

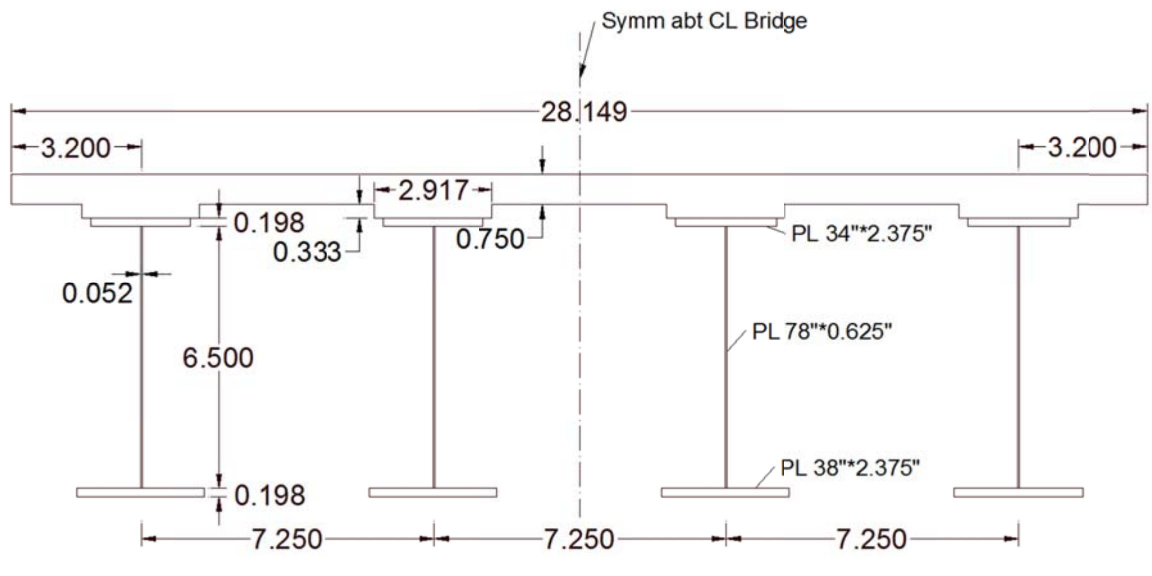

Figure 5-4 Typical steel I cross section (2) for L = 180ft at pier location

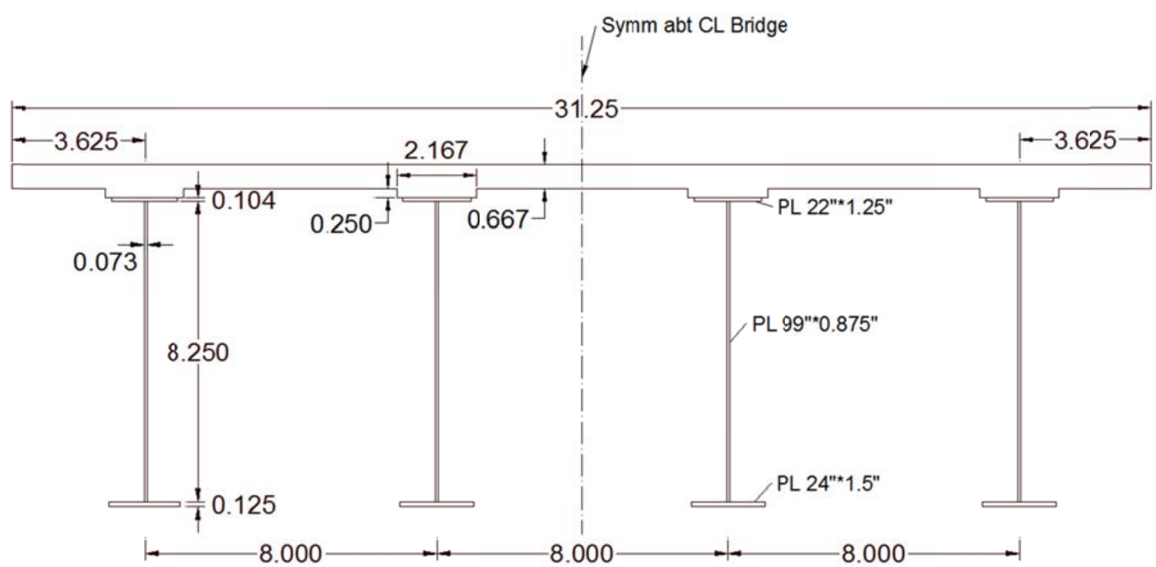

Figure 5-5 Typical steel I cross section (1) for L = 240ft

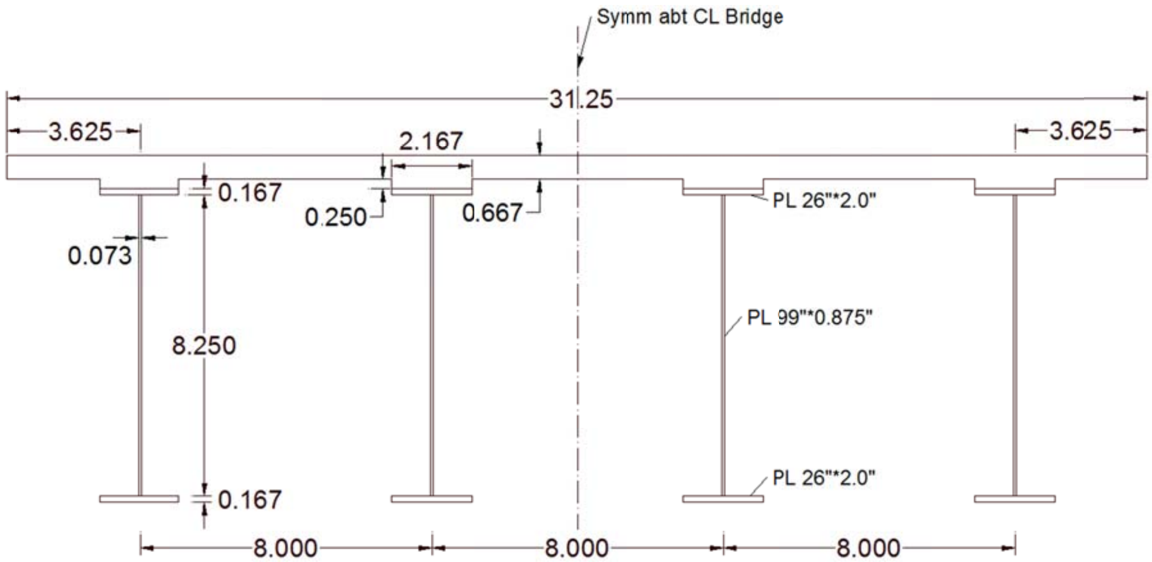

Figure 5-6 Typical steel I cross section (2) for L = 240ft at pier location

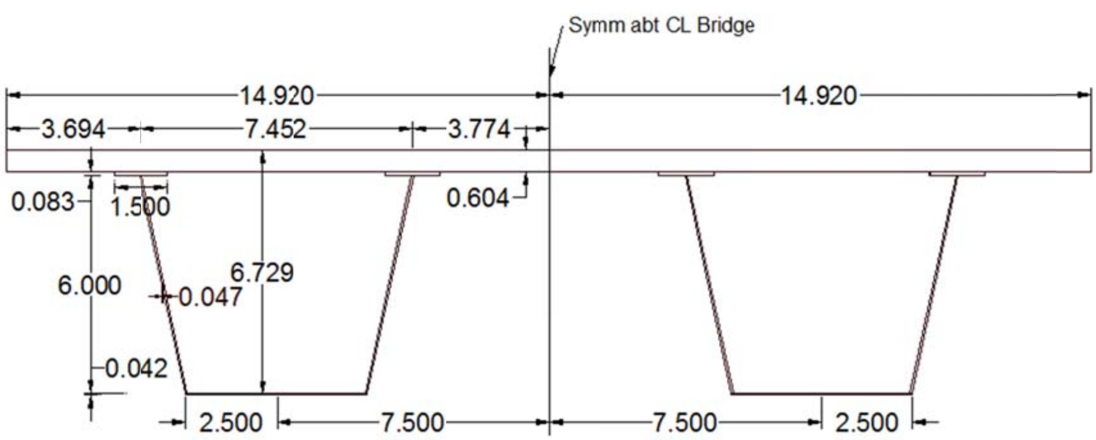

Figure 5-7 Typical steel BOX cross section (1) for L = 120ft

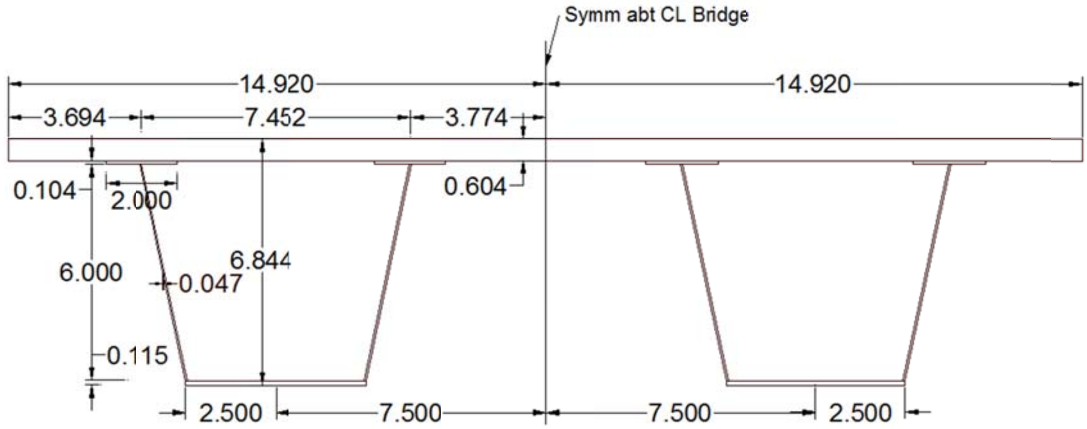

Figure 5-8 Typical steel BOX cross section (2) for L =120ft at pier location

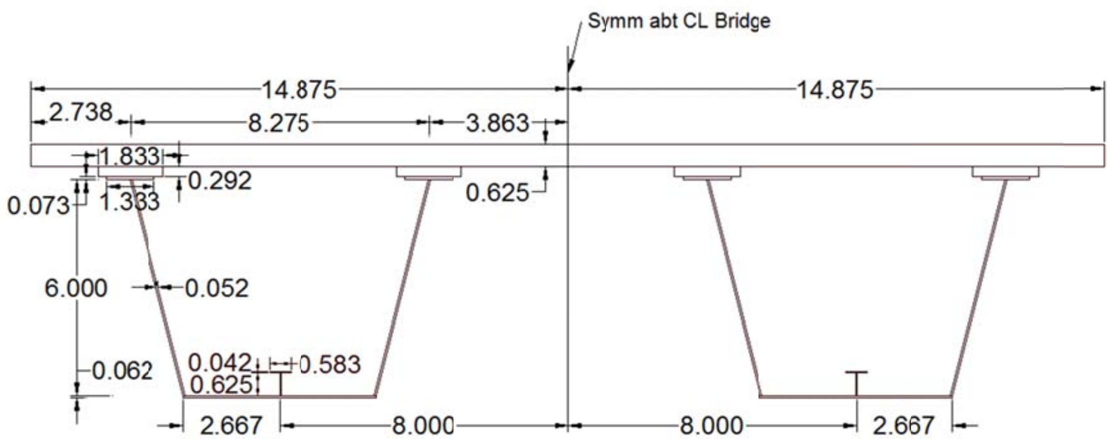

Figure 5-9 Typical steel BOX cross section (1) for L = 180ft

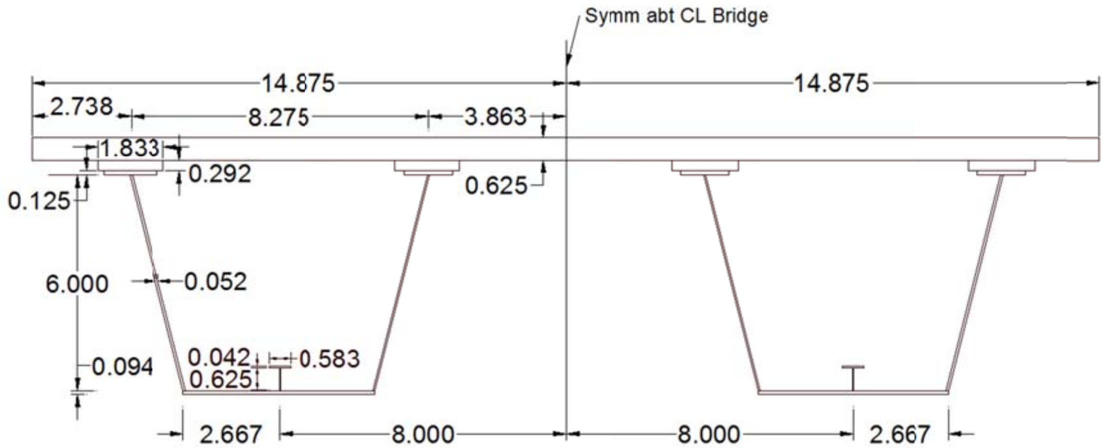

Figure 5-10 Typical steel BOX cross section (2) for L = 180ft at pier location

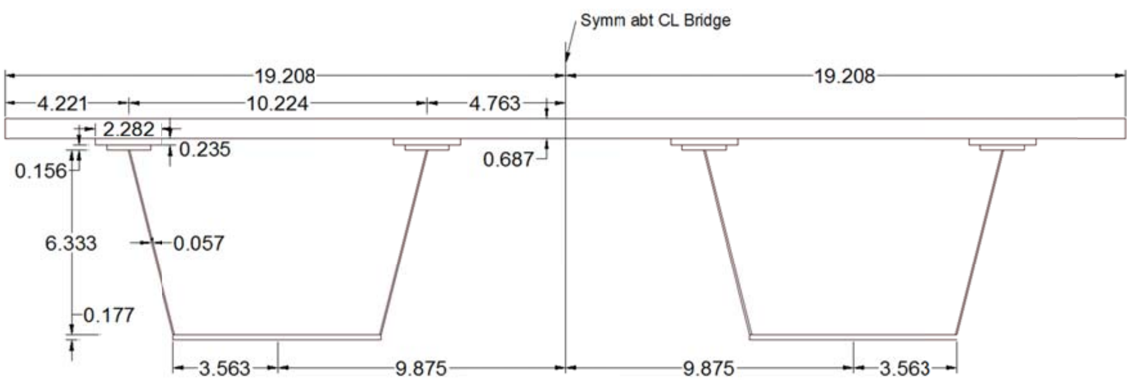

Figure 5-11 Typical steel BOX cross section (1) for L = 240ft

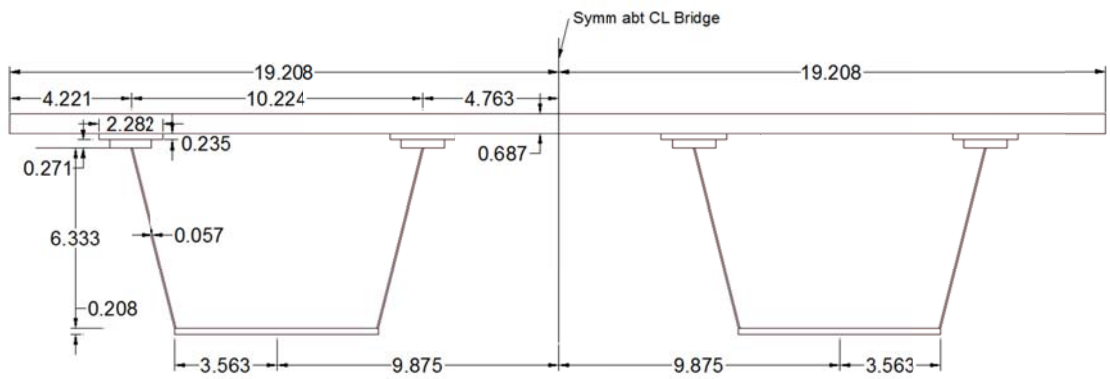

Figure 5-12 Typical steel BOX cross section (2) for L = 240ft at pier location

5.3 FINITE ELEMENT MODEL AND CROSS SECTIONS INFORMATION

SAP2000 is utilized to perform the nonlinear analysis. SAP2000 is a commercially available, general-purpose finite element-modeling package for numerically solving a wide variety of civil engineering problems. Each bridge configuration was modeled as a spine model (in which one line of elements was used for superstructure, located along the centerline of the bridge). Typical spine modeling technique is shown in Figure 5-13. SAP2000 input files for one case model required for analyzing the bridge using both MPA and NL-THA are shown in Appendix D.

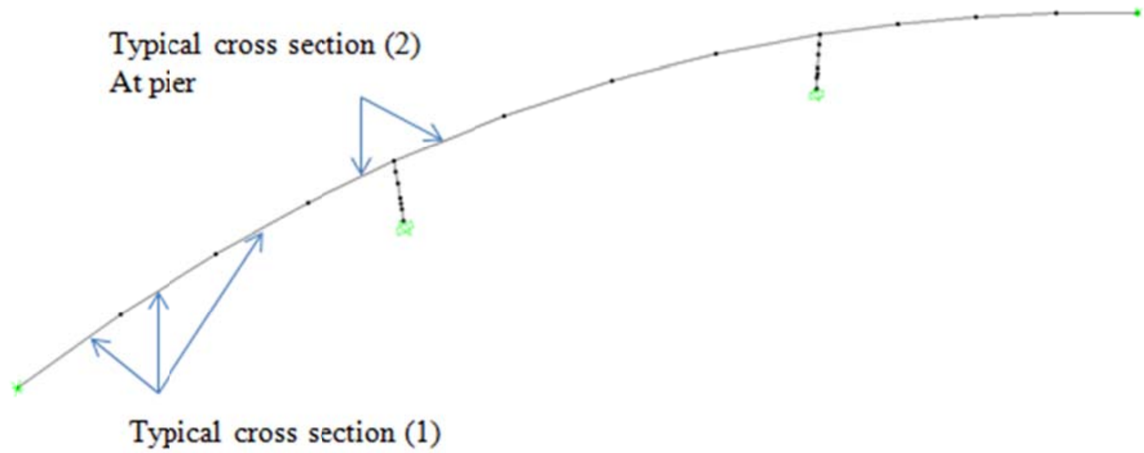

Figure 5-13 Typical curved line (spine beam) bridge model (showing 3-span unit)

Each model uses several elements per span in the longitudinal direction of the bridge. As shown in Figure 5-13, two different frame sections were utilized to model the superstructure elements of the bridge depending on the main span length, (L=120, 180, or 240ft). The section properties for the spine model were based on the entire section. Table 5-1 through Table 5-4 list the section properties used for both steel I and steel BOX cross sections used in the analysis for different span lengths. Each cross section (I or Box) was designed for two different locations along the bridge length; the first one is to define frame elements that are used to model the superstructure elements away from the pier locations (away from pier), while the second is to define frame elements used to model the superstructure elements to the right and left of each pier (at pier).

Table 5-1 Section properties for steel I cross sections for different span length bridge models (away from pier)

	120/120 ft 100/120/100 ft	180/180 ft 140/180/140 ft	240/240 ft 180/240/240 ft
Area (ft^2)	33.358	45.3845	56.2236
J (ft^4)	3.9203	5.6949	4.7058
I_{33} (ft^4)	108.7302	387.4543	697.5514
I_{22} (ft^4)	2705.6243	2991.0215	4531.5778
$Y_{c.g}$ (ft)	3.7885	5.1537	6.0336

Table 5-2 Section properties for steel I cross sections for different span length bridge models (at pier)

	120/120 ft 100/120/100 ft	180/180 ft 140/180/140 ft	240/240 ft 180/240/240 ft
Area (ft^2)	41.0393	73.99	65.6069
J (ft^4)	4.1582	9.1093	5.5169
I_{33} (ft^4)	156.883	761.92	871.4363
I_{22} (ft^4)	3400.2248	4897.3314	5287.266
$Y_{c.g}$ (ft)	3.6977	4.7221	5.9864

Table 5-3 Section properties for steel BOX cross sections for different span length bridge models (away from pier)

	120/120 ft 100/120/100 ft	180/180 ft 140/180/140 ft	240/240 ft 180/240/240 ft
Area (ft^2)	34.36167	39.82014	70.35483
J (ft^4)	4.312	5.2331	5.721
I_{33} (ft^4)	185.6136	273.3586	701.9582
I_{22} (ft^4)	2406.79	2948.364	8157.852
$Y_{c.g}$ (ft)	4.87891	4.74347	4.4409

Table 5-4 Section properties for steel BOX cross sections for different span length bridge models (at pier)

	120/120 ft 100/120/100 ft	180/180 ft 140/180/140 ft	240/240 ft 180/240/240 ft
Area (ft^2)	42.86167	45.2368	89.91733
J (ft^4)	5.332	5.4271	9.4762
I_{33} (ft^4)	317.1646	318.9432	865.6376
I_{22} (ft^4)	2935.909	3350.024	10514.86
$Y_{c.g}$ (ft)	4.368176	4.469949	4.730373

There are no elements to model the abutments; only support nodes as shown in Figure 5-13. Support nodes at abutments are modeled with full restraints for translations in both the longitudinal and transverse directions of the bridge and also the superstructure torsional rotation is fully restraint, while other degrees of freedom are released.

On the other hand, support nodes at the bottom of the piers' columns are modeled with full restraints in all degrees of freedom.

5.4 SEISMIC LOADING

All bridges were assumed to be in a seismic zone with an acceleration coefficient of PGA = 0.30g. The bridges will be assessed using the MPA procedure for a demand response spectrum equals 1.5 times the design response spectrum. Demand response spectrum (5% damped) used in this study is shown in Figure 5-14. Furthermore, nonlinear time history analysis (NL-THA) will be performed to all bridges in order to compare its results with the MPA procedure results. Three actual acceleration histories were implemented in this study; which were adjusted to match the response spectrum used in each analysis case. Information about acceleration time histories was previously introduced in section 3.5.2.

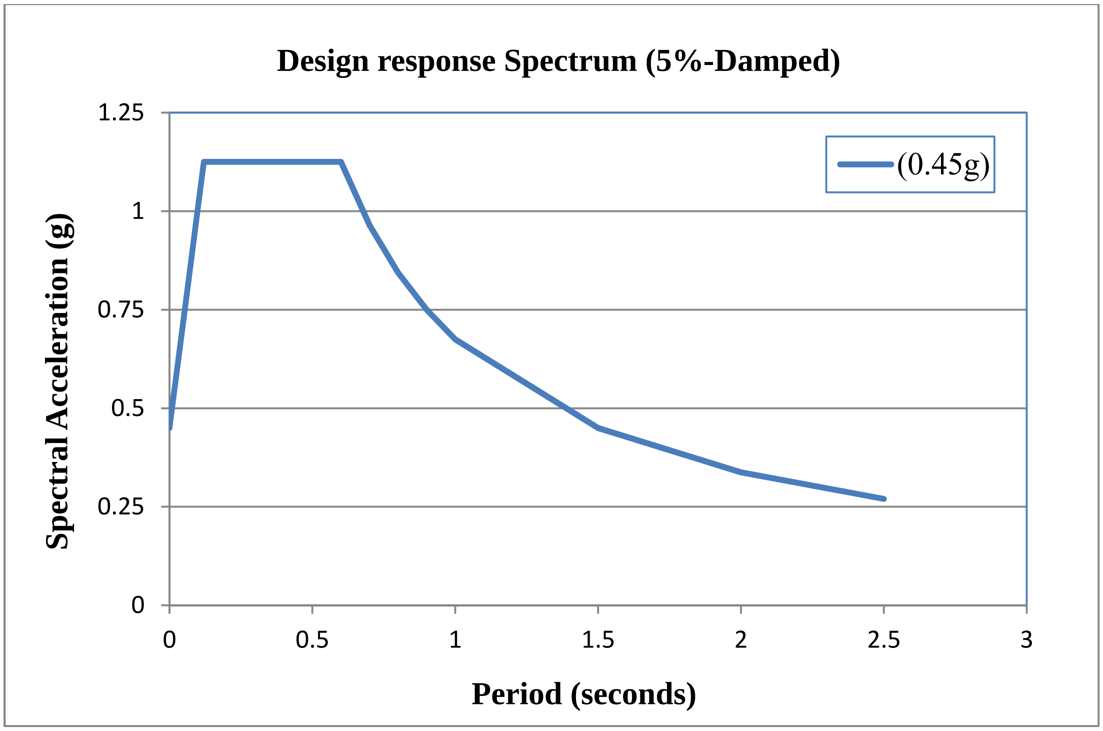

Figure 5-14 Demand response spectrum (5%-Damped) used in the parametric study

6. RESULTS OF PARAMETERIC STUDY

6.1 INTRODUCTION

This chapter presents the results of a parametric study of the effect of various parameters on the estimation of maximum demand displacement of curved bridges under seismic loading using the MPA procedure. Parameters investigated in the study were the span length, number of spans, girder cross section, radius of curvature and height of pier. Transverse displacements as well as base shear of the structure were the primary focus and results were examined in order to characterize seismic behavior. Results from the MPA were compared with results from the NL-THA in order to quantify the accuracy of the MPA procedure and then the effect of each of the parameters considered was studied.

6.2 ANALYSIS RESULTS

The analysis presented herein investigates the maximum demand displacement in the transverse direction of curved bridges with an increasing main span length (L) from 120ft to 240ft. For the case of 3-span Bridge, it was designed such that both left and right span lengths are a percentage (75-80%) of the main (middle) span length (i.e. 0.8L-L-0.8L). While for the 2-span Bridge, both spans have the same main span length (L).

6.2.1 For Steel I Bridges

As mentioned before, analysis was performed for different configurations of bridges with the previously designed steel I cross sections. The first group was for 3-span bridge models (with total spans ranged from 320 ft to 600 ft) with different radii of curvature (R=500 ft, 1000 ft, and 1600 ft) and different pier column heights (H=50 ft, and 20 ft).

The second group was for 2-span bridge models (with total spans ranged from 240 ft to 480 ft) with different radii of curvature (R=500 ft, 1000 ft, and 1600 ft) and different pier column heights (H=50 ft, and 20 ft). Table 6-1 and Table 6-2 list the data used for creating 3-span and 2-span Bridge models with steel I cross sections, respectively.

Table 6-1 3-span Bridge models with Steel I cross sections

Main Span length (L)	Bridge Configuration	Total Span Length (ft)	Radius of Curvature R (ft)	Curvature Angle θ (degree)	Pier Column Height H (ft)
120	100-120-100	320	500 1000 1600	37 18 11	50
180	140-180-140	460	500 1000 1600	53 26 17	50
240	180-240-180	600	500 1000 1600	69 34 22	50
120	100-120-100	320	500 1000 1600	37 18 11	20
180	140-180-140	460	500 1000 1600	53 26 17	20
240	180-240-180	600	500 1000 1600	69 34 22	20

Table 6-2 2-span Bridge models with Steel I cross sections

Main Span length (L)	Bridge Configuration	Total Span Length (ft)	Radius of Curvature R (ft)	Curvature Angle θ (degree)	Pier Column Height H (ft)
120	120-120	240	500 1000 1600	28 14 9	50
180	180-180	360	500 1000 1600	41 21 13	50
240	240-240	480	500 1000 1600	55 28 17	50
120	120-120	240	500 1000 1600	28 14 9	20
180	180-180	360	500 1000 1600	41 21 13	20
240	240-240	480	500 1000 1600	55 28 17	20

Figure 6-1 through Figure 6-6 illustrate the deck displacement profiles obtained from 3-span Bridge configurations for different pier column heights using the MPA procedure and also comparing the results with those results obtained from the NL-THA runs. Furthermore, Figure 6-7 through Figure 6-12 depict deck displacements obtained from both the MPA and NL-THA procedures for 2-span Bridge configurations used in the current study.

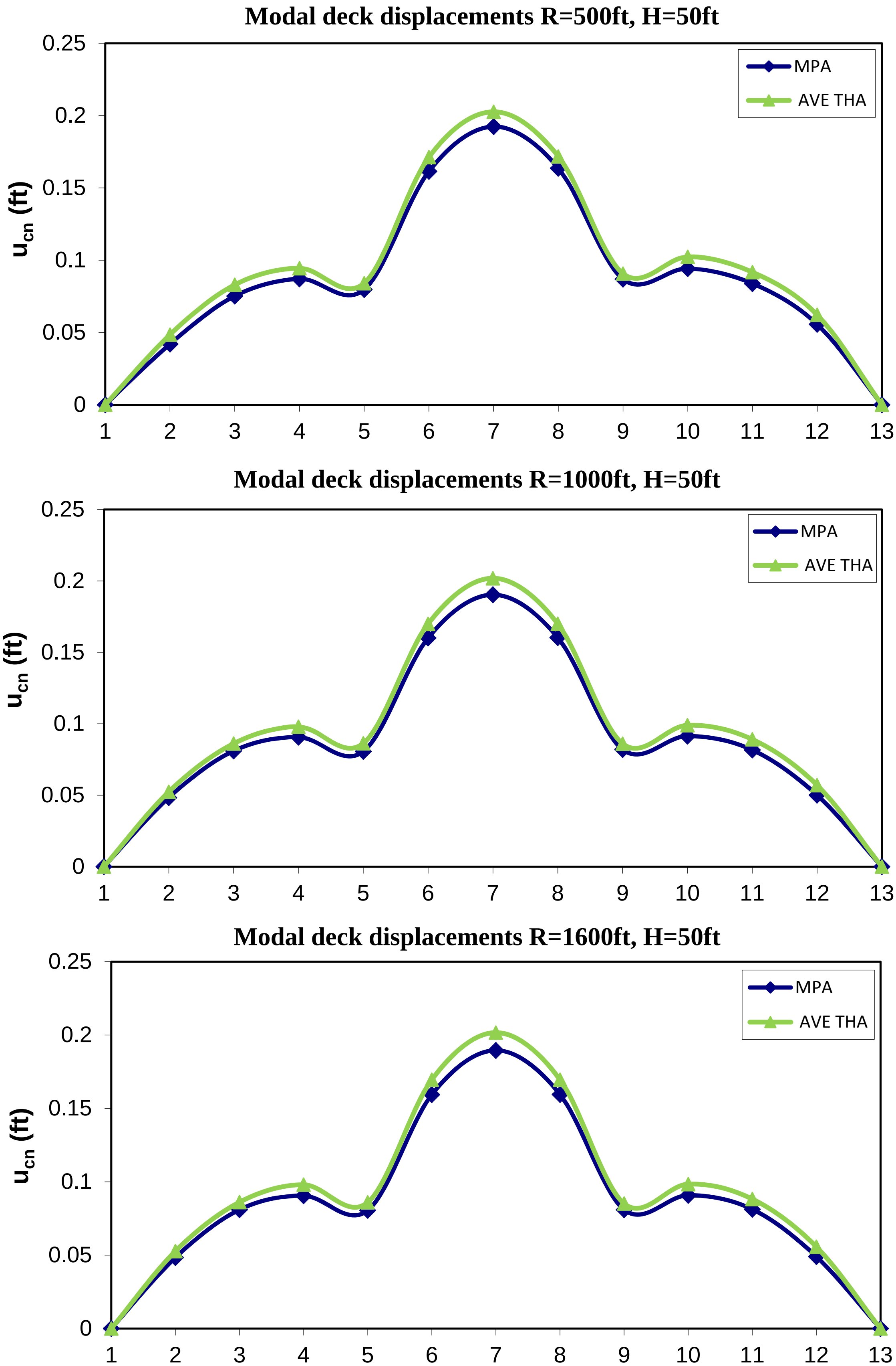

Figure 6-1 Deck Displacements for 3-span Steel I Bridge Model L=100-120-100ft, Pier Height = 50ft

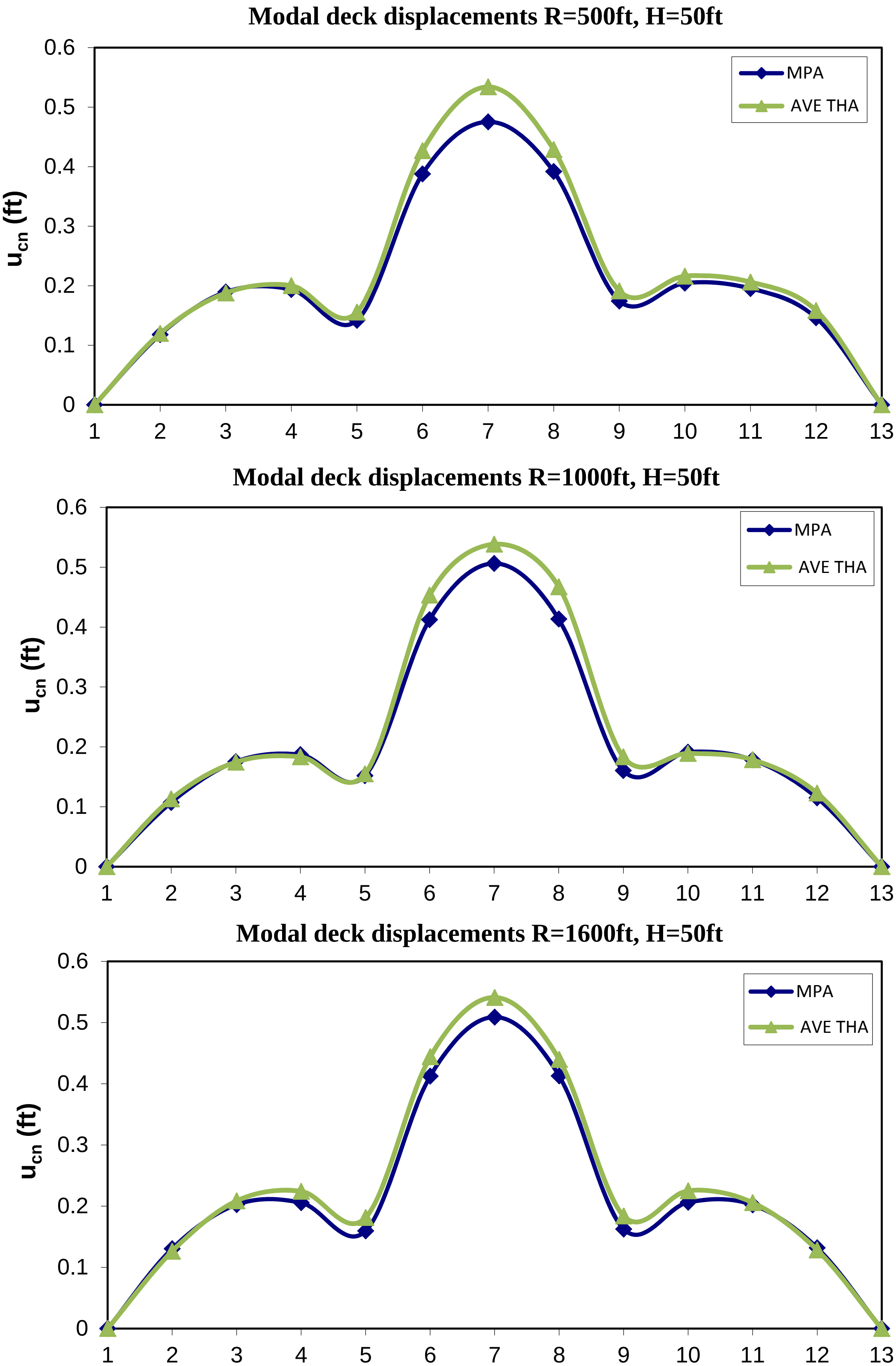

Figure 6-2 Deck Displacements for 3-span Steel I Bridge Model L=140-180-140ft, Pier Height = 50ft

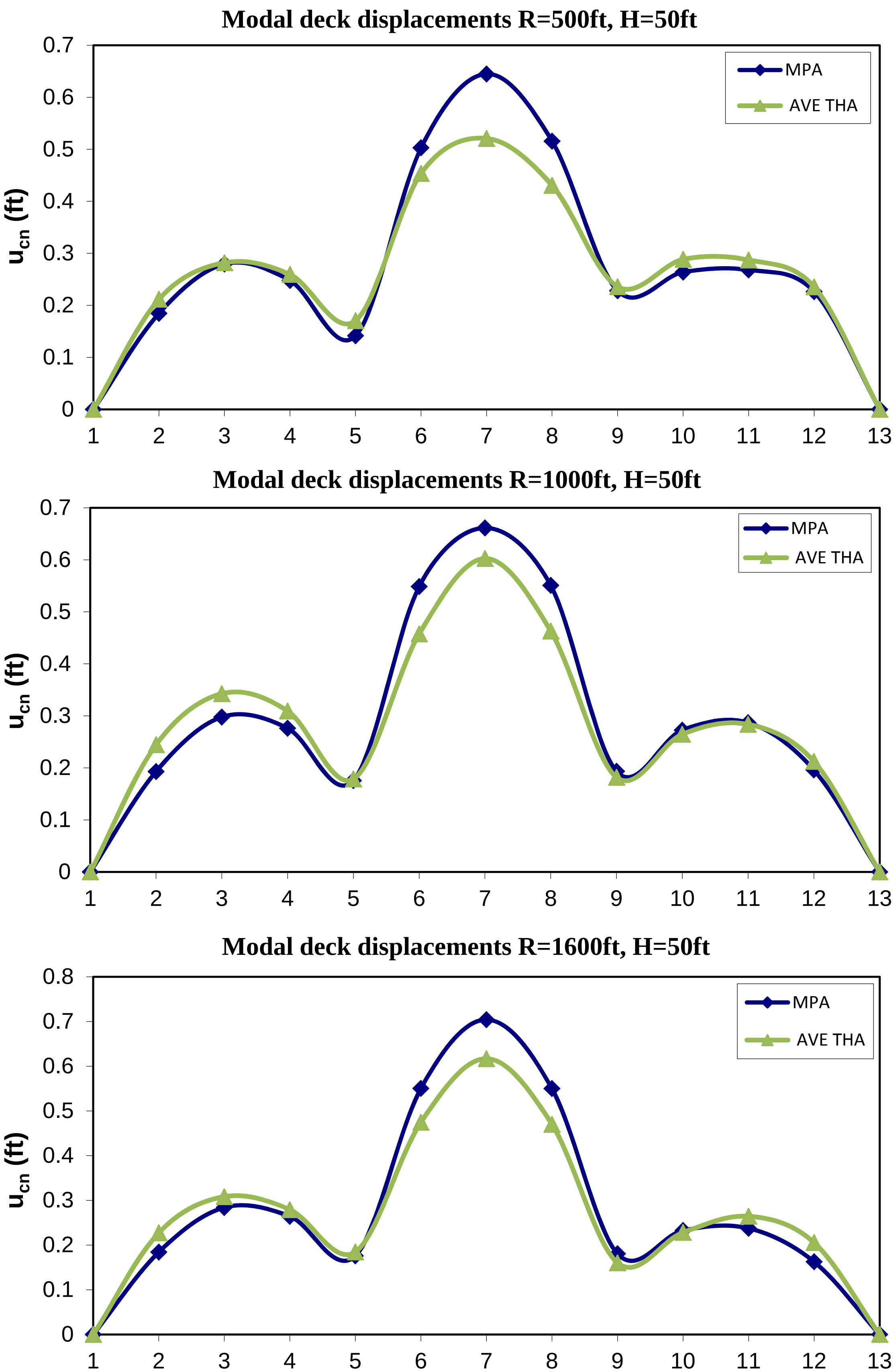

Figure 6-3 Deck Displacements for 3-span Steel I Bridge Model L=180-240-180ft, Pier Height = 50ft

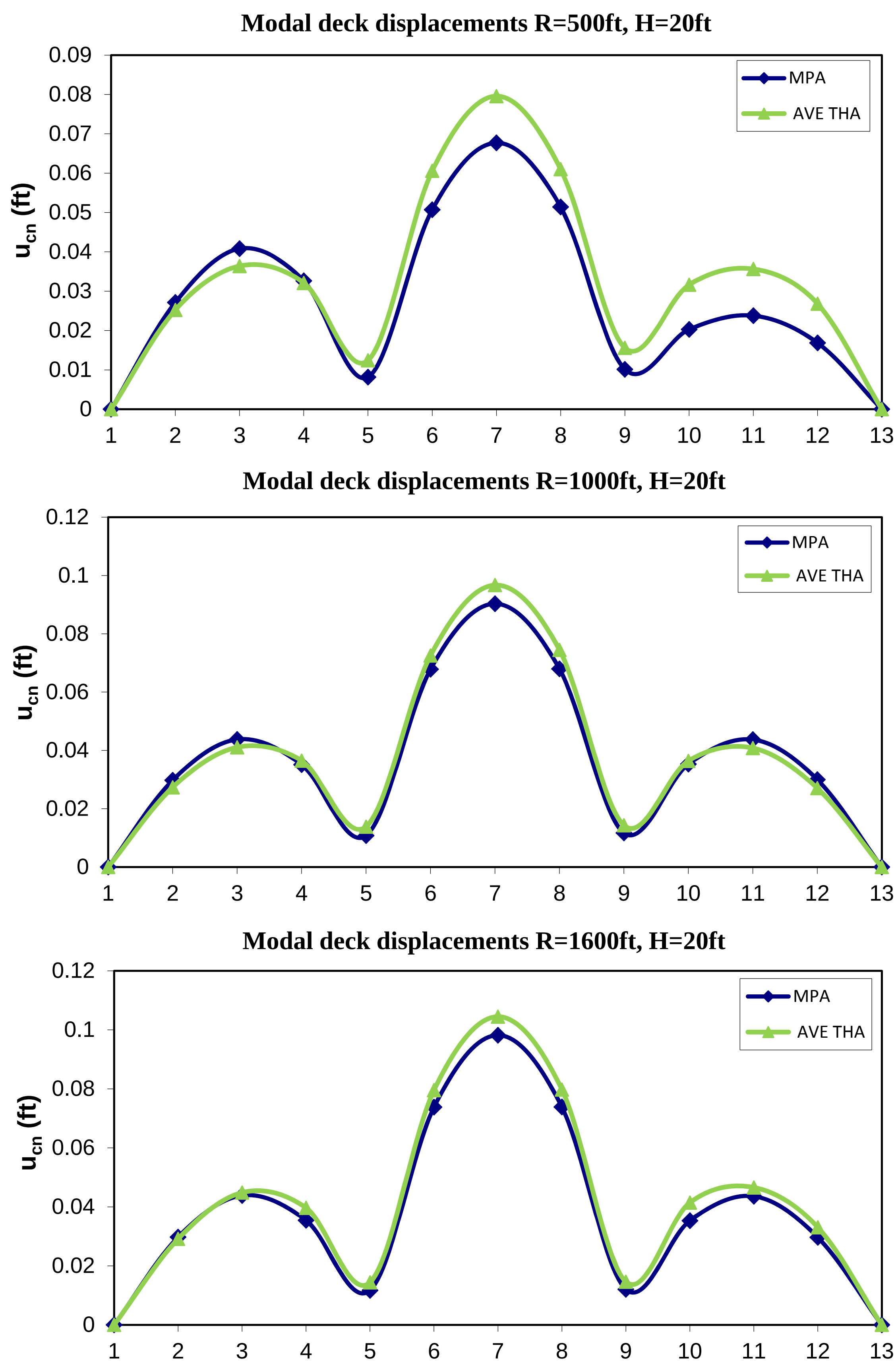

Figure 6-4 Deck Displacements for 3-span Steel I Bridge Model L=100-120-100ft, Pier Height = 20ft

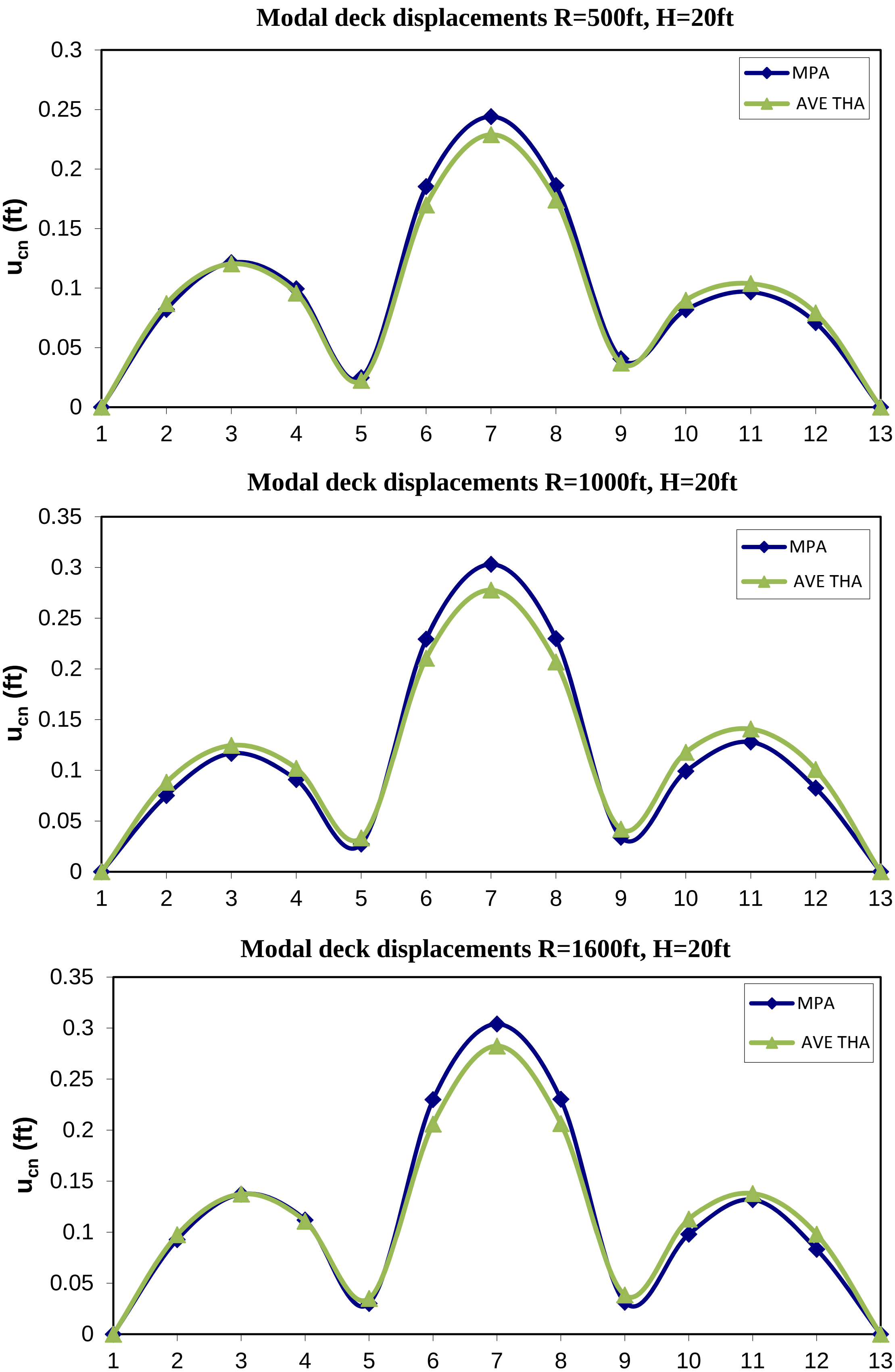

Figure 6-5 Deck Displacements for 3-span Steel I Bridge Model L=140-180-140ft, Pier Height = 20ft

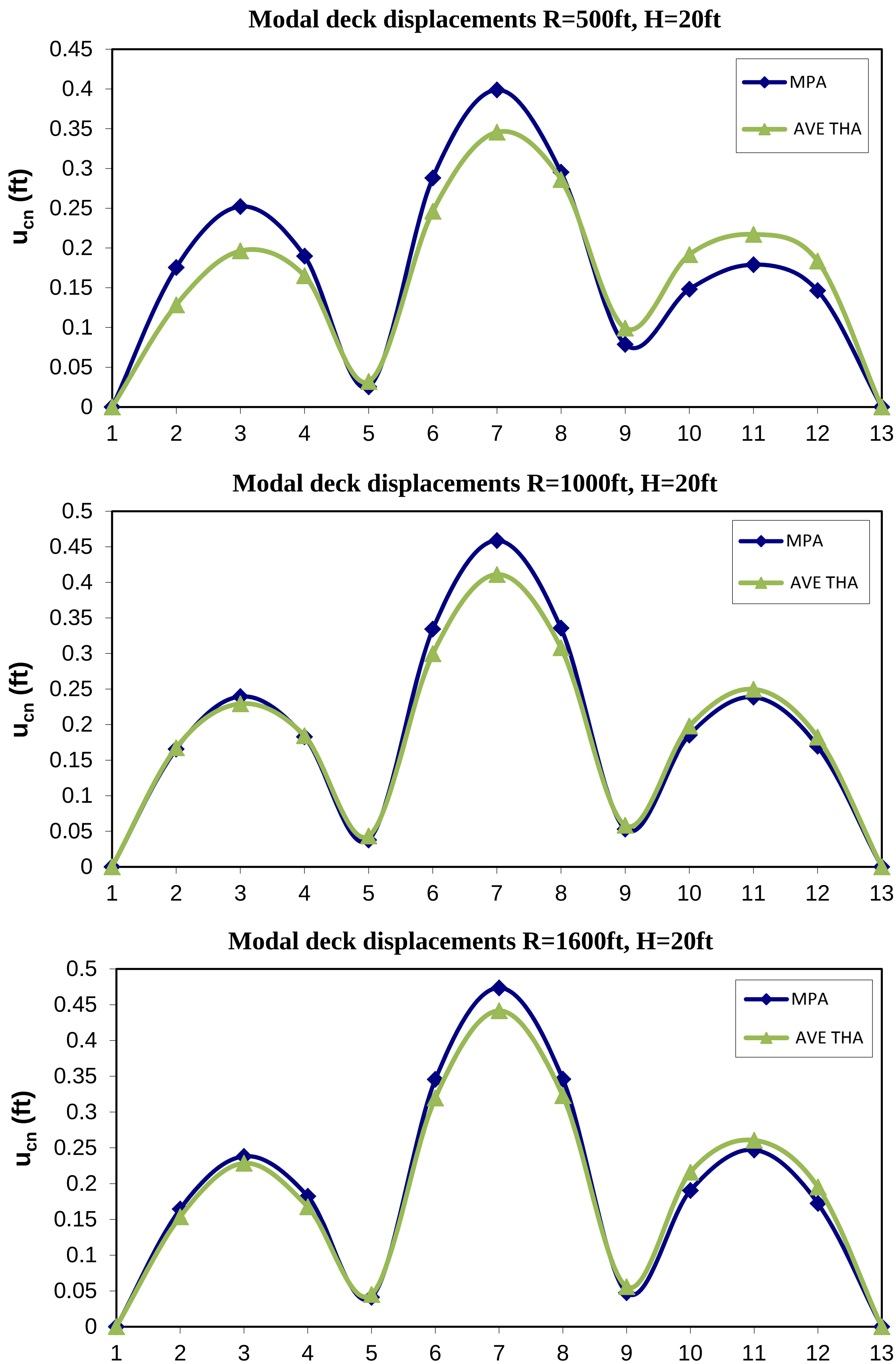

Figure 6-6 Deck Displacements for 3-span Steel I Bridge Model L=180-240-180ft, Pier Height = 20ft

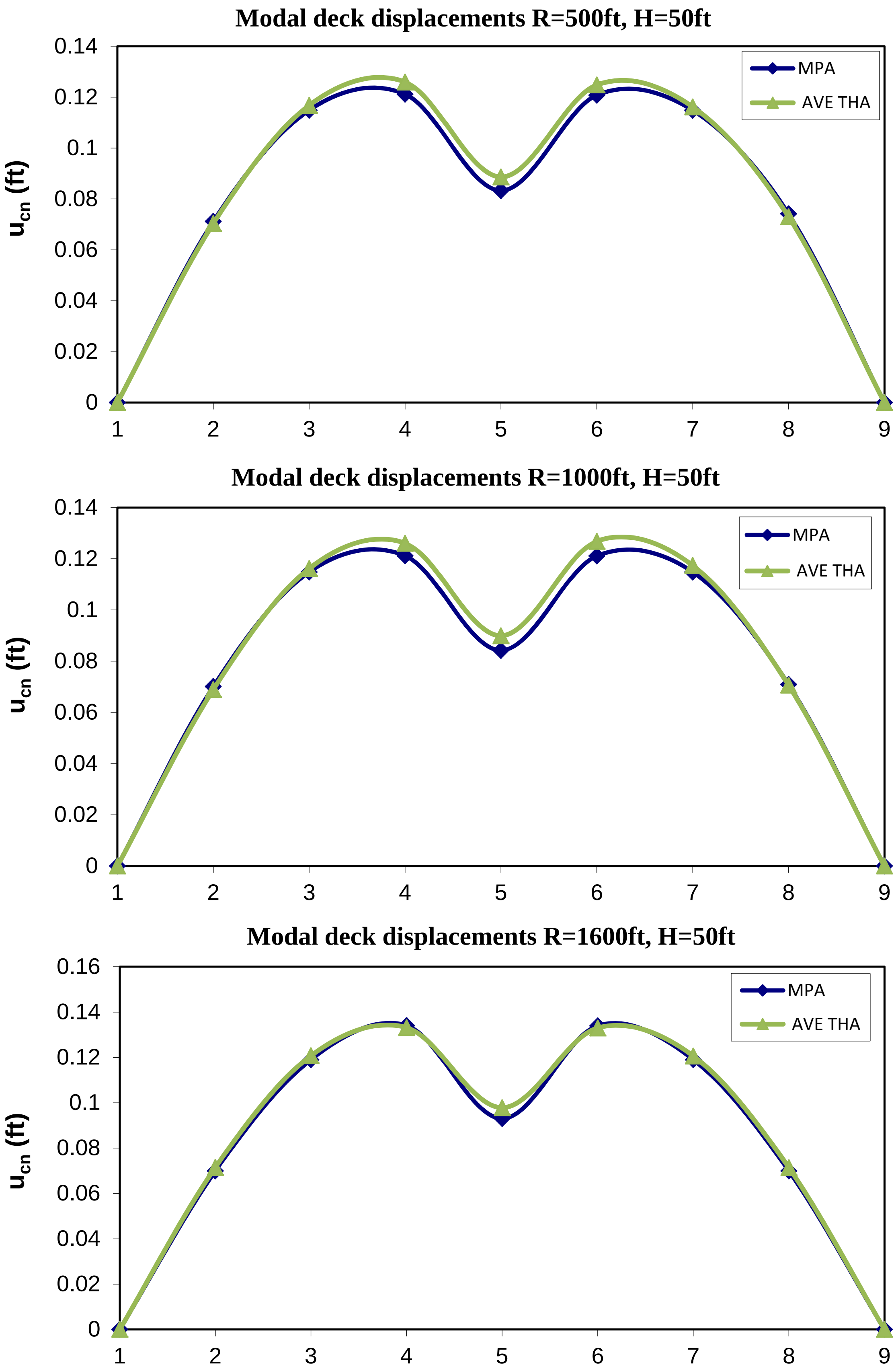

Figure 6-7 Deck Displacements for 2-span Steel I Bridge Model L=120-120ft, Pier Height = 50ft

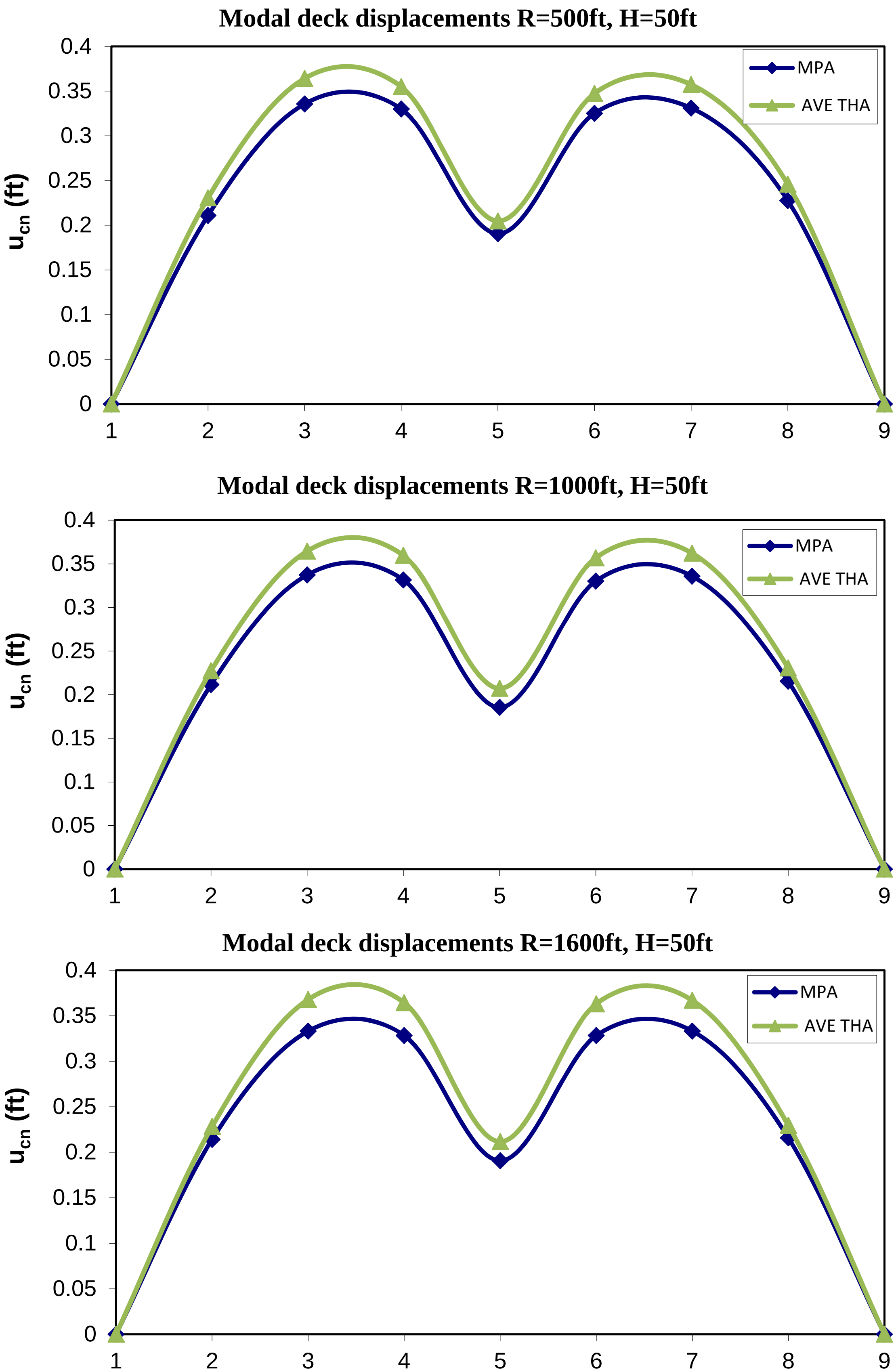

Figure 6-8 Deck Displacements for 2-span Steel I Bridge Model L=180-180ft, Pier Height = 50ft

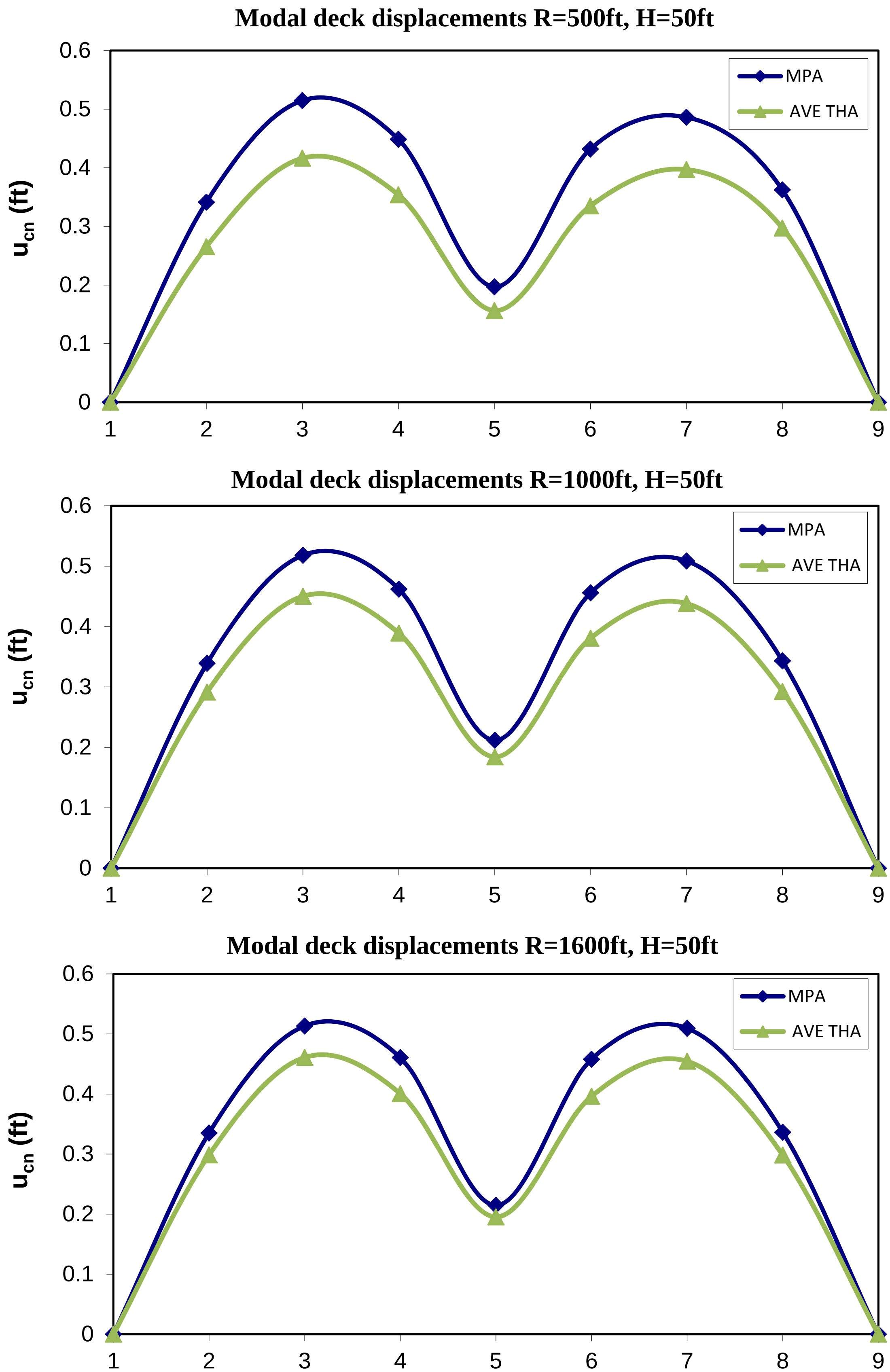

Figure 6-9 Deck Displacements for 2-span Steel I Bridge Model L=240-240ft, Pier Height = 50ft

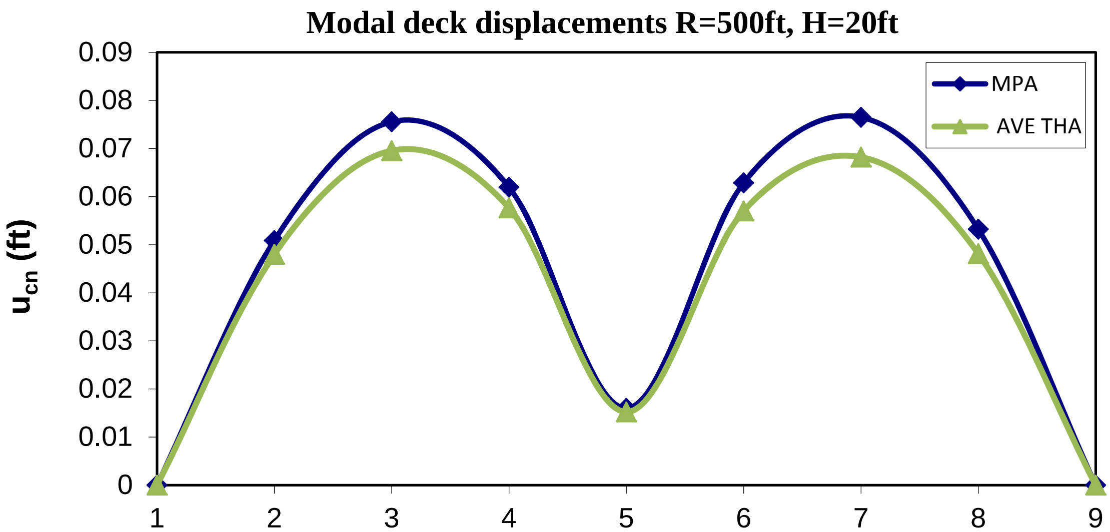

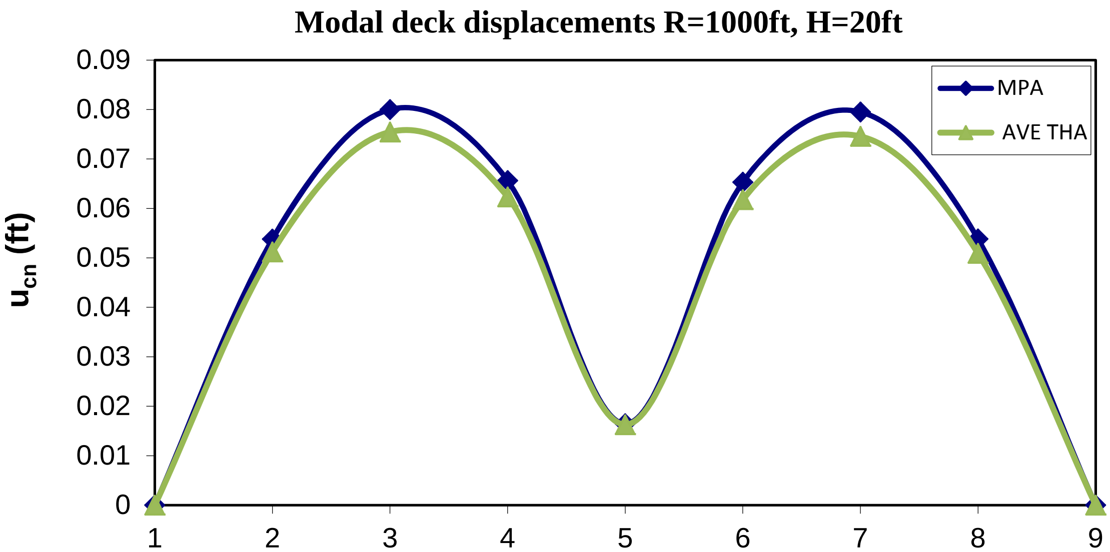

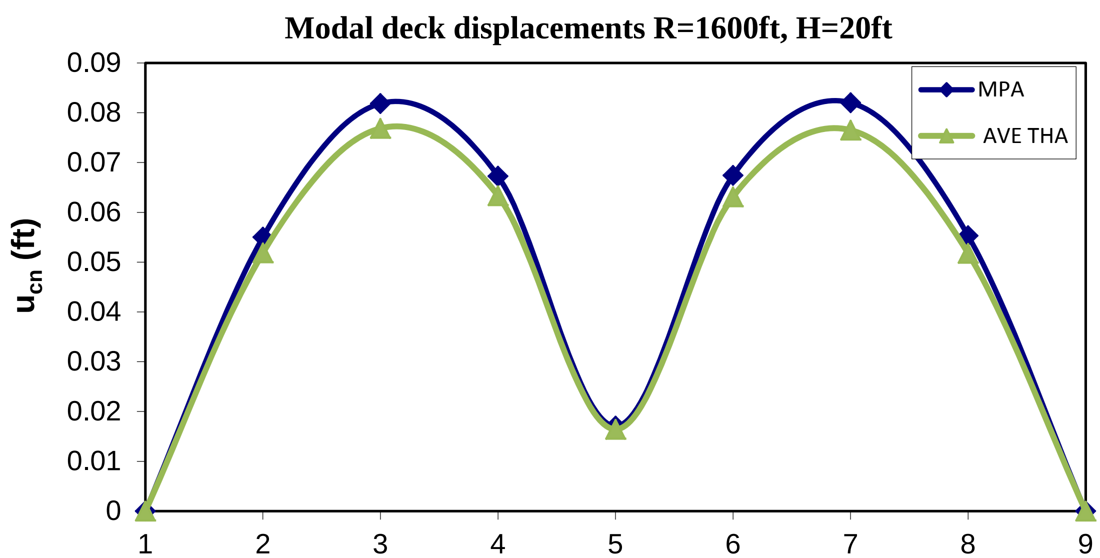

Figure 6-10 Deck Displacements for 2-span Steel I Bridge Model L=120-120ft, Pier Height=20ft

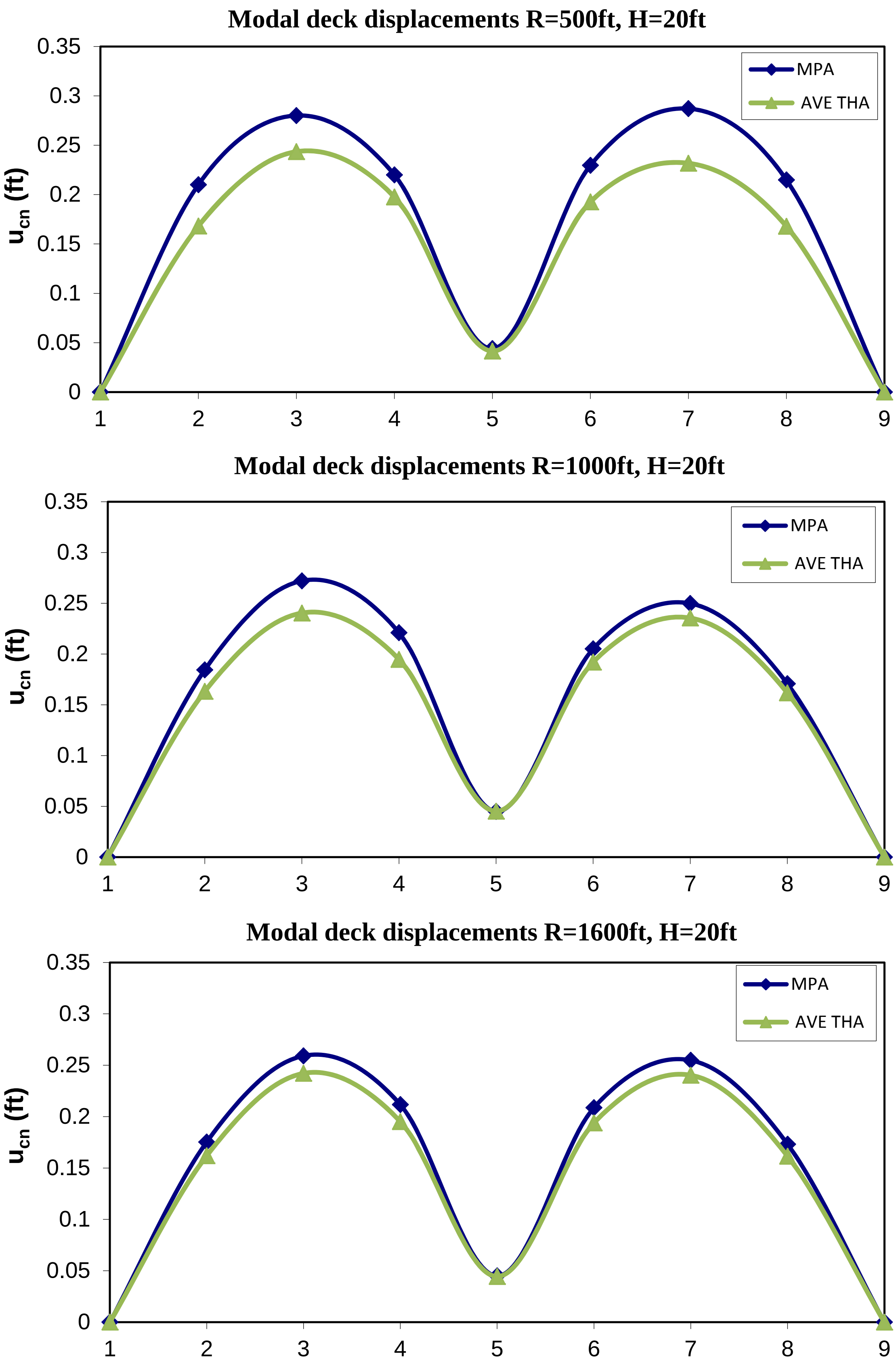

Figure 6-11 Deck Displacements for 2-span Steel I Bridge Model L=180-180ft, Pier Height=20ft

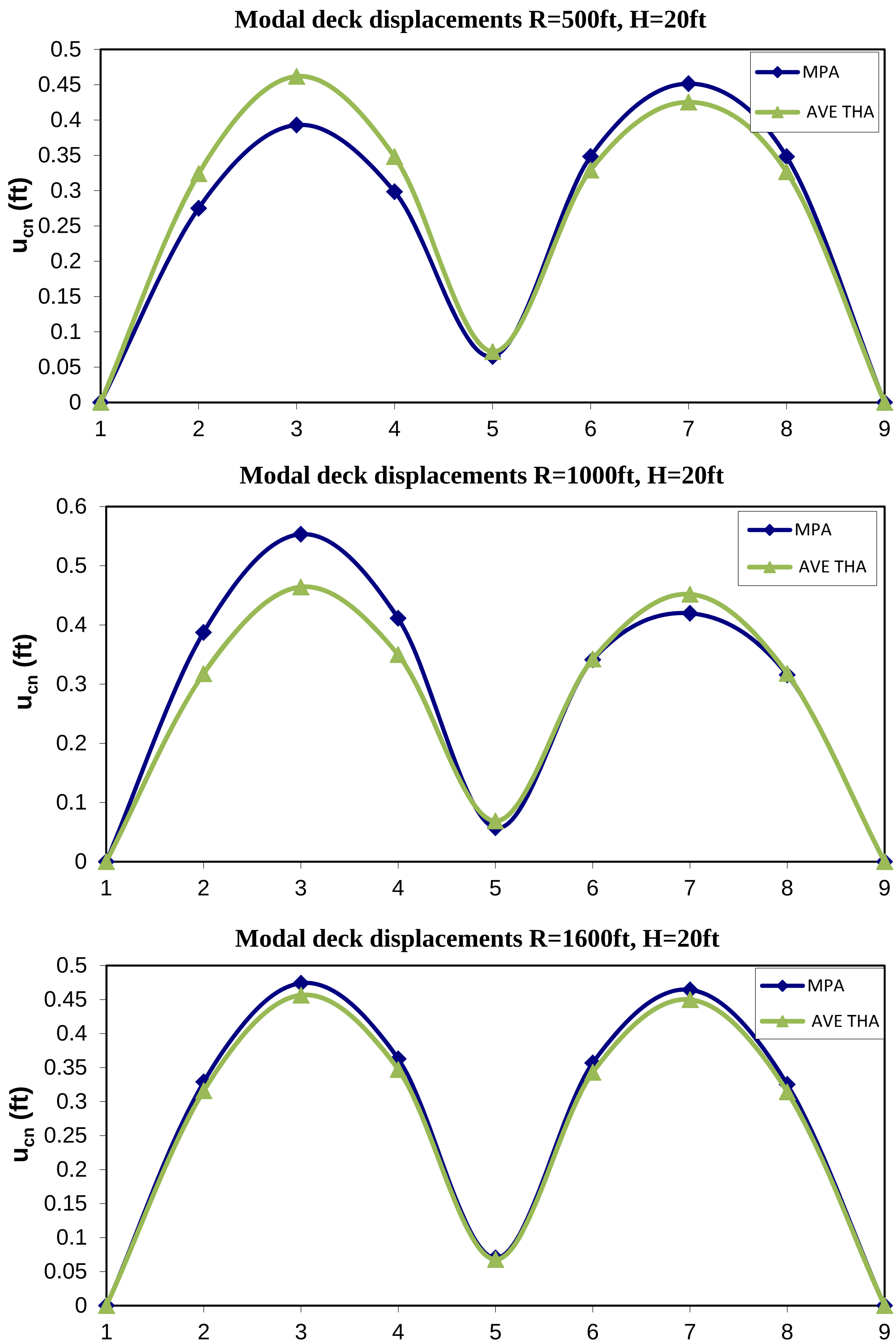

Figure 6-12 Deck Displacements for 2-span Steel I Bridge Model L=240-240ft, Pier Height=20ft

6.2.2 For Steel BOX Bridges

The study was further extended to include bridge models with steel BOX cross sections. Analysis was performed for different configurations of bridges with the previously designed steel BOX cross sections. The first group was for 3-span bridge models (with total spans ranged from 320 ft to 600 ft) with different radii of curvature (R=500 ft, 1000 ft, and 1600 ft) and different pier column heights (H=50 ft, and 20 ft).

The second group was for 2-span bridge models (with total spans ranged from 240 ft to 480 ft) with different radii of curvature (R=500 ft, 1000 ft, and 1600 ft) and different pier column heights (H=50 ft, and 20 ft). Same data that was previously used (as listed in Table 6-1 and Table 6-2) in creating bridge models with steel I sections using SAP2000, was utilized again for creating 3-span and 2-span Bridge models with steel box cross sections, respectively.

Figure 6-13 through Figure 6-18 illustrate the deck displacement profiles obtained from 3-span Bridge configurations for different pier column heights using the MPA procedure and also comparing the results with those results obtained from the NL-THA runs. Furthermore, Figure 6-19 through Figure 6-24 depict deck displacements obtained from both the MPA and NL-THA procedures for 2-span Bridge configurations used in the current study.

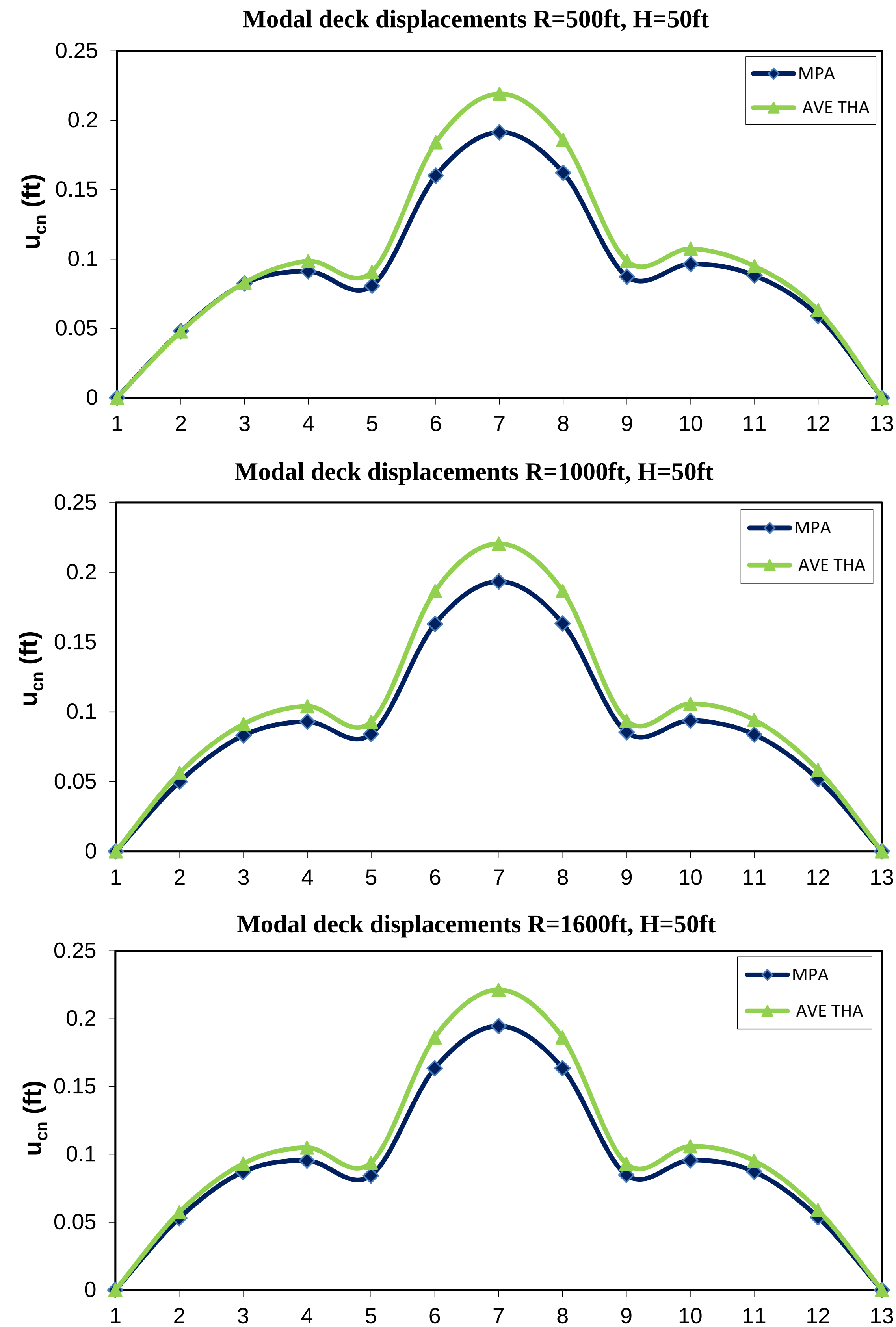

Figure 6-13 Deck Displacements for 3-span Steel BOX Bridge Model L=100-120-100ft, Pier Height = 50ft

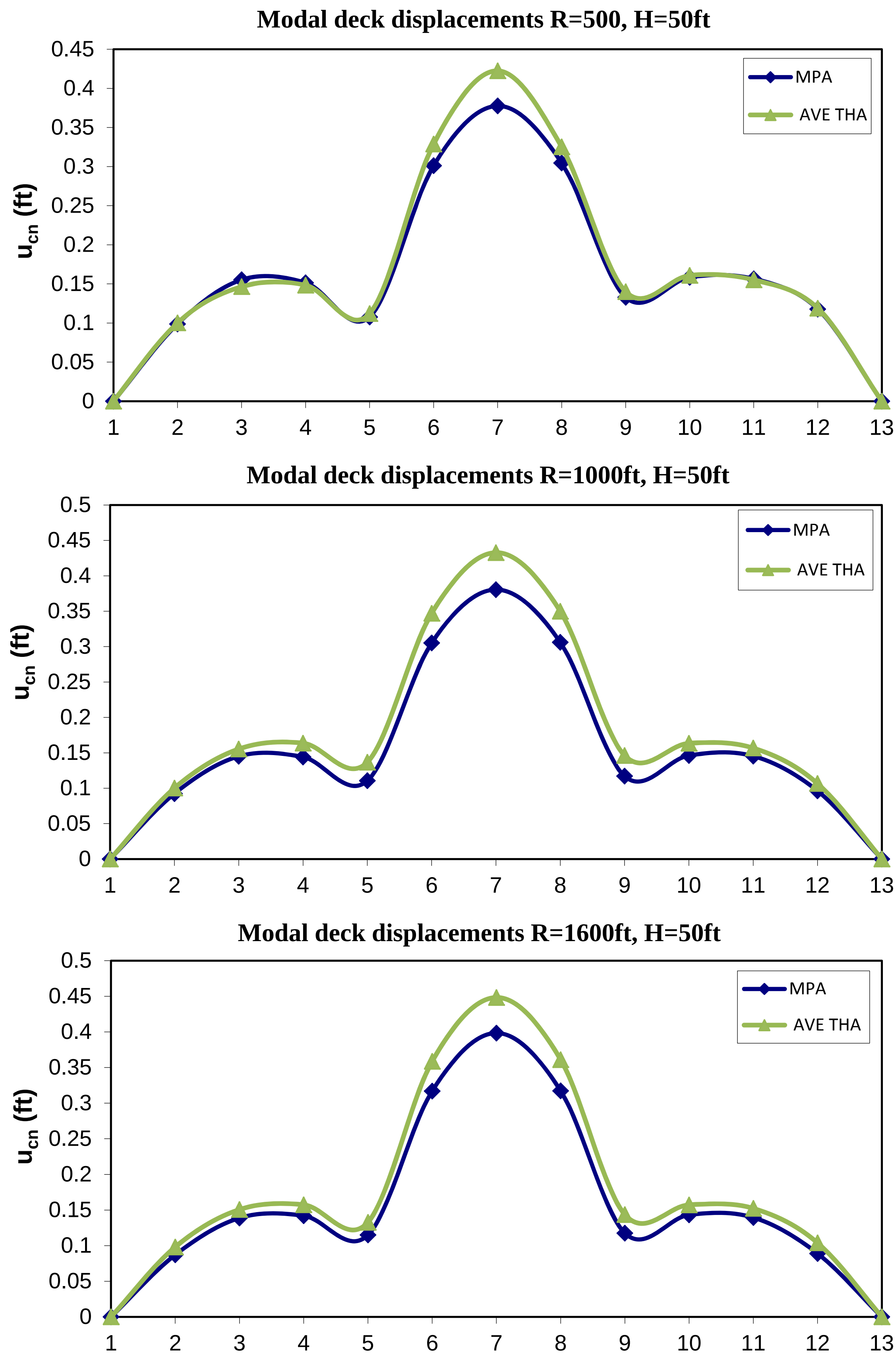

Figure 6-14 Deck Displacements for 3-span Steel BOX Bridge Model L=140-180-140ft, Pier Height = 50ft

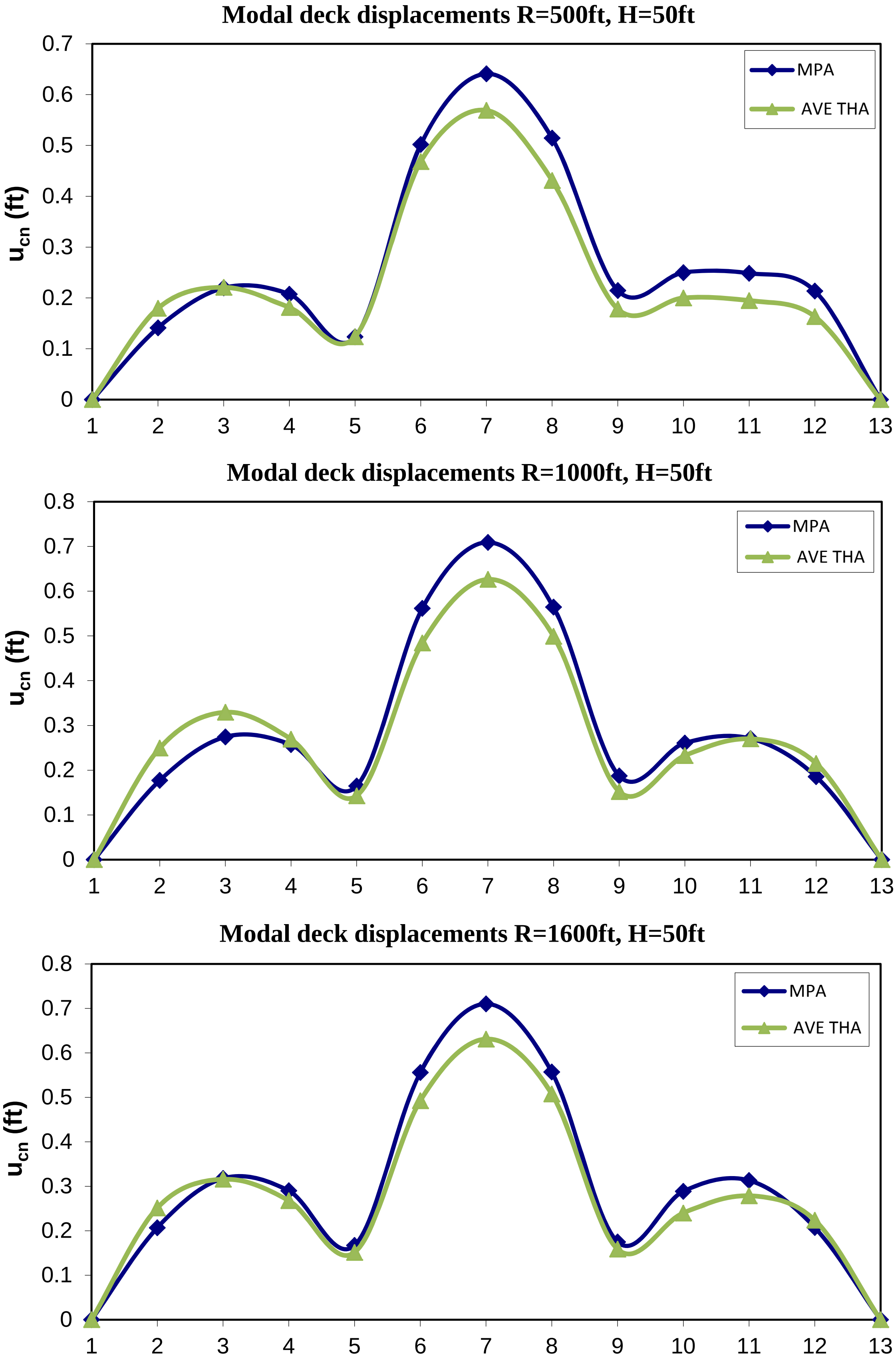

Figure 6-15 Deck Displacements for 3-span Steel BOX Bridge Model L=180-240-180ft, Pier Height = 50ft

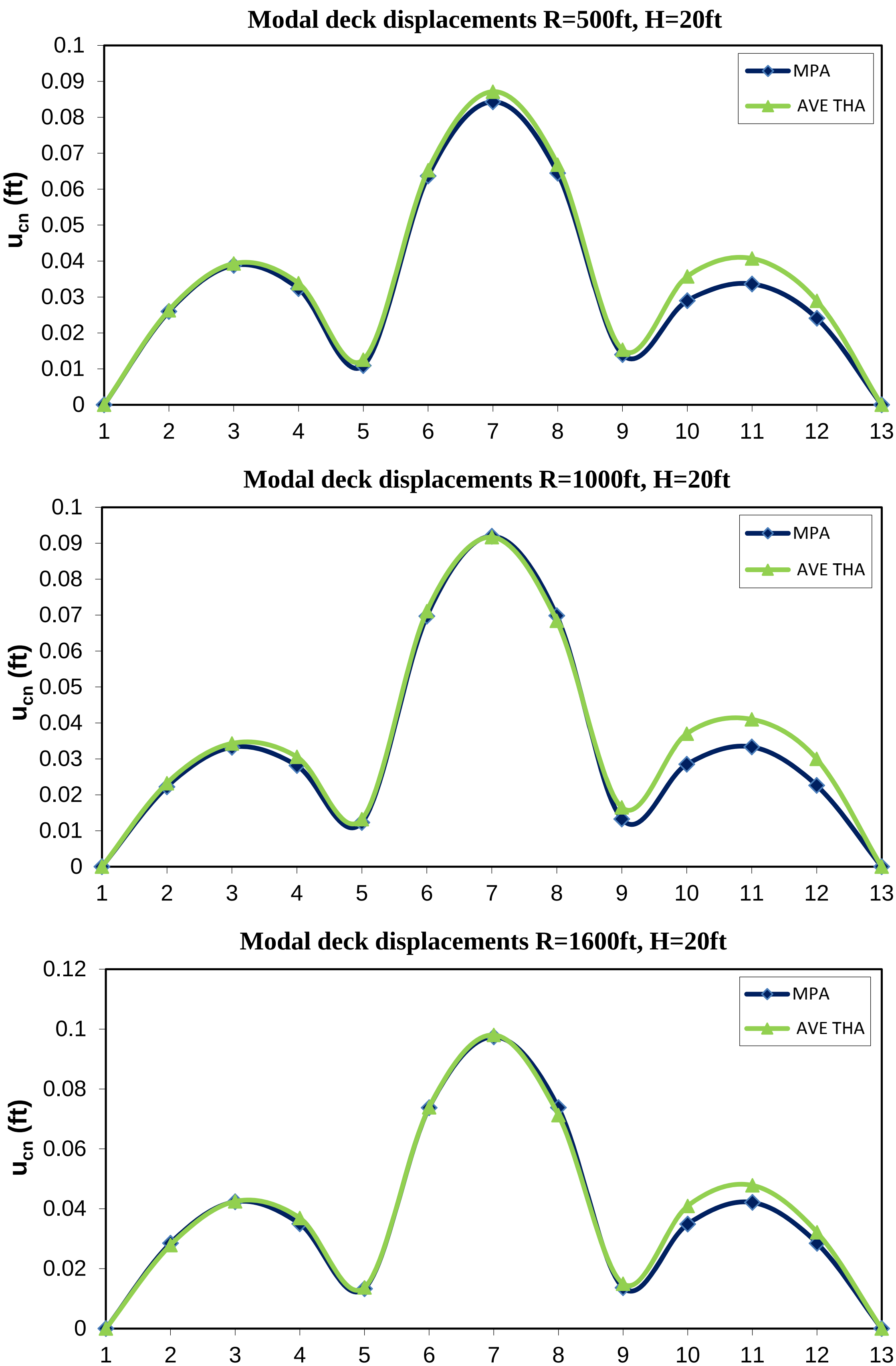

Figure 6-16 Deck Displacements for 3-span Steel BOX Bridge Model L=100-120-100ft, Pier Height = 20ft

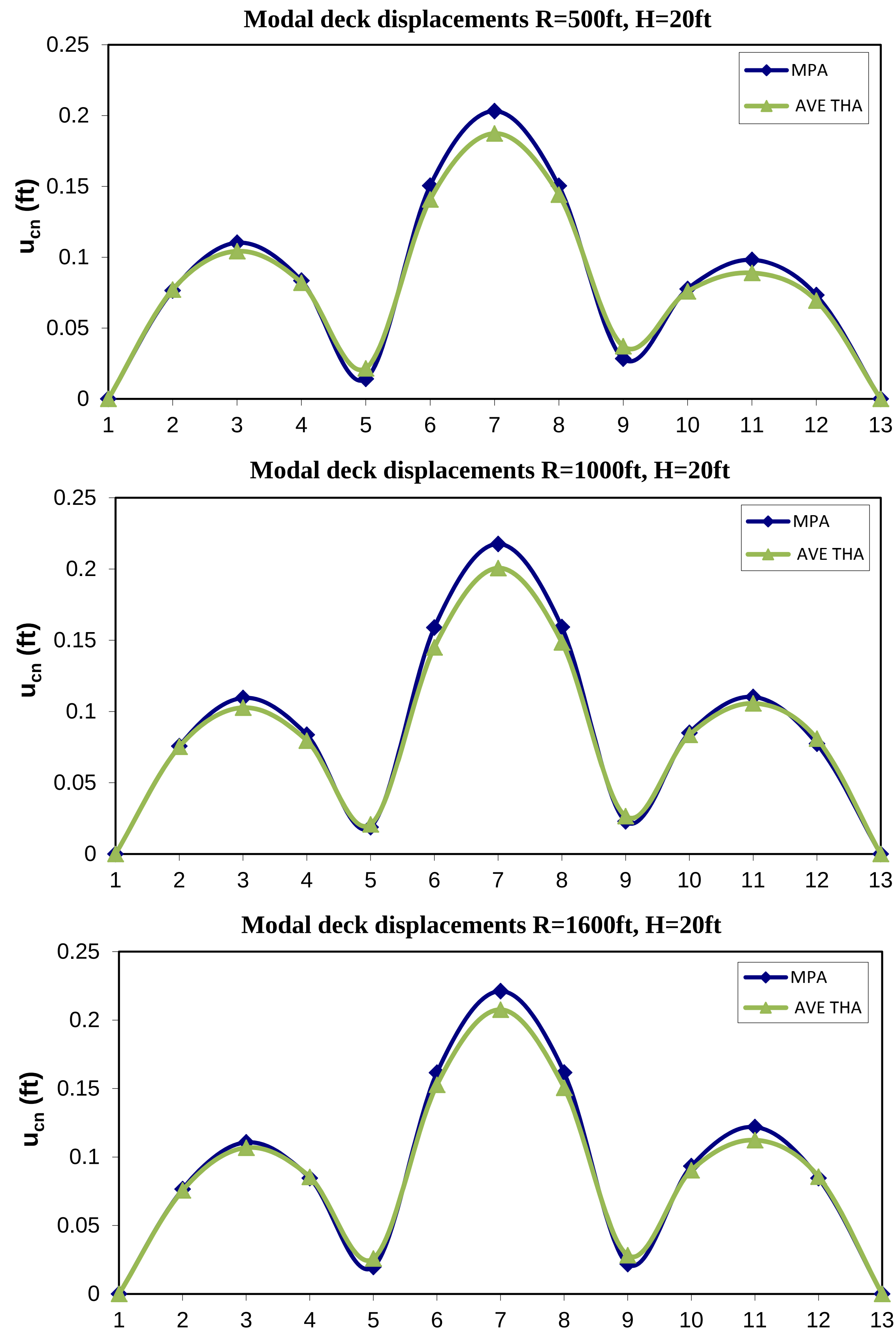

Figure 6-17 Deck Displacements for 3-span Steel BOX Bridge Model L=140-180-140ft, Pier Height = 20ft

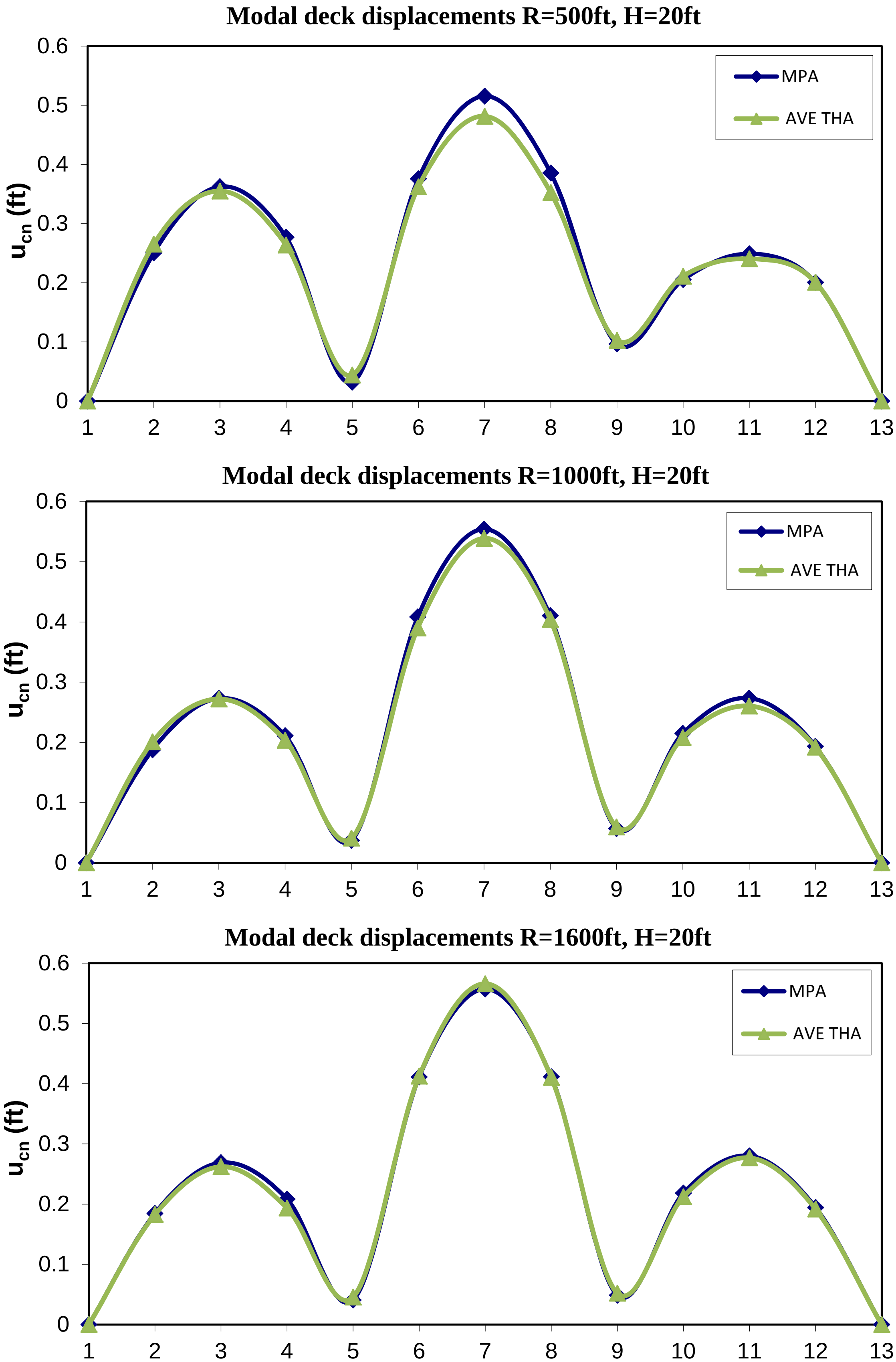

Figure 6-18 Deck Displacements for 3-span Steel BOX Bridge Model L=180-240-180ft, Pier Height = 20ft

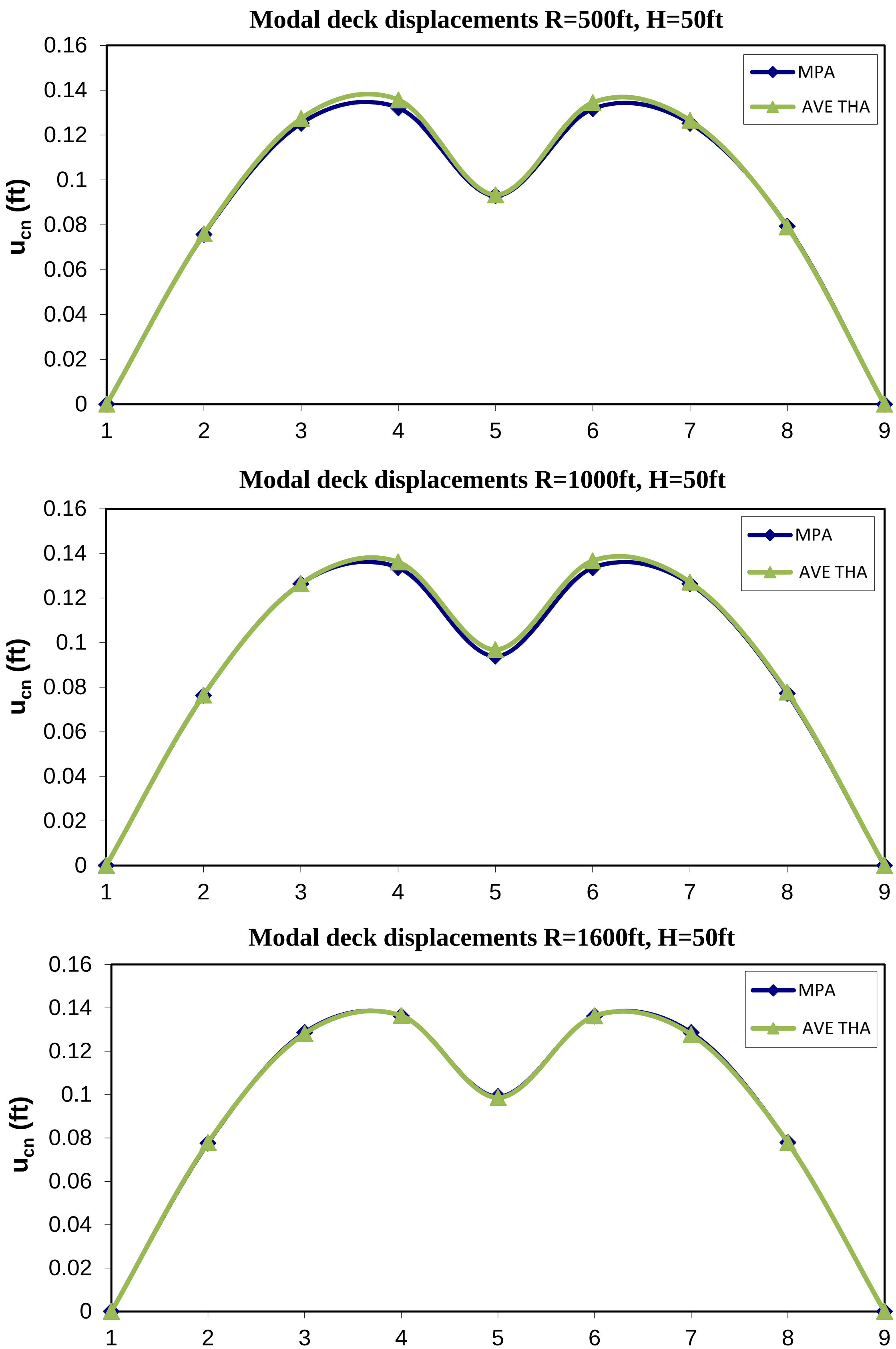

Figure 6-19 Deck Displacements for 2-span Steel BOX Bridge Model L=120-120ft, Pier Height = 50ft

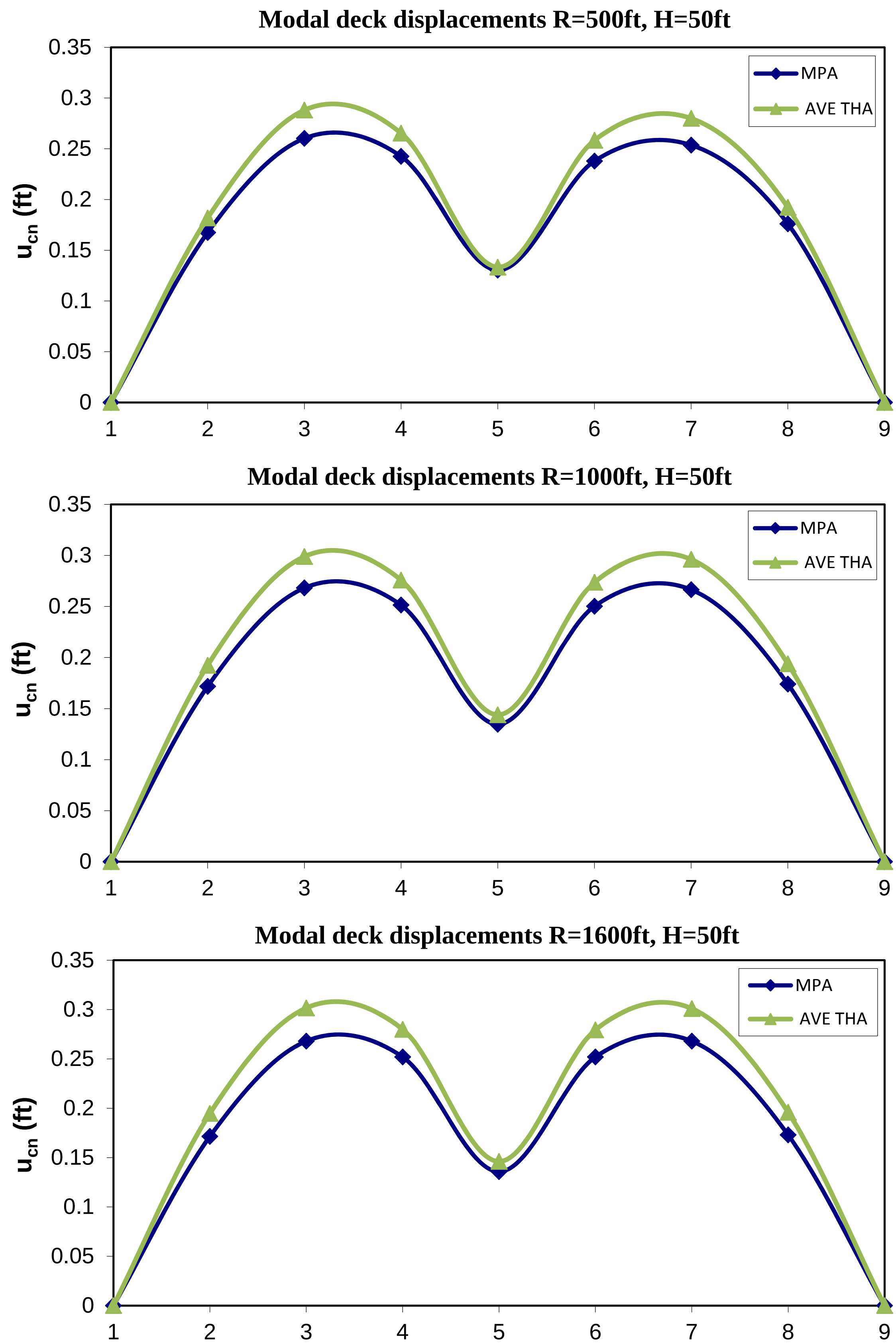

Figure 6-20 Deck Displacements for 2-span Steel BOX Bridge Model L=180-180ft, Pier Height = 50ft

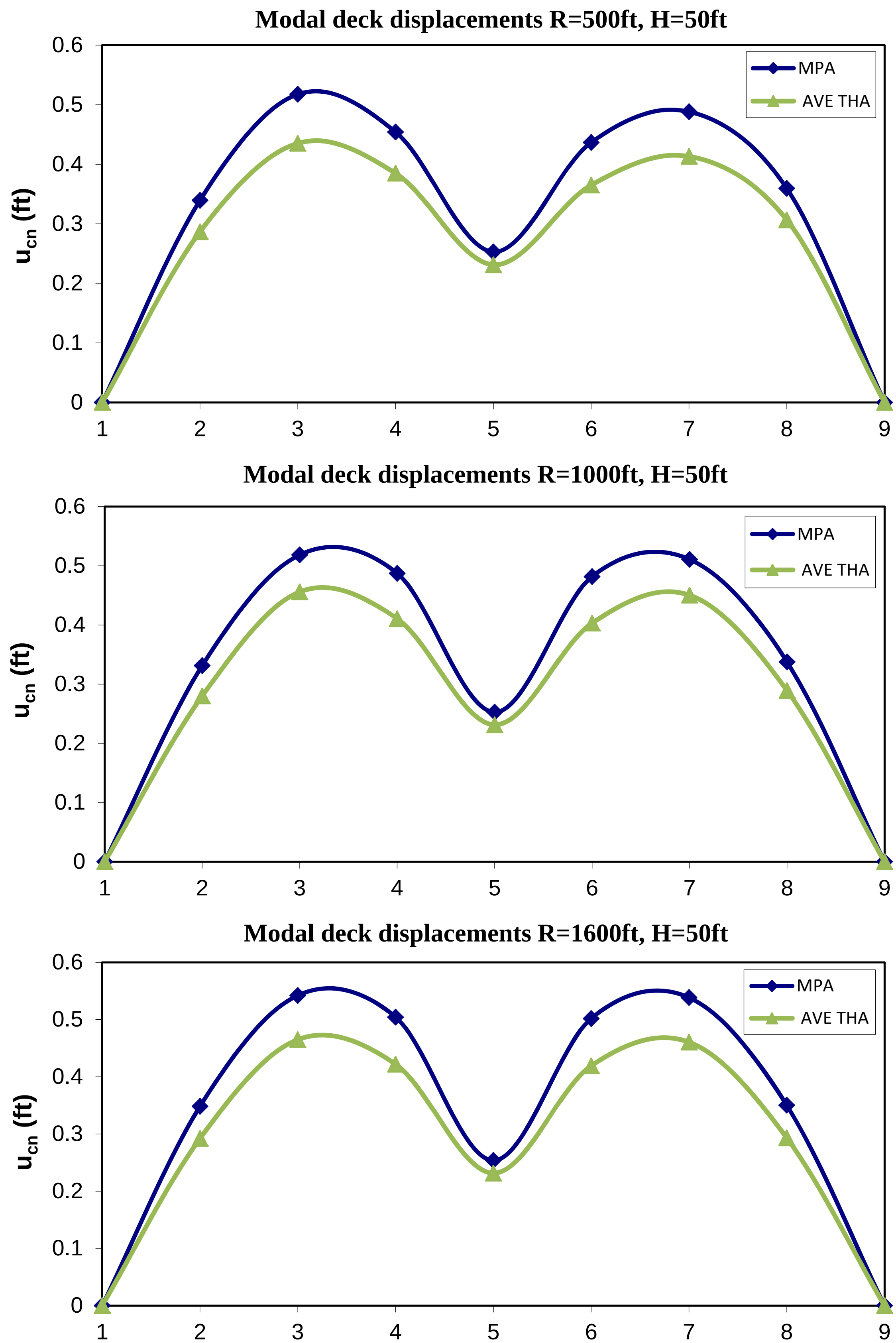

Figure 6-21 Deck Displacements for 2-span Steel BOX Bridge Model L=240-240ft, Pier Height = 50ft

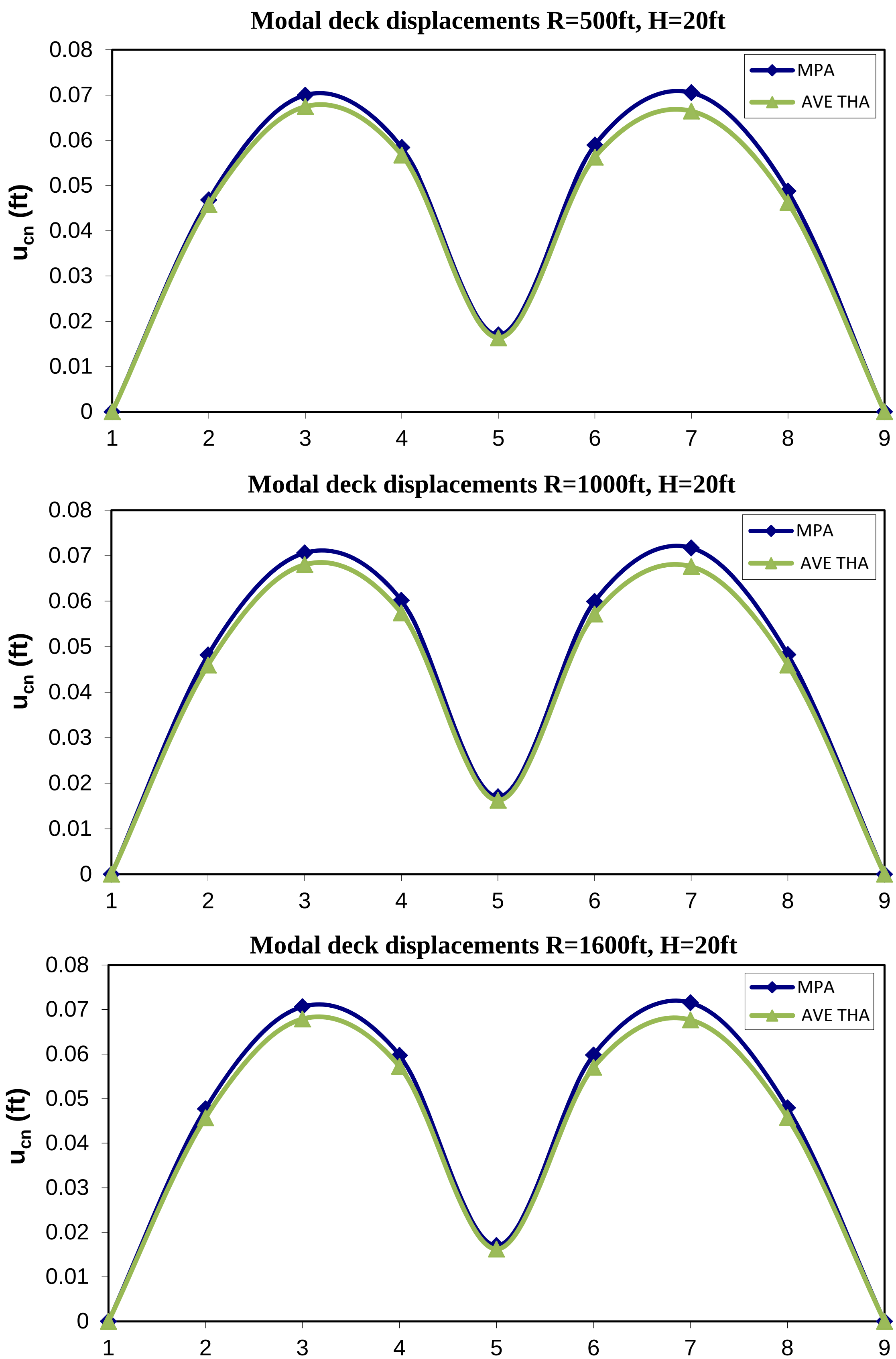

Figure 6-22 Deck Displacements for 2-span Steel BOX Bridge Model L=120-120ft, Pier Height = 20ft

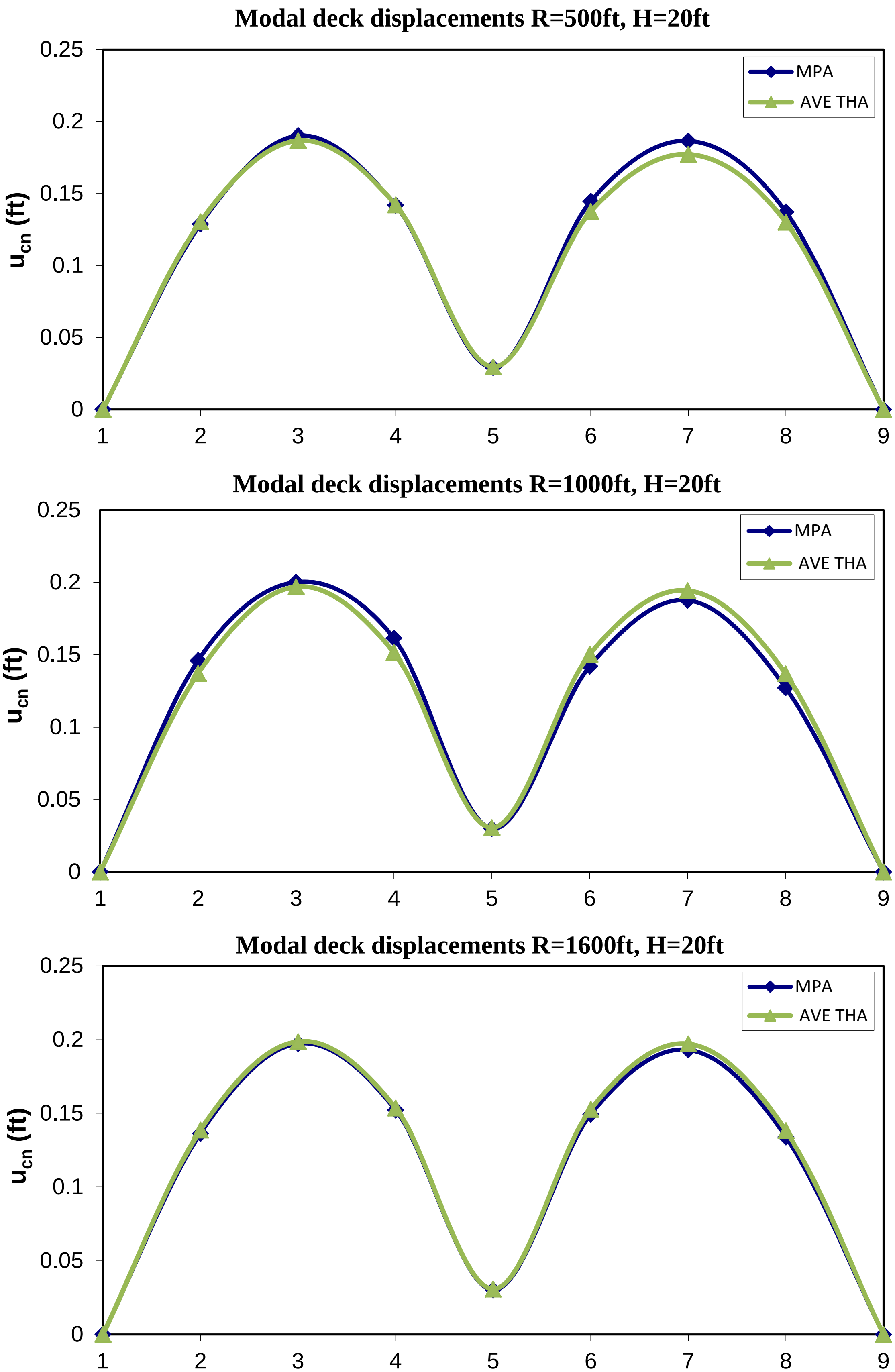

Figure 6-23 Deck Displacements for 2-span Steel BOX Bridge Model L=180-180ft, Pier Height = 20ft

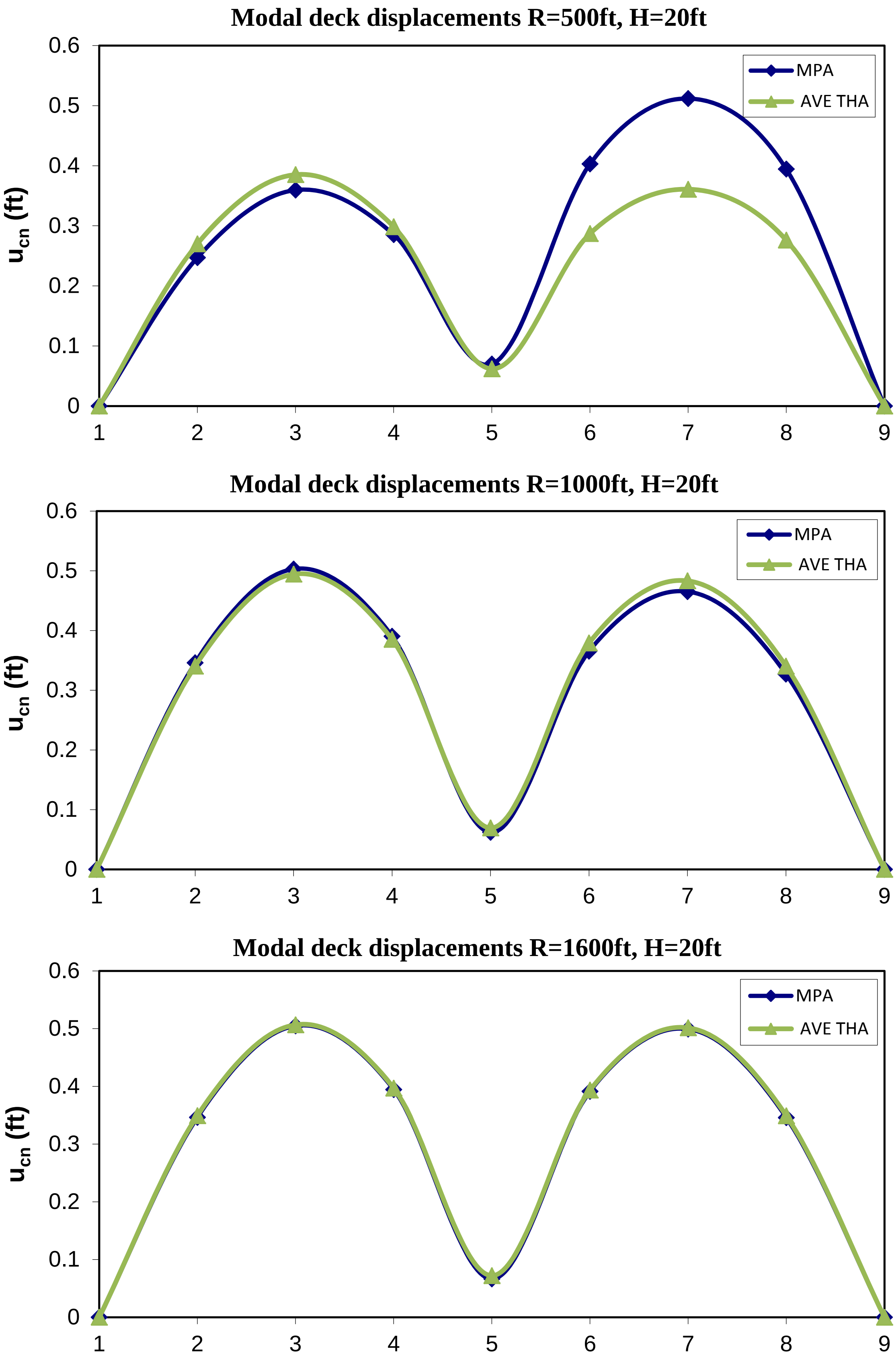

Figure 6-24 Deck Displacements for 2-span Steel BOX Bridge Model L=240-240ft, Pier Height = 20ft

6.3 DISCUSSION OF RESULTS

6.3.1 Demand Displacements

Results of the modal pushover analysis were evaluated by comparing them with those from NL-THA for three actual acceleration records compatible with the response spectrum. It is noted that the deck displacements shown in the figures as the AVE-THA case are the average of the peak displacements recorded in the structure during the three response-history analyses. Besides, in all results shown, the demand displacement is estimated independently in static and time-history inelastic analysis, whereas in some previous studies comparisons of displacement profiles are made assuming the same maximum displacement in both cases.

By evaluating all analysis cases, the proposed MPA procedure that accounts for more than one mode in the transverse direction (2 or 3 modes depending on the behavior of the bridge) is very accurate compared to NL-THA and the displacement profiles derived by the MPA method tend to match those obtained from the NL-THA.

For the cases of 3-span Bridge model with either steel I or steel BOX cross sections and pier height (H) of 50 ft (figures 6-1 to 6-3 & 6-13 to 6-15, respectively), the deck displacements derived using the MPA are very close to those obtained from NL-THA. It is also noticed that maximum demand displacement is slightly underestimated in the cases of short (100-120-100ft) and medium (140-180-140ft) spans, while for the case of long spans (180-240-180ft), the maximum demand displacement is slightly overestimated. Figure 6-25 illustrates a comparison between the maximum demand displacements obtained from the MPA method with those obtained from NL-THA method for the previously mentioned cases. Difference (%) in the figures can be defined as:

$$\text{Difference} = \frac{\delta_{MPA} - \delta_{THA}}{\delta_{THA}} \times 100\% \tag{6-1}$$

Where δ_{MPA} is the maximum transverse displacement resulting from the MPA method and δ_{THA} is the corresponding displacement resulting from the NL-THA method.

As shown in Figure 6-25, for steel I bridges, the differences range between 6.1% for the case of short spans (100-120-100ft) with largest radius of curvature (1600ft) and 23% for the case of long spans (180-240-180ft) with smallest radius of curvature (500ft). As the span length and curvature angle increases, the difference increases. While for the case of steel BOX bridges, the differences range between 11.8% and 13.4% for the same cases, respectively.

Furthermore, for the cases of 3-span Bridge models with steel I and steel BOX sections and pier height of 20 ft (figures 6-4 to 6-6 & 6-16 to 6-18, respectively), MPA method still predicts well the maximum transverse displacements and displacement profiles derived tend to match those obtained from NL-THA with the only difference that maximum demand displacements derived using MPA for the cases of medium spans (140-180-140ft) are slightly overestimated which is also noticed for the cases of long spans while results for short spans are still slightly underestimated. This would be explained as in those cases (medium and long spans) the superstructure is more flexible compared to the short stiff pier columns. Figure 6-26 shows the differences between the maximum demands derived from MPA compared to demands obtained from NL-THA for the 3-span cases with pier height of 20 ft. For the steel I cross sections models, the differences range between 5.7% and 15.3% (for short spans with R=1600ft and long spans with R=500ft, respectively), while for the cases with steel BOX cross sections, the differences range between 0.6% and 7% (for short spans with R=1600ft and long spans with R=500ft, respectively).

For the cases of 2-span Bridge models with steel I and steel BOX cross sections and pier height of 50 ft (figures 6-7 to 6-9 & 6-19 to 6-21, respectively), deck displacement profiles are still very close to profiles obtained from NL-THA and results deemed to be very accurate. As previously noticed in the cases for 3-span bridge models, MPA results for 2-span bridge models for short and medium spans are slightly underestimated when comparing to NL-THA results while results for long spans models are slightly overestimated. Figure 6-27 shows a comparison of the differences in maximum demand displacements predicted for the left span of each bridge model for both cases of steel I and BOX cross sections with regard to NL-THA demands. The differences in the steel I cases range between 0.60% (for the case of short spans (120-120ft) with radius of curvature = 1600ft) and 23.6% (for the case of large spans (240-240ft) with radius of curvature = 500 ft). For models with steel BOX cross sections, the differences range between 0.10% and 18.90%, respectively.

Lastly, for the cases of 2-span bridge models with steel I and steel BOX cross sections and pier height of 20 ft (figures 6-10 to 6-12 & 6-22 to 6-24, respectively), deck displacements results obtained from the MPA procedure are still in good agreement with those displacements obtained from the NL-THA except for the case of large spans (240-240ft) of steel BOX model (with radius of curvature = 500 ft). This case shows the effect of long span length when combined with short pier height (stiff column) and largest curvature angle. This bridge would be defined as highly irregular structure where stiff pier columns hinder free deformation of the superstructure in the transverse direction and therefore, MPA produces a displacement profile that has some discrepancies from those of NL-THA.

MPA procedure for all cases of 2-span Bridge model (short, medium, and long spans) with pier height of 20 ft slightly overestimated maximum demand displacements when compared to NL-THA method. Figure 6-28 illustrates the differences between the maximum demand displacements obtained from MPA and NL-THA for 2-span models with steel I and steel BOX sections and pier column height of 20 ft. Models with steel I show good agreement with the NL-THA results with differences range between 6.50% and 14.90% (for short spans with R=1600ft and long spans with R=500ft, respectively). Furthermore, models with steel box cross sections show very good agreement with the results from NL-THA except for the case of long spans. MPA predicts well the demand displacements for all cases with a maximum difference of 4.0% for the case of short spans with R=500 ft, while for the case of long spans with radius of curvature of 500 ft the difference is 41%.

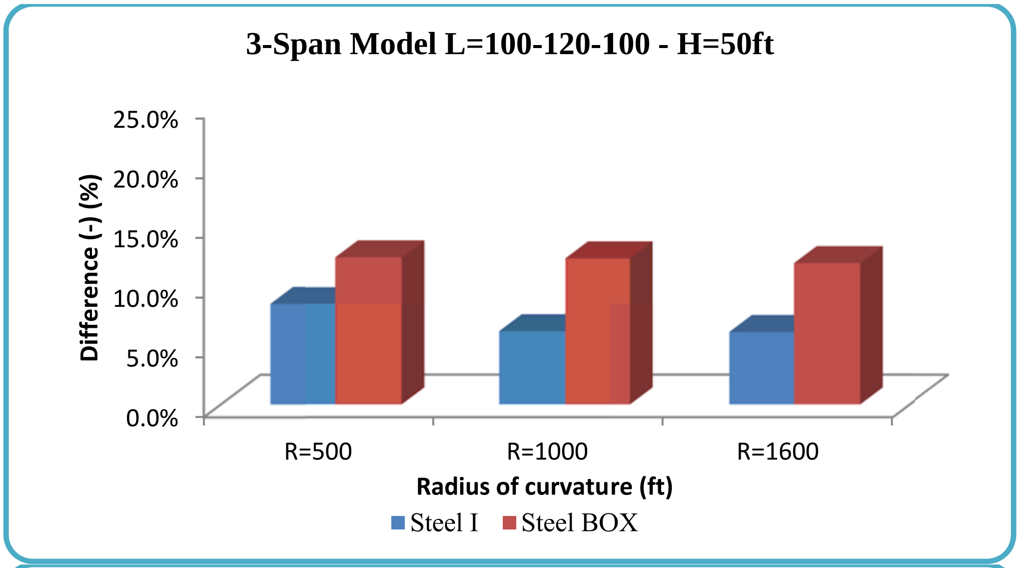

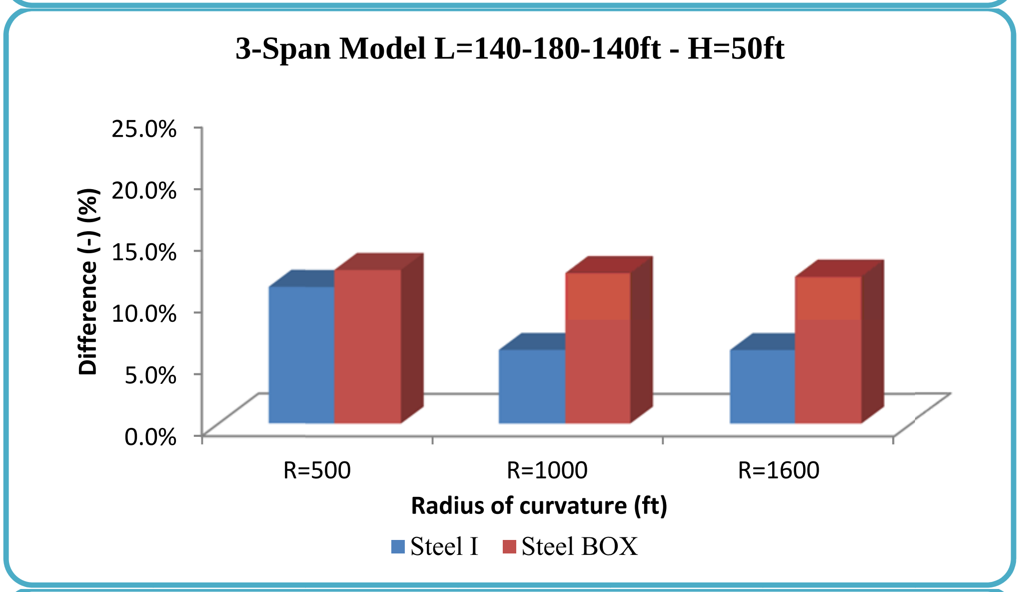

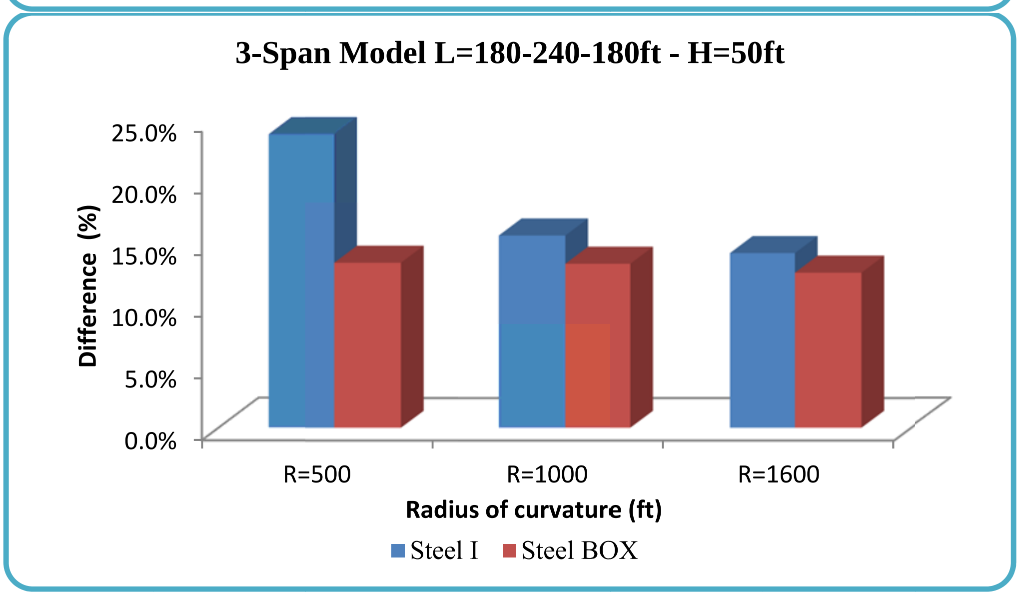

Figure 6-25 Differences between maximum demand displacements obtained from MPA and NL-THA for 3-span models Pier Height=50ft

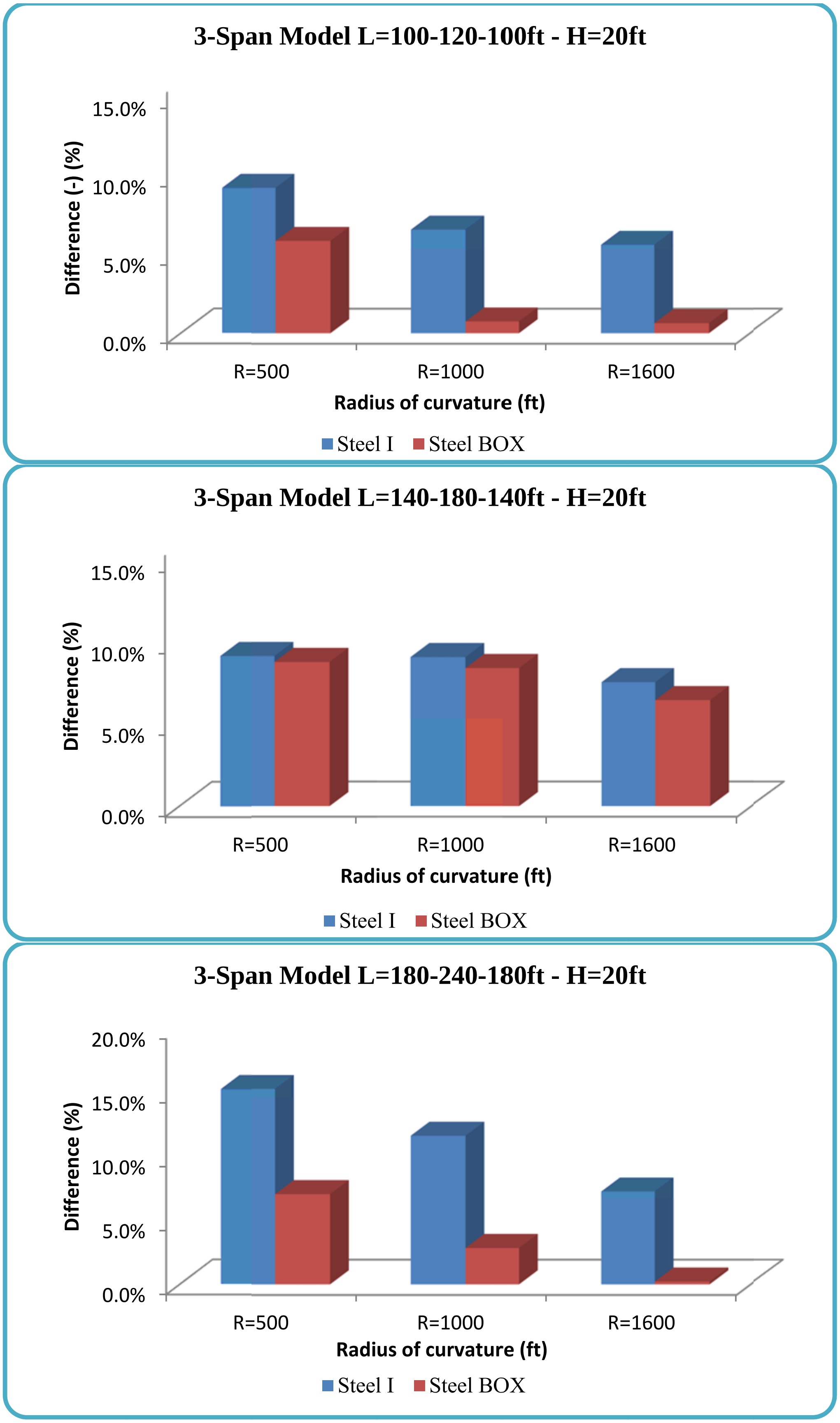

Figure 6-26 Differences between maximum demand displacements obtained from MPA and NL-THA for 3-span models, Pier Height=20ft

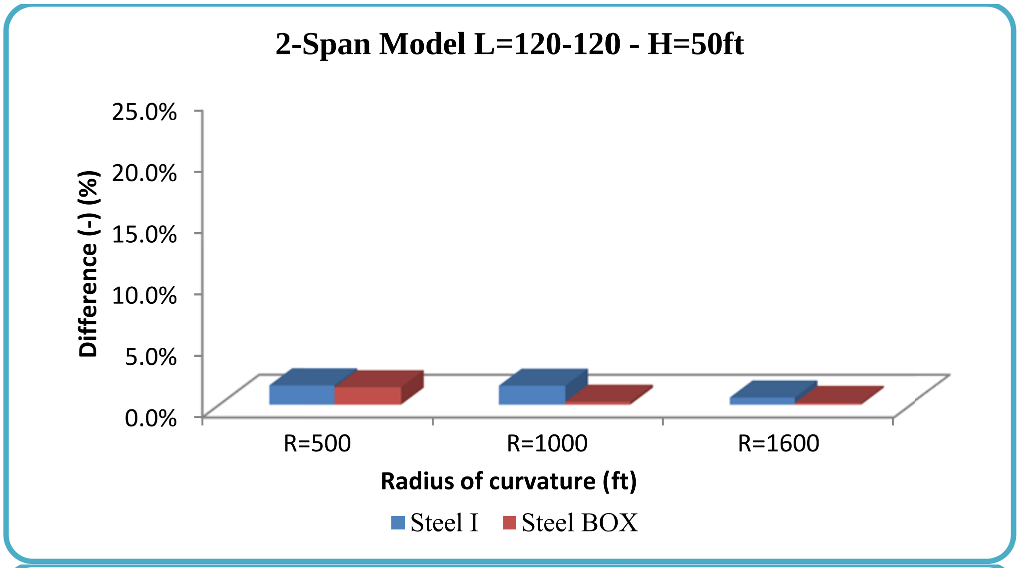

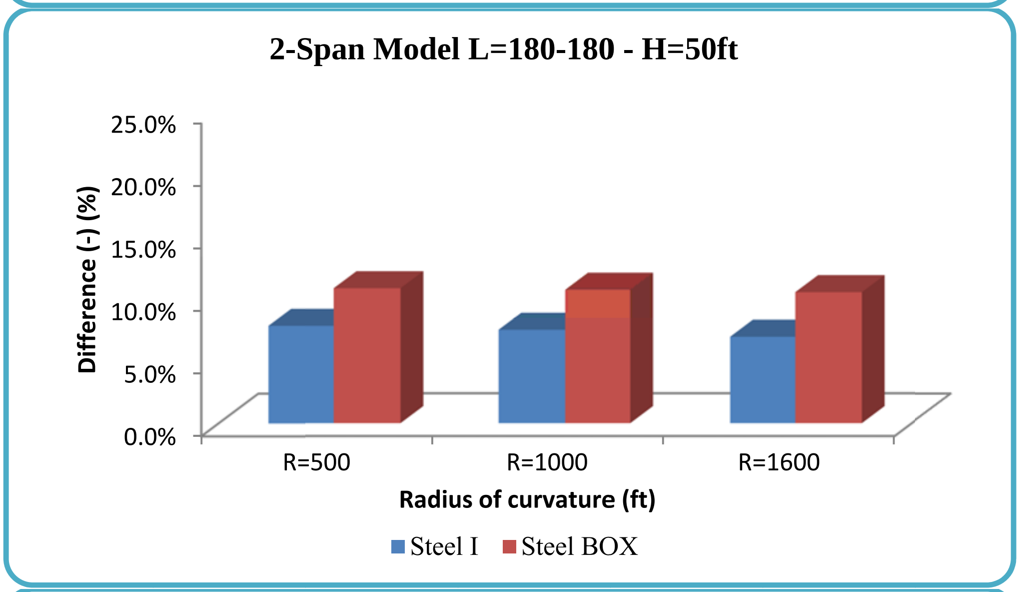

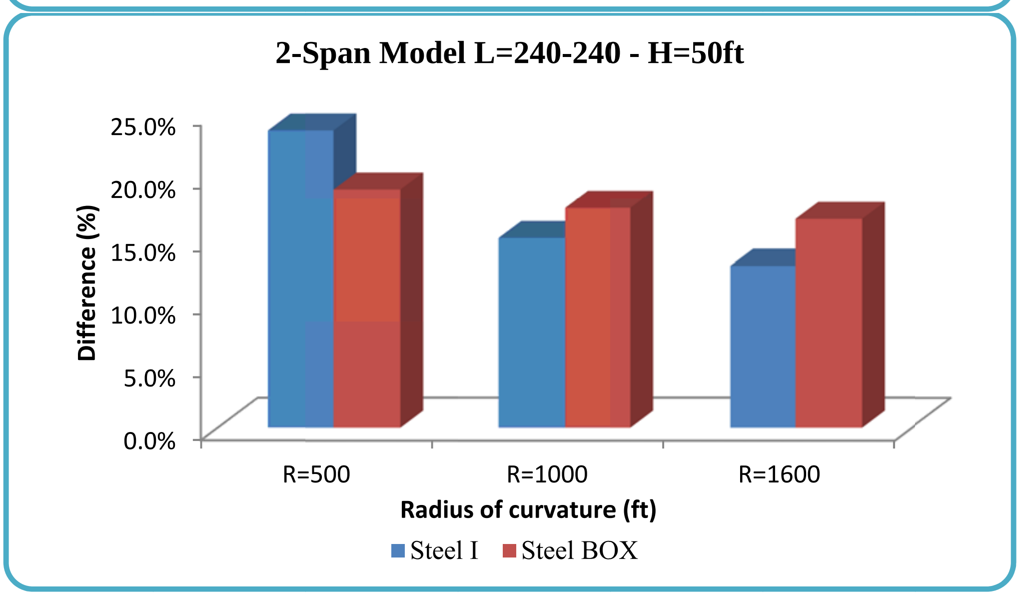

Figure 6-27 Differences between maximum demand displacements obtained from MPA and NL-THA for 2-span models Pier Height=50ft

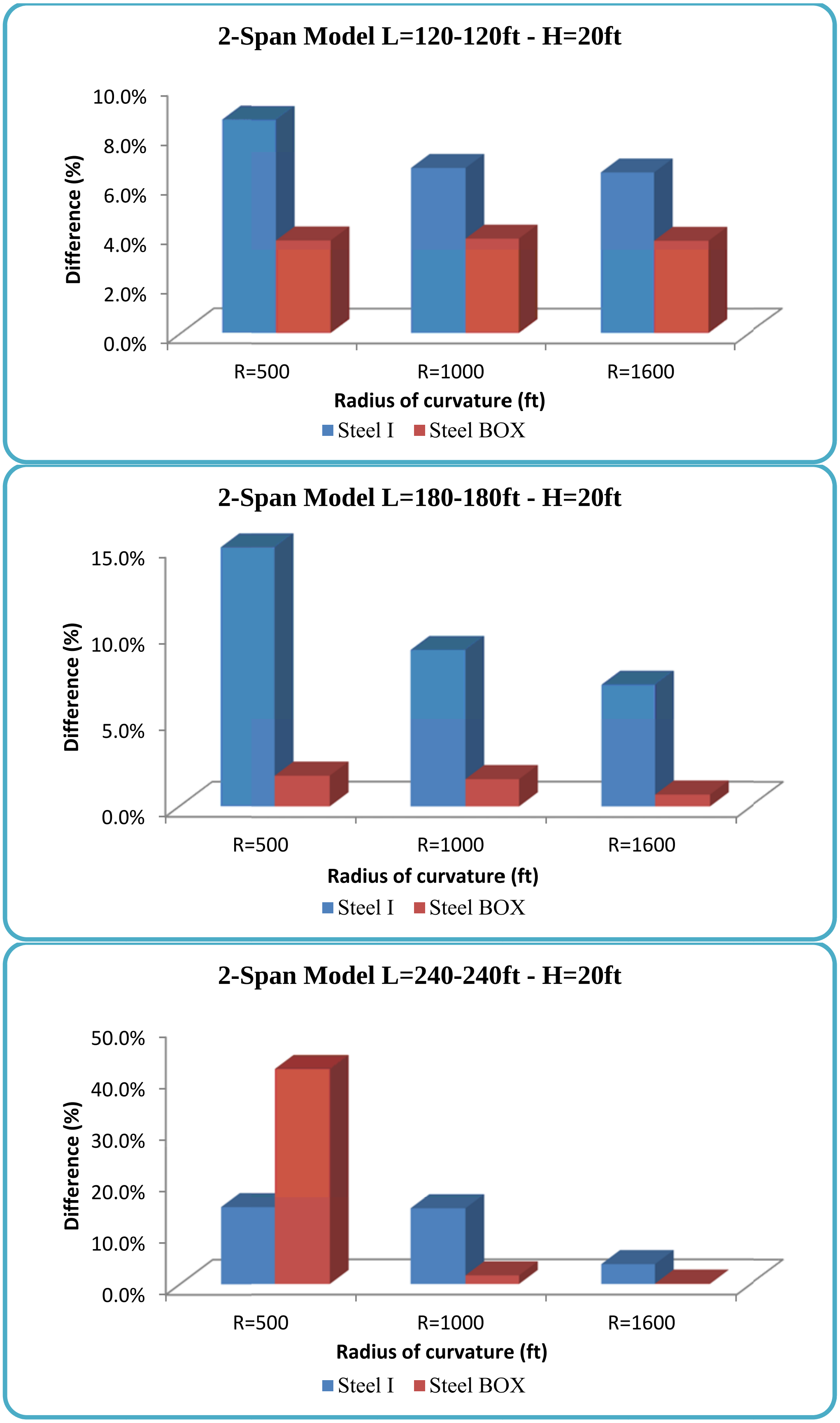

Figure 6-28 Differences between maximum demand displacements obtained from MPA and NL-THA for 2-span models Pier Height=20ft

6.3.2 Total Base Shear

Evaluation of the MPA procedure was further extended to compare the total base shear predicted for different bridge configurations with the results from the NL-THA procedure. Table 6-3 lists the total base shear for 3-span bridge models with both cross sections and different pier heights while Table 6-4 lists the total base shear for 2-span bridge models. It is noticed that for the wide range of bridge models used in the parametric study, MPA was slightly unconservative in estimating of the total bas shear.

For the 3-span bridge models with steel I girders and pier height = 50ft, MPA underestimated the base shear with differences range between 16% and 25% (with an average of 18.5% and a standard deviation of 869 kips) while for models with pier height = 20ft, differences range between 14% and 25% (with an average of 18.3% and a standard deviation of 872 kips).

For the 3-span bridge models with steel BOX girders, results tend to be more accurate and close from NL-THA results. For models with pier height = 50ft, MPA underestimated the base shear with differences range between 3.1% and 26.6% (with an average of 9.8% and a standard deviation of 1245 kips) while for models with pier height = 20ft, differences range between 5.3% and 23% (with an average of 15.5% and a standard deviation of 1612 kips).

As for the 2-span bridge models with steel I girders and pier height = 50ft, MPA underestimated the base shear with differences range between 11.8% and 24% (with an average of 18.16% and a standard deviation of 576 kips) while for models with pier height = 20ft, differences range between 7.5% and 21.9% (with an average of 14.3% and a standard deviation of 901 kips).

Lastly, for the 2-span bridge models with steel BOX girders and pier height = 50ft, MPA underestimated the base shear with differences range between 3.0% and 21.3% (with an average of 15.34% and a standard deviation of 806 kips) while for models with pier height = 20ft, differences range between 14.8% and 23.2% (with an average of 19.2% and a standard deviation of 1249 kips).

MPA predicts well total base shear and it underestimated results for all cases with an average of 16%.

Table 6-3 Total Base Shear for 3-span Bridge Models using NL-THA and MPA

		Base Shear for Steel I 3-Span Bridge Models (kips)					
		Pier Height (H) = 50ft			**Pier Height (H) = 20ft**		
Main Span (L)	R (ft)	THA	MPA	Diff. (%)	THA	MPA	Diff. (%)
L=120ft	500	4040.23	3342.3	-17.3%	2634	2098.3	-20.3%
	1000	4195.57	3500.7	-16.6%	3171	2670	-15.8%
	1600	4298.33	3604	-16.2%	3738	3221.5	-14.0%
L=180ft	500	5066	3772.6	-25%	4177	3357.14	-20.0%
	1000	5080	4111	-19%	4462	3625	-18.8%
	1600	5123	4304	-16%	4571	3787	-17.2%
L=240ft	500	6565	5073.6	-22.7%	5533	4150	-25.0%
	1000	6683	5497.8	-17.8%	5590	4677	-17.0%
	1600	6700	5585.98	-16.7%	5659.13	4724	-16.5%
		Base Shear for Steel BOX 3-Span Bridge Models (kips)					
		Pier Height (H) = 50ft			**Pier Height (H) = 20ft**		
Main Span (L)	R (ft)	THA	MPA	Diff. (%)	THA	MPA	Diff. (%)
L=120ft	500	3284.6	3077.45	-6.3%	2261	1806	-20.1%
	1000	3948.2	3707.34	-6.0%	2653	2207.5	-17.0%
	1600	4021.25	3897.6	-3.1%	2725.52	2404.7	-12.0%
L=180ft	500	4246.34	3871.41	-9.0%	3435.32	2645.2	-23.0%
	1000	4791.8	4503.6	-6.1%	3671.33	2886.025	-21.4%
	1600	5179.45	4848.13	-6.3%	4700	3741.27	-20.4%
L=240ft	500	6592.74	4837.16	-26.6%	6068	5340	-12.0%
	1000	7110.11	6070.25	-14.6%	6190	5653	-8.7%
	1600	7871.3	7051.22	-10.5%	6285	5952.13	-5.3%

Table 6-4 Total Base Shear for 2-span Bridge Models using NL-THA and MPA

		Base Shear for Steel I 2-Span Bridge Models (kips)					
		Pier Height (H) = 50ft			Pier Height (H) = 20ft		
Main Span (L)	R (ft)	THA	MPA	Diff. (%)	THA	MPA	Diff. (%)
L=120ft	500	3019.97	2432.5	-21.0%	1619.12	1263.95	-21.9%
	1000	3033.65	2408.95	-20.6%	1664.13	1341.46	-19.4%
	1600	3109.18	2471.8	-20.5%	1668.174	1387.77	-16.8%
L=180ft	500	4265.67	3237.35	-24.1%	2796.94	2257.76	-19.3%
	1000	4382	3560.02	-18.8%	2927.63	2706.52	-7.6%
	1600	4405.66	3580.62	-18.7%	3103.67	2871.51	-7.5%
L=240ft	500	4061	3429.6	-15.55%	3608.57	3108.68	-13.9%
	1000	4216.38	3689.1	-12.5%	3717	3214	-13.6%
	1600	4296.4	3791.25	-11.8%	3986.85	3654	-8.4%
		Base Shear for Steel BOX 2-Span Bridge Models (kips)					
		Pier Height (H) = 50ft			**Pier Height (H) = 20ft**		
Main Span (L)	R (ft)	THA	MPA	Diff. (%)	THA	MPA	Diff. (%)
L=120ft	500	2766.43	2192	-20.8%	1478.1	1135.68	-23.2%
	1000	2805	2247	-19.9%	1563.56	1233.56	-21.1%
	1600	2858.67	2299.7	-19.6%	1672	1323.88	-20.8%
L=180ft	500	3831.06	3015.8	-21.3%	2401	1900	-20.9%
	1000	3858	3152.04	-18.3%	2573.1	2072.38	-19.5%
	1600	3898	3198	-18.0%	2647	2144	-19.0%
L=240ft	500	4066.3	3662	-10.0%	4334.07	3529.25	-18.6%
	1000	4467	4118	-7.8%	4856.06	4127.39	-15.0%
	1600	4491.67	4385	-2.4%	5075.76	4319.59	-14.9%

6.4 INFLUENCES OF DIFFERENT PARAMETERS

Influences of different parameters included in the parametric study on maximum transverse displacements and the total base shear are shown in Figure 6-29 through Figure 6-32 for bridge models with steel I and steel BOX cross sections. (L) in the figures refers to the main span length of the bridge; for a 3-span Bridge it is the middle span length while for 2-span Bridge it is the length of one of the two equal spans.

6.4.1 Influence of Bridge length

As shown in Figure 6-29 for steel I bridges, maximum demand displacements are influenced significantly by bridge length. 3-span Bridge models with pier height of 50 ft generally produced higher displacements than corresponding 2-span bridges. For bridges with main span (L) of 120 ft and different radii of curvature, maximum demand displacements are increased by 70%, 65%, and 58% from demand displacements of 2-span bridges for radius of curvature (R) = 500, 1000, and 1600 ft, respectively. Bridges with L=180 ft, maximum displacements are increased by 41%, 49%, and 49% for R=500, 1000, and 1600 ft, respectively. While bridges with L= 240 ft, maximum displacements are increased 26%, 27%, and 35% for R=500, 1000, and 1600 ft, respectively. On the other hand, 3-span bridges with pier height of 20 ft showed less influence of bridge length on the maximum demand displacements. For bridge models with long spans (L=240ft), bridge length has insignificant effect. Demand displacements of bridges with L= 180 ft are increased by 14% for all radii of curvature used, while for bridges with L= 120 ft, demand displacements are increased by 17%.

Furthermore, results for steel BOX bridges are shown in Figure 6-30. Same trends as in the steel I cases are also noted. For 3-span steel box models with 50 ft pier heights, models with L= 120 ft have increased demand displacements by 53% than those of 2-span models for all radii of curvature. For models with L=180 ft, demand displacements are increase by 44% for all radii of curvature used, while models with L=240 ft, maximum demand displacements are increased by 25%, 31%, and 31% for R= 500, 1000, 1600 ft, respectively. For 3-span steel box models with 20 ft pier heights, demand displacements for models with L=120 ft are increased by 17%, 28%, and 37% for R=500, 1000, and 1600 ft, respectively. For models with L=180 ft, demand displacements are increased by 9% for all radii of curvature, while for models with L=240 ft, displacements are increased by 1%, 10%, and 10% for R=500, 1000, 1600 ft, respectively.

As for the total base shear, Figure 6-31 shows calculated base shear for different bridge models with steel I cross sections and Table 6-5 list the percentages of increase. 3-span bridge models with pier column height = 20ft are more affected by increasing bridge length than other models with column height = 50ft. Short spans models (L=120ft) with H=20ft are the most affected and had increased base shear by 66%, 99%, and 132% for R=500, 1000, and 1600ft, respectively.

Figure 6-32 and Table 6-6 list the total base shear for bridge models with steel box cross sections. Same trends are observed as in the case of steel I girders and also short spans models with pier column height = 20ft were the most affected sections by increasing bridge length.

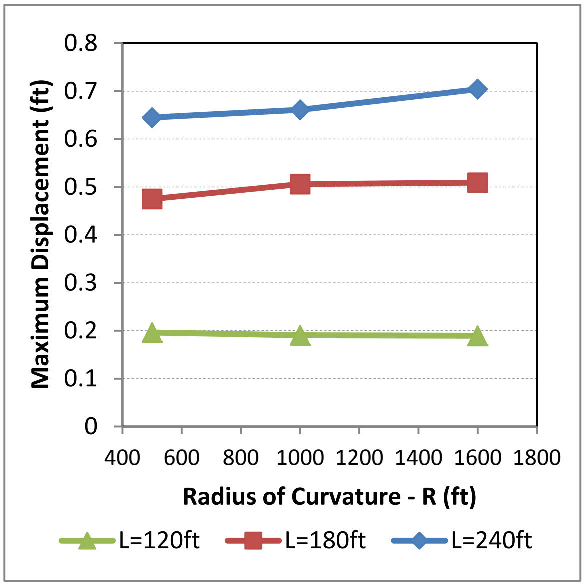

3-span Bridge model with pier height = 50ft

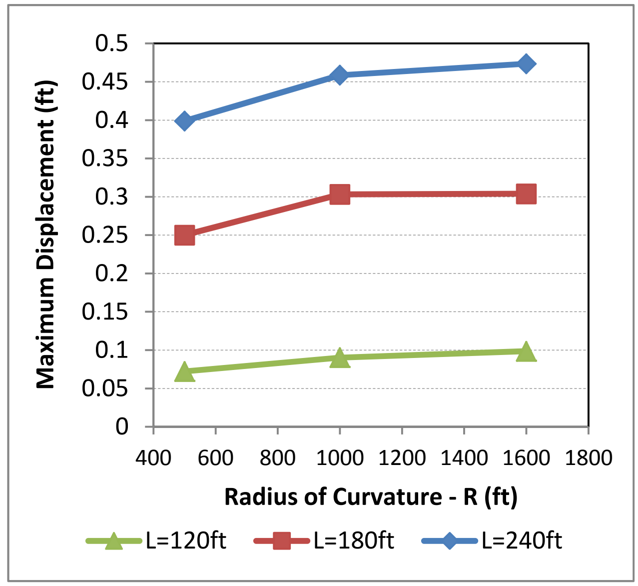

3-span Bridge model with pier height = 20ft

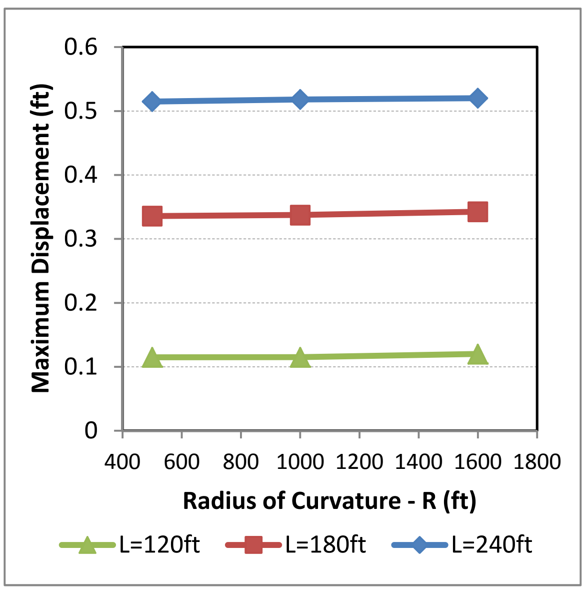

2-span Bridge model with pier height = 50ft

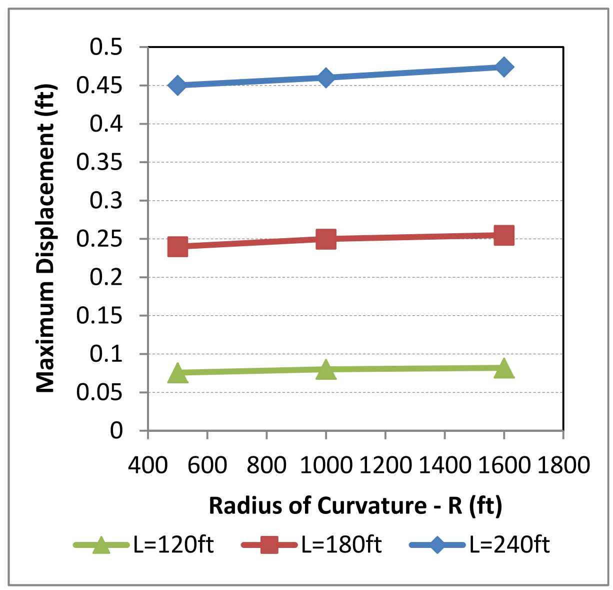

2-span Bridge model with pier height = 20ft

Figure 6-29 Variation of maximum displacements with radius of curvature for bridge models with steel I girders

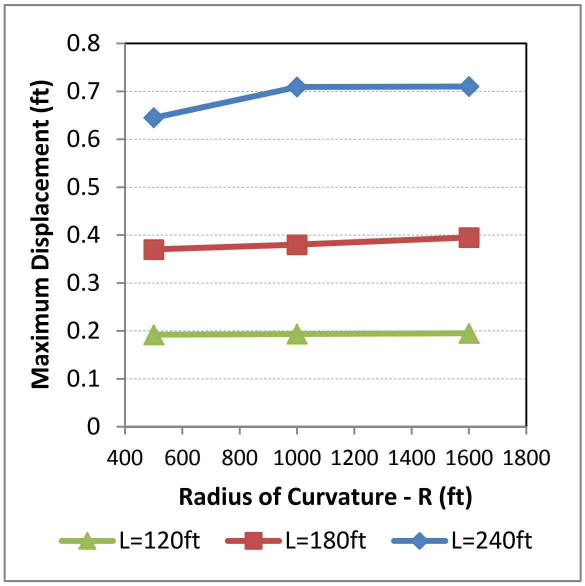

3-span Bridge model with pier height = 50ft

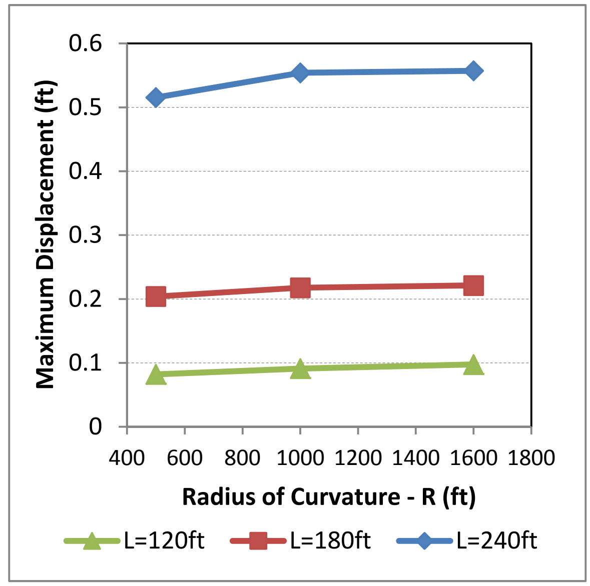

3-span Bridge model with pier height = 20ft

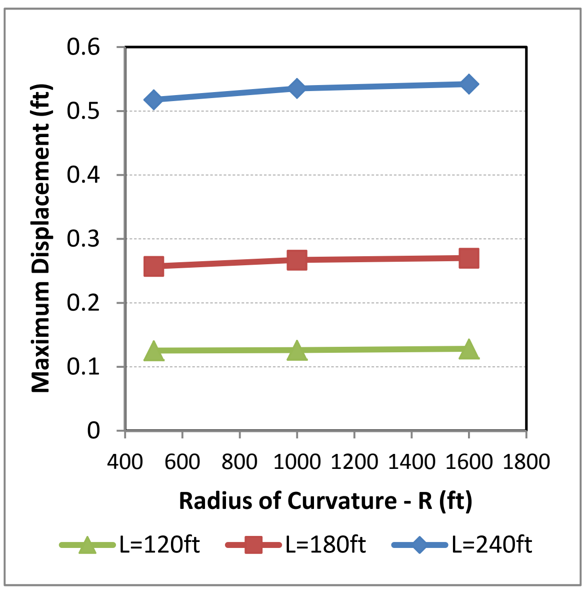

2-span Bridge model with pier height = 50ft

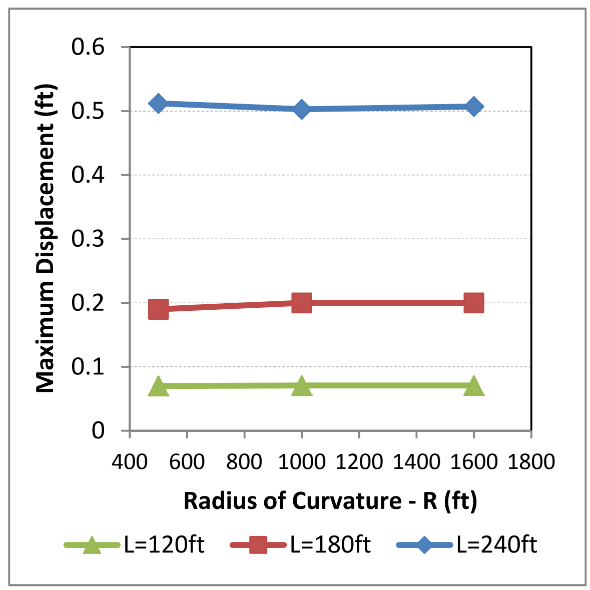

2-span Bridge model with pier height = 20ft

Figure 6-30 Variation of maximum displacements with radius of curvature for bridge models with steel BOX girders

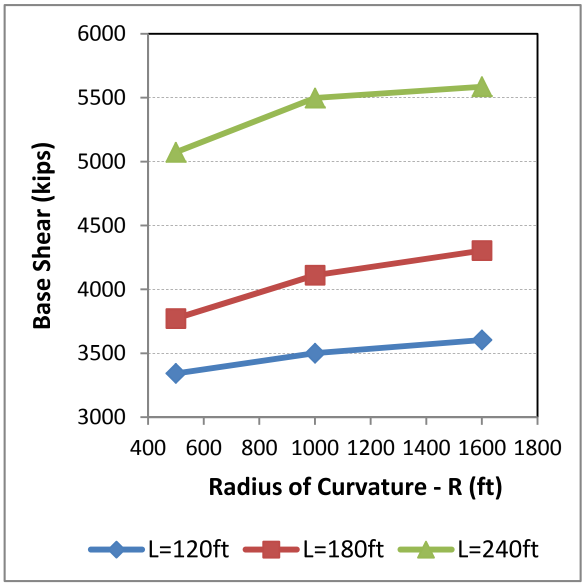

3-span Bridge model with pier height = 50ft

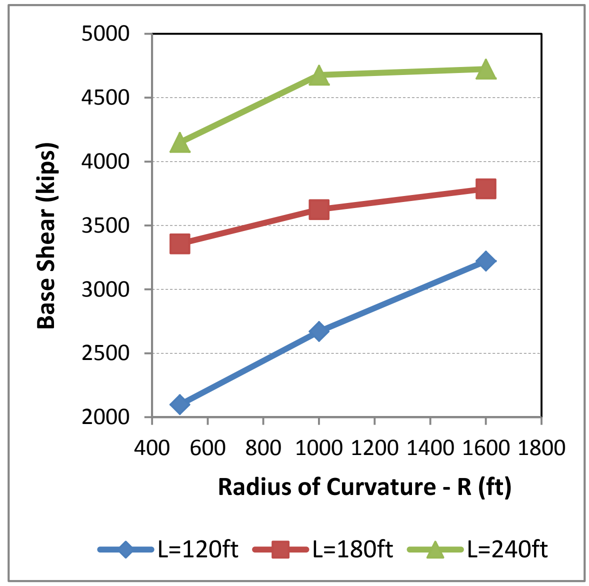

3-span Bridge model with pier height = 20ft

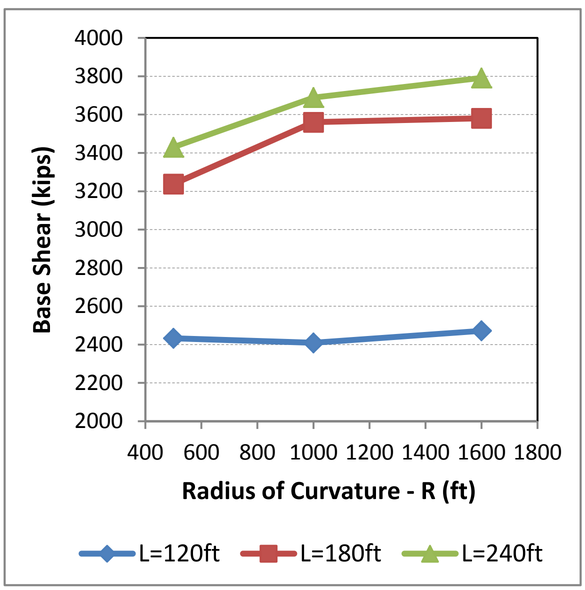

2-span Bridge model with pier height = 50ft

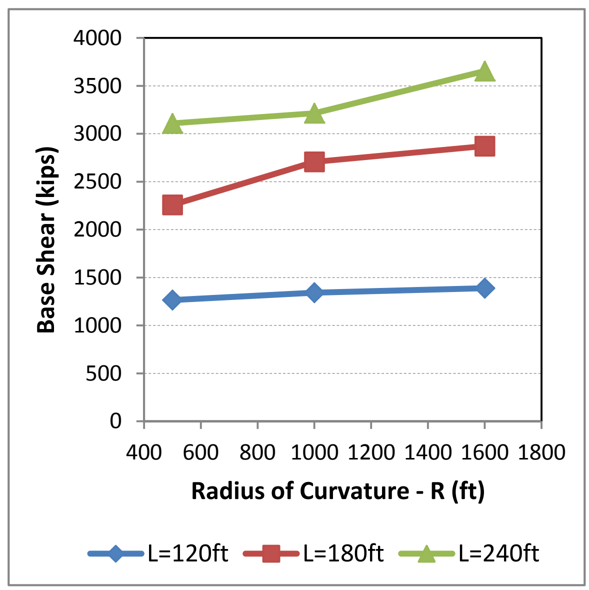

2-span Bridge model with pier height = 20ft

Figure 6-31 Variation of total base shear with radius of curvature for bridge models with steel I girders

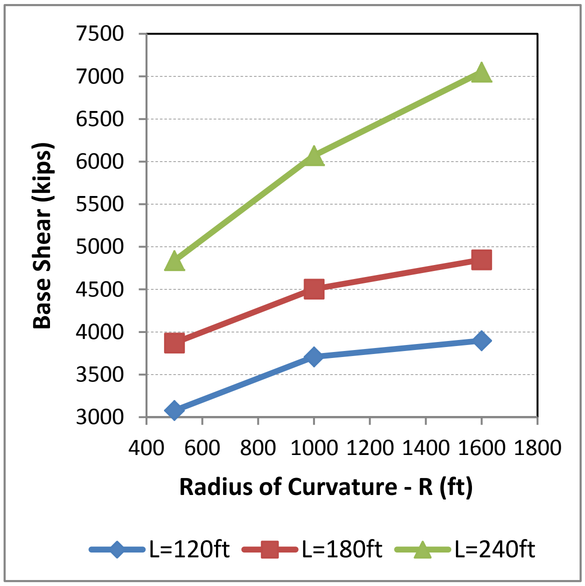

3-span Bridge model with pier height = 50ft

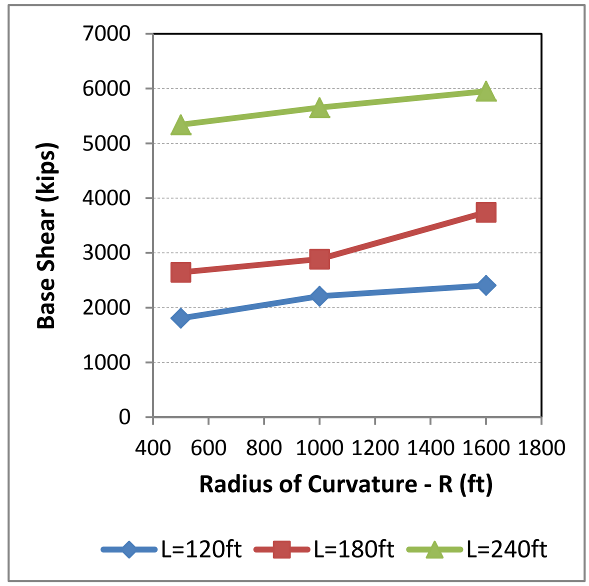

3-span Bridge model with pier height = 20ft

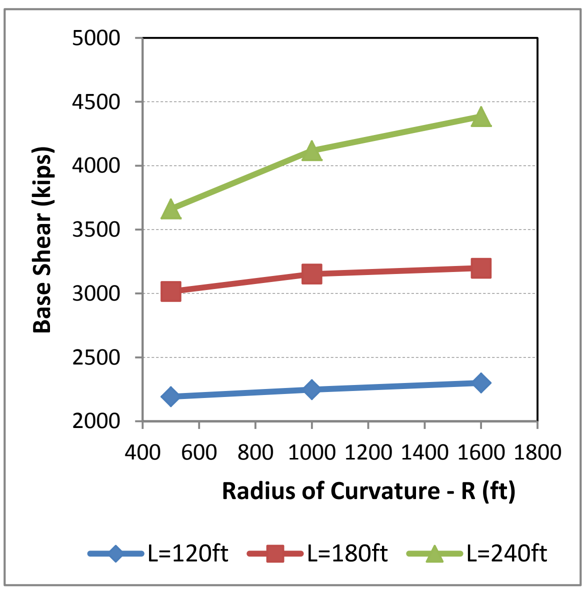

2-span Bridge model with pier height = 50ft

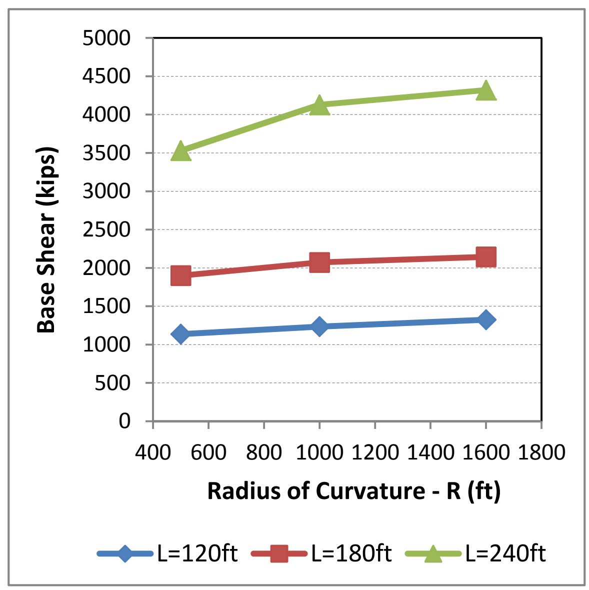

2-span Bridge model with pier height = 20ft

Figure 6-32 Variation of total base shear with radius of curvature for bridge models with steel BOX girders

Table 6-5 Total base shear increase (%) for 3-span bridge models with steel I sections

3-span models with Steel I cross sections, H=50ft			
	R=500 ft	R=1000 ft	R=1600 ft
L=120 ft	37%	45%	46%
L=180 ft	17%	15%	20%
L= 240 ft	48%	49%	47%
3-span models with Steel I cross sections, H=20ft			
	R=500 ft	R=1000 ft	R=1600 ft
L=120 ft	66%	99%	132%
L=180 ft	49%	34%	32%
L= 240 ft	33%	46%	29%

Table 6-6 Total base shear increase (%) for 3-span bridge models with steel BOX sections

3-span models with Steel BOX cross sections, H=50ft			
	R=500 ft	R=1000 ft	R=1600 ft
L=120 ft	40%	65%	69%
L=180 ft	28%	43%	52%
L= 240 ft	32%	47%	61%
3-span models with Steel BOX cross sections, H=20ft			
	R=500 ft	R=1000 ft	R=1600 ft
L=120 ft	59%	79%	82%
L=180 ft	39%	39%	74%
L= 240 ft	51%	37%	38%

6.4.2 Influence of radius of curvature (R)

The influence of radius of curvature on the maximum demand displacements is shown in Figure 6-29 and Figure 6-30 for steel I and steel BOX models, respectively. The effect is more noticeable for the 3-span models than in the 2-span models. For 3-span steel I models with pier height of 50 ft, the maximum demands displacements are increased with an average of 7% when the radius of curvature is increased from 500 ft to 1600 ft, while for models with pier height of 20 ft, maximum displacements are increased with an average of 25%. For 3-span steel BOX models with pier height of 50 ft, maximum displacements are also increased with an average of 7% while for models with pier height of 20 ft, the average increase is 12%. For all cases of 2-span models with either steel I or steel BOX and pier height of 50 or 20 ft, maximum demand displacements are slightly increased within a range of 1% to 4%.

Same trends were also noticed for the influence of radius of curvature on the total base shear. For 3-span models with steel I sections, base shear was increased by an average of 11% and 27% for models with H=50, 20ft respectively when increasing the radius of curvature from 500ft to 1600ft while for 2-span models, it was increased by 8% and 18%.

For 3-span models with steel BOX, base shear was increased by an average of 33% and 29% for models with H=50, 20ft respectively when increasing the radius of curvature from 500ft to 1600ft while for 2-span models, it was increased by 10% and 17%.

6.4.3 Influence of Pier height (H)

Two cases were considered in the study. Bridge models with pier column heights of 20 and 50 ft were studied. Maximum demand displacements are significantly influenced by pier column's height. 3-span models are more affected by pier's height than 2-span models for both cross sections considered. Demand displacements' increases are listed as a percentage in Table 6-7and Table 6-8 for steel I and steel BOX models, respectively. The increase percentage was calculated as follow:

$$\text{Percentage} = \frac{\delta_{i\,(\mathrm{H}=50)} - \delta_{j\,(\mathrm{H}=20)}}{\delta_{j\,(\mathrm{H}=20)}} \times 100\,\%$$

Where δ_i is the demand displacement for the case considered where pier height = 50 ft, and δ_j is the corresponding demand displacement value when pier height, H=20 ft.

From the results shown, it is clear that demand displacements calculated from 3-span Bridge models with steel I & BOX cross sections for short and medium spans (L) are significantly influenced by changing pier height from 20 ft to 50 ft and have the largest increase percentages.

Table 6-9 and Table 6-10 list the percentages for total base shear increases for models with steel I and steel BOX, respectively after increasing the pier height from 20ft to 50ft. Changing pier height also has significant effect on base shear for 2-span models especially for those with short and medium spans.

Table 6-7 Demand displacements increase for Steel I models

3-span models with Steel I cross sections			
	R=500 ft	R=1000 ft	R=1600 ft
L=120 ft	170%	107%	92%
L=180 ft	90%	66%	66%
L= 240 ft	61.6%	45%	45%
2-span models with Steel I cross sections			
	R=500 ft	R=1000 ft	R=1600 ft
L=120 ft	52%	45%	45%
L=180 ft	40%	35%	34%
L= 240 ft	14.4%	12.6%	9.7%

Table 6-8 Demand displacements increase for Steel BOX models

3-span models with Steel BOX cross sections			
	R=500 ft	R=1000 ft	R=1600 ft
L=120 ft	134%	126%	100%
L=180 ft	81%	74%	74%
L= 240 ft	28%	28%	27%
2-span models with Steel BOX cross sections			
	R=500 ft	R=1000 ft	R=1600 ft
L=120 ft	79%	78%	78%
L=180 ft	35%	34%	34%
L= 240 ft	2%	6%	7%

Table 6-9 Base shear differences for Steel I models

3-span models with Steel I cross sections			
	R=500 ft	R=1000 ft	R=1600 ft
L=120 ft	59.24%	31.11%	11.87%
L=180 ft	12.38%	13.41%	13.65%
L= 240 ft	22.26%	17.55%	18.25%
2-span models with Steel I cross sections			
	R=500 ft	R=1000 ft	R=1600 ft
L=120 ft	92.45%	79.58%	78.11%
L=180 ft	43.39%	31.53%	24.69%
L= 240 ft	10.32%	14.78%	3.76%

Table 6-10 Base shear differences for Steel BOX models

3-span models with Steel BOX cross sections			
	R=500 ft	R=1000 ft	R=1600 ft
L=120 ft	70.40%	67.94%	62.08%
L=180 ft	46.36%	56.05%	29.59%
L= 240 ft	-9.42%	7.38%	18.47%
2-span models with Steel BOX cross sections			
	R=500 ft	R=1000 ft	R=1600 ft
L=120 ft	93.01%	82.16%	73.71%
L=180 ft	58.73%	52.1%	49.16%
L= 240 ft	3.76%	-0.23%	1.51%

7. SUMMARY AND CONCLUSIONS

7.1 SUMMARY

The objectives of this research investigation were to evaluate the accuracy of the modal pushover analysis (MPA) procedure in estimating seismic demands for a wide range of bridges after proposing some modifications that would render the MPA procedure applicable for bridges.

Principles of the MPA were presented along with the theoretical background of the procedure. A review of the available literature indicated that important advancements have been made to apply this approach for high-rise buildings and frames. However, only a few researchers implemented this procedure for bridges.

The main key steps of the MPA were investigated and some modifications were proposed that would assure that the procedure is applicable for bridge assessment. Definition of the monitoring point was presented and different appropriate locations; deck mass center, equivalent SDOF location, or most critical pier location, were proposed and investigated. Development of the pushover curve with regard to different control points was investigated. Modal load pattern used for pushover analysis was evaluated and a correction was proposed when inelastic behavior of bridge is developed. Estimation of the demand displacement was investigated to quantify the accuracy of the MPA procedure for bridges.

Case studies of three bridges were presented for MPA verification. Description of the finite element model for each bridge was presented along with the bridge properties. Calculations of different parameters needed to define plastic hinges as well as nonlinear link elements needed to perform modal pushover and nonlinear time history analyses using the SAP2000 were presented in Appendix A. Design response spectra needed for MPA as well as acceleration time histories for time history analyses were presented.

For Bridge no. 1 of the case studies, comparisons of results obtained from the SPA and MPA procedures with the results of the NL-THA, which is considered the most reliable method for nonlinear analysis, were performed to validate the MPA procedure. Observations obtained from the comparison of results can be summarized as following:

- Control node is the node used to monitor the displacement of the structure and to draw the pushover curve. Among the proposed locations; most critical pier location was deemed to give the most accurate results compared to NL-THA results.

- There was a little merit from adding more modes whose mass participation factor is less than 1%, while calculating demand displacements and less rigid rule than the 90% mass participation could be adopted. On the other hand, adding more modes slightly improved base shear prediction by 5%.

- As for the modal load pattern implemented to represent the distribution of inertia forces, it produced good results with regard to maximum demand displacement if the structure remains elastic or close to the yield point.

- For increasing levels of earthquake excitation, more inelasticity is developed in the structure. The correction proposed in section 2.4.3 to calculate an improved target displacement of the monitoring point (u'_{cn}) was found to give accurate results compared to the NL-THA results and better displacement profiles are obtained.

- SPA procedure poorly predicted the transverse displacement at the end areas of the bridge and gave better estimates only in the area of the central piers; such area is dominated by the first fundamental transverse mode.

- MPA procedure which accounts for more transverse modes than SPA predicted well the deck displacements of the bridge with more enhancements to the end areas of the bridge.

- Modified MPA procedure overestimated the maximum demand displacements by only 8% for both levels of earthquake excitation used in the analysis (PGA=0.45g and 0.60g).

- As for the total base shear, MPA procedure tends to underestimate the base shear results by 28% and 26% for both cases of earthquake levels (0.45g and 0.60g), respectively.

- MPA predicted well the rotations of plastic hinges compared to rotations from NL-THA. MPA underestimated rotations of most critical pier by only 8.8% and 4.6% for PGA=0.45g and 0.60g, respectively.

For bridges no. 2 & 3 of the case studies, results obtained from the MPA procedure were also compared with results from the NL-THA in order to verify the former procedure. Observations obtained from the comparison of results can be summarized as following:

- Calculated demands using the SPA and MPA procedures are in very good agreement with those results from the NL-THA and results are deemed very accurate.

- As for the demand displacement in the transverse direction; for PGA=0.30g, SPA and MPA slightly underestimated maximum demand displacements by 6.0% and 3.0%, respectively. As the level of excitations increases (PGA=0.45g), both methods slightly overestimated the maximum demand displacement by 4.0%

- As for the plastic rotations at the top of the piers; for bridge no. 2, MPA underestimated the plastic rotations by an average of 21% for PGA=0.30g and overestimated it by 4% for PGA=0.45g. While for bridge no. 3, MPA underestimated the plastic rotations by 22% for PGA=0.30g and overestimated rotations by 8% for PGA=0.45g.

- MPA predicted very well the total base shear for both bridges. It slightly underestimated the results with an average difference of 4% for all levels of earthquake considered.

- By analyzing results from bridge no 2 and 3 where the only difference between the two models was a skew angle of 30 degrees in bridge no. 2, skewness was only found to increase bridge responses by 10% and 2% for load cases of PGA=0.30g and 0.45g, respectively.

Also, results obtained from analyzing bridge no.1 and bridge no.2 using MPA procedure were compared with results from previous study (AlAyed, 2002) where the displacement coefficient method (DCM) was applied to assess the behavior of bridge structures. Comparison showed that:

- For long curved-in-plan bridge model (bridge no. 1), MPA tends to slightly overestimate the maximum demand displacement by 6.3% while DCM is more unconservative and it slightly underestimated demand displacement by 5.7%.

- For regular bridge model (bridge no. 2), MPA and DCM methods slightly underestimated demand displacements by 3.2% and 4.5%, respectively and results are found to be in good agreement with those results from the NL-THA.

The current study was then extended to furthermore evaluate the applicability of the MPA method for a wide range of bridges and quantify its accuracy; a parametric study was performed in order to study the influence of different parameters on the behavior of horizontally curved bridges. Parameters included the girder cross section (steel I vs. steel BOX), span length, number of spans, radius of curvature, and pier column's height. Nonlinear time history analysis was also performed as a benchmark in order to compare its results with results from the MPA. Observations obtained from the comparison of results can be summarized as following:

- For 3-span bridge model configurations adopted in the study with pier height of 50 ft, MPA tends to underestimate the maximum demand displacements for short (100-120-100ft), and medium (140-180-140ft) spans while overestimate it for long (180-240-180) spans with displacement differences range between 6.1 – 23% and 11.8 – 13.4% for models with steel I and steel BOX, respectively.

- Same observations are noted for 2-span bridges with pier height of 50 ft with displacement differences range between 0.6 – 23.6% and 0.1 – 18.9% for models with steel I and steel BOX, respectively.

- For 3-span bridge model configurations with pier height of 20 ft, MPA tends to underestimate the maximum demand displacements for short spans while overestimate displacements for both medium and long spans with displacement differences range between 5.7 – 15.3% and 0.6 – 7% for models with steel I and steel BOX, respectively.

- For all 2-span bridge models adopted in the study with pier height of 20 ft, MPA tends to overestimate the maximum demand displacement for short, medium and long spans with displacement differences range between 6.5 – 14.9% and 1 – 4% for models with steel I and steel BOX, respectively.

- MPA procedure tends to underestimate the predicted total base shear for all configurations considered in the study with an average difference of 16%.

- Span length is found to have a significant influence on the estimated maximum demand displacements. It is more noticeable in cases with short spans with taller pier height than in other medium or long spans.

- Radius of curvature influences 3-span models more than 2-span models with regard to maximum demand displacements. Displacements are increased by 7% and 25% for 3-span steel I models with pier height of 50 and 20 ft, respectively when radius of curvature is changed from 500 ft to 1600 ft. For steel BOX models, displacements are increased by 7% and 12 % for models with pier height of 50 ft and 20 ft, respectively when radius of curvature is changed from 500 ft to 1600 ft. For all cases of 2 span models with either steel I or steel BOX, displacements are slightly increased within a range of 1.0% to 4.0%.

- Maximum demand displacements are significantly influenced by pier column's height. 3-span models are more affected by pier's height than 2-span models for both cross sections considered.

- Total base shear is also significantly influenced by increasing bridge length and pier height while less influenced by radius of curvature. Cases of short spans and shorter pier height were the most affected with base shear increase of 99% and 70% for models with steel I and steel BOX, respectively.

- For the wide range of curved bridges used in the parametric study, MPA is deemed to give accurate results reasonably matching the results of the more refined NL-THA method.

7.2 CONCLUSIONS

Based on the results obtained from the current study, the following conclusions were made:

1. Most critical pier location was found to be the most appropriate location to be considered as the control point. Pushover curve and calculated transverse demand displacements with regard to the most critical pier location were deemed to be accurate for practical applications.

2. The improved MPA procedure introduced was found to yield better results when the level of earthquake excitation was increased and more inelasticity developed in the structure.

3. From the first case study (bridge no.1) considered to evaluate the modal pushover analysis procedure, all three methods yielded similar values of maximum inelastic deck displacement; however the variation of displacements along the bridge was rather different. The SPA method predicted well the displacement only in the central, first mode dominated, area of the bridge. On the contrary, MPA provided a significantly improved estimate with respect to maximum displacement pattern, reasonably matching the results of the more refined NL-THA method, even for increasing levels of earthquake loading that trigger increased contribution of higher modes.

4. From the other two cases considered where bridges no. 2 and 3 could be classified as regular structures without curvature, all three pushover methods yielded similar

values of maximum demand displacements. Results also indicated that SPA generally works reasonably well when applied to bridges of regular configuration.

5. On the basis of the results obtained, MPA seems to be a promising approach that yields more accurate results compared to the standard pushover, without requiring the higher modeling effort and computational cost, as well as the other complications involved in NL-THA (like the selection and scaling of natural records, or the generation of synthetic ones).

6. Parametric study performed for the wide range of bridges showed that MPA predicts well demand displacements. MPA underestimated demand displacements for all models with pier height =50ft except for the case with long spans where displacements were slightly overestimated while for all other cases with pier height = 20ft, MPA overestimated the results except for 3-span models with short spans where demand displacements were underestimated.

7. As for the base shear, MPA predicts well total base shear and it underestimated results for all cases with an average of 16%.

8. Span length and pier height had significant effect on the maximum demand displacements with the effect is more pronounced for models with short spans (L=120ft) and pier height = 50ft.

9. Also, span length and pier height significantly increased total base shear results. Steel I models with short spans and pier height = 20ft had the maximum base shear increase.

10. Radius of curvature had the least effect on demand displacements. Maximum demand displacements for 3-span bridge models with pier height = 50ft were increased by 7% when changing radius of curvature from 500ft to 1600ft, while for models with H=20ft displacements were increased by 25% and 12% for steel I and BOX sections, respectively. All 2-span bridge models showed less influence of radius of curvature where displacements were only increased by 4%.

11. For the wide range of bridge configurations used in the parametric study, MPA provided accurate results for both demand displacements and base shear closely matching results from the NL-THA procedure and proved to be acceptable for practical use.

More work is clearly required to further investigate the effectiveness of MPA by applying it to bridge structures with different configuration and study the effect of superstructure-pier stiffness ratio on the behavior of bridges since MPA is expected to be even more valuable for the assessment of the actual inelastic response of bridges with significant higher modes.

APPENDIX A

This appendix includes calculations of different parameters needed to define plastic hinges as well as nonlinear link elements needed to perform modal pushover and nonlinear time history analyses using the SAP2000. First a moment-curvature analysis is required to obtain the moment-curvature curve for each column cross section. Then, the moment-rotation curve is generated.

A.1 Bridge No. 1

1. Weak axis of the column:

From the M-ϕ curve, $\phi_y = 4.416*10^{-4}$ 1/ft & $M_n = 37443$ k-ft

Using Eq. 3.2, $I_e = \dfrac{37443}{518400 x 4.416*10^{-4}} = 163.6\ \text{ft}^4$

$I_e = 163.6/407 = 0.402\ I_g$

Using Eq. 3.1, $L_p = 6.85$ ft (for the 70 ft column)

$L_p = 5.25$ ft (for the 50 ft column)

$L_p = 2.76$ ft (for the 20 ft column)

$\theta_y = \phi_y * L_p = 3.025*10^{-3}$ (70 ft column)

$= 2.318*10^{-3}$ (50 ft column)

$= 1.2188*10^{-3}$ (20 ft column)

Flexural stiffness for nonlinear springs (70 ft column)

K_e (stiffness before yielding) = M_n/θ_y=12380278 k-ft/rad

$$K_p \text{ (stiffness after yielding)} = \alpha K_e = \frac{M_u - M_n}{\theta_u - \theta_y} = 287222 \text{ k-ft/rad}$$

Flexural stiffness for nonlinear springs (50 ft column)

K_e (stiffness before yielding) = M_n/θ_y=16153316 k-ft/rad

$$K_p \text{ (stiffness after yielding)} = \alpha K_e = \frac{M_u - M_n}{\theta_u - \theta_y} = 374750 \text{ k-ft/rad}$$

Flexural stiffness for nonlinear springs (20 ft column)

K_e (stiffness before yielding) = M_n/θ_y=$3.07*10^7$ k-ft/rad

$$K_p \text{ (stiffness after yielding)} = \alpha K_e = \frac{M_u - M_n}{\theta_u - \theta_y} = 712240 \text{ k-ft/rad}$$

Stiffness of the shear springs for nonlinear link elements:

$K_{2\text{-}2} = 12EI_{cr}/L^3$ = 12*518400*163.6 / $(6.85)^3$ = 3166342 k/ft (70 ft column)

$K_{2\text{-}2} = 12EI_{cr}/L^3$ = 12*518400*163.6 / $(5.25)^3$ = 7033178 k/ft (50 ft column)

$K_{2\text{-}2}$ = $12EI_{cr}/L^3$ = 12*518400*163.6 / $(2.76)^3$ = 48406345.03 k/ft (20 ft column)

2. **Strong axis of the column:**

From the $M\text{-}\phi$ curve, ϕ_y = 1.4856*10^{-4} 1/ft & M_n = 113268 k-ft

Using Eq. 3.2, $$I_e = \frac{113268}{518400\text{x}1.4856*10^{-4}} = 1471\text{ft}^4$$

I_e=1471/4167=0.353 I_g

Using Eq. 3.1, L_p = 6.85 ft (for the 70 ft column)

L_p = 5.25 ft (for the 50 ft column)

$\theta_y = \phi_y * L_p$ = 1.017*10^{-3} (70 ft column)

= 7.80*10^{-4} (50 ft column)

= 4.1*10^{-4} (20 ft column)

Flexural stiffness for nonlinear springs (70 ft column)

K_e (stiffness before yielding) = M_n/θ_y=1.11*10^8 k-ft/rad

K_p (stiffness after yielding) = αK_e = $$\frac{M_u - M_n}{\theta_u - \theta_y} = 957000 \text{ k-ft/rad}$$

Flexural stiffness for nonlinear springs (50 ft column)

K_e (stiffness before yielding) = M_n/θ_y=1.45*10^8 k-ft/rad

K_p (stiffness after yielding) = αK_e = $\dfrac{M_u - M_n}{\theta_u - \theta_y} = 1261500$ k - ft/rad

Flexural stiffness for nonlinear springs (20 ft column)

K_e (stiffness before yielding) = M_n/θ_y=2.76*10^8 k-ft/rad

K_p (stiffness after yielding) = αK_e = $\dfrac{M_u - M_n}{\theta_u - \theta_y} = 2401200$ k - ft/rad

Stiffness of the shear springs for nonlinear link elements:

$K_{3\text{-}3} = 12EI_{cr}/L^3$ = 12*518400*163.6 / $(6.85)^3$ = 28470000 k/ft (70 ft column)

$K_{3\text{-}3} = 12EI_{cr}/L^3$ = 12*518400*163.6 / $(5.25)^3$ = 63238419 k/ft (50 ft column)

$K_{3\text{-}3} = 12EI_{cr}/L^3$ = 12*518400*163.6 / $(5.25)^3$ = 4.35*10^8 k/ft (20 ft column)

A.2 Bridge No. 2 & 3

From the M-ϕ curve, $\phi_y = 1.008*10^{-3}$ 1/ft & $M_n = 4703$ k-ft

Using Eq. 3.2, $I_e = \dfrac{4703}{518400\text{x}1.008*10^{-3}} = 9.0\,\text{ft}^4$

I_e=9.0/12.57=$0.716\ I_g$

Using Eq. 3.1, $L_p = 4.97$ ft (for the 50 ft column)

$L_p = 2.57$ ft (for the 20 ft column)

$\theta_y = \phi_y * L_p = 5.011*10^{-3}$ (50 ft column)

$= 2.5915*10^{-3}$ (20 ft column)

<u>Flexural stiffness for nonlinear springs (50 ft column)</u>

K_e (stiffness before yielding) = M_n/θ_y=938535 k-ft/rad

K_p (stiffness after yielding) = $\alpha K_e = \dfrac{M_u - M_n}{\theta_u - \theta_y} = 52426$ k - ft/rad

<u>Flexural stiffness for nonlinear springs (20 ft column)</u>

K_e (stiffness before yielding) = M_n/θ_y=1815000 k-ft/rad

K_p (stiffness after yielding) = $\alpha K_e = \dfrac{M_u - M_n}{\theta_u - \theta_y} = 101386$ k-ft/rad

Stiffness of the shear springs for nonlinear link elements:

$K_{2\text{-}2} = 12EI_{cr}/L^3$ = 12*518400*9.0 / $(5.25)^3$ = 456057.5 k/ft (50 ft column)

$K_{2\text{-}2} = 12EI_{cr}/L^3$ = 12*518400*9.0 / $(2.57)^3$ = 3270700 k/ft (20 ft column)

APPENDIX B

This appendix studies the influence of number of modes to be included in the MPA procedure in order to calculate the maximum demand displacement.

Bridge No. 1 is considered for the analysis. Analyses were performed for different number of modes included for one level of earthquake excitation, PGA=0.45g. The first analysis considered the first four transverse modes to calculate the demand displacement. These modes contributed to 75% of the total mass of the bridge. The second analysis considered eight transverse modes to calculate the demand displacement. Such modes contributed to 87% of the total mass of the structure. Figures B.1 and B.2 illustrate modal deck displacements considering 4 and 8 transverse modes, respectively. Also, Table B.1 lists the displacements with the difference ratios between the two cases.

Results show that adding more modes, to capture all modes whose masses contribute to at least 90% of the total mass of the bridges (a criterion commonly used in seismic codes), has insignificant effect on the results of demand displacements and there is little merit in adding modes whose participation factor is very low, say less than 1%, and less rigid rules than the 90% one (calibrated only for buildings) could be adopted. While for total base shear, adding more modes slightly improved the prediction (from 8640 kips to 9132 kips) and base shear was underestimated by 24%.

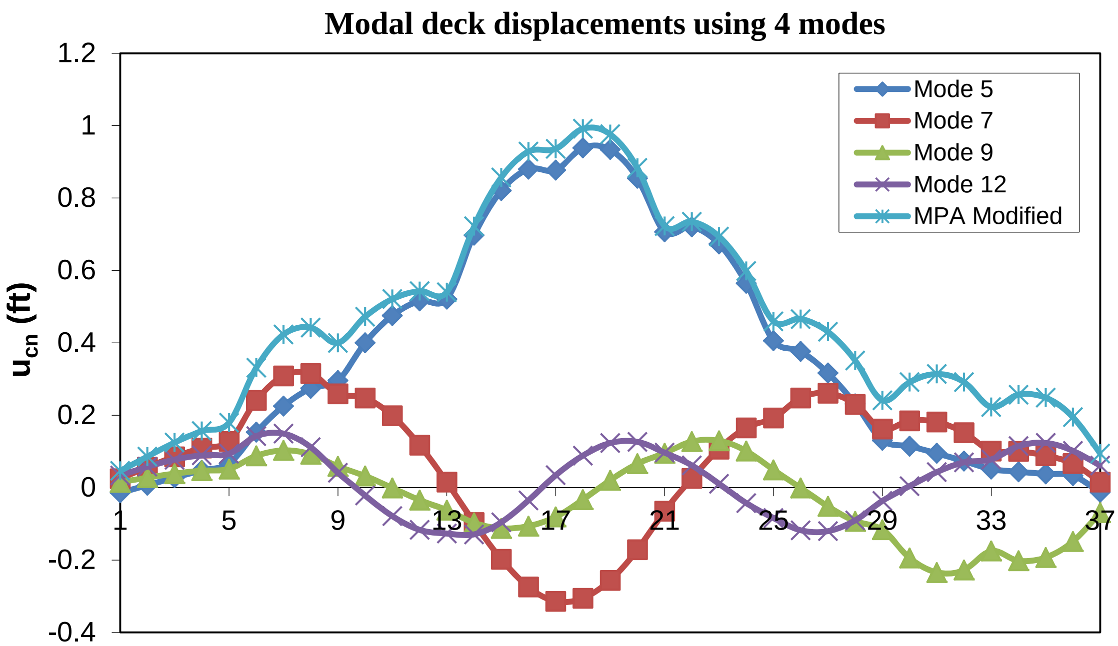

Figure B. 1 Modal deck displacements using 4 transverse modes

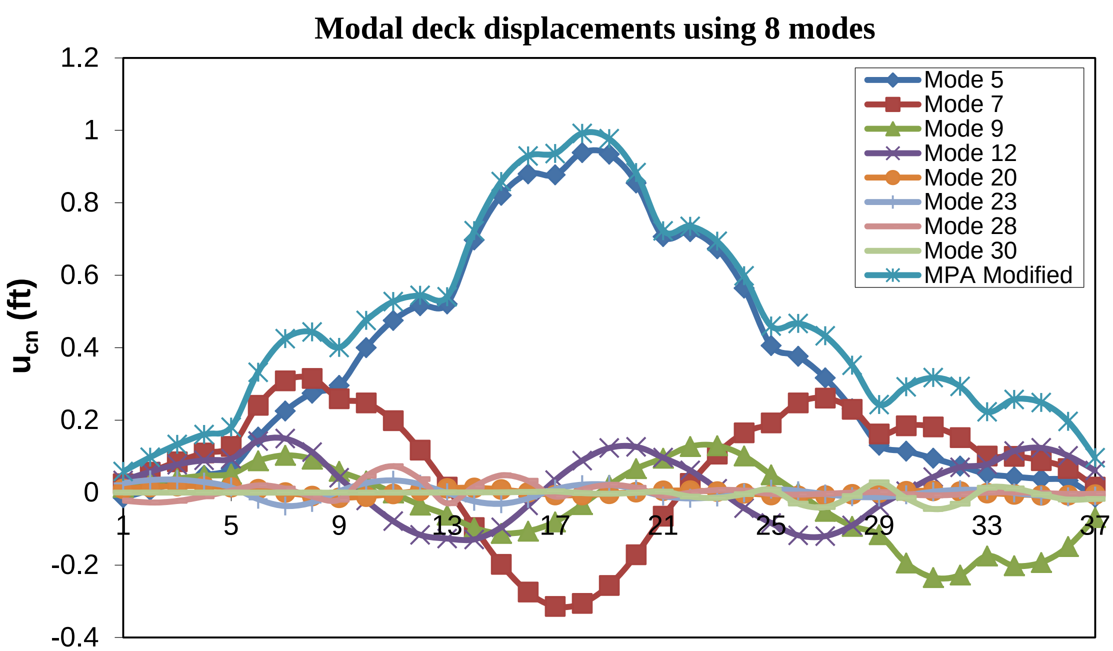

Figure B. 2 Modal deck displacement using 8 transverse modes

Table B.1 Comparison between modal deck displacements for the two cases considered

		Displacement Using 4 Modes (ft)	Displacement Using 8 Modes (ft)	Difference (%)
Deck Nodes	**A1**	0.046387594	0.058375439	25.8428%
	702	0.085872068	0.097832925	13.9287%
	703	0.12457116	0.132908716	6.6930%
	704	0.156477017	0.160445699	2.5363%
	P1	0.179408836	0.180737564	0.7406%
	712	0.331128318	0.332395705	0.3827%
	713	0.423049044	0.42480451	0.4150%
	714	0.442268589	0.443327649	0.2395%
	P2	0.399933503	0.400689634	0.1891%
	722	0.47230418	0.475382731	0.6518%
	723	0.521237497	0.527419687	1.1861%
	724	0.542861742	0.544664452	0.3321%
	P3	0.539890842	0.540830965	0.1741%
	732	0.722222628	0.72293432	0.0985%
	733	0.856882939	0.858801876	0.2239%
	734	0.928421647	0.929140777	0.0775%
	P4	0.935893305	0.936039721	0.0156%
	742	0.991407935	0.991710423	0.0305%
	743	0.97658496	0.977082508	0.0509%
	744	0.883401823	0.883546775	0.0164%
	P5	0.722665248	0.722809163	0.0199%
	752	0.734618562	0.734897083	0.0379%
	753	0.693691692	0.693995869	0.0438%
	754	0.598500559	0.598543608	0.0072%
	P6	0.45958892	0.459828998	0.0522%
	762	0.465776422	0.46691403	0.2442%
	763	0.430794009	0.432760806	0.4566%
	764	0.351374794	0.351722142	0.0989%
	P7	0.241158535	0.243118364	0.8127%
	772	0.291387932	0.291900337	0.1758%
	773	0.314232501	0.317614018	1.0761%
	774	0.291719874	0.293500653	0.6104%
	P8	0.222642807	0.223135026	0.2211%
	782	0.256849392	0.257166709	0.1235%
	783	0.248573653	0.248883427	0.1246%
	784	0.195023498	0.196466746	0.7400%
	A2	0.094204384	0.096445225	2.3787%

APPENDIX C

This appendix includes a sample of input files for analyzing and designing two bridge configurations with steel I & BOX cross sections using DESCUS I&II, respectively.

Steel I 3-span Bridge (240-240ft)

```
0101
0101Two 230ft spans
0102I-73 Bridge 70B/72B
0103
0103     1    0    10         2          1    10.             1          0 1
0104
0104   1     3  8.12      2     3  8.12      3     3  8.12      4     3  8.12
0104   5     3  8.12
0105
0105     2     1     1
0201
02015 05      2     0         0         13.9
02013 03      1    1.090417
02013 03      1    2.090417
02013 03      1    3.090417
02013 03      1    4.090417
02013 03      1    5.090417
0301
0301   1    1    .000  1   2    1    2    .625  1   2    1    3    .625  1   2
0301   1    4    .625  1   2    1    5    .125  1   2
0301   2    1    .375  1   2    2    2    .750  1   2    2    3    .625  1   2
0301   2    4    .250  1   2    2    5    .000  1   2
0301   3    1    .000  1   2    3    2    .375  1   2    3    3    .750  1   2
0301   3    4    .625  1   2    3    5    .250  1   2
0301   4    1    .000  1   2    4    2    .250  1   2    4    3    .625  1   2
0301   4    4    .750  1   2    4    5    .375  1   2
0301   5    1    .000  1   2    5    2    .125  1   2    5    3    .625  1   2
0301   5    4    .625  1   2    5    5    .625  1   2
0401
0401      5    8.         .25        3.   26.  15.        1.15
0402
04020       820.    36.     3.625  3.625  1.625  1.625  24. 8.  4.      150.
0403
0403  HL 93    1      2
0501
0501  150.  PG          99.    .875  22.   1.25  24.   1.5
0501  250.  PG          99.    .875  24.   1.75  20.   1.75
0501  350.  PG          99.    .875  26.   2.    26.   2.
0501  450.  TR                                             103.613.612.6892.
0601
0601  1    0.000  0.0000   1  65 125
0601  2    0.000  8.0000   2  64 124
0601  3    0.000  8.0000   3  63 123
0601  4    0.000  8.0000   4  62 122
0601  5    0.000  8.0000   5  61 121
0701
```

```
0701    1       1    10   15.20270     1-1200.0000    10    15   20.27027      1-
1200.0000
0701    1      15    20   20.27027     1-1200.0000    20    25   20.27027      1-
1200.0000
0701    1      25    30   20.27027     1-1200.0000    30    35   20.27027      1-
1200.0000
0701    1      35    40   20.27027     1-1200.0000    40    45   20.27027      1-
1200.0000
0701    1      45    50   20.27027     1-1200.0000    50    55   20.27027      1-
1200.0000
0701    1      55    60   20.27027     2-1200.0000    60    65   15.20270      3-
1200.0000
0701    1      65    70   15.20270     3-1200.0000    70    75   20.27027      2-
1200.0000
0701    1      75    80   20.27027     1-1200.0000    80    85   20.27027      1-
1200.0000
0701    1      85    90   20.27027     1-1200.0000    90    95   20.27027      1-
1200.0000
0701    1      95   100   20.27027     1-1200.0000   100   105   20.27027      1-
1200.0000
0701    1     105   110   20.27027     1-1200.0000   110   115   20.27027      1-
1200.0000
0701    1     115   120   20.27027     1-1200.0000   120   125   15.20270      1-
1200.0000
0701    2       2     9   15.10135     1-1192.0000     9    14   20.13514      1-
1192.0000
0701    2      14    19   20.13514     1-1192.0000    19    24   20.13514      1-
1192.0000
0701    2      24    29   20.13514     1-1192.0000    29    34   20.13514      1-
1192.0000
0701    2      34    39   20.13514     1-1192.0000    39    44   20.13514      1-
1192.0000
0701    2      44    49   20.13514     1-1192.0000    49    54   20.13514      1-
1192.0000
0701    2      54    59   20.13514     2-1192.0000    59    64   15.10135      3-
1192.0000
0701    2      64    69   15.10135     3-1192.0000    69    74   20.13514      2-
1192.0000
0701    2      74    79   20.13514     1-1192.0000    79    84   20.13514      1-
1192.0000
0701    2      84    89   20.13514     1-1192.0000    89    94   20.13514      1-
1192.0000
0701    2      94    99   20.13514     1-1192.0000    99   104   20.13514      1-
1192.0000
0701    2     104   109   20.13514     1-1192.0000   109   114   20.13514      1-
1192.0000
0701    2     114   119   20.13514     1-1192.0000   119   124   15.10135      1-
1192.0000
0701    3       3     8   15.00000     1-1184.0000     8    13   20.00000      1-
1184.0000
0701    3      13    18   20.00000     1-1184.0000    18    23   20.00000      1-
1184.0000
0701    3      23    28   20.00000     1-1184.0000    28    33   20.00000      1-
1184.0000
0701    3      33    38   20.00000     1-1184.0000    38    43   20.00000      1-
1184.0000
0701    3      43    48   20.00000     1-1184.0000    48    53   20.00000      1-
1184.0000
```

```
0701    3       53    58   20.00000     2-1184.0000    58    63   15.00000      3-
1184.0000
0701    3       63    68   15.00000     3-1184.0000    68    73   20.00000      2-
1184.0000
0701    3       73    78   20.00000     1-1184.0000    78    83   20.00000      1-
1184.0000
0701    3       83    88   20.00000     1-1184.0000    88    93   20.00000      1-
1184.0000
0701    3       93    98   20.00000     1-1184.0000    98   103   20.00000      1-
1184.0000
0701    3      103   108   20.00000     1-1184.0000   108   113   20.00000      1-
1184.0000
0701    3      113   118   20.00000     1-1184.0000   118   123   15.00000      1-
1184.0000
0701    4        4     7   14.89865     1-1176.0000     7    12   19.86486      1-
1176.0000
0701    4       12    17   19.86486     1-1176.0000    17    22   19.86486      1-
1176.0000
0701    4       22    27   19.86486     1-1176.0000    27    32   19.86486      1-
1176.0000
0701    4       32    37   19.86486     1-1176.0000    37    42   19.86486      1-
1176.0000
0701    4       42    47   19.86486     1-1176.0000    47    52   19.86486      1-
1176.0000
0701    4       52    57   19.86486     2-1176.0000    57    62   14.89865      3-
1176.0000
0701    4       62    67   14.89865     3-1176.0000    67    72   19.86486      2-
1176.0000
0701    4       72    77   19.86486     1-1176.0000    77    82   19.86486      1-
1176.0000
0701    4       82    87   19.86486     1-1176.0000    87    92   19.86486      1-
1176.0000
0701    4       92    97   19.86486     1-1176.0000    97   102   19.86486      1-
1176.0000
0701    4      102   107   19.86486     1-1176.0000   107   112   19.86486      1-
1176.0000
0701    4      112   117   19.86486     1-1176.0000   117   122   14.89865      1-
1176.0000
0701    5        5     6   14.79730     1-1168.0000     6    11   19.72973      1-
1168.0000
0701    5       11    16   19.72973     1-1168.0000    16    21   19.72973      1-
1168.0000
0701    5       21    26   19.72973     1-1168.0000    26    31   19.72973      1-
1168.0000
0701    5       31    36   19.72973     1-1168.0000    36    41   19.72973      1-
1168.0000
0701    5       41    46   19.72973     1-1168.0000    46    51   19.72973      1-
1168.0000
0701    5       51    56   19.72973     2-1168.0000    56    61   14.79730      3-
1168.0000
0701    5       61    66   14.79730     3-1168.0000    66    71   19.72973      2-
1168.0000
0701    5       71    76   19.72973     1-1168.0000    76    81   19.72973      1-
1168.0000
0701    5       81    86   19.72973     1-1168.0000    86    91   19.72973      1-
1168.0000
0701    5       91    96   19.72973     1-1168.0000    96   101   19.72973      1-
1168.0000
```

```
0701    5      101   106   19.72973      1-1168.0000   106   111   19.72973      1-
1168.0000
0701    5      111   116   19.72973      1-1168.0000   116   121   14.79730      1-
1168.0000
0801
0801    1   10    9   4    2    9    8   4    3    8    7   4    4    7    6   4    5   15   14
4
0801    6   14   13   4    7   13   12   4    8   12   11   4    9   20   19   4   10   19   18
4
0801   11   18   17   4   12   17   16   4   13   25   24   4   14   24   23   4   15   23   22
4
0801   16   22   21   4   17   30   29   4   18   29   28   4   19   28   27   4   20   27   26
4
0801   21   35   34   4   22   34   33   4   23   33   32   4   24   32   31   4   25   40   39
4
0801   26   39   38   4   27   38   37   4   28   37   36   4   29   45   44   4   30   44   43
4
0801   31   43   42   4   32   42   41   4   33   50   49   4   34   49   48   4   35   48   47
4
0801   36   47   46   4   37   55   54   4   38   54   53   4   39   53   52   4   40   52   51
4
0801   41   60   59   4   42   59   58   4   43   58   57   4   44   57   56   4   45   70   69
4
0801   46   69   68   4   47   68   67   4   48   67   66   4   49   75   74   4   50   74   73
4
0801   51   73   72   4   52   72   71   4   53   80   79   4   54   79   78   4   55   78   77
4
0801   56   77   76   4   57   85   84   4   58   84   83   4   59   83   82   4   60   82   81
4
0801   61   90   89   4   62   89   88   4   63   88   87   4   64   87   86   4   65   95   94
4
0801   66   94   93   4   67   93   92   4   68   92   91   4   69  100   99   4   70   99   98
4
0801   71   98   97   4   72   97   96   4   73  105  104   4   74  104  103   4   75  103  102
4
0801   76  102  101   4   77  110  109   4   78  109  108   4   79  108  107   4   80  107  106
4
0801   81  115  114   4   82  114  113   4   83  113  112   4   84  112  111   4   85  120  119
4
0801   86  119  118   4   87  118  117   4   88  117  116   4
```

Steel BOX 3-span Bridge (240-240ft)

```
0101TxDOT IH610/Katy Freeway Direct Connector 2-F
0102
0103
0103     2    0    20          2          0    3.              1          2
0104
0104   2     8  4.21      3     8  4.21
0301
0301   2    1 2.933    1   3    2    2 2.933    1   3    2    3 2.933    1   3
0301   2    4 2.933    1   3
0301   3    1 2.933    1   3    3    2 2.933    1   3    3    3 2.933    1   3
0301   3    4 2.933    1   3
0311
0311  1  .158    .158    .158    .158    .158    .158      1  .158
0311  2  .133    .133    .133    .133    .133    .133      2  .158
0311  3  .158    .158    .158    .158    .158    .158      3  .158
0311                                                       4  .158
0313
0313.09      .09      .09
0401
0401      4    8.25       0          2.82 27.380          1.20       0
0402
04020       376.    36.     4.33   4.33   1.208331.2083324. 8.  4.      150.
0403
0403  HS 25    1      1
0501
0501  1  1   5014.0476.   .687522.   1.37585.5  1.   .039  2.375
0501  2  1   5014.0476.   .687522.   1.37585.5  1.375.039  2.375
0501  3  1   5014.0476.   .687536.   1.37585.5  1.875.039  2.375
0501  4  1   5014.0476.   .687536.   2.12585.5  1.875.039  3.125
0501  5  1   5014.0476.   .687536.   3.25 85.5  2.5  .04   4.25
0501  6  1   5014.0476.   .687524.   1.37585.5  1.375.039  2.375
0501  7  1   5014.0476.   .687524.   1.87585.5  2.125.039  2.875
0501  8  0 1  00.   0.    0.   0.    0.   0.    0.   0.    0.
0502
0502 10 501.  16.  1.  16.  1.  82.75
0502 11 501.  20.  1.  16.  1.  79.
0502 12 501.  16.  1.  16.  1.  44.38
0502 14                                                       702.     2808.
0502 13 50                           6.31 6.31 4.   65.38
0503
0503  1228.     15.3    5.3125
0601
0601  1 0.0     0.0      101 123 151 172
0601  2 0.0     5.0      201 223 251 272
0601  3 0.0     19.75    301 323 351 372
0601  4 0.0     5.0      401 423 451 472
0602
060219.     24.     19.
0701
0701   1    101  1021.784         8-898.35     102  10310.218        8-898.35
0701   1    103  10410.218        8-898.35     104  1055.109         8-898.35
0701   1    105  1065.109         8-898.35     106  10710.218        8-898.35
0701   1    107  10810.218        8-898.35     108  10910.218        8-898.35
0701   1    109  11010.218        8-898.35     110  11110.218        8-898.35
0701   1    111  11210.218        8-898.35     112  11310.218        8-898.35
0701   1    113  11410.218        8-898.35     114  11510.218        8-898.35
0701   1    115  11610.218        8-898.35     116  1175.109         8-898.35
```

0701	1	117	1185.109	8-898.35	118	11910.218	8-898.35
0701	1	119	12010.218	8-898.35	120	12110.218	8-898.35
0701	1	121	12210.218	8-898.35	122	12310.218	8-898.35
0701	1	123	12410.616	8-898.35	124	12510.616	8-898.35
0701	1	125	12610.616	8-898.35	126	12710.616	8-898.35
0701	1	127	12810.616	8-898.35	128	1295.308	8-898.35
0701	1	129	1305.308	8-898.35	130	13110.616	8-898.35
0701	1	131	1325.308	8-898.35	132	1335.308	8-898.35
0701	1	133	13410.616	8-898.35	134	13510.616	8-898.35
0701	1	135	13610.616	8-898.35	136	13710.616	8-898.35
0701	1	137	13810.616	8-898.35	138	13910.616	8-898.35
0701	1	139	14010.616	8-898.35	140	14110.616	8-898.35
0701	1	141	1425.308	8-898.35	142	1435.308	8-898.35
0701	1	143	14410.616	8-898.35	144	1455.308	8-898.35
0701	1	145	1465.308	8-898.35	146	14710.616	8-898.35
0701	1	147	14810.616	8-898.35	148	14910.616	8-898.35
0701	1	149	15010.616	8-898.35	150	15110.616	8-898.35
0701	1	151	15210.224	8-898.35	152	15310.224	8-898.35
0701	1	153	15410.224	8-898.35	154	15510.224	8-898.35
0701	1	155	15610.224	8-898.35	156	1575.112	8-898.35
0701	1	157	1585.112	8-898.35	158	15910.224	8-898.35
0701	1	159	16010.224	8-898.35	160	16110.224	8-898.35
0701	1	161	16210.224	8-898.35	162	16310.224	8-898.35
0701	1	163	16410.224	8-898.35	164	16510.224	8-898.35
0701	1	165	16610.224	8-898.35	166	16710.224	8-898.35
0701	1	167	16810.224	8-898.35	168	1695.112	8-898.35
0701	1	169	1705.112	8-898.35	170	17110.224	8-898.35
0701	1	171	17210.224	8-898.35			
0701	2	201	2021.774	1-893.35	202	20310.161	1-893.35
0701	2	203	20410.161	1-893.35	204	2055.0805	1-893.35
0701	2	205	2065.0805	2-893.35	206	20710.161	2-893.35
0701	2	207	20810.161	2-893.35	208	20910.161	2-893.35
0701	2	209	21010.161	2-893.35	210	21110.161	2-893.35
0701	2	211	21210.161	2-893.35	212	21310.161	2-893.35
0701	2	213	21410.161	2-893.35	214	21510.161	2-893.35
0701	2	215	21610.161	2-893.35	216	2175.0805	2-893.35
0701	2	217	2185.0805	3-893.35	218	21910.161	3-893.35
0701	2	219	22010.161	4-893.35	220	22110.161	4-893.35
0701	2	221	22210.161	5-893.35	222	22310.161	5-893.35
0701	2	223	22410.557	5-893.35	224	22510.557	5-893.35
0701	2	225	22610.557	4-893.35	226	22710.557	4-893.35
0701	2	227	22810.557	3-893.35	228	2295.2785	3-893.35
0701	2	229	2305.2785	6-893.35	230	23110.557	6-893.35
0701	2	231	2325.2785	6-893.35	232	2335.2785	6-893.35
0701	2	233	23410.557	7-893.35	234	23510.557	7-893.35
0701	2	235	23610.557	7-893.35	236	23710.557	7-893.35
0701	2	237	23810.557	7-893.35	238	23910.557	7-893.35
0701	2	239	24010.557	7-893.35	240	24110.557	7-893.35
0701	2	241	2425.2785	6-893.35	242	2435.2785	6-893.35
0701	2	243	24410.557	6-893.35	244	2455.2785	6-893.35
0701	2	245	2465.2785	3-893.35	246	24710.557	3-893.35
0701	2	247	24810.557	4-893.35	248	24910.557	4-893.35
0701	2	249	25010.557	5-893.35	250	25110.557	5-893.35
0701	2	251	25210.167	5-893.35	252	25310.167	5-893.35
0701	2	253	25410.167	4-893.35	254	25510.167	4-893.35
0701	2	255	25610.167	3-893.35	256	2575.0835	3-893.35
0701	2	257	2585.0835	2-893.35	258	25910.167	2-893.35
0701	2	259	26010.167	2-893.35	260	26110.167	2-893.35
0701	2	261	26210.167	2-893.35	262	26310.167	2-893.35

0701	2	263	26410.167	2-893.35	264	26510.167	2-893.35
0701	2	265	26610.167	2-893.35	266	26710.167	2-893.35
0701	2	267	26810.167	2-893.35	268	2695.0835	2-893.35
0701	2	269	2705.0835	1-893.35	270	27110.167	1-893.35
0701	2	271	27210.167	1-893.35			
0701	3	301	3021.735	1-873.6	302	3039.937	1-873.6
0701	3	303	3049.937	1-873.6	304	3054.9685	1-873.6
0701	3	305	3064.9685	2-873.6	306	3079.937	2-873.6
0701	3	307	3089.937	2-873.6	308	3099.937	2-873.6
0701	3	309	3109.937	2-873.6	310	3119.937	2-873.6
0701	3	311	3129.937	2-873.6	312	3139.937	2-873.6
0701	3	313	3149.937	2-873.6	314	3159.937	2-873.6
0701	3	315	3169.937	2-873.6	316	3174.9685	2-873.6
0701	3	317	3184.9685	3-873.6	318	3199.937	3-873.6
0701	3	319	3209.937	4-873.6	320	3219.937	4-873.6
0701	3	321	3229.937	5-873.6	322	3239.937	5-873.6
0701	3	323	32410.324	5-873.6	324	32510.324	5-873.6
0701	3	325	32610.324	4-873.6	326	32710.324	4-873.6
0701	3	327	32810.324	3-873.6	328	3295.162	3-873.6
0701	3	329	3305.162	6-873.6	330	33110.324	6-873.6
0701	3	331	3325.162	6-873.6	332	3335.162	6-873.6
0701	3	333	33410.324	6-873.6	334	33510.324	6-873.6
0701	3	335	33610.324	6-873.6	336	33710.324	6-873.6
0701	3	337	33810.324	6-873.6	338	33910.324	6-873.6
0701	3	339	34010.324	6-873.6	340	34110.324	6-873.6
0701	3	341	3425.162	6-873.6	342	3435.162	6-873.6
0701	3	343	34410.324	6-873.6	344	3455.162	6-873.6
0701	3	345	3465.162	3-873.6	346	34710.324	3-873.6
0701	3	347	34810.324	4-873.6	348	34910.324	4-873.6
0701	3	349	35010.324	5-873.6	350	35110.324	5-873.6
0701	3	351	3529.943	5-873.6	352	3539.943	5-873.6
0701	3	353	3549.943	4-873.6	354	3559.943	4-873.6
0701	3	355	3569.943	3-873.6	356	3574.9715	3-873.6
0701	3	357	3584.9715	2-873.6	358	3599.943	2-873.6
0701	3	359	3609.943	2-873.6	360	3619.943	2-873.6
0701	3	361	3629.943	2-873.6	362	3639.943	2-873.6
0701	3	363	3649.943	2-873.6	364	3659.943	2-873.6
0701	3	365	3669.943	2-873.6	366	3679.943	2-873.6
0701	3	367	3689.943	2-873.6	368	3694.9715	2-873.6
0701	3	369	3704.9715	1-873.6	370	3719.943	1-873.6
0701	3	371	3729.943	1-873.6			
0701	4	401	4021.725	8-868.6	402	4039.880	8-868.6
0701	4	403	4049.880	8-868.6	404	4054.940	8-868.6
0701	4	405	4064.940	8-868.6	406	4079.880	8-868.6
0701	4	407	4089.880	8-868.6	408	4099.880	8-868.6
0701	4	409	4109.880	8-868.6	410	4119.880	8-868.6
0701	4	411	4129.880	8-868.6	412	4139.880	8-868.6
0701	4	413	4149.880	8-868.6	414	4159.880	8-868.6
0701	4	415	4169.880	8-868.6	416	4174.940	8-868.6
0701	4	417	4184.940	8-868.6	418	4199.880	8-868.6
0701	4	419	4209.880	8-868.6	420	4219.880	8-868.6
0701	4	421	4229.880	8-868.6	422	4239.880	8-868.6
0701	4	423	42410.265	8-868.6	424	42510.265	8-868.6
0701	4	425	42610.265	8-868.6	426	42710.265	8-868.6
0701	4	427	42810.265	8-868.6	428	4295.1325	8-868.6
0701	4	429	4305.1325	8-868.6	430	43110.265	8-868.6
0701	4	431	4325.1325	8-868.6	432	4335.1325	8-868.6
0701	4	433	43410.265	8-868.6	434	43510.265	8-868.6
0701	4	435	43610.265	8-868.6	436	43710.265	8-868.6

```
0701   4    437  43810.265        8-868.6      438  43910.265        8-868.6
0701   4    439  44010.265        8-868.6      440  44110.265        8-868.6
0701   4    441  4425.1325        8-868.6      442  4435.1325        8-868.6
0701   4    443  44410.265        8-868.6      444  4455.1325        8-868.6
0701   4    445  4465.1325        8-868.6      446  44710.265        8-868.6
0701   4    447  44810.265        8-868.6      448  44910.265        8-868.6
0701   4    449  45010.265        8-868.6      450  45110.265        8-868.6
0701   4    451  4529.886         8-868.6      452  4539.886         8-868.6
0701   4    453  4549.886         8-868.6      454  4559.886         8-868.6
0701   4    455  4569.886         8-868.6      456  4574.943         8-868.6
0701   4    457  4584.943         8-868.6      458  4599.886         8-868.6
0701   4    459  4609.886         8-868.6      460  4619.886         8-868.6
0701   4    461  4629.886         8-868.6      462  4639.886         8-868.6
0701   4    463  4649.886         8-868.6      464  4659.886         8-868.6
0701   4    465  4669.886         8-868.6      466  4679.886         8-868.6
0701   4    467  4689.886         8-868.6      468  4694.943         8-868.6
0701   4    469  4704.943         8-868.6      470  4719.886         8-868.6
0701   4    471  4729.886         8-868.6
0801
0801    1 101  201 14    2 102  202 14    3 103  203 14    4 104  204 14    5 105  205
14
0801    6 106  206 14    7 107  207 14    8 108  208 14    9 109  209 14   10 110  210
14
0801   11 111  211 14   12 112  212 14   13 113  213 14   14 114  214 14   15 115  215
14
0801   16 116  216 14   17 117  217 14   18 118  218 14   19 119  219 14   20 120  220
14
0801   21 121  221 14   22 122  222 14   23 123  223 14   24 124  224 14   25 125  225
14
0801   26 126  226 14   27 127  227 14   28 128  228 14   29 129  229 14   30 130  230
14
0801   31 131  231 14   32 132  232 14   33 133  233 14   34 134  234 14   35 135  235
14
0801   36 136  236 14   37 137  237 14   38 138  238 14   39 139  239 14   40 140  240
14
0801   41 141  241 14   42 142  242 14   43 143  243 14   44 144  244 14   45 145  245
14
0801   46 146  246 14   47 147  247 14   48 148  248 14   49 149  249 14   50 150  250
14
0801   51 151  251 14   52 152  252 14   53 153  253 14   54 154  254 14   55 155  255
14
0801   56 156  256 14   57 157  257 14   58 158  258 14   59 159  259 14   60 160  260
14
0801   61 161  261 14   62 162  262 14   63 163  263 14   64 164  264 14   65 165  265
14
0801   66 166  266 14   67 167  267 14   68 168  268 14   69 169  269 14   70 170  270
14
0801   71 171  271 14   72 172  272 14   73 201  301 14   74 202  302 14   75 203  303
14
0801   76 204  304 14   77 205  305 14   78 206  306 14   79 207  307 14   80 208  308
14
0801   81 209  309 14   82 210  310 14   83 211  311 14   84 212  312 14   85 213  313
14
0801   86 214  314 14   87 215  315 14   88 216  316 14   89 217  317 14   90 218  318
14
0801   91 219  319 14   92 220  320 14   93 221  321 14   94 222  322 14   95 223  323
14
0801   96 224  324 14   97 225  325 14   98 226  326 14   99 227  327 14 100 228  328
14
```

```
0801 101 229 329 14 102 230 330 14 103 231 331 14 104 232 332 14 105 233 333
14
0801 106 234 334 14 107 235 335 14 108 236 336 14 109 237 337 14 110 238 338
14
0801 111 239 339 14 112 240 340 14 113 241 341 14 114 242 342 14 115 243 343
14
0801 116 244 344 14 117 245 345 14 118 246 346 14 119 247 347 14 120 248 348
14
0801 121 249 349 14 122 250 350 14 123 251 351 14 124 252 352 14 125 253 353
14
0801 126 254 354 14 127 255 355 14 128 256 356 14 129 257 357 14 130 258 358
14
0801 131 259 359 14 132 260 360 14 133 261 361 14 134 262 362 14 135 263 363
14
0801 136 264 364 14 137 265 365 14 138 266 366 14 139 267 367 14 140 268 368
14
0801 141 269 369 14 142 270 370 14 143 271 371 14 144 272 372 14 145 301 401
14
0801 146 302 402 14 147 303 403 14 148 304 404 14 149 305 405 14 150 306 406
14
0801 151 307 407 14 152 308 408 14 153 309 409 14 154 310 410 14 155 311 411
14
0801 156 312 412 14 157 313 413 14 158 314 414 14 159 315 415 14 160 316 416
14
0801 161 317 417 14 162 318 418 14 163 319 419 14 164 320 420 14 165 321 421
14
0801 166 322 422 14 167 323 423 14 168 324 424 14 169 325 425 14 170 326 426
14
0801 171 327 427 14 172 328 428 14 173 329 429 14 174 330 430 14 175 331 431
14
0801 176 332 432 14 177 333 433 14 178 334 434 14 179 335 435 14 180 336 436
14
0801 181 337 437 14 182 338 438 14 183 339 439 14 184 340 440 14 185 341 441
14
0801 186 342 442 14 187 343 443 14 188 344 444 14 189 345 445 14 190 346 446
14
0801 191 347 447 14 192 348 448 14 193 349 449 14 194 350 450 14 195 351 451
14
0801 196 352 452 14 197 353 453 14 198 354 454 14 199 355 455 14 200 356 456
14
0801 201 357 457 14 202 358 458 14 203 359 459 14 204 360 460 14 205 361 461
14
0801 206 362 462 14 207 363 463 14 208 364 464 14 209 365 465 14 210 366 466
14
0801 211 367 467 14 212 368 468 14 213 369 469 14 214 370 470 14 215 371 471
14
0801 216 372 472 14 217 201 301 11 218 206 306 13 219 209 309 13 220 212 312
13
0801 221 216 316 13 222 220 320 13 223 223 323 10 224 226 326 13 225 231 331
13
0801 226 235 335 13 227 237 337 13 228 239 339 13 229 243 343 13 230 248 348
13
0801 231 251 351 10 232 254 354 13 233 259 359 13 234 262 362 13 235 265 365
13
0801 236 268 368 13 237 272 372 12
0910
0910     1    2
```

Appendix D

This appendix includes input files for analyzing a 3-span bridge model (140-180-140ft) with steel BOX cross section and pier height = 50ft using MPA and NL-THA, respectively

D.1 SAP2000 INPUT DATA FILE FOR MPA

File C:\Users\MAhmed\Documents\My Dropbox\Public\0714-Parametric-Steel BOX-L140-180-140-H50-R500.s2k was saved on 10/31/10 at 21:18:06

TABLE: "PROGRAM CONTROL"
  ProgramName=SAP2000 Version=14.0.0 ProgLevel=Advanced LicenseOS=Yes LicenseSC=Yes LicenseBR=Yes LicenseHT=No CurrUnits="Kip, ft, F" SteelCode=AISC-LRFD93 ConcCode="ACI 318-05/IBC2003" AlumCode="AA-ASD 2000" _
    ColdCode=AISI-ASD96 BridgeCode="AASHTO LRFD 2007" RegenHinge=Yes

TABLE: "ACTIVE DEGREES OF FREEDOM"
  UX=Yes UY=Yes UZ=Yes RX=Yes RY=Yes RZ=Yes

TABLE: "ANALYSIS OPTIONS"
  Solver=Advanced SolverProc=Auto Force32Bit=No StiffCase=None GeomMod=No

TABLE: "COORDINATE SYSTEMS"
  Name=GLOBAL Type=Cartesian X=0 Y=0 Z=0 AboutZ=0 AboutY=0 AboutX=0

TABLE: "GRID LINES"
  CoordSys=GLOBAL AxisDir=X GridID=A XRYZCoord=0 LineType=Primary LineColor=Gray8Dark Visible=Yes BubbleLoc=End AllVisible=No BubbleSize=9.25
  CoordSys=GLOBAL AxisDir=X GridID=B XRYZCoord=105 LineType=Primary LineColor=Gray8Dark Visible=Yes BubbleLoc=End
  CoordSys=GLOBAL AxisDir=Y GridID=1 XRYZCoord=0 LineType=Primary LineColor=Gray8Dark Visible=Yes BubbleLoc=Start
  CoordSys=GLOBAL AxisDir=Z GridID=Z8 XRYZCoord=-84.5 LineType=Primary LineColor=Gray8Dark Visible=Yes BubbleLoc=End
  CoordSys=GLOBAL AxisDir=Z GridID=Z7 XRYZCoord=-78 LineType=Primary LineColor=Gray8Dark Visible=Yes BubbleLoc=End
  CoordSys=GLOBAL AxisDir=Z GridID=Z6 XRYZCoord=-64.5 LineType=Primary LineColor=Gray8Dark Visible=Yes BubbleLoc=End
  CoordSys=GLOBAL AxisDir=Z GridID=Z5 XRYZCoord=-58 LineType=Primary LineColor=Gray8Dark Visible=Yes BubbleLoc=End
  CoordSys=GLOBAL AxisDir=Z GridID=Z4 XRYZCoord=-25 LineType=Primary LineColor=Gray8Dark Visible=Yes BubbleLoc=End
  CoordSys=GLOBAL AxisDir=Z GridID=Z3 XRYZCoord=-15 LineType=Primary LineColor=Gray8Dark Visible=Yes BubbleLoc=End
  CoordSys=GLOBAL AxisDir=Z GridID=Z2 XRYZCoord=-6.5 LineType=Primary LineColor=Gray8Dark Visible=Yes BubbleLoc=End
  CoordSys=GLOBAL AxisDir=Z GridID=Z1 XRYZCoord=0 LineType=Primary LineColor=Gray8Dark

Visible=Yes BubbleLoc=End

TABLE: "MATERIAL PROPERTIES 01 - GENERAL"
Material=4000Psi Type=Concrete SymType=Isotropic TempDepend=No Color=Cyan Notes="Normalweight f'c = 4 ksi added 4/23/2010 12:39:57 PM"
Material=A615Gr60 Type=Rebar SymType=Uniaxial TempDepend=No Color=Cyan Notes="ASTM A615 Grade 60 added 4/23/2010 3:10:32 PM"
Material=A992Fy50 Type=Steel SymType=Isotropic TempDepend=No Color=Green Notes="ASTM A992 Fy=50 ksi added 4/23/2010 12:39:57 PM"
Material=CONC Type=Concrete SymType=Isotropic TempDepend=No Color=Blue Notes="Normalweight f'c = 4 ksi added 4/23/2010 3:04:41 PM"
Material=RIGID Type=Concrete SymType=Isotropic TempDepend=No Color=Blue Notes="Normalweight f'c = 4 ksi added 4/23/2010 3:02:20 PM"
Material=SUB Type=Concrete SymType=Isotropic TempDepend=No Color=Blue Notes="Normalweight f'c = 4 ksi added 4/23/2010 3:02:20 PM"
Material=SUPER Type=Concrete SymType=Isotropic TempDepend=No Color=Blue Notes="Normalweight f'c = 4 ksi added 4/23/2010 2:59:44 PM"

TABLE: "MATERIAL PROPERTIES 02 - BASIC MECHANICAL PROPERTIES"
Material=4000Psi UnitWeight=0.15 UnitMass=4.66214231655636E-03 E1=519119.500693241 G12=216299.791955517 U12=0.2 A1=0.0000055
Material=A615Gr60 UnitWeight=0.49 UnitMass=1.52296649007508E-02 E1=4176000 A1=0.0000065
Material=A992Fy50 UnitWeight=0.49 UnitMass=1.52296649007508E-02 E1=4176000 G12=1606153.84615385 U12=0.3 A1=0.0000065
Material=CONC UnitWeight=0 UnitMass=0 E1=518400 G12=216000 U12=0.2 A1=0.0000055
Material=RIGID UnitWeight=0 UnitMass=0 E1=518400 G12=219661.016949153 U12=0.18 A1=0.000006
Material=SUB UnitWeight=0.15 UnitMass=0.004658385 E1=518400 G12=219661.016949153 U12=0.18 A1=0.000006
Material=SUPER UnitWeight=0.152 UnitMass=0.00472049 E1=518400 G12=219661.016949153 U12=0.18 A1=0.000006

TABLE: "MATERIAL PROPERTIES 03A - STEEL DATA"
Material=A992Fy50 Fy=7200 Fu=9360 EffFy=7920 EffFu=10296 SSCurveOpt=Simple SSHysType=Kinematic SHard=0.015 SMax=0.11 SRup=0.17 FinalSlope=-0.1

TABLE: "MATERIAL PROPERTIES 03B - CONCRETE DATA"
Material=4000Psi Fc=576 LtWtConc=No SSCurveOpt=Mander SSHysType=Takeda SFc=2.21914221766202E-03 SCap=0.005 FinalSlope=-0.1 FAngle=0 DAngle=0
Material=CONC Fc=576 LtWtConc=No SSCurveOpt=Mander SSHysType=Kinematic SFc=2.21914221766202E-03 SCap=0.005 FinalSlope=-0.1 FAngle=0 DAngle=0
Material=RIGID Fc=576 LtWtConc=No SSCurveOpt=Mander SSHysType=Kinematic SFc=2.21914221766202E-03 SCap=0.005 FinalSlope=-0.1 FAngle=0 DAngle=0
Material=SUB Fc=576 LtWtConc=No SSCurveOpt=Mander SSHysType=Kinematic SFc=2.21914221766202E-03 SCap=0.005 FinalSlope=-0.1 FAngle=0 DAngle=0
Material=SUPER Fc=576 LtWtConc=No SSCurveOpt=Mander SSHysType=Kinematic SFc=2.21914221766202E-03 SCap=0.005 FinalSlope=-0.1 FAngle=0 DAngle=0

TABLE: "MATERIAL PROPERTIES 03E - REBAR DATA"
Material=A615Gr60 Fy=8640 Fu=12960 EffFy=9504 EffFu=14256 SSCurveOpt=Simple SSHysType=Kinematic SHard=0.01 SCap=0.09 FinalSlope=-0.1 UseCTDef=No

TABLE: "MATERIAL PROPERTIES 06 - DAMPING PARAMETERS"
Material=4000Psi ModalRatio=0 VisMass=0 VisStiff=0 HysMass=0 HysStiff=0
Material=A615Gr60 ModalRatio=0 VisMass=0 VisStiff=0 HysMass=0 HysStiff=0
Material=A992Fy50 ModalRatio=0 VisMass=0 VisStiff=0 HysMass=0 HysStiff=0
Material=CONC ModalRatio=0 VisMass=0 VisStiff=0 HysMass=0 HysStiff=0
Material=RIGID ModalRatio=0 VisMass=0 VisStiff=0 HysMass=0 HysStiff=0
Material=SUB ModalRatio=0 VisMass=0 VisStiff=0 HysMass=0 HysStiff=0

Material=SUPER ModalRatio=0 VisMass=0 VisStiff=0 HysMass=0 HysStiff=0

TABLE: "FRAME SECTION PROPERTIES 01 - GENERAL"
SectionName=BLINK Material=SUB Shape=Rectangular t3=25 t2=25 Area=625 TorsConst=55013.0208333333 I33=32552.0833333333 I22=32552.0833333333 AS2=520.833333333333 AS3=520.833333333333 S33=2604.16666666667 _
S22=2604.16666666667 Z33=3906.25 Z22=3906.25 R33=7.21687836487032 R22=7.21687836487032 ConcCol=Yes ConcBeam=No Color=Gray8Dark TotalWt=1218.75 TotalMass=37.849378125 FromFile=No AMod=1 A2Mod=0 A3Mod=0 _
JMod=1 I2Mod=1 I3Mod=1 MMod=1 WMod=1 Notes="Added 4/23/2010 3:12:01 PM"
SectionName=COL Material=SUB Shape=Rectangular t3=6.25 t2=20 Area=125 TorsConst=1307.42425487066 I33=406.901041666667 I22=4166.66666666667 AS2=104.166666666667 AS3=104.166666666667 S33=130.208333333333 _
S22=416.666666666667 Z33=195.3125 Z22=625 R33=1.80421959121758 R22=5.77350269189626 ConcCol=Yes ConcBeam=No Color=Yellow TotalWt=1237.5 TotalMass=38.43167625 FromFile=No AMod=1 A2Mod=0 A3Mod=0 JMod=1 _
I2Mod=0.353 I3Mod=0.402 MMod=1 WMod=1 Notes="Added 4/23/2010 3:11:18 PM"
SectionName=COLH Material=SUB Shape=Rectangular t3=6.25 t2=40 Area=250 TorsConst=2934.78967917811 I33=813.802083333333 I22=33333.3333333333 AS2=208.333333333333 AS3=208.333333333333 S33=260.416666666667 _
S22=1666.66666666667 Z33=390.625 Z22=2500 R33=1.80421959121758 R22=11.5470053837925 ConcCol=Yes ConcBeam=No Color=Red TotalWt=525 TotalMass=16.3043475 FromFile=No AMod=1 A2Mod=0 A3Mod=0 JMod=1 I2Mod=1 _
I3Mod=1 MMod=1 WMod=1 Notes="Added 4/23/2010 3:10:32 PM"
SectionName=COLT Shape=Nonprismatic Color=Blue Notes="Added 4/23/2010 3:12:36 PM"
SectionName=RIGID Material=RIGID Shape=General t3=1.5 t2=0.8333 Area=2500 TorsConst=100000 I33=100000 I22=100000 AS2=1 AS3=1 S33=1 S22=1 Z33=1 Z22=1 R33=1 R22=1 ConcCol=No ConcBeam=No Color=Blue _
TotalWt=0 TotalMass=0 FromFile=No AMod=1 A2Mod=1 A3Mod=1 JMod=1 I2Mod=1 I3Mod=1 MMod=1 WMod=1 Notes="Added 4/23/2010 3:09:53 PM"
SectionName=SUPER Material=SUPER Shape=General t3=1.5 t2=0.8333 Area=39.8201 TorsConst=5.7 I33=273.3586 I22=2948.364 AS2=1 AS3=1 S33=1 S22=1 Z33=1 Z22=1 R33=1 R22=1 ConcCol=No ConcBeam=No Color=White _
TotalWt=1815.63125119602 TotalMass=56.38598134841 FromFile=No AMod=1 A2Mod=1 A3Mod=1 JMod=1 I2Mod=1 I3Mod=1 MMod=1 WMod=1 Notes="Added 4/23/2010 3:08:54 PM"
SectionName=SUPER-PIER Material=SUPER Shape=General t3=1.5 t2=0.8333 Area=45.2368 TorsConst=9.1 I33=318.9432 I22=3350.024 AS2=1 AS3=1 S33=1 S22=1 Z33=1 Z22=1 R33=1 R22=1 ConcCol=No ConcBeam=No _
Color=White TotalWt=1099.989524661 TotalMass=34.1611154688618 FromFile=No AMod=1 A2Mod=1 A3Mod=1 JMod=1 I2Mod=1 I3Mod=1 MMod=1 WMod=1 Notes="Added 7/17/2010 11:41:37 PM"

TABLE: "FRAME SECTION PROPERTIES 02 - CONCRETE COLUMN"
SectionName=BLINK RebarMatL=A615Gr60 RebarMatC=A615Gr60 ReinfConfig=Rectangular LatReinf=Ties Cover=0.25 NumBars3Dir=26 NumBars2Dir=26 BarSizeL=#9 BarSizeC=#4 SpacingC=0.5 NumCBars2=3 NumCBars3=3 ReinfType=Check
SectionName=COL RebarMatL=A615Gr60 RebarMatC=A615Gr60 ReinfConfig=Rectangular LatReinf=Ties Cover=0.33 NumBars3Dir=45 NumBars2Dir=12 BarSizeL=#11 BarSizeC=#7 SpacingC=1 NumCBars2=6 NumCBars3=20 ReinfType=Design
SectionName=COLH RebarMatL=A615Gr60 RebarMatC=A615Gr60 ReinfConfig=Rectangular LatReinf=Ties Cover=0.33 NumBars3Dir=44 NumBars2Dir=15 BarSizeL=#11 BarSizeC=#7 SpacingC=0.5 NumCBars2=6 NumCBars3=20 ReinfType=Check

TABLE: "FRAME SECTION PROPERTIES 05 - NONPRISMATIC"
SectionName=COLT NumSegments=1 SegmentNum=1 StartSect=COLH EndSect=COL LengthType=Absolute AbsLength=10 EI33Var=Linear EI22Var=Cubic

TABLE: "HINGES DEF 01 - OVERVIEW"
HingeName=HINGE DOFType="Interacting P-M2-M3" Behavior="Deformation Controlled"

TABLE: "HINGES DEF 06 - INTERACTING - DEFORM CONTROL - GENERAL"
HingeName=HINGE DOFType="Interacting P-M2-M3" FDType=Moment-Rot LengthType=Relative SSRelLen=0.1 SFType="User Defined" UserSFRot=1 BeyondE="To Zero" PMMorMMSym=Circular NumAxForce=1 NumAngle=1

TABLE: "HINGES DEF 07 - INTERACTING - DEFORM CONTROL - FS AND ANGS"
HingeName=HINGE DOFType="Interacting P-M2-M3" AxForce=0 Angle=0

TABLE: "HINGES DEF 08 - INTERACTING - DEFORM CONTROL - FORCE-DEFORM"
HingeName=HINGE DOFType="Interacting P-M2-M3" CurveNum=1 AxForce=0 Angle=0 FDPoint=A MomRatio=0 RCRatio=0
HingeName=HINGE DOFType="Interacting P-M2-M3" CurveNum=1 AxForce=0 Angle=0 FDPoint=B MomRatio=1 RCRatio=0
HingeName=HINGE DOFType="Interacting P-M2-M3" CurveNum=1 AxForce=0 Angle=0 FDPoint=C MomRatio=1.2 RCRatio=0.02
HingeName=HINGE DOFType="Interacting P-M2-M3" CurveNum=1 AxForce=0 Angle=0 FDPoint=D MomRatio=0.2 RCRatio=0.02
HingeName=HINGE DOFType="Interacting P-M2-M3" CurveNum=1 AxForce=0 Angle=0 FDPoint=E MomRatio=0.2 RCRatio=0.03

TABLE: "HINGES DEF 09 - INTERACTING - DEFORM CONTROL - ACCEPTANCE"
HingeName=HINGE DOFType="Interacting P-M2-M3" CurveNum=1 AxForce=0 Angle=0 ACPoint=IO AC=0.005
HingeName=HINGE DOFType="Interacting P-M2-M3" CurveNum=1 AxForce=0 Angle=0 ACPoint=LS AC=0.01
HingeName=HINGE DOFType="Interacting P-M2-M3" CurveNum=1 AxForce=0 Angle=0 ACPoint=CP AC=0.02

TABLE: "HINGES DEF 11 - INTERACTING - INTERACTION SURFACE - GENERAL"
HingeName=HINGE DOFType="Interacting P-M2-M3" IntType=User PCurve=Elastic-Plastic SymMMandPMM=Double NumCurves=5 NumPoints=11 ScaleP=71262.65 ScaleM2=72161.39 ScaleM3=72161.39

TABLE: "HINGES DEF 12 - INTERACTING - INTERACTION SURFACE - DATA"
HingeName=HINGE DOFType="Interacting P-M2-M3" CurveNum=1 PointNum=1 P=-1 M2=0 M3=0
HingeName=HINGE DOFType="Interacting P-M2-M3" CurveNum=1 PointNum=2 P=-0.851 M2=1.1841 M3=0
HingeName=HINGE DOFType="Interacting P-M2-M3" CurveNum=1 PointNum=3 P=-0.7516 M2=1.8246 M3=0
HingeName=HINGE DOFType="Interacting P-M2-M3" CurveNum=1 PointNum=4 P=-0.6452 M2=2.3201 M3=0
HingeName=HINGE DOFType="Interacting P-M2-M3" CurveNum=1 PointNum=5 P=-0.5362 M2=2.6631 M3=0
HingeName=HINGE DOFType="Interacting P-M2-M3" CurveNum=1 PointNum=6 P=-0.4099 M2=2.8372 M3=0
HingeName=HINGE DOFType="Interacting P-M2-M3" CurveNum=1 PointNum=7 P=-0.3189 M2=2.7895 M3=0
HingeName=HINGE DOFType="Interacting P-M2-M3" CurveNum=1 PointNum=8 P=-0.2282 M2=2.5685 M3=0
HingeName=HINGE DOFType="Interacting P-M2-M3" CurveNum=1 PointNum=9 P=-0.1374 M2=2.179 M3=0
HingeName=HINGE DOFType="Interacting P-M2-M3" CurveNum=1 PointNum=10 P=-0.0337 M2=1.5546 M3=0
HingeName=HINGE DOFType="Interacting P-M2-M3" CurveNum=1 PointNum=11 P=0.1497 M2=0 M3=0
HingeName=HINGE DOFType="Interacting P-M2-M3" CurveNum=2 PointNum=1 P=-1 M2=0 M3=0
HingeName=HINGE DOFType="Interacting P-M2-M3" CurveNum=2 PointNum=2 P=-0.851 M2=1.1167 M3=0.7045

HingeName=HINGE DOFType="Interacting P-M2-M3" CurveNum=2 PointNum=3 P=-0.7516 M2=1.7348 M3=0.966
HingeName=HINGE DOFType="Interacting P-M2-M3" CurveNum=2 PointNum=4 P=-0.6452 M2=2.2229 M3=1.0959
HingeName=HINGE DOFType="Interacting P-M2-M3" CurveNum=2 PointNum=5 P=-0.5362 M2=2.55 M3=1.1944
HingeName=HINGE DOFType="Interacting P-M2-M3" CurveNum=2 PointNum=6 P=-0.4099 M2=2.7021 M3=1.2639
HingeName=HINGE DOFType="Interacting P-M2-M3" CurveNum=2 PointNum=7 P=-0.3189 M2=2.6659 M3=1.2517
HingeName=HINGE DOFType="Interacting P-M2-M3" CurveNum=2 PointNum=8 P=-0.2282 M2=2.4335 M3=1.2063
HingeName=HINGE DOFType="Interacting P-M2-M3" CurveNum=2 PointNum=9 P=-0.1374 M2=2.083 M3=1.1192
HingeName=HINGE DOFType="Interacting P-M2-M3" CurveNum=2 PointNum=10 P=-0.0337 M2=1.4977 M3=0.8903
HingeName=HINGE DOFType="Interacting P-M2-M3" CurveNum=2 PointNum=11 P=0.1497 M2=0 M3=0
HingeName=HINGE DOFType="Interacting P-M2-M3" CurveNum=3 PointNum=1 P=-1 M2=0 M3=0
HingeName=HINGE DOFType="Interacting P-M2-M3" CurveNum=3 PointNum=2 P=-0.859355003741443 M2=0.873794599643073 M3=0.873794599643073
HingeName=HINGE DOFType="Interacting P-M2-M3" CurveNum=3 PointNum=3 P=-0.762037630399016 M2=1.31807221332363 M3=1.31807221332363
HingeName=HINGE DOFType="Interacting P-M2-M3" CurveNum=3 PointNum=4 P=-0.65809587561594 M2=1.63579322880561 M3=1.63579322880561
HingeName=HINGE DOFType="Interacting P-M2-M3" CurveNum=3 PointNum=5 P=-0.55577543531639 M2=1.85207851246629 M3=1.85207851246629
HingeName=HINGE DOFType="Interacting P-M2-M3" CurveNum=3 PointNum=6 P=-0.410639738177721 M2=1.9850404410749 M3=1.9850404410749
HingeName=HINGE DOFType="Interacting P-M2-M3" CurveNum=3 PointNum=7 P=-0.294991131405852 M2=1.94055216697559 M3=1.94055216697559
HingeName=HINGE DOFType="Interacting P-M2-M3" CurveNum=3 PointNum=8 P=-0.207592564040144 M2=1.79090799726159 M3=1.79090799726159
HingeName=HINGE DOFType="Interacting P-M2-M3" CurveNum=3 PointNum=9 P=-0.112557757697182 M2=1.528794056407 M3=1.528794056407
HingeName=HINGE DOFType="Interacting P-M2-M3" CurveNum=3 PointNum=10 P=-2.16590406561296E-02 M2=1.14281407088648 M3=1.14281407088648
HingeName=HINGE DOFType="Interacting P-M2-M3" CurveNum=3 PointNum=11 P=0.1497 M2=0 M3=0
HingeName=HINGE DOFType="Interacting P-M2-M3" CurveNum=4 PointNum=1 P=-1 M2=0 M3=0
HingeName=HINGE DOFType="Interacting P-M2-M3" CurveNum=4 PointNum=2 P=-0.851 M2=0.7045 M3=1.1167
HingeName=HINGE DOFType="Interacting P-M2-M3" CurveNum=4 PointNum=3 P=-0.7516 M2=0.966 M3=1.7348
HingeName=HINGE DOFType="Interacting P-M2-M3" CurveNum=4 PointNum=4 P=-0.6452 M2=1.0959 M3=2.2229
HingeName=HINGE DOFType="Interacting P-M2-M3" CurveNum=4 PointNum=5 P=-0.5362 M2=1.1944 M3=2.55
HingeName=HINGE DOFType="Interacting P-M2-M3" CurveNum=4 PointNum=6 P=-0.4099 M2=1.2639 M3=2.7021
HingeName=HINGE DOFType="Interacting P-M2-M3" CurveNum=4 PointNum=7 P=-0.3189 M2=1.2517 M3=2.6659
HingeName=HINGE DOFType="Interacting P-M2-M3" CurveNum=4 PointNum=8 P=-0.2282 M2=1.2063 M3=2.4335
HingeName=HINGE DOFType="Interacting P-M2-M3" CurveNum=4 PointNum=9 P=-0.1374 M2=1.1192 M3=2.083
HingeName=HINGE DOFType="Interacting P-M2-M3" CurveNum=4 PointNum=10 P=-0.0337 M2=0.8903 M3=1.4977
HingeName=HINGE DOFType="Interacting P-M2-M3" CurveNum=4 PointNum=11 P=0.1497 M2=0 M3=0
HingeName=HINGE DOFType="Interacting P-M2-M3" CurveNum=5 PointNum=1 P=-1 M2=0 M3=0

HingeName=HINGE DOFType="Interacting P-M2-M3" CurveNum=5 PointNum=2 P=-0.851 M2=0 M3=1.1841
HingeName=HINGE DOFType="Interacting P-M2-M3" CurveNum=5 PointNum=3 P=-0.7516 M2=0 M3=1.8246
HingeName=HINGE DOFType="Interacting P-M2-M3" CurveNum=5 PointNum=4 P=-0.6452 M2=0 M3=2.3201
HingeName=HINGE DOFType="Interacting P-M2-M3" CurveNum=5 PointNum=5 P=-0.5362 M2=0 M3=2.6631
HingeName=HINGE DOFType="Interacting P-M2-M3" CurveNum=5 PointNum=6 P=-0.4099 M2=0 M3=2.8372
HingeName=HINGE DOFType="Interacting P-M2-M3" CurveNum=5 PointNum=7 P=-0.3189 M2=0 M3=2.7895
HingeName=HINGE DOFType="Interacting P-M2-M3" CurveNum=5 PointNum=8 P=-0.2282 M2=0 M3=2.5685
HingeName=HINGE DOFType="Interacting P-M2-M3" CurveNum=5 PointNum=9 P=-0.1374 M2=0 M3=2.179
HingeName=HINGE DOFType="Interacting P-M2-M3" CurveNum=5 PointNum=10 P=-0.0337 M2=0 M3=1.5546
HingeName=HINGE DOFType="Interacting P-M2-M3" CurveNum=5 PointNum=11 P=0.1497 M2=0 M3=0

TABLE: "LOAD PATTERN DEFINITIONS"
LoadPat=DEAD DesignType=DEAD SelfWtMult=1

TABLE: "LOAD CASE DEFINITIONS"
Case=DEAD Type=LinStatic InitialCond=Zero DesTypeOpt="Prog Det" DesignType=DEAD AutoType=None RunCase=Yes CaseStatus="Not Run"
Case=MODAL Type=LinModal InitialCond=Zero DesTypeOpt="Prog Det" DesignType=OTHER AutoType=None RunCase=Yes CaseStatus="Not Run"
Case=ModalRitz Type=LinModal InitialCond=Zero DesTypeOpt="Prog Det" DesignType=OTHER AutoType=None RunCase=No CaseStatus="Not Run"
Case=RITZ Type=LinModal InitialCond=Zero DesTypeOpt="Prog Det" DesignType=QUAKE AutoType=None RunCase=No CaseStatus="Not Run"
Case=GRAV Type=NonStatic InitialCond=Zero DesTypeOpt="Prog Det" DesignType=DEAD AutoType=None RunCase=Yes CaseStatus="Not Run"
Case=MODE4 Type=NonStatic InitialCond=GRAV ModalCase=MODAL DesTypeOpt="Prog Det" AutoType=None RunCase=Yes CaseStatus="Not Run"
Case=MODE6 Type=NonStatic InitialCond=GRAV ModalCase=MODAL DesTypeOpt="Prog Det" AutoType=None RunCase=Yes CaseStatus="Not Run"
Case=MODE7 Type=NonStatic InitialCond=GRAV ModalCase=MODAL DesTypeOpt="Prog Det" AutoType=None RunCase=Yes CaseStatus="Not Run"
Case=MODE12 Type=NonStatic InitialCond=GRAV ModalCase=MODAL DesTypeOpt="Prog Det" AutoType=None RunCase=Yes CaseStatus="Not Run"

TABLE: "CASE - STATIC 1 - LOAD ASSIGNMENTS"
Case=DEAD LoadType="Load pattern" LoadName=DEAD LoadSF=1
Case=GRAV LoadType="Load pattern" LoadName=DEAD LoadSF=1
Case=MODE4 LoadType=Mode LoadName="Mode 4" LoadSF=1
Case=MODE6 LoadType=Mode LoadName="Mode 6" LoadSF=1
Case=MODE7 LoadType=Mode LoadName="Mode 7" LoadSF=1
Case=MODE12 LoadType=Mode LoadName="Mode 12" LoadSF=1

TABLE: "CASE - STATIC 2 - NONLINEAR LOAD APPLICATION"
Case=GRAV LoadApp="Full Load" MonitorDOF=U1 MonitorJt=711
Case=MODE4 LoadApp="Displ Ctrl" DisplType=Monitored TargetDispl=1 MonitorDOF=U2 MonitorJt=711
Case=MODE6 LoadApp="Displ Ctrl" DisplType=Conjugate TargetDispl=1 MonitorDOF=U2 MonitorJt=711
Case=MODE7 LoadApp="Displ Ctrl" DisplType=Conjugate TargetDispl=1 MonitorDOF=U2 MonitorJt=711
Case=MODE12 LoadApp="Displ Ctrl" DisplType=Monitored TargetDispl=1 MonitorDOF=U2 MonitorJt=711

TABLE: "CASE - STATIC 4 - NONLINEAR PARAMETERS"
Case=GRAV Unloading="Unload Entire" GeoNonLin=None ResultsSave="Final State" MaxTotal=200 MaxNull=50 MaxIterCS=10 MaxIterNR=40 ItConvTol=0.0001 UseEvStep=Yes EvLumpTol=0.01 LSPerIter=20 LSTol=0.1 _
LSStepFact=1.618 FrameTC=Yes FrameHinge=Yes CableTC=Yes LinkTC=Yes LinkOther=Yes TFMaxIter=10 TFTol=0.01 TFAccelFact=1 TFNoStop=No
Case=MODE4 Unloading="Unload Entire" GeoNonLin=P-Delta ResultsSave="Multiple States" MinNumState=20 MaxNumState=200 PosIncOnly=Yes MaxTotal=200 MaxNull=50 MaxIterCS=10 MaxIterNR=40 ItConvTol=0.0001 UseEvStep=Yes _
EvLumpTol=0.01 LSPerIter=20 LSTol=0.1 LSStepFact=1.618 FrameTC=Yes FrameHinge=Yes CableTC=Yes LinkTC=Yes LinkOther=Yes TFMaxIter=10 TFTol=0.01 TFAccelFact=1 TFNoStop=No
Case=MODE6 Unloading="Unload Entire" GeoNonLin=P-Delta ResultsSave="Multiple States" MinNumState=20 MaxNumState=200 PosIncOnly=Yes MaxTotal=200 MaxNull=50 MaxIterCS=10 MaxIterNR=40 ItConvTol=0.0001 UseEvStep=Yes _
EvLumpTol=0.01 LSPerIter=20 LSTol=0.1 LSStepFact=1.618 FrameTC=Yes FrameHinge=Yes CableTC=Yes LinkTC=Yes LinkOther=Yes TFMaxIter=10 TFTol=0.01 TFAccelFact=1 TFNoStop=No
Case=MODE7 Unloading="Unload Entire" GeoNonLin=P-Delta ResultsSave="Multiple States" MinNumState=20 MaxNumState=200 PosIncOnly=Yes MaxTotal=200 MaxNull=50 MaxIterCS=10 MaxIterNR=40 ItConvTol=0.0001 UseEvStep=Yes _
EvLumpTol=0.01 LSPerIter=20 LSTol=0.1 LSStepFact=1.618 FrameTC=Yes FrameHinge=Yes CableTC=Yes LinkTC=Yes LinkOther=Yes TFMaxIter=10 TFTol=0.01 TFAccelFact=1 TFNoStop=No
Case=MODE12 Unloading="Unload Entire" GeoNonLin=P-Delta ResultsSave="Multiple States" MinNumState=20 MaxNumState=200 PosIncOnly=Yes MaxTotal=200 MaxNull=50 MaxIterCS=10 MaxIterNR=40 ItConvTol=0.0001 UseEvStep=Yes _
EvLumpTol=0.01 LSPerIter=20 LSTol=0.1 LSStepFact=1.618 FrameTC=Yes FrameHinge=Yes CableTC=Yes LinkTC=Yes LinkOther=Yes TFMaxIter=10 TFTol=0.01 TFAccelFact=1 TFNoStop=No

TABLE: "CASE - MODAL 1 - GENERAL"
Case=MODAL ModeType=Eigen MaxNumModes=12 MinNumModes=1 EigenShift=0 EigenCutoff=0 EigenTol=0.000000001 AutoShift=Yes
Case=ModalRitz ModeType=Ritz MaxNumModes=12 MinNumModes=1
Case=RITZ ModeType=Ritz MaxNumModes=12 MinNumModes=1

TABLE: "CASE - MODAL 3 - LOAD ASSIGNMENTS - RITZ"
Case=ModalRitz LoadType="Load pattern" LoadName=DEAD MaxCycles=0 TargetPar=0
Case=ModalRitz LoadType=Accel LoadName="Accel UY" MaxCycles=0 TargetPar=0
Case=ModalRitz LoadType=Link LoadName="All Links" MaxCycles=0 TargetPar=0
Case=RITZ LoadType=Accel LoadName="Accel UY" MaxCycles=0 TargetPar=0
Case=RITZ LoadType=Link LoadName="All Links" MaxCycles=0 TargetPar=0

TABLE: "JOINT COORDINATES"
Joint=211 CoordSys=GLOBAL CoordType=Cartesian XorR=138.1947 Y=-19.4771 Z=-60.9757 SpecialJt=No GlobalX=138.1947 GlobalY=-19.4771 GlobalZ=-60.9757
Joint=221 CoordSys=GLOBAL CoordType=Cartesian XorR=298.63 Y=-98.9762 Z=-60.9757 SpecialJt=No GlobalX=298.63 GlobalY=-98.9762 GlobalZ=-60.9757
Joint=311 CoordSys=GLOBAL CoordType=Cartesian XorR=138.1947 Y=-19.4771 Z=-54.4757 SpecialJt=No GlobalX=138.1947 GlobalY=-19.4771 GlobalZ=-54.4757
Joint=315 CoordSys=GLOBAL CoordType=Cartesian XorR=138.1947 Y=-19.4771 Z=-49.2301154751892 SpecialJt=No GlobalX=138.1947 GlobalY=-19.4771 GlobalZ=-49.2301154751892
Joint=321 CoordSys=GLOBAL CoordType=Cartesian XorR=298.63 Y=-98.9762 Z=-54.4757 SpecialJt=No GlobalX=298.63 GlobalY=-98.9762 GlobalZ=-54.4757
Joint=325 CoordSys=GLOBAL CoordType=Cartesian XorR=298.63 Y=-98.9762 Z=-49.2301154751892 SpecialJt=No GlobalX=298.63 GlobalY=-98.9762 GlobalZ=-49.2301154751892
Joint=411 CoordSys=GLOBAL CoordType=Cartesian XorR=138.1947 Y=-19.4771 Z=-21.4757 SpecialJt=No GlobalX=138.1947 GlobalY=-19.4771 GlobalZ=-21.4757
Joint=421 CoordSys=GLOBAL CoordType=Cartesian XorR=298.63 Y=-98.9762 Z=-21.4757 SpecialJt=No GlobalX=298.63 GlobalY=-98.9762 GlobalZ=-21.4757
Joint=511 CoordSys=GLOBAL CoordType=Cartesian XorR=138.1947 Y=-19.4771 Z=-11.4757

SpecialJt=No GlobalX=138.1947 GlobalY=-19.4771 GlobalZ=-11.4757
Joint=521 CoordSys=GLOBAL CoordType=Cartesian XorR=298.63 Y=-98.9762 Z=-11.4757 SpecialJt=No GlobalX=298.63 GlobalY=-98.9762 GlobalZ=-11.4757
Joint=611 CoordSys=GLOBAL CoordType=Cartesian XorR=138.1947 Y=-19.4771 Z=-4.4757 SpecialJt=No GlobalX=138.1947 GlobalY=-19.4771 GlobalZ=-4.4757
Joint=621 CoordSys=GLOBAL CoordType=Cartesian XorR=298.63 Y=-98.9762 Z=-4.4757 SpecialJt=No GlobalX=298.63 GlobalY=-98.9762 GlobalZ=-4.4757
Joint=701 CoordSys=GLOBAL CoordType=Cartesian XorR=0 Y=0 Z=0 SpecialJt=No GlobalX=0 GlobalY=0 GlobalZ=0
Joint=702 CoordSys=GLOBAL CoordType=Cartesian XorR=34.9758 Y=-1.2248 Z=0 SpecialJt=No GlobalX=34.9758 GlobalY=-1.2248 GlobalZ=0
Joint=703 CoordSys=GLOBAL CoordType=Cartesian XorR=69.7802 Y=-4.8932 Z=0 SpecialJt=No GlobalX=69.7802 GlobalY=-4.8932 GlobalZ=0
Joint=704 CoordSys=GLOBAL CoordType=Cartesian XorR=104.2428 Y=-10.9873 Z=0 SpecialJt=No GlobalX=104.2428 GlobalY=-10.9873 GlobalZ=0
Joint=711 CoordSys=GLOBAL CoordType=Cartesian XorR=138.1947 Y=-19.4771 Z=0 SpecialJt=No GlobalX=138.1947 GlobalY=-19.4771 GlobalZ=0
Joint=712 CoordSys=GLOBAL CoordType=Cartesian XorR=180.8294 Y=-33.8447 Z=0 SpecialJt=No GlobalX=180.8294 GlobalY=-33.8447 GlobalZ=0
Joint=713 CoordSys=GLOBAL CoordType=Cartesian XorR=222 Y=-51.9866 Z=0 SpecialJt=No GlobalX=222 GlobalY=-51.9866 GlobalZ=0
Joint=714 CoordSys=GLOBAL CoordType=Cartesian XorR=261.3731 Y=-73.7558 Z=0 SpecialJt=No GlobalX=261.3731 GlobalY=-73.7558 GlobalZ=0
Joint=721 CoordSys=GLOBAL CoordType=Cartesian XorR=298.63 Y=-98.9762 Z=0 SpecialJt=No GlobalX=298.63 GlobalY=-98.9762 GlobalZ=0
Joint=722 CoordSys=GLOBAL CoordType=Cartesian XorR=325.9507 Y=-120.848 Z=0 SpecialJt=No GlobalX=325.9507 GlobalY=-120.848 GlobalZ=0
Joint=723 CoordSys=GLOBAL CoordType=Cartesian XorR=351.6746 Y=-144.578 Z=0 SpecialJt=No GlobalX=351.6746 GlobalY=-144.578 GlobalZ=0
Joint=724 CoordSys=GLOBAL CoordType=Cartesian XorR=375.8239 Y=-170.049 Z=0 SpecialJt=No GlobalX=375.8239 GlobalY=-170.049 GlobalZ=0
Joint=731 CoordSys=GLOBAL CoordType=Cartesian XorR=397.8358 Y=-197.136 Z=0 SpecialJt=No GlobalX=397.8358 GlobalY=-197.136 GlobalZ=0

TABLE: "CONNECTIVITY - FRAME"
Frame=211 JointI=311 JointJ=211 IsCurved=No Length=6.5 CentroidX=138.1947 CentroidY=-19.4771 CentroidZ=-57.7257
Frame=221 JointI=321 JointJ=221 IsCurved=No Length=6.5 CentroidX=298.63 CentroidY=-98.9762 CentroidZ=-57.7257
Frame=311 JointI=315 JointJ=311 IsCurved=No Length=5.24558452481077 CentroidX=138.1947 CentroidY=-19.4771 CentroidZ=-51.8529077375946
Frame=315 JointI=411 JointJ=315 IsCurved=No Length=27.7544154751892 CentroidX=138.1947 CentroidY=-19.4771 CentroidZ=-35.3529077375946
Frame=321 JointI=325 JointJ=321 IsCurved=No Length=5.24558452481077 CentroidX=298.63 CentroidY=-98.9762 CentroidZ=-51.8529077375946
Frame=325 JointI=421 JointJ=325 IsCurved=No Length=27.7544154751892 CentroidX=298.63 CentroidY=-98.9762 CentroidZ=-35.3529077375946
Frame=411 JointI=511 JointJ=411 IsCurved=No Length=10 CentroidX=138.1947 CentroidY=-19.4771 CentroidZ=-16.4757
Frame=421 JointI=521 JointJ=421 IsCurved=No Length=10 CentroidX=298.63 CentroidY=-98.9762 CentroidZ=-16.4757
Frame=511 JointI=611 JointJ=511 IsCurved=No Length=7 CentroidX=138.1947 CentroidY=-19.4771 CentroidZ=-7.9757
Frame=521 JointI=621 JointJ=521 IsCurved=No Length=7 CentroidX=298.63 CentroidY=-98.9762 CentroidZ=-7.9757
Frame=611 JointI=711 JointJ=611 IsCurved=No Length=4.4757 CentroidX=138.1947 CentroidY=-19.4771 CentroidZ=-2.23785
Frame=621 JointI=721 JointJ=621 IsCurved=No Length=4.4757 CentroidX=298.63 CentroidY=-98.9762

CentroidZ=-2.23785
Frame=701 JointI=701 JointJ=702 IsCurved=No Length=34.9972387579363 CentroidX=17.4879 CentroidY=-0.6124 CentroidZ=0
Frame=702 JointI=702 JointJ=703 IsCurved=No Length=34.9971915718962 CentroidX=52.378 CentroidY=-3.059 CentroidZ=0
Frame=703 JointI=703 JointJ=704 IsCurved=No Length=34.9972692301842 CentroidX=87.0115 CentroidY=-7.94025 CentroidZ=0
Frame=704 JointI=704 JointJ=711 IsCurved=No Length=34.9972601449028 CentroidX=121.21875 CentroidY=-15.2322 CentroidZ=0
Frame=711 JointI=711 JointJ=712 IsCurved=No Length=44.9905053744676 CentroidX=159.51205 CentroidY=-26.6609 CentroidZ=0
Frame=712 JointI=712 JointJ=713 IsCurved=No Length=44.9905194454343 CentroidX=201.4147 CentroidY=-42.91565 CentroidZ=0
Frame=713 JointI=713 JointJ=714 IsCurved=No Length=44.9904331191644 CentroidX=241.68655 CentroidY=-62.8712 CentroidZ=0
Frame=714 JointI=714 JointJ=721 IsCurved=No Length=44.9905009281959 CentroidX=280.00155 CentroidY=-86.366 CentroidZ=0
Frame=721 JointI=721 JointJ=722 IsCurved=No Length=34.9970896465692 CentroidX=312.29035 CentroidY=-109.9121 CentroidZ=0
Frame=722 JointI=722 JointJ=723 IsCurved=No Length=34.997598934927 CentroidX=338.81265 CentroidY=-132.713 CentroidZ=0
Frame=723 JointI=723 JointJ=724 IsCurved=No Length=35.0992953132965 CentroidX=363.74925 CentroidY=-157.3135 CentroidZ=0
Frame=724 JointI=724 JointJ=731 IsCurved=No Length=34.9031418443956 CentroidX=386.82985 CentroidY=-183.5925 CentroidZ=0

TABLE: "JOINT RESTRAINT ASSIGNMENTS"
Joint=211 U1=Yes U2=Yes U3=Yes R1=Yes R2=Yes R3=Yes
Joint=221 U1=Yes U2=Yes U3=Yes R1=Yes R2=Yes R3=Yes
Joint=701 U1=No U2=Yes U3=Yes R1=Yes R2=No R3=No
Joint=731 U1=No U2=Yes U3=Yes R1=Yes R2=No R3=No

TABLE: "JOINT LOCAL AXES ASSIGNMENTS 1 - TYPICAL"
Joint=211 AngleA=-16 AngleB=0 AngleC=0 AdvanceAxes=No
Joint=221 AngleA=-36 AngleB=0 AngleC=0 AdvanceAxes=No
Joint=731 AngleA=-52 AngleB=0 AngleC=0 AdvanceAxes=No

TABLE: "JOINT SPRING ASSIGNMENTS 1 - UNCOUPLED"
Joint=211 CoordSys=Local U1=0 U2=0 U3=0 R1=0 R2=0 R3=0
Joint=701 CoordSys=Local U1=0 U2=0 U3=0 R1=0 R2=0 R3=0
Joint=731 CoordSys=Local U1=0 U2=0 U3=0 R1=0 R2=0 R3=0
Joint=221 CoordSys=Local U1=0 U2=0 U3=0 R1=0 R2=0 R3=0

TABLE: "FRAME SECTION ASSIGNMENTS"
Frame=211 SectionType=Rectangular AutoSelect=N.A. AnalSect=BLINK DesignSect=BLINK MatProp=Default
Frame=221 SectionType=Rectangular AutoSelect=N.A. AnalSect=BLINK DesignSect=BLINK MatProp=Default
Frame=311 SectionType=Rectangular AutoSelect=N.A. AnalSect=COL DesignSect=COL MatProp=Default
Frame=315 SectionType=Rectangular AutoSelect=N.A. AnalSect=COL DesignSect=COL MatProp=Default
Frame=321 SectionType=Rectangular AutoSelect=N.A. AnalSect=COL DesignSect=COL MatProp=Default
Frame=325 SectionType=Rectangular AutoSelect=N.A. AnalSect=COL DesignSect=COL MatProp=Default
Frame=411 SectionType=Nonprismatic AutoSelect=N.A. AnalSect=COLT DesignSect=COLT MatProp=Default NPSectType=Default
Frame=421 SectionType=Nonprismatic AutoSelect=N.A. AnalSect=COLT DesignSect=COLT MatProp=Default NPSectType=Default
Frame=511 SectionType=Rectangular AutoSelect=N.A. AnalSect=COLH DesignSect=COLH MatProp=Default

Frame=521 SectionType=Rectangular AutoSelect=N.A. AnalSect=COLH DesignSect=COLH MatProp=Default
Frame=611 SectionType=General AutoSelect=N.A. AnalSect=RIGID DesignSect=N.A. MatProp=Default
Frame=621 SectionType=General AutoSelect=N.A. AnalSect=RIGID DesignSect=N.A. MatProp=Default
Frame=701 SectionType=General AutoSelect=N.A. AnalSect=SUPER DesignSect=N.A. MatProp=Default
Frame=702 SectionType=General AutoSelect=N.A. AnalSect=SUPER DesignSect=N.A. MatProp=Default
Frame=703 SectionType=General AutoSelect=N.A. AnalSect=SUPER DesignSect=N.A. MatProp=Default
Frame=704 SectionType=General AutoSelect=N.A. AnalSect=SUPER-PIER DesignSect=N.A. MatProp=Default
Frame=711 SectionType=General AutoSelect=N.A. AnalSect=SUPER-PIER DesignSect=N.A. MatProp=Default
Frame=712 SectionType=General AutoSelect=N.A. AnalSect=SUPER DesignSect=N.A. MatProp=Default
Frame=713 SectionType=General AutoSelect=N.A. AnalSect=SUPER DesignSect=N.A. MatProp=Default
Frame=714 SectionType=General AutoSelect=N.A. AnalSect=SUPER-PIER DesignSect=N.A. MatProp=Default
Frame=721 SectionType=General AutoSelect=N.A. AnalSect=SUPER-PIER DesignSect=N.A. MatProp=Default
Frame=722 SectionType=General AutoSelect=N.A. AnalSect=SUPER DesignSect=N.A. MatProp=Default
Frame=723 SectionType=General AutoSelect=N.A. AnalSect=SUPER DesignSect=N.A. MatProp=Default
Frame=724 SectionType=General AutoSelect=N.A. AnalSect=SUPER DesignSect=N.A. MatProp=Default

TABLE: "FRAME RELEASE ASSIGNMENTS 1 - GENERAL"
Frame=611 PI=No V2I=No V3I=No TI=No M2I=No M3I=No PJ=No V2J=No V3J=No TJ=No M2J=No M3J=Yes PartialFix=No
Frame=621 PI=No V2I=No V3I=No TI=No M2I=No M3I=No PJ=No V2J=No V3J=No TJ=No M2J=No M3J=Yes PartialFix=No

TABLE: "FRAME LOCAL AXES ASSIGNMENTS 1 - TYPICAL"
Frame=211 Angle=16 MirrorAbt2=No MirrorAbt3=No AdvanceAxes=No
Frame=221 Angle=36 MirrorAbt2=No MirrorAbt3=No AdvanceAxes=No
Frame=311 Angle=16 MirrorAbt2=No MirrorAbt3=No AdvanceAxes=No
Frame=315 Angle=16 MirrorAbt2=No MirrorAbt3=No AdvanceAxes=No
Frame=321 Angle=36 MirrorAbt2=No MirrorAbt3=No AdvanceAxes=No
Frame=325 Angle=36 MirrorAbt2=No MirrorAbt3=No AdvanceAxes=No
Frame=411 Angle=16 MirrorAbt2=No MirrorAbt3=No AdvanceAxes=No
Frame=421 Angle=36 MirrorAbt2=No MirrorAbt3=No AdvanceAxes=No
Frame=511 Angle=16 MirrorAbt2=No MirrorAbt3=No AdvanceAxes=No
Frame=521 Angle=36 MirrorAbt2=No MirrorAbt3=No AdvanceAxes=No
Frame=611 Angle=16 MirrorAbt2=No MirrorAbt3=No AdvanceAxes=No
Frame=621 Angle=36 MirrorAbt2=No MirrorAbt3=No AdvanceAxes=No

TABLE: "FRAME OUTPUT STATION ASSIGNMENTS"
Frame=211 StationType=MinNumSta MinNumSta=3 AddAtElmInt=Yes AddAtPtLoad=Yes
Frame=221 StationType=MinNumSta MinNumSta=3 AddAtElmInt=Yes AddAtPtLoad=Yes
Frame=311 StationType=MinNumSta MinNumSta=3 AddAtElmInt=Yes AddAtPtLoad=Yes
Frame=315 StationType=MinNumSta MinNumSta=3 AddAtElmInt=Yes AddAtPtLoad=Yes
Frame=321 StationType=MinNumSta MinNumSta=3 AddAtElmInt=Yes AddAtPtLoad=Yes
Frame=325 StationType=MinNumSta MinNumSta=3 AddAtElmInt=Yes AddAtPtLoad=Yes
Frame=411 StationType=MinNumSta MinNumSta=3 AddAtElmInt=Yes AddAtPtLoad=Yes
Frame=421 StationType=MinNumSta MinNumSta=3 AddAtElmInt=Yes AddAtPtLoad=Yes
Frame=511 StationType=MinNumSta MinNumSta=3 AddAtElmInt=Yes AddAtPtLoad=Yes
Frame=521 StationType=MinNumSta MinNumSta=3 AddAtElmInt=Yes AddAtPtLoad=Yes
Frame=611 StationType=MinNumSta MinNumSta=3 AddAtElmInt=Yes AddAtPtLoad=Yes
Frame=621 StationType=MinNumSta MinNumSta=3 AddAtElmInt=Yes AddAtPtLoad=Yes
Frame=701 StationType=MaxStaSpcg MaxStaSpcg=2 AddAtElmInt=Yes AddAtPtLoad=Yes
Frame=702 StationType=MaxStaSpcg MaxStaSpcg=2 AddAtElmInt=Yes AddAtPtLoad=Yes
Frame=703 StationType=MaxStaSpcg MaxStaSpcg=2 AddAtElmInt=Yes AddAtPtLoad=Yes
Frame=704 StationType=MaxStaSpcg MaxStaSpcg=2 AddAtElmInt=Yes AddAtPtLoad=Yes

Frame=711 StationType=MaxStaSpcg MaxStaSpcg=2 AddAtElmInt=Yes AddAtPtLoad=Yes
Frame=712 StationType=MaxStaSpcg MaxStaSpcg=2 AddAtElmInt=Yes AddAtPtLoad=Yes
Frame=713 StationType=MaxStaSpcg MaxStaSpcg=2 AddAtElmInt=Yes AddAtPtLoad=Yes
Frame=714 StationType=MaxStaSpcg MaxStaSpcg=2 AddAtElmInt=Yes AddAtPtLoad=Yes
Frame=721 StationType=MaxStaSpcg MaxStaSpcg=2 AddAtElmInt=Yes AddAtPtLoad=Yes
Frame=722 StationType=MaxStaSpcg MaxStaSpcg=2 AddAtElmInt=Yes AddAtPtLoad=Yes
Frame=723 StationType=MaxStaSpcg MaxStaSpcg=2 AddAtElmInt=Yes AddAtPtLoad=Yes
Frame=724 StationType=MaxStaSpcg MaxStaSpcg=2 AddAtElmInt=Yes AddAtPtLoad=Yes

TABLE: "FRAME HINGE ASSIGNS 01 - OVERVIEW"
Frame=311 AssignType="Auto FEMA356 - P-M2-M3" HingeTable="Table 6-8 (Concrete Columns - Flexure) Item i" GenHinge=311H1 RelDist=1 AbsDist=5.24558452481077 ActualDist=5.24558452481077 OverWrites=No
Frame=321 AssignType="Auto FEMA356 - P-M2-M3" HingeTable="Table 6-8 (Concrete Columns - Flexure) Item i" GenHinge=321H1 RelDist=1 AbsDist=5.24558452481077 ActualDist=5.24558452481077 OverWrites=No

TABLE: "FRAME HINGE ASSIGNS 05 - AUTO FEMA 356 - CONCRETE COLUMN"
Frame=311 GenHinge=311H1 CompType=Primary DOF=P-M2-M3 PandVFrom=Case PandVCase=DEAD Conforming=Yes BeyondE="To Zero" DistType=RelDist RelDist=1 AbsDist=5.24558452481077 ActualDist=5.24558452481077
Frame=321 GenHinge=321H1 CompType=Primary DOF=P-M2-M3 PandVFrom=Case PandVCase=DEAD Conforming=Yes BeyondE="To Zero" DistType=RelDist RelDist=1 AbsDist=5.24558452481077 ActualDist=5.24558452481077

TABLE: "FRAME AUTO MESH ASSIGNMENTS"
Frame=211 AutoMesh=Yes AtJoints=Yes AtFrames=No NumSegments=0 MaxLength=0 MaxDegrees=0
Frame=221 AutoMesh=Yes AtJoints=Yes AtFrames=No NumSegments=0 MaxLength=0 MaxDegrees=0
Frame=311 AutoMesh=Yes AtJoints=Yes AtFrames=No NumSegments=0 MaxLength=0 MaxDegrees=0
Frame=315 AutoMesh=Yes AtJoints=Yes AtFrames=No NumSegments=0 MaxLength=0 MaxDegrees=0
Frame=321 AutoMesh=Yes AtJoints=Yes AtFrames=No NumSegments=0 MaxLength=0 MaxDegrees=0
Frame=325 AutoMesh=Yes AtJoints=Yes AtFrames=No NumSegments=0 MaxLength=0 MaxDegrees=0
Frame=411 AutoMesh=Yes AtJoints=Yes AtFrames=No NumSegments=0 MaxLength=0 MaxDegrees=0
Frame=421 AutoMesh=Yes AtJoints=Yes AtFrames=No NumSegments=0 MaxLength=0 MaxDegrees=0
Frame=511 AutoMesh=Yes AtJoints=Yes AtFrames=No NumSegments=0 MaxLength=0 MaxDegrees=0
Frame=521 AutoMesh=Yes AtJoints=Yes AtFrames=No NumSegments=0 MaxLength=0 MaxDegrees=0
Frame=611 AutoMesh=Yes AtJoints=Yes AtFrames=No NumSegments=0 MaxLength=0 MaxDegrees=0
Frame=621 AutoMesh=Yes AtJoints=Yes AtFrames=No NumSegments=0 MaxLength=0 MaxDegrees=0
Frame=701 AutoMesh=Yes AtJoints=Yes AtFrames=No NumSegments=0 MaxLength=0 MaxDegrees=0
Frame=702 AutoMesh=Yes AtJoints=Yes AtFrames=No NumSegments=0 MaxLength=0 MaxDegrees=0
Frame=703 AutoMesh=Yes AtJoints=Yes AtFrames=No NumSegments=0 MaxLength=0 MaxDegrees=0
Frame=704 AutoMesh=Yes AtJoints=Yes AtFrames=No NumSegments=0 MaxLength=0 MaxDegrees=0
Frame=711 AutoMesh=Yes AtJoints=Yes AtFrames=No NumSegments=0 MaxLength=0 MaxDegrees=0
Frame=712 AutoMesh=Yes AtJoints=Yes AtFrames=No NumSegments=0 MaxLength=0 MaxDegrees=0
Frame=713 AutoMesh=Yes AtJoints=Yes AtFrames=No NumSegments=0 MaxLength=0 MaxDegrees=0
Frame=714 AutoMesh=Yes AtJoints=Yes AtFrames=No NumSegments=0 MaxLength=0 MaxDegrees=0
Frame=721 AutoMesh=Yes AtJoints=Yes AtFrames=No NumSegments=0 MaxLength=0 MaxDegrees=0
Frame=722 AutoMesh=Yes AtJoints=Yes AtFrames=No NumSegments=0 MaxLength=0 MaxDegrees=0
Frame=723 AutoMesh=Yes AtJoints=Yes AtFrames=No NumSegments=0 MaxLength=0 MaxDegrees=0
Frame=724 AutoMesh=Yes AtJoints=Yes AtFrames=No NumSegments=0 MaxLength=0 MaxDegrees=0

END TABLE DATA

D.2 SAP2000 INPUT DATA FILE FOR NL-THA

File C:\Users\MAhmed\Documents\My Dropbox\Public\0714-Parametric-Steel BOX-L140-180-140-H50-R500-THA-045g.s2k was saved on 10/31/10 at 21:27:57

TABLE: "PROGRAM CONTROL"
ProgramName=SAP2000 Version=14.0.0 ProgLevel=Advanced LicenseOS=Yes LicenseSC=Yes LicenseBR=Yes LicenseHT=No CurrUnits="Kip, ft, F" SteelCode=AISC-LRFD93 ConcCode="ACI 318-05/IBC2003" AlumCode="AA-ASD 2000" _
ColdCode=AISI-ASD96 BridgeCode="AASHTO LRFD 2007" RegenHinge=Yes

TABLE: "ACTIVE DEGREES OF FREEDOM"
UX=Yes UY=Yes UZ=Yes RX=Yes RY=Yes RZ=Yes

TABLE: "ANALYSIS OPTIONS"
Solver=Advanced SolverProc=Auto Force32Bit=No StiffCase=None GeomMod=No

TABLE: "COORDINATE SYSTEMS"
Name=GLOBAL Type=Cartesian X=0 Y=0 Z=0 AboutZ=0 AboutY=0 AboutX=0

TABLE: "GRID LINES"
CoordSys=GLOBAL AxisDir=X GridID=A XRYZCoord=0 LineType=Primary LineColor=Gray8Dark Visible=Yes BubbleLoc=End AllVisible=No BubbleSize=9.25
CoordSys=GLOBAL AxisDir=X GridID=B XRYZCoord=105 LineType=Primary LineColor=Gray8Dark Visible=Yes BubbleLoc=End
CoordSys=GLOBAL AxisDir=Y GridID=1 XRYZCoord=0 LineType=Primary LineColor=Gray8Dark Visible=Yes BubbleLoc=Start
CoordSys=GLOBAL AxisDir=Z GridID=Z8 XRYZCoord=-84.5 LineType=Primary LineColor=Gray8Dark Visible=Yes BubbleLoc=End
CoordSys=GLOBAL AxisDir=Z GridID=Z7 XRYZCoord=-78 LineType=Primary LineColor=Gray8Dark Visible=Yes BubbleLoc=End
CoordSys=GLOBAL AxisDir=Z GridID=Z6 XRYZCoord=-64.5 LineType=Primary LineColor=Gray8Dark Visible=Yes BubbleLoc=End
CoordSys=GLOBAL AxisDir=Z GridID=Z5 XRYZCoord=-58 LineType=Primary LineColor=Gray8Dark Visible=Yes BubbleLoc=End
CoordSys=GLOBAL AxisDir=Z GridID=Z4 XRYZCoord=-25 LineType=Primary LineColor=Gray8Dark Visible=Yes BubbleLoc=End
CoordSys=GLOBAL AxisDir=Z GridID=Z3 XRYZCoord=-15 LineType=Primary LineColor=Gray8Dark Visible=Yes BubbleLoc=End
CoordSys=GLOBAL AxisDir=Z GridID=Z2 XRYZCoord=-6.5 LineType=Primary LineColor=Gray8Dark Visible=Yes BubbleLoc=End
CoordSys=GLOBAL AxisDir=Z GridID=Z1 XRYZCoord=0 LineType=Primary LineColor=Gray8Dark Visible=Yes BubbleLoc=End

TABLE: "MATERIAL PROPERTIES 01 - GENERAL"
Material=4000Psi Type=Concrete SymType=Isotropic TempDepend=No Color=Cyan Notes="Normalweight f'c = 4 ksi added 4/23/2010 12:39:57 PM"
Material=A615Gr60 Type=Rebar SymType=Uniaxial TempDepend=No Color=Cyan Notes="ASTM A615 Grade 60 added 4/23/2010 3:10:32 PM"
Material=A992Fy50 Type=Steel SymType=Isotropic TempDepend=No Color=Green Notes="ASTM A992 Fy=50 ksi added 4/23/2010 12:39:57 PM"
Material=CONC Type=Concrete SymType=Isotropic TempDepend=No Color=Blue Notes="Normalweight f'c = 4 ksi added 4/23/2010 3:04:41 PM"
Material=RIGID Type=Concrete SymType=Isotropic TempDepend=No Color=Blue Notes="Normalweight f'c = 4 ksi added 4/23/2010 3:02:20 PM"
Material=SUB Type=Concrete SymType=Isotropic TempDepend=No Color=Blue Notes="Normalweight f'c =

4 ksi added 4/23/2010 3:02:20 PM"
Material=SUPER Type=Concrete SymType=Isotropic TempDepend=No Color=Blue Notes="Normalweight f'c = 4 ksi added 4/23/2010 2:59:44 PM"

TABLE: "MATERIAL PROPERTIES 02 - BASIC MECHANICAL PROPERTIES"
Material=4000Psi UnitWeight=0.15 UnitMass=4.66214231655636E-03 E1=519119.500693241 G12=216299.791955517 U12=0.2 A1=0.0000055
Material=A615Gr60 UnitWeight=0.49 UnitMass=1.52296649007508E-02 E1=4176000 A1=0.0000065
Material=A992Fy50 UnitWeight=0.49 UnitMass=1.52296649007508E-02 E1=4176000 G12=1606153.84615385 U12=0.3 A1=0.0000065
Material=CONC UnitWeight=0 UnitMass=0 E1=518400 G12=216000 U12=0.2 A1=0.0000055
Material=RIGID UnitWeight=0 UnitMass=0 E1=518400 G12=219661.016949153 U12=0.18 A1=0.000006
Material=SUB UnitWeight=0.15 UnitMass=0.004658385 E1=518400 G12=219661.016949153 U12=0.18 A1=0.000006
Material=SUPER UnitWeight=0.152 UnitMass=0.00472049 E1=518400 G12=219661.016949153 U12=0.18 A1=0.000006

TABLE: "MATERIAL PROPERTIES 03A - STEEL DATA"
Material=A992Fy50 Fy=7200 Fu=9360 EffFy=7920 EffFu=10296 SSCurveOpt=Simple SSHysType=Kinematic SHard=0.015 SMax=0.11 SRup=0.17 FinalSlope=-0.1

TABLE: "MATERIAL PROPERTIES 03B - CONCRETE DATA"
Material=4000Psi Fc=576 LtWtConc=No SSCurveOpt=Mander SSHysType=Takeda SFc=2.21914221766202E-03 SCap=0.005 FinalSlope=-0.1 FAngle=0 DAngle=0
Material=CONC Fc=576 LtWtConc=No SSCurveOpt=Mander SSHysType=Kinematic SFc=2.21914221766202E-03 SCap=0.005 FinalSlope=-0.1 FAngle=0 DAngle=0
Material=RIGID Fc=576 LtWtConc=No SSCurveOpt=Mander SSHysType=Kinematic SFc=2.21914221766202E-03 SCap=0.005 FinalSlope=-0.1 FAngle=0 DAngle=0
Material=SUB Fc=576 LtWtConc=No SSCurveOpt=Mander SSHysType=Kinematic SFc=2.21914221766202E-03 SCap=0.005 FinalSlope=-0.1 FAngle=0 DAngle=0
Material=SUPER Fc=576 LtWtConc=No SSCurveOpt=Mander SSHysType=Kinematic SFc=2.21914221766202E-03 SCap=0.005 FinalSlope=-0.1 FAngle=0 DAngle=0

TABLE: "MATERIAL PROPERTIES 03E - REBAR DATA"
Material=A615Gr60 Fy=8640 Fu=12960 EffFy=9504 EffFu=14256 SSCurveOpt=Simple SSHysType=Kinematic SHard=0.01 SCap=0.09 FinalSlope=-0.1 UseCTDef=No

TABLE: "MATERIAL PROPERTIES 06 - DAMPING PARAMETERS"
Material=4000Psi ModalRatio=0 VisMass=0 VisStiff=0 HysMass=0 HysStiff=0
Material=A615Gr60 ModalRatio=0 VisMass=0 VisStiff=0 HysMass=0 HysStiff=0
Material=A992Fy50 ModalRatio=0 VisMass=0 VisStiff=0 HysMass=0 HysStiff=0
Material=CONC ModalRatio=0 VisMass=0 VisStiff=0 HysMass=0 HysStiff=0
Material=RIGID ModalRatio=0 VisMass=0 VisStiff=0 HysMass=0 HysStiff=0
Material=SUB ModalRatio=0 VisMass=0 VisStiff=0 HysMass=0 HysStiff=0
Material=SUPER ModalRatio=0 VisMass=0 VisStiff=0 HysMass=0 HysStiff=0

TABLE: "FRAME SECTION PROPERTIES 01 - GENERAL"
SectionName=BLINK Material=SUB Shape=Rectangular t3=25 t2=25 Area=625 TorsConst=55013.0208333333 I33=32552.0833333333 I22=32552.0833333333 AS2=520.833333333333 AS3=520.833333333333 S33=2604.16666666667 _
S22=2604.16666666667 Z33=3906.25 Z22=3906.25 R33=7.21687836487032 R22=7.21687836487032 ConcCol=Yes ConcBeam=No Color=Gray8Dark TotalWt=1218.75 TotalMass=37.849378125 FromFile=No AMod=1 A2Mod=0 A3Mod=0 _
JMod=1 I2Mod=1 I3Mod=1 MMod=1 WMod=1 Notes="Added 4/23/2010 3:12:01 PM"
SectionName=COL Material=SUB Shape=Rectangular t3=6.25 t2=20 Area=125 TorsConst=1307.42425487066 I33=406.901041666667 I22=4166.66666666667 AS2=104.166666666667 AS3=104.166666666667 S33=130.208333333333 _
S22=416.666666666667 Z33=195.3125 Z22=625 R33=1.80421959121758 R22=5.77350269189626

ConcCol=Yes ConcBeam=No Color=Yellow TotalWt=1040.7905803196 TotalMass=32.3226881833473 FromFile=No AMod=1 A2Mod=0 A3Mod=0 _
JMod=1 I2Mod=0.353 I3Mod=0.402 MMod=1 WMod=1 Notes="Added 4/23/2010 3:11:18 PM"
SectionName=COLH Material=SUB Shape=Rectangular t3=6.25 t2=40 Area=250 TorsConst=2934.78967917811 I33=813.802083333333 I22=33333.3333333333 AS2=208.333333333333 AS3=208.333333333333 S33=260.416666666667 _
S22=1666.66666666667 Z33=390.625 Z22=2500 R33=1.80421959121758 R22=11.5470053837925 ConcCol=Yes ConcBeam=No Color=Red TotalWt=525 TotalMass=16.3043475 FromFile=No AMod=1 A2Mod=0 A3Mod=0 JMod=1 I2Mod=1 _
I3Mod=1 MMod=1 WMod=1 Notes="Added 4/23/2010 3:10:32 PM"
SectionName=COLT Shape=Nonprismatic Color=Blue Notes="Added 4/23/2010 3:12:36 PM"
SectionName=RIGID Material=RIGID Shape=General t3=1.5 t2=0.8333 Area=2500 TorsConst=100000 I33=100000 I22=100000 AS2=1 AS3=1 S33=1 S22=1 Z33=1 Z22=1 R33=1 R22=1 ConcCol=No ConcBeam=No Color=Blue _
TotalWt=0 TotalMass=0 FromFile=No AMod=1 A2Mod=1 A3Mod=1 JMod=1 I2Mod=1 I3Mod=1 MMod=1 WMod=1 Notes="Added 4/23/2010 3:09:53 PM"
SectionName=SUPER Material=SUPER Shape=General t3=1.5 t2=0.8333 Area=39.8201 TorsConst=5.6949 I33=273.3586 I22=2948.364 AS2=1 AS3=1 S33=1 S22=1 Z33=1 Z22=1 R33=1 R22=1 ConcCol=No ConcBeam=No _
Color=White TotalWt=1815.63125119602 TotalMass=56.38598134841 FromFile=No AMod=1 A2Mod=1 A3Mod=1 JMod=1 I2Mod=1 I3Mod=1 MMod=1 WMod=1 Notes="Added 4/23/2010 3:08:54 PM"
SectionName=SUPER-PIER Material=SUPER Shape=General t3=1.5 t2=0.8333 Area=45.2368 TorsConst=9.1093 I33=318.9432 I22=3350.024 AS2=1 AS3=1 S33=1 S22=1 Z33=1 Z22=1 R33=1 R22=1 ConcCol=No ConcBeam=No _
Color=White TotalWt=1099.989524661 TotalMass=34.1611154688618 FromFile=No AMod=1 A2Mod=1 A3Mod=1 JMod=1 I2Mod=1 I3Mod=1 MMod=1 WMod=1 Notes="Added 7/17/2010 11:41:37 PM"

TABLE: "FRAME SECTION PROPERTIES 02 - CONCRETE COLUMN"
SectionName=BLINK RebarMatL=A615Gr60 RebarMatC=A615Gr60 ReinfConfig=Rectangular LatReinf=Ties Cover=0.25 NumBars3Dir=26 NumBars2Dir=26 BarSizeL=#9 BarSizeC=#4 SpacingC=0.5 NumCBars2=3 NumCBars3=3 ReinfType=Check
SectionName=COL RebarMatL=A615Gr60 RebarMatC=A615Gr60 ReinfConfig=Rectangular LatReinf=Ties Cover=0.33 NumBars3Dir=45 NumBars2Dir=12 BarSizeL=#11 BarSizeC=#7 SpacingC=1 NumCBars2=6 NumCBars3=20 ReinfType=Design
SectionName=COLH RebarMatL=A615Gr60 RebarMatC=A615Gr60 ReinfConfig=Rectangular LatReinf=Ties Cover=0.33 NumBars3Dir=44 NumBars2Dir=15 BarSizeL=#11 BarSizeC=#7 SpacingC=0.5 NumCBars2=6 NumCBars3=20 ReinfType=Check

TABLE: "FRAME SECTION PROPERTIES 05 - NONPRISMATIC"
SectionName=COLT NumSegments=1 SegmentNum=1 StartSect=COLH EndSect=COL LengthType=Absolute AbsLength=10 EI33Var=Linear EI22Var=Cubic

TABLE: "LINK PROPERTY DEFINITIONS 01 - GENERAL"
Link=PH1 LinkType="Plastic (Wen)" Mass=0.001 Weight=0 RotInert1=0.1 RotInert2=0.1 RotInert3=0.1 DefLength=1 DefArea=1 PDM2I=0 PDM2J=0 PDM3I=0 PDM3J=0 Color=Yellow Notes="Added 7/19/2010 4:13:36 PM"

TABLE: "LINK PROPERTY DEFINITIONS 10 - PLASTIC (WEN)"
Link=PH1 DOF=U1 Fixed=No NonLinear=No TransKE=12300000 TransCE=0
Link=PH1 DOF=U2 Fixed=No NonLinear=No TransKE=7033178 TransCE=0 DJ=2.625
Link=PH1 DOF=U3 Fixed=No NonLinear=No TransKE=63238419 TransCE=0 DJ=2.625
Link=PH1 DOF=R1 Fixed=No NonLinear=No RotKE=64200000 RotCE=0
Link=PH1 DOF=R2 Fixed=No NonLinear=Yes RotKE=145000000 RotCE=0 RotK=145000000 RotYield=113268 Ratio=0.008 YieldExp=20
Link=PH1 DOF=R3 Fixed=No NonLinear=Yes RotKE=16153316 RotCE=0 RotK=16153316 RotYield=37443 Ratio=0.0232 YieldExp=20

TABLE: "LOAD PATTERN DEFINITIONS"

LoadPat=DEAD   DesignType=DEAD   SelfWtMult=1

TABLE: "FUNCTION - TIME HISTORY - FROM FILE"
Name=northcc   Time=0   Value=0.778   HeaderLines=2   PrefixChars=0   PtsPerLine=8   DataType="Equal Interval"   FormatType=Free   Interval=0.02   FileName="c:\program files\computers and structures\sap2000 14\time history functions\lacc_nor-1.th"
Name=northcc   Time=0.02   Value=-0.246
Name=northcc   Time=0.04   Value=0.164
....
Name=northcc   Time=59.94   Value=-5.557
Name=northcc   Time=59.96   Value=-4.9
Name=northcc   Time=59.98   Value=-3.523

Name=Elcentro   Time=0   Value=0.0108   HeaderLines=0   PrefixChars=0   PtsPerLine=3   DataType="Time and Value"   FormatType=Free   FileName="c:\program files\computers and structures\sap2000 14\time history functions\elcentro"
Name=Elcentro   Time=0.042   Value=0.001
Name=Elcentro   Time=0.097   Value=0.0159
....
Name=Elcentro   Time=11.988   Value=0.1354
Name=Elcentro   Time=12.043   Value=0.0673
Name=Elcentro   Time=12.113   Value=0.0865

TABLE: "FUNCTION - TIME HISTORY - USER"
Name=Monica   Time=0   Value=1.245
Name=Monica   Time=0.02   Value=-0.441
Name=Monica   Time=0.04   Value=-0.93
Name=Monica   Time=0.06   Value=-2.185
Name=Monica   Time=0.08   Value=-2.94
....
Name=Monica   Time=59.96   Value=-1.588
Name=Monica   Time=59.98   Value=-0.819
Name=Monica   Time=59.96   Value=-1.588
Name=Monica   Time=59.98   Value=-0.819
Name=Monica

TABLE: "CONSTRAINT DEFINITIONS - EQUAL"
Name=EQUAL1   CoordSys=GLOBAL   UX=No   UY=Yes   UZ=Yes   RX=Yes   RY=No   RZ=No

TABLE: "LOAD CASE DEFINITIONS"
Case=DEAD   Type=LinStatic   InitialCond=Zero   DesTypeOpt="Prog Det"   DesignType=DEAD   AutoType=None   RunCase=Yes   CaseStatus="Not Run"
Case=MODAL   Type=LinModal   InitialCond=Zero   DesTypeOpt="Prog Det"   DesignType=OTHER   AutoType=None   RunCase=Yes   CaseStatus="Not Run"
Case=ModalRitz   Type=LinModal   InitialCond=Zero   DesTypeOpt="Prog Det"   DesignType=OTHER   AutoType=None   RunCase=Yes   CaseStatus="Not Run"
Case=RITZ   Type=LinModal   InitialCond=Zero   DesTypeOpt="Prog Det"   DesignType=QUAKE   AutoType=None   RunCase=Yes   CaseStatus="Not Run"
Case=GRAV   Type=NonStatic   InitialCond=Zero   DesTypeOpt="Prog Det"   DesignType=DEAD   AutoType=None   RunCase=Yes   CaseStatus="Not Run"
Case=Elcentro   Type=NonModHist   InitialCond=Zero   ModalCase=RITZ   DesTypeOpt="Prog Det"   DesignType=QUAKE   AutoType=None   RunCase=Yes   CaseStatus="Not Run"
Case=NorthCC   Type=NonModHist   InitialCond=Zero   ModalCase=RITZ   DesTypeOpt="Prog Det"   DesignType=QUAKE   AutoType=None   RunCase=Yes   CaseStatus="Not Run"
Case=NorthCC-1   Type=NonModHist   InitialCond=Zero   ModalCase=RITZ   DesTypeOpt="Prog Det"   DesignType=QUAKE   AutoType=None   RunCase=Yes   CaseStatus="Not Run"
Case=S.Monica   Type=NonModHist   InitialCond=Zero   ModalCase=ModalRitz   DesTypeOpt="Prog Det"   DesignType=QUAKE   AutoType=None   RunCase=Yes   CaseStatus="Not Run"

TABLE: "CASE - STATIC 1 - LOAD ASSIGNMENTS"
Case=DEAD LoadType="Load pattern" LoadName=DEAD LoadSF=1
Case=GRAV LoadType="Load pattern" LoadName=DEAD LoadSF=1

TABLE: "CASE - STATIC 2 - NONLINEAR LOAD APPLICATION"
Case=GRAV LoadApp="Full Load" MonitorDOF=U1 MonitorJt=711

TABLE: "CASE - STATIC 4 - NONLINEAR PARAMETERS"
Case=GRAV Unloading="Unload Entire" GeoNonLin=None ResultsSave="Final State" MaxTotal=200 MaxNull=50 MaxIterCS=10 MaxIterNR=40 ItConvTol=0.0001 UseEvStep=Yes EvLumpTol=0.01 LSPerIter=20 LSTol=0.1 _
LSStepFact=1.618 FrameTC=Yes FrameHinge=Yes CableTC=Yes LinkTC=Yes LinkOther=Yes TFMaxIter=10 TFTol=0.01 TFAccelFact=1 TFNoStop=No

TABLE: "CASE - MODAL 1 - GENERAL"
Case=MODAL ModeType=Eigen MaxNumModes=12 MinNumModes=1 EigenShift=0 EigenCutoff=0 EigenTol=0.000000001 AutoShift=Yes
Case=ModalRitz ModeType=Ritz MaxNumModes=12 MinNumModes=1
Case=RITZ ModeType=Ritz MaxNumModes=12 MinNumModes=1

TABLE: "CASE - MODAL 3 - LOAD ASSIGNMENTS - RITZ"
Case=ModalRitz LoadType="Load pattern" LoadName=DEAD MaxCycles=0 TargetPar=0
Case=ModalRitz LoadType=Accel LoadName="Accel UY" MaxCycles=0 TargetPar=0
Case=ModalRitz LoadType=Link LoadName="All Links" MaxCycles=0 TargetPar=0
Case=RITZ LoadType=Accel LoadName="Accel UY" MaxCycles=0 TargetPar=0
Case=RITZ LoadType=Link LoadName="All Links" MaxCycles=0 TargetPar=0

TABLE: "JOINT COORDINATES"
Joint=211 CoordSys=GLOBAL CoordType=Cartesian XorR=138.1947 Y=-19.4771 Z=-60.9757 SpecialJt=No GlobalX=138.1947 GlobalY=-19.4771 GlobalZ=-60.9757
Joint=221 CoordSys=GLOBAL CoordType=Cartesian XorR=298.63 Y=-98.9762 Z=-60.9757 SpecialJt=No GlobalX=298.63 GlobalY=-98.9762 GlobalZ=-60.9757
Joint=311 CoordSys=GLOBAL CoordType=Cartesian XorR=138.1947 Y=-19.4771 Z=-54.4757 SpecialJt=No GlobalX=138.1947 GlobalY=-19.4771 GlobalZ=-54.4757
Joint=315 CoordSys=GLOBAL CoordType=Cartesian XorR=138.1947 Y=-19.4771 Z=-49.2301154751892 SpecialJt=No GlobalX=138.1947 GlobalY=-19.4771 GlobalZ=-49.2301154751892
Joint=321 CoordSys=GLOBAL CoordType=Cartesian XorR=298.63 Y=-98.9762 Z=-54.4757 SpecialJt=No GlobalX=298.63 GlobalY=-98.9762 GlobalZ=-54.4757
Joint=325 CoordSys=GLOBAL CoordType=Cartesian XorR=298.63 Y=-98.9762 Z=-49.2301154751892 SpecialJt=No GlobalX=298.63 GlobalY=-98.9762 GlobalZ=-49.2301154751892
Joint=411 CoordSys=GLOBAL CoordType=Cartesian XorR=138.1947 Y=-19.4771 Z=-21.4757 SpecialJt=No GlobalX=138.1947 GlobalY=-19.4771 GlobalZ=-21.4757
Joint=421 CoordSys=GLOBAL CoordType=Cartesian XorR=298.63 Y=-98.9762 Z=-21.4757 SpecialJt=No GlobalX=298.63 GlobalY=-98.9762 GlobalZ=-21.4757
Joint=511 CoordSys=GLOBAL CoordType=Cartesian XorR=138.1947 Y=-19.4771 Z=-11.4757 SpecialJt=No GlobalX=138.1947 GlobalY=-19.4771 GlobalZ=-11.4757
Joint=521 CoordSys=GLOBAL CoordType=Cartesian XorR=298.63 Y=-98.9762 Z=-11.4757 SpecialJt=No GlobalX=298.63 GlobalY=-98.9762 GlobalZ=-11.4757
Joint=611 CoordSys=GLOBAL CoordType=Cartesian XorR=138.1947 Y=-19.4771 Z=-4.4757 SpecialJt=No GlobalX=138.1947 GlobalY=-19.4771 GlobalZ=-4.4757
Joint=621 CoordSys=GLOBAL CoordType=Cartesian XorR=298.63 Y=-98.9762 Z=-4.4757 SpecialJt=No GlobalX=298.63 GlobalY=-98.9762 GlobalZ=-4.4757
Joint=701 CoordSys=GLOBAL CoordType=Cartesian XorR=0 Y=0 Z=0 SpecialJt=No GlobalX=0 GlobalY=0 GlobalZ=0
Joint=702 CoordSys=GLOBAL CoordType=Cartesian XorR=34.9758 Y=-1.2248 Z=0 SpecialJt=No GlobalX=34.9758 GlobalY=-1.2248 GlobalZ=0
Joint=703 CoordSys=GLOBAL CoordType=Cartesian XorR=69.7802 Y=-4.8932 Z=0 SpecialJt=No GlobalX=69.7802 GlobalY=-4.8932 GlobalZ=0

Joint=704 CoordSys=GLOBAL CoordType=Cartesian XorR=104.2428 Y=-10.9873 Z=0 SpecialJt=No GlobalX=104.2428 GlobalY=-10.9873 GlobalZ=0
Joint=711 CoordSys=GLOBAL CoordType=Cartesian XorR=138.1947 Y=-19.4771 Z=0 SpecialJt=No GlobalX=138.1947 GlobalY=-19.4771 GlobalZ=0
Joint=712 CoordSys=GLOBAL CoordType=Cartesian XorR=180.8294 Y=-33.8447 Z=0 SpecialJt=No GlobalX=180.8294 GlobalY=-33.8447 GlobalZ=0
Joint=713 CoordSys=GLOBAL CoordType=Cartesian XorR=222 Y=-51.9866 Z=0 SpecialJt=No GlobalX=222 GlobalY=-51.9866 GlobalZ=0
Joint=714 CoordSys=GLOBAL CoordType=Cartesian XorR=261.3731 Y=-73.7558 Z=0 SpecialJt=No GlobalX=261.3731 GlobalY=-73.7558 GlobalZ=0
Joint=721 CoordSys=GLOBAL CoordType=Cartesian XorR=298.63 Y=-98.9762 Z=0 SpecialJt=No GlobalX=298.63 GlobalY=-98.9762 GlobalZ=0
Joint=722 CoordSys=GLOBAL CoordType=Cartesian XorR=325.9507 Y=-120.848 Z=0 SpecialJt=No GlobalX=325.9507 GlobalY=-120.848 GlobalZ=0
Joint=723 CoordSys=GLOBAL CoordType=Cartesian XorR=351.6746 Y=-144.578 Z=0 SpecialJt=No GlobalX=351.6746 GlobalY=-144.578 GlobalZ=0
Joint=724 CoordSys=GLOBAL CoordType=Cartesian XorR=375.8239 Y=-170.049 Z=0 SpecialJt=No GlobalX=375.8239 GlobalY=-170.049 GlobalZ=0
Joint=731 CoordSys=GLOBAL CoordType=Cartesian XorR=397.8358 Y=-197.136 Z=0 SpecialJt=No GlobalX=397.8358 GlobalY=-197.136 GlobalZ=0

TABLE: "CONNECTIVITY - FRAME"
Frame=211 JointI=311 JointJ=211 IsCurved=No Length=6.5 CentroidX=138.1947 CentroidY=-19.4771 CentroidZ=-57.7257
Frame=221 JointI=321 JointJ=221 IsCurved=No Length=6.5 CentroidX=298.63 CentroidY=-98.9762 CentroidZ=-57.7257
Frame=315 JointI=411 JointJ=315 IsCurved=No Length=27.7544154751892 CentroidX=138.1947 CentroidY=-19.4771 CentroidZ=-35.3529077375946
Frame=325 JointI=421 JointJ=325 IsCurved=No Length=27.7544154751892 CentroidX=298.63 CentroidY=-98.9762 CentroidZ=-35.3529077375946
Frame=411 JointI=511 JointJ=411 IsCurved=No Length=10 CentroidX=138.1947 CentroidY=-19.4771 CentroidZ=-16.4757
Frame=421 JointI=521 JointJ=421 IsCurved=No Length=10 CentroidX=298.63 CentroidY=-98.9762 CentroidZ=-16.4757
Frame=511 JointI=611 JointJ=511 IsCurved=No Length=7 CentroidX=138.1947 CentroidY=-19.4771 CentroidZ=-7.9757
Frame=521 JointI=621 JointJ=521 IsCurved=No Length=7 CentroidX=298.63 CentroidY=-98.9762 CentroidZ=-7.9757
Frame=611 JointI=711 JointJ=611 IsCurved=No Length=4.4757 CentroidX=138.1947 CentroidY=-19.4771 CentroidZ=-2.23785
Frame=621 JointI=721 JointJ=621 IsCurved=No Length=4.4757 CentroidX=298.63 CentroidY=-98.9762 CentroidZ=-2.23785
Frame=701 JointI=701 JointJ=702 IsCurved=No Length=34.9972387579363 CentroidX=17.4879 CentroidY=-0.6124 CentroidZ=0
Frame=702 JointI=702 JointJ=703 IsCurved=No Length=34.9971915718962 CentroidX=52.378 CentroidY=-3.059 CentroidZ=0
Frame=703 JointI=703 JointJ=704 IsCurved=No Length=34.9972692301842 CentroidX=87.0115 CentroidY=-7.94025 CentroidZ=0
Frame=704 JointI=704 JointJ=711 IsCurved=No Length=34.9972601449028 CentroidX=121.21875 CentroidY=-15.2322 CentroidZ=0
Frame=711 JointI=711 JointJ=712 IsCurved=No Length=44.9905053744676 CentroidX=159.51205 CentroidY=-26.6609 CentroidZ=0
Frame=712 JointI=712 JointJ=713 IsCurved=No Length=44.9905194454343 CentroidX=201.4147 CentroidY=-42.91565 CentroidZ=0
Frame=713 JointI=713 JointJ=714 IsCurved=No Length=44.9904331191644 CentroidX=241.68655 CentroidY=-62.8712 CentroidZ=0
Frame=714 JointI=714 JointJ=721 IsCurved=No Length=44.9905009281959 CentroidX=280.00155 CentroidY=-86.366 CentroidZ=0

Frame=721 JointI=721 JointJ=722 IsCurved=No Length=34.9970896465692 CentroidX=312.29035 CentroidY=-109.9121 CentroidZ=0
Frame=722 JointI=722 JointJ=723 IsCurved=No Length=34.997598934927 CentroidX=338.81265 CentroidY=-132.713 CentroidZ=0
Frame=723 JointI=723 JointJ=724 IsCurved=No Length=35.0992953132965 CentroidX=363.74925 CentroidY=-157.3135 CentroidZ=0
Frame=724 JointI=724 JointJ=731 IsCurved=No Length=34.9031418443956 CentroidX=386.82985 CentroidY=-183.5925 CentroidZ=0

TABLE: "JOINT RESTRAINT ASSIGNMENTS"
Joint=211 U1=Yes U2=Yes U3=Yes R1=Yes R2=Yes R3=Yes
Joint=221 U1=Yes U2=Yes U3=Yes R1=Yes R2=Yes R3=Yes
Joint=701 U1=No U2=Yes U3=Yes R1=Yes R2=No R3=No
Joint=731 U1=No U2=Yes U3=Yes R1=Yes R2=No R3=No

TABLE: "JOINT LOCAL AXES ASSIGNMENTS 1 - TYPICAL"
Joint=211 AngleA=-16 AngleB=0 AngleC=0 AdvanceAxes=No
Joint=221 AngleA=-36 AngleB=0 AngleC=0 AdvanceAxes=No
Joint=731 AngleA=-52 AngleB=0 AngleC=0 AdvanceAxes=No

TABLE: "JOINT SPRING ASSIGNMENTS 1 - UNCOUPLED"
Joint=211 CoordSys=Local U1=0 U2=0 U3=0 R1=0 R2=0 R3=0
Joint=701 CoordSys=Local U1=0 U2=0 U3=0 R1=0 R2=0 R3=0
Joint=731 CoordSys=Local U1=0 U2=0 U3=0 R1=0 R2=0 R3=0
Joint=221 CoordSys=Local U1=0 U2=0 U3=0 R1=0 R2=0 R3=0

TABLE: "FRAME SECTION ASSIGNMENTS"
Frame=211 SectionType=Rectangular AutoSelect=N.A. AnalSect=BLINK DesignSect=BLINK MatProp=Default
Frame=221 SectionType=Rectangular AutoSelect=N.A. AnalSect=BLINK DesignSect=BLINK MatProp=Default
Frame=315 SectionType=Rectangular AutoSelect=N.A. AnalSect=COL DesignSect=COL MatProp=Default
Frame=325 SectionType=Rectangular AutoSelect=N.A. AnalSect=COL DesignSect=COL MatProp=Default
Frame=411 SectionType=Nonprismatic AutoSelect=N.A. AnalSect=COLT DesignSect=COLT MatProp=Default NPSectType=Default
Frame=421 SectionType=Nonprismatic AutoSelect=N.A. AnalSect=COLT DesignSect=COLT MatProp=Default NPSectType=Default
Frame=511 SectionType=Rectangular AutoSelect=N.A. AnalSect=COLH DesignSect=COLH MatProp=Default
Frame=521 SectionType=Rectangular AutoSelect=N.A. AnalSect=COLH DesignSect=COLH MatProp=Default
Frame=611 SectionType=General AutoSelect=N.A. AnalSect=RIGID DesignSect=N.A. MatProp=Default
Frame=621 SectionType=General AutoSelect=N.A. AnalSect=RIGID DesignSect=N.A. MatProp=Default
Frame=701 SectionType=General AutoSelect=N.A. AnalSect=SUPER DesignSect=N.A. MatProp=Default
Frame=702 SectionType=General AutoSelect=N.A. AnalSect=SUPER DesignSect=N.A. MatProp=Default
Frame=703 SectionType=General AutoSelect=N.A. AnalSect=SUPER DesignSect=N.A. MatProp=Default
Frame=704 SectionType=General AutoSelect=N.A. AnalSect=SUPER-PIER DesignSect=N.A. MatProp=Default
Frame=711 SectionType=General AutoSelect=N.A. AnalSect=SUPER-PIER DesignSect=N.A. MatProp=Default
Frame=712 SectionType=General AutoSelect=N.A. AnalSect=SUPER DesignSect=N.A. MatProp=Default
Frame=713 SectionType=General AutoSelect=N.A. AnalSect=SUPER DesignSect=N.A. MatProp=Default
Frame=714 SectionType=General AutoSelect=N.A. AnalSect=SUPER-PIER DesignSect=N.A. MatProp=Default
Frame=721 SectionType=General AutoSelect=N.A. AnalSect=SUPER-PIER DesignSect=N.A. MatProp=Default
Frame=722 SectionType=General AutoSelect=N.A. AnalSect=SUPER DesignSect=N.A. MatProp=Default
Frame=723 SectionType=General AutoSelect=N.A. AnalSect=SUPER DesignSect=N.A. MatProp=Default

Frame=724   SectionType=General   AutoSelect=N.A.   AnalSect=SUPER   DesignSect=N.A.   MatProp=Default

TABLE: "FRAME RELEASE ASSIGNMENTS 1 - GENERAL"
Frame=611   PI=No   V2I=No   V3I=No   TI=No   M2I=No   M3I=No   PJ=No   V2J=No   V3J=No   TJ=No   M2J=No   M3J=Yes   PartialFix=No
Frame=621   PI=No   V2I=No   V3I=No   TI=No   M2I=No   M3I=No   PJ=No   V2J=No   V3J=No   TJ=No   M2J=No   M3J=Yes   PartialFix=No

TABLE: "FRAME LOCAL AXES ASSIGNMENTS 1 - TYPICAL"
Frame=211   Angle=16   MirrorAbt2=No   MirrorAbt3=No   AdvanceAxes=No
Frame=221   Angle=36   MirrorAbt2=No   MirrorAbt3=No   AdvanceAxes=No
Frame=315   Angle=16   MirrorAbt2=No   MirrorAbt3=No   AdvanceAxes=No
Frame=325   Angle=36   MirrorAbt2=No   MirrorAbt3=No   AdvanceAxes=No
Frame=411   Angle=16   MirrorAbt2=No   MirrorAbt3=No   AdvanceAxes=No
Frame=421   Angle=36   MirrorAbt2=No   MirrorAbt3=No   AdvanceAxes=No
Frame=511   Angle=16   MirrorAbt2=No   MirrorAbt3=No   AdvanceAxes=No
Frame=521   Angle=36   MirrorAbt2=No   MirrorAbt3=No   AdvanceAxes=No
Frame=611   Angle=16   MirrorAbt2=No   MirrorAbt3=No   AdvanceAxes=No
Frame=621   Angle=36   MirrorAbt2=No   MirrorAbt3=No   AdvanceAxes=No

TABLE: "LINK PROPERTY ASSIGNMENTS"
Link=1   LinkType="Plastic (Wen)"   LinkJoints=TwoJoint   LinkProp=PH1   LinkFDProp=None
Link=2   LinkType="Plastic (Wen)"   LinkJoints=TwoJoint   LinkProp=PH1   LinkFDProp=None

TABLE: "LINK LOCAL AXES ASSIGNMENTS 1 - TYPICAL"
Link=1   Angle=-16   AdvanceAxes=No
Link=2   Angle=-36   AdvanceAxes=No

END TABLE DATA

REFERENCES

AASHTO. (2009). *AASHTO Guide Specification for LRFD Seismic Bridge Design.* American Association of State Highway and Transportation Officials.

AlAyed, H. S. (2002). Seismic analysis of bridges using nonlinear static procedure. *PhD Dissertation*. College Park, MD: Department of Civil & Environmental Engineering, University of Maryland.

Antoniou, S., Rovithakis, A., & Pinho, R. (2002). Development and verification of a fully adaptive pushover procedure. *Proceedings of the 12th European Conference on Earthquake Engineering.* London, U.K.

ATC-40. (1996). *Seismic Evaluation and Retrofit of Concrete Buildings.* Redwood City, CA.: Applied Technology Council.

Aydinoglu, M. N. (2004). *An improved pushover procedure for engineering practice: incremental response spectrum analysis (IRSA).* PEER Report 2004-5 (UC Berkeley).

Bracci, J. M., Kunnath, S. K., & Reinhorn, A. M. (1997). Seismic performance and retrofit evaluation for reinforced concrete structures. *Jornal of Structural Engineering (ASCE), 123*(1), 3-10.

Chopra, A. K. (2001). *Dynamics of Structures: Theory and Applications to Earthquake Engineering* (Second ed.). Englewood Cliffs, New Jersey: Prentice Hall.

Chopra, A. K., & Goel, R. K. (2001). *A Modal Pushover Analysis Procedure to Estimating Seismic Demands for Buildings: Theory and Preliminary Evaluation.* University of California. Berkely, California: Pacific Earthquake Engineering Research Center.

Chopra, A. K., & Goel, R. K. (2002). A Modal pushover analysis procedure for estimating seismic demands for buildings. *Earthquake Engineering and Structural Dynamics, 31*(3), 561-582.

Chopra, A. K., & Goel, R. K. (2004). A modal pushover analysis procedure to estimate seismic demands for unsymmetrical-plan buildings. *Earthquake Engineering and Structural Dynamics, 33*(8), 903-927.

CSI. (2009). SAP 2000 Advanced version 14.0. Berkeley, CA: Computers and Structures, Inc.

Eurocode 8. (2004). *Design of structures for earthquake resistance - Part2: Bridges.* Brussels: CEN (Comite Europeen de Normalisation).

Fajfar, P. (1999). Capacity spectrum method based on inelastic demand spectra. *Earthquake Engineering & Structural Dynamics, 28*(9), 979-993.

Fajfar, P., & Fischinger, M. (1989). N2 - A method for non-linear seismic analysis of regular buildings. *The 9th World Conference on Earthquake Engineering*, *V*, pp. 111-116. Tokyo-Kyoto, Japan.

FEMA-273. (1997). *NEHRP Guidelines for the Seismic Rehabilitation of Buildings.* Washington, D.C.: Federal Emergency Management Agency.

FEMA-356. (2000). *Prestandard and Commentary for the Seismic Rehabilitation of Buildings.* Washington, D.C.: Fedral Emergency Management Agency.

FHWA, 1996-a. (1996). *Seismic Design of Bridges: Design Example No. 4 Three span Continous CIP Concrete Bridge.* Springfield, VA: Federal Highway Administration, Publication No. FHWA-SA-97-009.

FHWA, 1996-b. (1996). *Seismic Design of Bridges: Design Example No. 5 Nine span Viaduct Steel Girder Bridge.* Springfield, VA: Fedral Highway Administration; Publication No. FHWA-SA-97-009.

Fischinger, M., Beg, M., Isakovic, T., Tomazevic, M., & Zarnic, R. (2004). *Performance based assessment - from general methodologies to specific implementations.* published in PEER Report 2004-05 (UC Berkeley).

Freeman, S. A., Nicoletti, J. P., & Tyrell, J. V. (1975). Evaluations of Existing Buildings for Seismic Risk - A Case Study of Puget Sound Naval Shipyard. *The first U.S. Nat. Conf. on Earthq. Engng*, (pp. 113-122). Oakland, California.

Fu, C. C. (2009). DESCUS I. *Win-DESCUS I User's manual for Design and Analysis of Curved I-Girder Bridge Systems, 12*. College Park, MD: The BEST Center, University of Maryland.

Fu, C. C. (2009). DESCUS II. *Win-DESCUS User's manual for Design and Analysis of Curved BOX-Girder Bridge Systems, 12*. College Park, MD: The BEST Center, University of Maryland.

Gupta, B., & Kunnath, S. K. (2000). Adaptive spectra-based pushover procedure for seismic evaluation of structures. *Earthquake spectra, 16*(2), 367-392.

Isakovic, T., & Fischinger, M. (2006). Higher modes in simplified inelastic seismic analysis of single column bent viaducts. *Earthquake Engineering and Structural Dynamics, 35*(1), 95-114.

Kappos, A. J., & Paraskeva, T. S. (2008). Nonlinear static analysis of bridges accounting for higher mode effects. *Nonlinear Static Methods for design/Assessment of 3D Structures*. Portugal.

Kappos, A. J., & Petrains, C. (2001). Reliability of pushover analysis - based methods for seismic assessment of R/C buildings. *Earthquake Resistant Engineering Structures III; WIT Press*, 407-416.

Kappos, A. J., Paraskeva, T. S., & Sextos, A. G. (2004). Seismic assessment of a major bridge using modal pushover analysis and dynamic time-history analysis. *Advances in Computational and Experimental Engineering and Science*, 673-680.

Paraskeva, T. S., Kappos, A. J., & Sextos, A. G. (2006). Extension of modal pushover analysis to seismic assessment of bridges. *Earthquake Engineering and Structural Dynamics, 35*, 1269-1293.

PEER. (2005). *Pacific Earthquake Engineering Research Center*. Retrieved September 2010, from http://peer.berkeley.edu/nga/.

Pinho, R., Antoniou, S., Casarotti, C., & Lopez, M. (2005). A displacement-based adaptive pushover for assessment of buildings and bridges. *NATO International Workshop on Advances in Earthquake Engineering for Urban Risk Reduction*. Istanbul, Turkey.

Priestly, M. J., Seible, F., & Calvi, G. M. (1996). *Seismic design and retrofit of bridges.* New York: John Wiley & Sons.

Sasaki, K. K., Freeman, S. A., & Paret, T. F. (1998). Multimode pushover procedure (MMP) - a method to identify the effects of higher modes in a pushover analysis. *Proceedings of the 6th US National Conference on Earthquake Engineering*. Seattle.

Vidic, T., Fajfar, P., & Fischinger, M. (1994). Consistent inelastic design spectra: strength and displacement. *Earthquake Engineering & Structural Dynamics, 23*, 502-521.